# STRONG BOND ACTIVATION WITH LATE TRANSITION-METAL PINCER COMPLEXES AS A FOUNDATION FOR POTENTIAL CATALYSIS

A Dissertation

by

YANJUN ZHU

Submitted to the Office of Graduate Studies of
Texas A&M University
in partial fulfillment of the requirements for the degree of

DOCTOR OF PHILOSOPHY

May 2012

Major Subject: Chemsitry

Strong Bond Activation with Late Transition-Metal Pincer Complexes as a Foundation for Potential Catalysis

# STRONG BOND ACTIVATION WITH LATE TRANSITION-METAL PINCER COMPLEXES AS A FOUNDATION FOR POTENTIAL CATALYSIS

A Dissertation

by

YANJUN ZHU

Submitted to the Office of Graduate Studies of
Texas A&M University
in partial fulfillment of the requirements for the degree of

DOCTOR OF PHILOSOPHY

Approved by:

| | |
|---|---|
| Chair of Committee, | Oleg V. Ozerov |
| Committee Members, | Fran ̧ois P. Gabbaï |
| | John A. Gladysz |
| | Robert Lane |
| Head of Department, | David H. Russell |

May 2012

Major Subject: Chemsitry

# ABSTRACT

Strong Bond Activation with Late Transition-Metal Pincer Complexes as a Foundation for Potential Catalysis.

(May 2012)

Yanjun Zhu, B.S., Soochow University, China; M.S., Brandeis University, USA

Chair of Advisory Committee: Dr. Oleg V. Ozerov

Strong bond activation mediated by pincer ligated transiton-metal complexes has been the subject of intense study in recent years, due to its potential involvement in catalytic transformations. This dissertation has focused on the net heterolytic cleavage of B-H and B-B bonds across the N-Pd bond in a cationic (PNP)Pd fragment, the C-H oxidative addition to a (PNP)Ir center and the recent results on the C-H and C-O oxidative addition in reactions of aryl carboxylates with the (PNP)Rh fragment.

Transition metal carbene and carbyne complexes are of great interest because of their role in a wide variety of catalytic reactions. Our work has resulted in the isolation of a rhodium(I) difluorocarbene. Reaction of the rhodium difluorocarbene complex with a silylium salt led to the C-F bond cleavage and the formation of a terminal fluorocarbyne complex.

Reductive elimination is a critical step of cross coupling reactions. In order to examine the effect of the pincer ligand on the reductive elimination reactions from Rh(III), the first π-accepting PNP ligand bearing pyrrolyl substituents was prepared and

installed onto the rhodium center. Arylhalide (halide = Br, I) oxidative addition was achieved in the presence of donor ligands such as acetonitrile to form stable six-coordinate Rh(III) compounds. The C-O reductive elimination reactions in this system were also explored.

# ACKNOWLEDGEMENTS

I am heartily thankful to my supervisor, Prof. Oleg Ozerov, who has supported me in the past five years with his patience, knowledge, and encouragement. I appreciate all his contributions of time and ideas to make my Ph.D experiences wonderful. I am also thankful for the excellent example he has provided as a successful chemist.

I am very thankful to Professor Bruce Foxman, Dr. Chun-Hsing Chen, Dr. David Herbert and Rafael Huacuja for their work on X-ray crystallography. I also want to thank my committee members Dr. Gladysz, Dr. Gabbaï and Dr. Lane for their time in reading and correcting this dissertation.

Thanks also go to the group members both in Brandeis and Texas A&M University. The group has been a source of friendship, inspirations and good collaborations. Thanks go to Dr. Mason Haneline, who taught me lots of lab skills when I was a fresh graduate student. I would also like to acknowledge Samuel Timpa, a very brilliant and organized person, who has worked with me since 2008. I very much appreciate his passion in chemistry, his work in changing the gas cylinders, filling the liquid $N_2$ tanks as well as numerous lunch sandwiches he brought me. Many thanks to Rafael Huacuja and Chun-I Lee, who I always share ideas with and always give me very creative ideas. Thank other group members who I had a great pleasure to work with: Dr. Wei Weng, Dr. Sylvain Gatard, Dr. Chris Douvris, Dr. Deborha Bacciu, Dr. Anthony Fernandez, Dr. Nagaraja, Dr. Panida Surawatanawong, Dr. Justin Walensky, Dr. Dan Smith, Dr. David Herbert, Dr. Jia Zhou, Dr. Morgan Maclnnis, Dr. Claudia Fafard, Dr. Weixing Gu, Alyson

Christopher, Baofei Pan, Dan Graham, Mayank Puri, Shoshanna Barnett, Laura Gerber, Lauren Gregor, Emily Pelton, Billy McCulloch, Rodrigo Ramirez, Jillian Davidson, Loren Press, Aaron Hollas, Jessica DeMott, Adam Miller, Chrissy Brammell, Chandra Mouli Palit, Chris Pell, Chan Park and Samantha Yruegas.

Finally, I want to thank my family for their love and support. As the only child in the family, I am very sorry that I am not able to be with my parents and take good care of them. Thanks for their understanding and encouragement. I also want to express my gratitude to my grandmother, who passed away a few months ago while I was writing this dissertation. She was the best grandmother in the world. Thank you!

# TABLE OF CONTENTS

Page

CHAPTER Page

CHAPTER Page

# LIST OF FIGURES

# LIST OF SCHEMES

Page

Page

Page

Page

# CHAPTER I

# INTRODUCTION AND OVERVIEW

## *1.1 General introduction for pincer ligands*

The ability to control properties of metal centers by a well-defined ligand system is of great importance in inorganic and organometallic chemistry. Pincer ligands, tridentate ligands that coordinate in a meridional fashion, are one of the most well defined ligand systems. Pincer ligands have attracted a lot of attention, especially in the past decade, due to the stability and activity of their transition metal complexes as well as their variability. For example, pincer metal complexes have been studied in strong bond activation, such as C-H,[1] C-N,[2] C-O[3] bonds, as well as small molecule activation, such as $NH_3$,[4] $CO_2$,[5] $CH_4$,[6] and alcohols.[7]

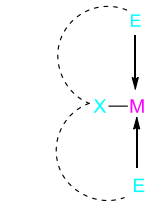


**Scheme 1-1.** General scheme for pincer metal complexes.

---

This dissertation follows the style of *Journal of the American Chemical Society*.

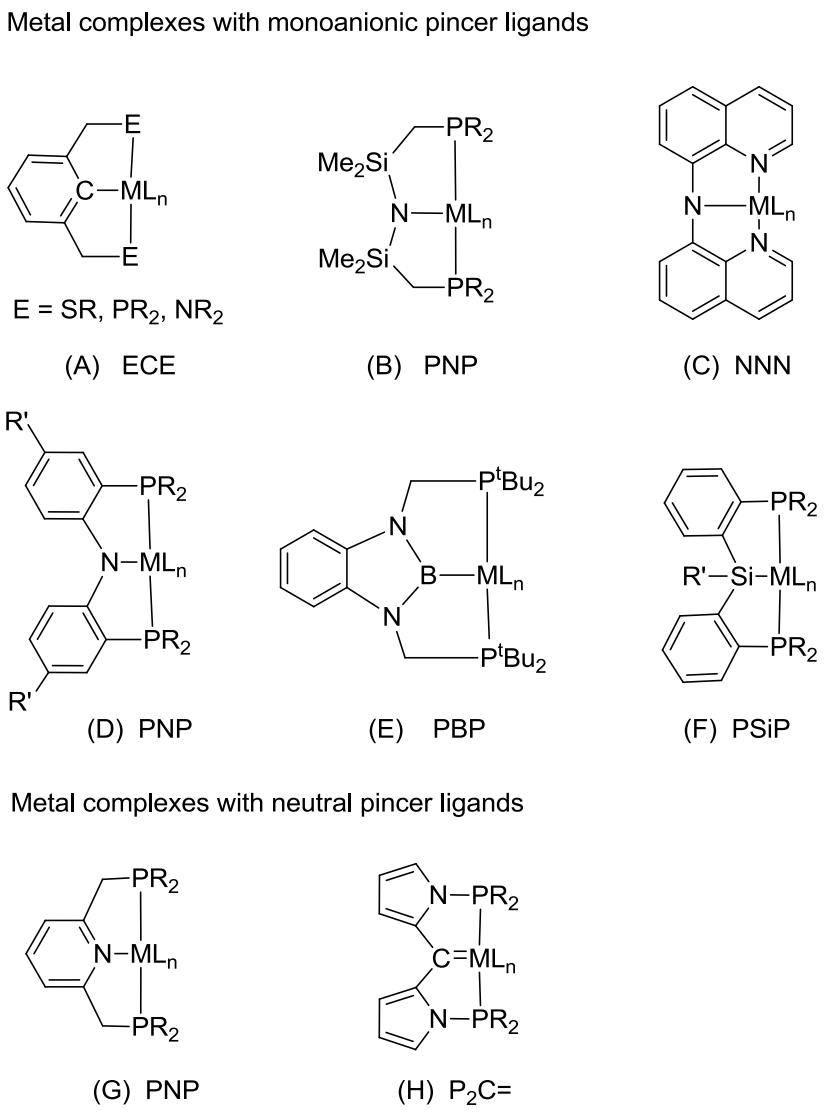


**Scheme 1-2.** Metal complexes bearing anionic or neutral pincer ligand motifs.

Pincer ligands are frequently referred to by their donor atoms, EXE (side arm donors, E; center donor, X) (Scheme 1-1) and can be generally divided into two main categories. The first one is the anionic ligand, where the two ligand arms are neutral donors and the one in the middle is an anionic donor. Representative examples of anionic pincer ligands include ECE (E = P, S, N, etc.) ligands (**A**),[8] Fryzuk's PNP ligand (**B**)[9], the NNN

ligand from the Peters' group (**C**),[10] diarylamido based PNP ligands (**D**)[11] and the most recently developed PBP (**E**)[12] and PSiP (**F**)[13] ligands. The second type is the neutral pincer ligand with all three donors being neutral. Most of these types of ligands are often based on the pyridine backbone (**G**)[14] or carbene (**H**)[15] frameworks. Among all these pincer ligands, the PXP ligands are the most prevalent. The incorporation of phosphine arms in the ligand not only allows for steric and electronic control by using substituent effects, but also provides a useful $^{31}$P NMR spectroscopic probe, which makes it convenient to monitor the reaction transformations by $^{31}$P NMR spectroscopy.

### *1.2 Synthesis of pincer ligated transition metal complexes*

#### *1.2.1 Transmetalation*

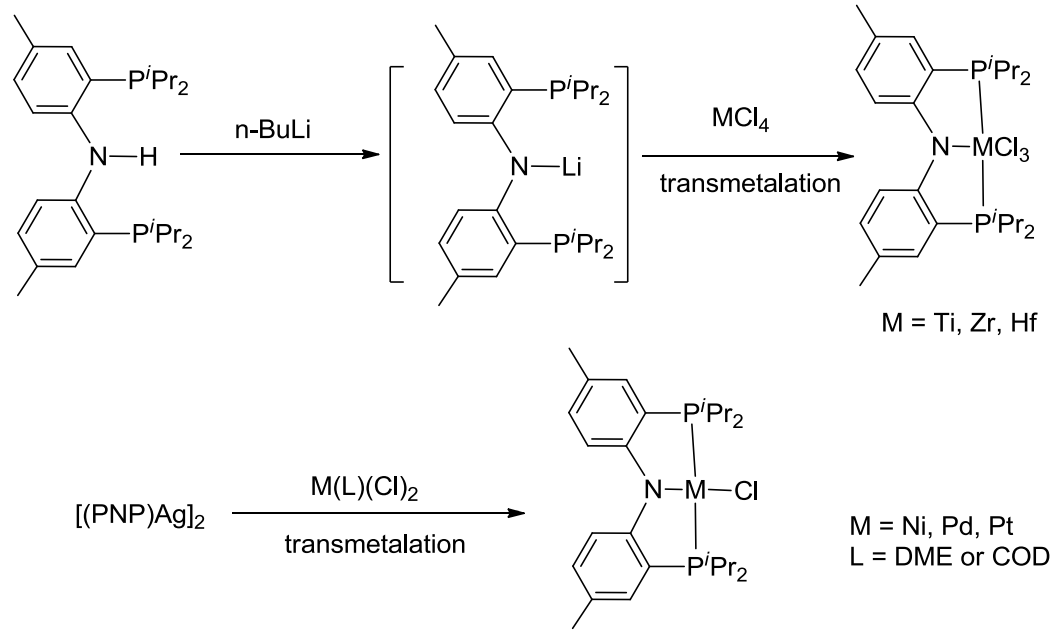


**Scheme 1-3.** Installation of ligand onto metal via transmetalation.

Organometallic complexes of the alkali or alkaline earth metals, such as organolithium or organomagnesium complexes, are very useful synthetic reagents. Pincer lithium /sodium or magnesium salts are truly the workhorse reagents for synthetic methods to generate transition metal and other main group complexes via transmetallation (TM). For example, our group reported the synthesis of a series Group 4 (PNP)$ML_n$ complexes via the TM of (PNP)Li salt with $MCl_4$ metal precursors (Scheme 1-3).[16] The soft metal salt $[(PNP)Ag]_2$[17] has also been developed and shown the ability to transfer the ligand to a Group 10 metal center. However, this method may be problematic in some other ligand sets since the synthesis of the lithium salt requires well controlled lithiation (typically through Li-halogen exchange or selective deprotonation) of pincer ligands and sometimes the lithiation is not selective.[18]

*1.2.2 Oxidative addition (OA) of low valent metal precursors*

Another recently developed method to install the pincer ligand onto a metal center is through oxidative addition reactions. Oxidative addition reactions form products containing two new metal-ligand bonds through cleavage of a bond (Scheme 1-4). By this overall process, the oxidation state of metal is increased by two. The Milstein group reported the first example of metal insertion into the strong C-C bond in Ar-$CF_3$ by utilizing a PCP ligand bearing a $CF_3$ group between the chelate phosphine moieties.[19] It was later observed that Rh(I) precursors can also cleave the aryl-Et bond in PC(Et)P, providing the synthesis of (PCP)Rh(III) complexes through oxidative addition. Inspired by Milstein's work, our group has also successfully accomplished the intramolecular N-

H, N-C, and C-H oxidative additions reactions at Group 9 metal centers with PNP ligands to afford Rh(III) or Ir(III) complexes (Scheme 1-5).[1b,2b,20]

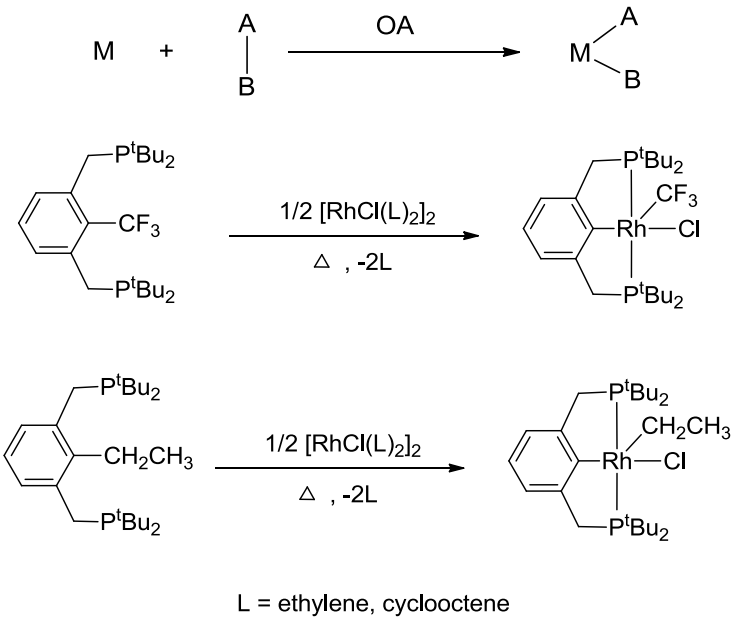


**Scheme 1-4.** Installation of ligand onto metal via oxidative addition.

*1.2.3 Direct cyclometalation without changing oxidation state of metals*

Besides TM and OA reactions, direct cyclometalation is another commonly used method to make pincer metal complexes especially when TM method is a problem. The coordinating functionalities of the ligand (such as P, S, N, etc) induce "precoordination" which brings the bond that will be activated closer to the metal center. This "precoordination" mode facilitates the insertion of the metal into the bond. Milstein and

coworkers reported the first example of metal insertion into an unstrained, unactivated C-C bond by employing Ph-PCP with $[HRh(PPh_3)_4]$[21] (Scheme 1-6A).

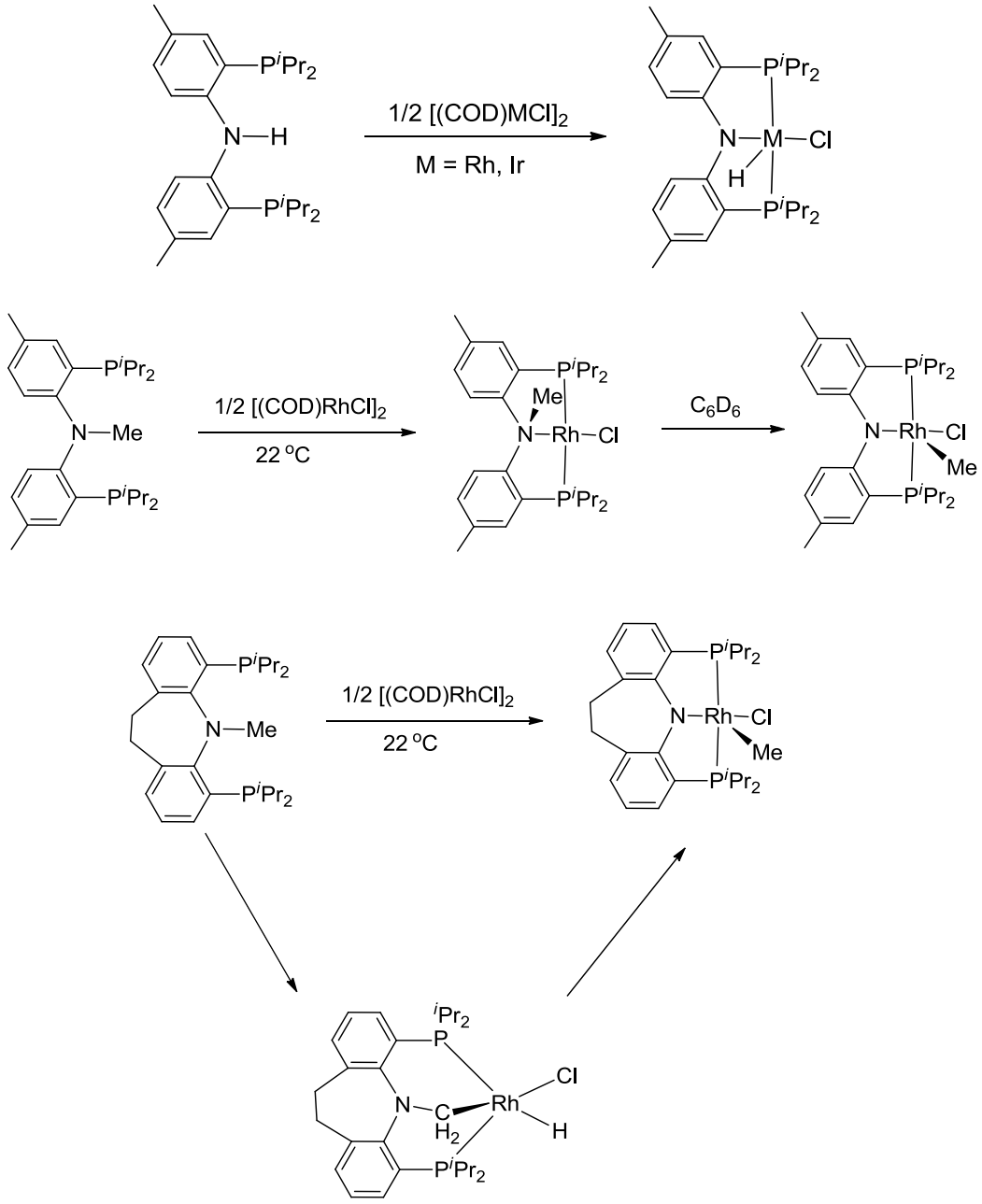


**Scheme 1-5.** N-H or N-C OA onto Ir/Rh center.

Direct cyclometalation usually involves the release of HX (X= H, R, halide, etc) as by product. For example, the Ozerov group reported the synthesis of (PNP)PdCl by reacting the ligand PN(H)P with $Pd(COD)Cl_2$ in the presence of $Et_3N$ (Scheme 1-6B).[11b] In this reaction, $Et_3N$ serves as a base to react with the HCl generated in the process. It is worth noting that in contrast to OA reactions, the oxidation state of the metal does not change in direct cyclometallation reactions.

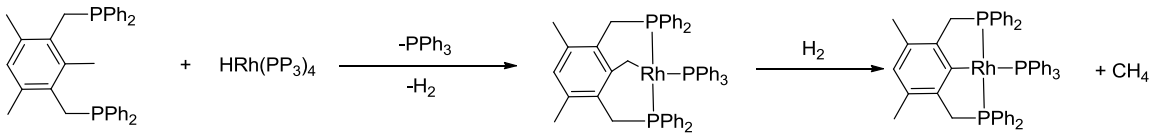


**Scheme 1-6A.** Installation of ligand onto metal via direct cyclometalation.

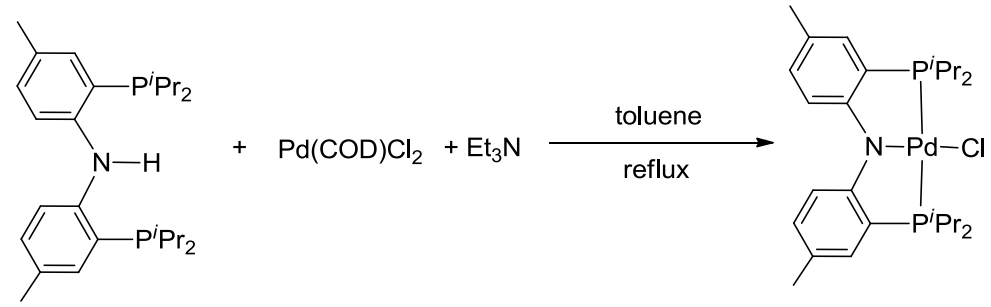


**Scheme 1-6B.** Installation of PNP ligand onto Pd via direct cyclometalation.

*1.2.4 Transcyclometalation*

The so called transcyclometalation method to form new pincer metal complexes was first introduced by von Koten and coworkers.[22] In analogy to transesterfication in

organic chemistry, the transcyclometalation process involves the interconversion of one cyclometalated ligand metal complex [(ECE)M] into another one [(E'CE')M] with the concomitant consumption and formation of the ligand E'CE' and ECE, respectively (Scheme 1-7). For example, Ru(NCN)(Cl)($PPh_3$) is a very useful synthetic precursor in

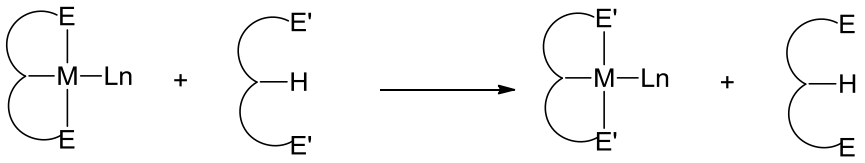


**Scheme 1-7.** Installation of ligand onto metal via transcyclometalation.

the process of making other pincer ruthenium complexes through transcyclometalation (Scheme 1-8). This method allows for the synthesis of (PCP)Ru complexes which are difficult or impossible to make through conventional ways.[22] The driving force for the transcyclometalation reaction is the difference in heteroatom-metal bond strength which is highest for the P-M bond in the case of the late transition metals such as Pd(II), Pt(II), or Ru(II).

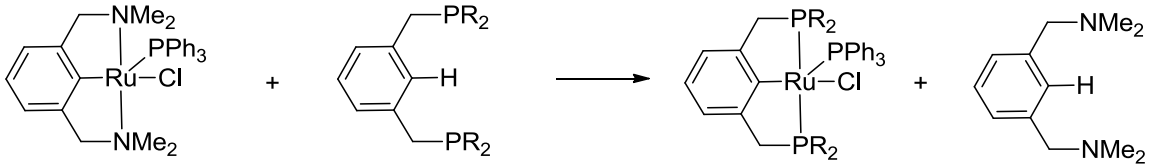


**Scheme 1-8.** Installation of PCP ligand onto Ru via transcyclometalation.

### *1.3 Structural preference for group 9/10 metal complexes (4d and 5d)*[23]

Transition metal complexes can adopt many types of geometries depending on the nature of the metal and the coordination number. The geometry is normally determined by electronic and steric effects. From the steric aspect, the preferred geometry for a three-coordinate compound is trigonal planar, for a four-coordinate complex is tetrahedral, for a five-coordinate is trigonal bipyramidal and for a six-coordinate complex is octahedral. However, these sterically preferred geometries are not always observed. For transition metal complexes, the electronic preference often overrides the steric effects. The geometries of transition metals bearing d-electrons can be predicted by their energy diagram of d-orbitals. From the electronic aspect, certain d-electron configurations cause their metal complexes to adopt particular geometries. Because this thesis mainly involves group 9 and group 10 metals, this section will focus on the structural preference for the second and third row group 9/10 metal complexes.

#### *1.3.1 Geometry for $ML_3$*

##### 1.3.1.1 Trigonal planar $ML_3$ complexes

A trigonal planar complex can be viewed by removing the two axial ligands from a TBP $ML_5$ complex (Scheme 1-9). The d-orbital energy diagram is shown in Scheme 1-9. These five d-orbitals are sufficiently low in energy and can be occupied by electrons. As a results, many 16-electron, $d^{10}$ metal complexes adopt this geometry, such as $M(CO)_3$ (M = Ni, Pd, Pt), $[Pt(PPh_3)_3]$, $[Pt(\eta^2\text{-ethylene})(PR_3)_2]$ etc.[24]

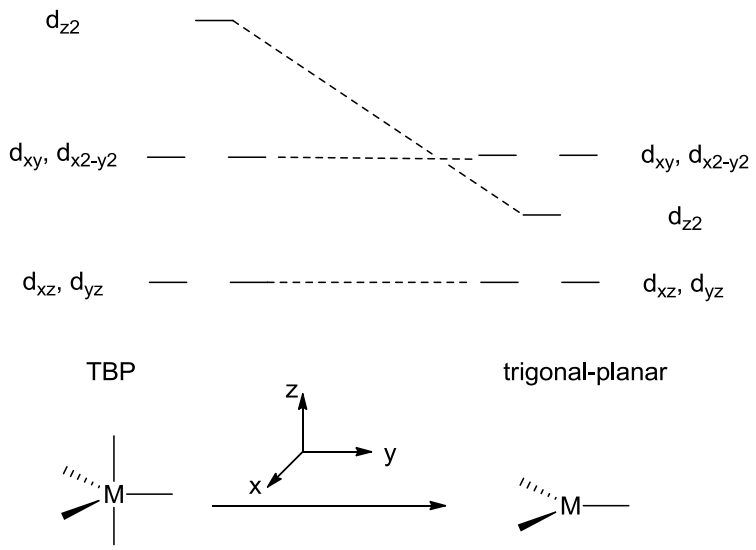


**Scheme 1-9.** d-orbital energy diagram of $ML_3$ trigonal planar complexes.

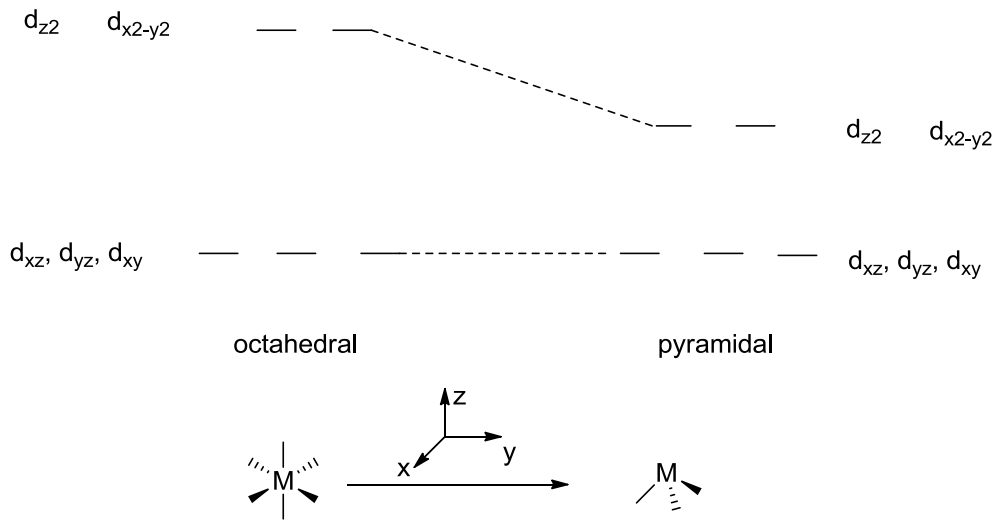


**Scheme 1-10.** d-orbital energy diagram of $ML_3$ pyramidal complexes.

1.3.1.2 Pyramidal $ML_3$ Complexes

A pyramidal geometry can be viewed as removing the adjacent three ligands from an octahedral complex. The d-orbital energy diagram for this geometry is shown in Scheme 1-10. This type of geometry is not common but is observed for low-spin $d^6$ complexes, such as $[M(Mes)_3]$ (M = Rh, Ir).[25]

1.3.1.3 T-shaped $ML_3$ complexes

The T-shaped geometry can be envisioned as arising from a removal of one ligand from a square planar complex. The d-orbital energy diagram is shown in Scheme 1-11. Similar to the square planar structure, the T-shaped $ML_3$ fragment is characterized by the presence of four low-energy d-orbitals. Typical examples bearing this structure include diamagnetic $d^8$ metal complexes such as $[Rh(PPh_3)_3]^+$, $[Pt(Cl)_3(\eta^2\text{-ethylene})]^-$. It is worth noting that three-coordinate pincer metal complexes or intermediates adopt the T-shaped structure as well. For example, Chris Douvris in our group was able to isolate a three-coordinate $(PNP)Ni^+CHB_{11}Cl_{11}^-$ compound. This species was characterized by solid state X-ray crystal structure and the three-coordinate nickel center adopts the T-shaped geometry. It is also postulated that other three-coordinate $d^8$ metal fragments (PNP)M (M = Rh, Ir) or $[(PNP)M]^+$ (M = Pd, Pt) are T-shaped as well.

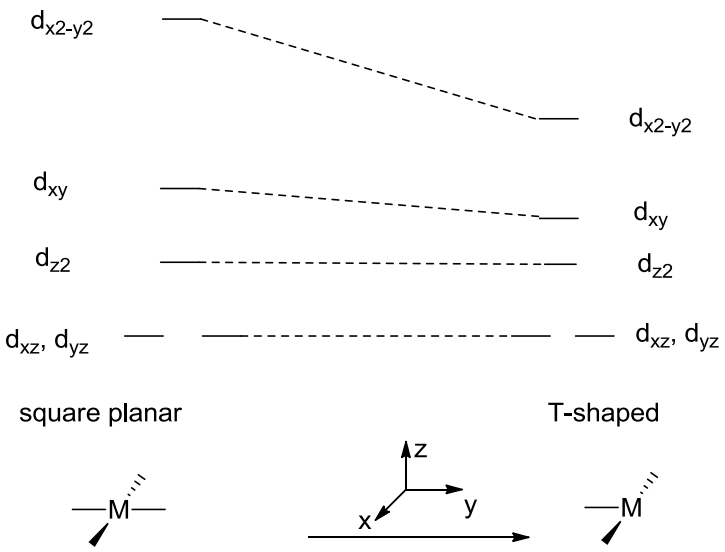


**Scheme 1-11.** d-orbital energy diagram of $ML_3$ T-shaped complexes.

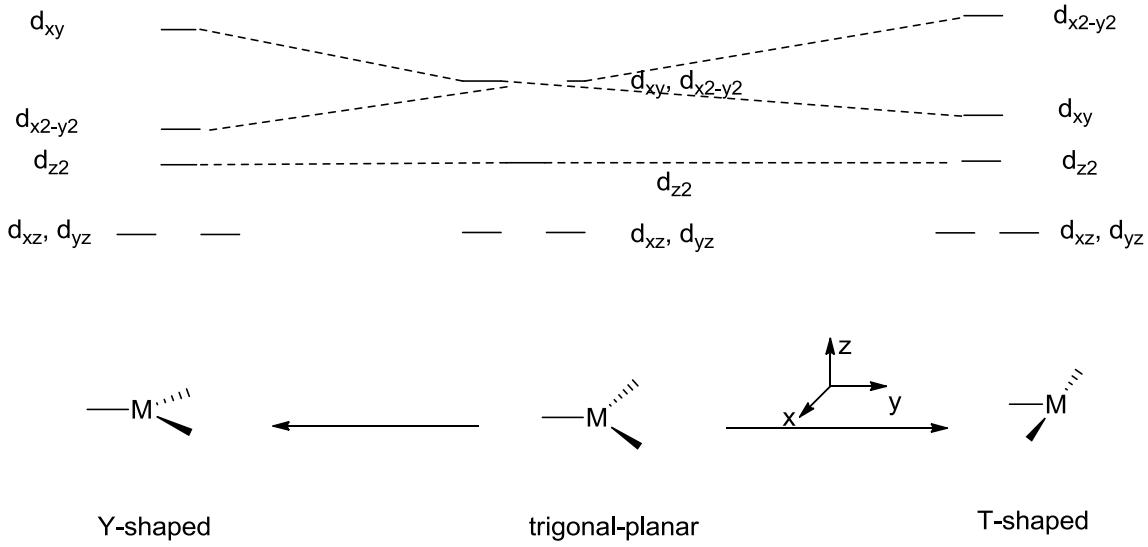


**Scheme 1-12.** d-orbital energy diagram of $ML_3$ Y-shaped complexes.

The $ML_3$ T-shaped geometry can be viewed as the distortion from the trigonal planar geometry. Another possible distortion from trigonal planar is the so called "Y" shape.

The d-orbital energy diagram of $ML_3$ Y-shaped complexes is shown in Scheme 1-12. Examples of three-coordinate $d^8$ metal center adopting the Y-shaped geometry are known. For example, Hillhouse et al.[26] reported the structure of the three-coordinate nickel complex containing the chelating phosphine ligand and imido nitrogen-donor ligand. The nickel center is distorted from trigonal planar and adopts the Y-shaped geometry. More detailed discussion about the origins for the T-shaped and Y-shaped geometries will be presented in Section 1.3.3.1.

*1.3.2 Geometry for $ML_4$*

1.3.2.1 Square planar $ML_4$ complexes

Scheme 1-11 shows the d-orbital energy diagram for four-coordinate square planar geometry. Indeed, diamagnetic four-coordinate $d^8$ complexes of the second and third row metals almost always adopt square planar geometry.

1.3.2.2 Tetrahedral $ML_4$ complexes

The d-orbital energy diagram for a tetrahedral metal complex is shown in Scheme 1-13. All five orbitals can be occupied since the separation between the two d-levels is small. It is straightforward to understand that four-coordinate $d^{10}$ diamagnetic metal complexes such as $Ni(CO)_4$ and $[Pt(dppe)_2]$ (dppe = diphenylphosphinoethane) adopt this geometry.[27]

As mentioned above, it is not very difficult to predict the geometries for diamagnetic four-coordinate $d^8$ metal complexes (square planar) and $d^{10}$ metal complexes (tetrahedral). However, it is harder to predict, for a given $d^8$ metal complex, whether it will adopt low-spin square planar geometry or high-spin tetrahedral structure (Scheme 1-

13). Both electronic and steric factors play important roles and the balance between these factors is subtle. For example, it has been reported that the complex $[Ni(PPh_2Et)_2Br_2]$ can be isolated in both geometries.[28]

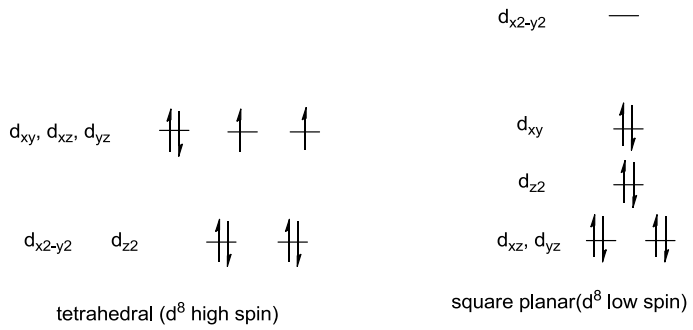


**Scheme 1-13.** d-orbital energy diagram of $ML_4$ tetrahedral and square planar complexes.

*1.3.3 Geometry for $ML_5$*

The sterically preferred geometry of a five-coordinate metal complex is trigonal bipyramidal (TBP) and the d-orbital energy diagram is shown in Scheme 1-14. However, diamagnetic $d^6$ $ML_5$ complexes usually do not adopt a regular TBP geometry. As can be seen from the diagram, the TBP geometry is not favored for diamagnetic $d^6$ complexes because this leads to a partially filled set of degenerate orbitals, but is stable for the lowest energy triplet state. So $d^6$ $ML_5$ complexes adopting TBP geometry would be paramagnetic.

1.3.3.1 Square pyramidal vs. Y-shaped

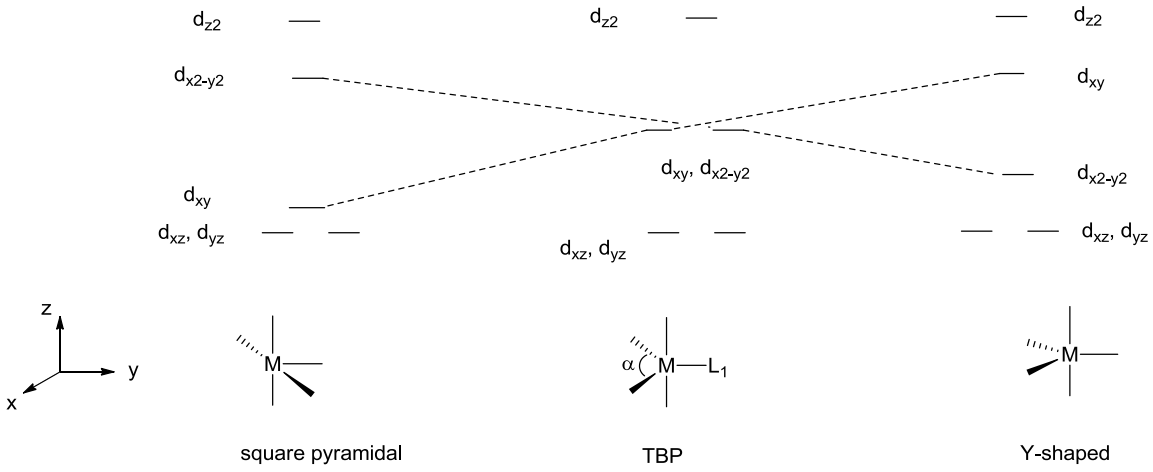


**Scheme 1-14.** d-orbital energy diagram of $ML_5$ complexes (SP, TBP, Y-shaped).

A singlet ground state of $d^6$ $ML_5$ complexes can be obtained by distortion of the TBP geometry: a square-based pyramid (SP) with $\alpha = 180\ °$ or a distorted trigonal bipyramid with a Y configuration of equatorial ligands (normally $\alpha < 80\ °$). The distortion of TBP geometry to either SP or Y-shaped structures lowers one of the degenerate orbitals so that they are no longer degenerate (Scheme 1-14). Whether a diamagnetic $d^6$ $ML_5$ complex adopts SP or Y-shaped geometry is governed by the electronic properties of the ligand $L_1$ that is *trans* to the angle α. The SP geometry results from the stabilization of $d_{xy}$ orbital and occurs when $L_1$ is a strong σ donor. Examples have shown that complexes with one strong trans influence ligand such as hyride or alkyl adopt the SP geometry with the strong trans influence ligand trans to the empty site.[1b,2b] The Y-shaped geometry results from the stabilization of $d_{x^2-y^2}$ orbital and it occurs when the

equatorial plane contains a single π donor ligand and two strong σ donors. Y-shaped geometry is commonly found in five-coordinate $d^6$ 16-electron of Ir and Rh complexes.

*1.3.4 Geometry for $ML_6$*

The steric preferred geometry for six-coordinate metal complexes is octahedral. And indeed most six-coordinate $d^6$, 18-electron Rh(III) and Ir(III) metal complexes adopt octahedral structures.

***1.4 Application of group 9/10 pincer complexes in bond activation and catalysis***

*1.4.1 C-H, C-X (X= halide) and C-O bond activation by group 9/10 pincer complexes*

Metal insertion into a strong bond and the subsequent functionalization to make more useful organic molecules are the key transformations for the rational design of both metal-mediated stoichiometric and catalytic reactions. Extensive studies have shown that pincer metal complexes are capable of activating various strong bonds such as C-H,[1] N-H,[2b] N-C,[2] C-halide,[29] etc. In this section, some background about C-H, C-X and C-O bond activation by group 9/10 metals will be covered, because these are relevant to the work described within the body of this thesis. Three-coordinate T-shaped $d^8$ $(EXE)M^+$ (M = Ni, Pd, Pt) or (EXE)M (M = Rh, Ir) fragments demonstrate high Lewis acidity and are the proposed intermediate for the strong bond activation.

1.4.1.1 C-H bond activation

Selective C-H activation and functionalization is one of the hottest areas in organometallic chemistry, and pincer metal complexes have made great contributions in this field. There are just a few examples for intermolecular C-H activation by group 10 pincer complexes.[30,31] The lack of group 10 metal complexes capable of facilitating this

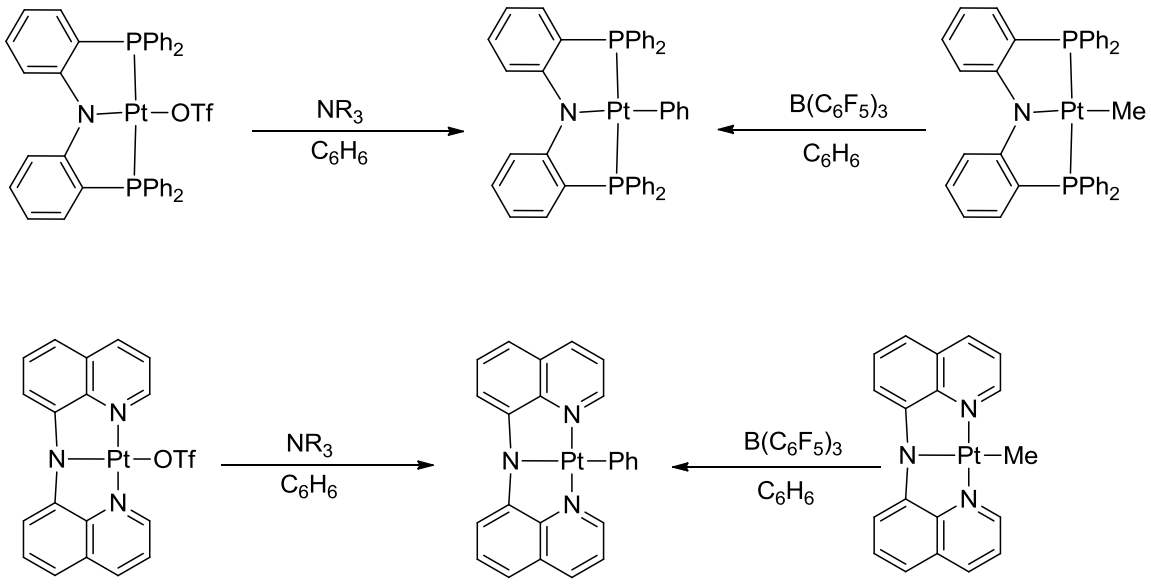


**Scheme 1-15.** Benzene C-H activation at (PNP)Pt and (NNN)Pt center.

reactivity is likely due to the difficulty of supporting their higher oxidation state metal compelxes (e.g. Pd(IV)). The process of C-H activation can be divided into five categories: oxidative addition, σ-bond metathasis, electrophilic metallation, 1,2-addition and metalloradical activation.

Liang[30] and coworkers reported an example of C-H activation with benzene at the (PNP)Pt enter (Scheme 1-15). Treatment of (PNP)PtOTf with a base such as $NEt_3$ or $MeNCy_2$ in benzene led to complex (PNP)PtPh quantitatively. On the other hand, treatment of (PNP)PtMe with the Lewis acid $B(C_6F_5)$ in benzene afforded (PNP)PtPh as well, a C-H activation product. Although the defined mechanism for this reaction is unknown, it is suggested that prior dissociation or displacement of a ligand is essential

for intermolecular C-H bond activation in the process. This reactivity is reminiscent of that reported earlier by Peters et al.[31] for using a biquinolylamido pincer Pt complex.

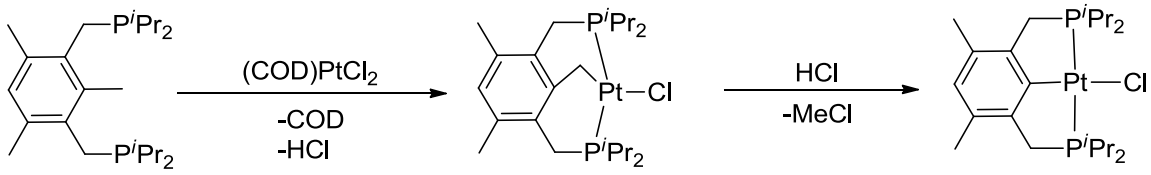


**Scheme 1-16.** Kinetic C-H activation and thermodynamic C-C activation by Pt.

In another example, Milstein et al.[32] reported the reaction of Pt(COD)$Cl_2$ with the PCP ligand that resulted in HCl elimination and the formation of the kinetic C-H activation product (Scheme 1-16). The kinetic C-H activation product was quantitatively converted into the C-C activation product by the addition of HCl, releasing MeCl.

C-H activation by Rh and Ir complexes has been examined extensively. The greater strength of M-C bonds of third-row transition metals makes oxidative addition to Ir very common. For example, arene C-H activation by (PCP)Ir,[33] (PNP)Ir,[1b] and (PSiP)Ir[34] complexes are all known. Importantly, alkane C-H activation is also feasible in the (PCP)Ir system (Scheme 1-17).[33] The three-coordinate (PCP)Ir generated from the reductive elimination of Ph-H from (PCP)Ir(H)(Ph) was able to activate C-H bonds in alkanes such as cyclooctane. C-H oxidative addition followed by β-hydride elimination led to the formation of (PCP)Ir$(H)_2$ with concomitant release of cyclooctene.

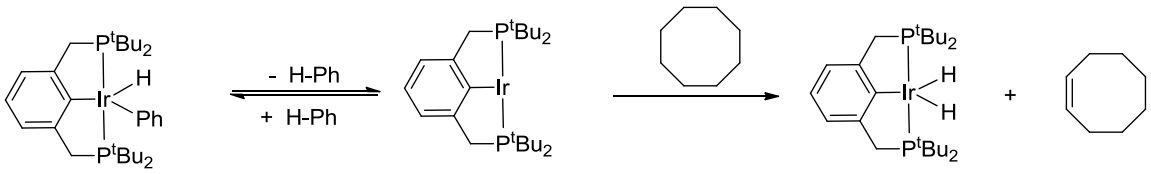


**Scheme 1-17.** Alkane C-H activation/dehydrogenation by (PCP)Ir.

1.4.1.2 C-X (X = halide) oxidative addition

Oxidative addition of aryl or vinyl halides to transition metal centers is a very important step in catalytic reactions, especially in metal catalyzed cross-coupling reactions.[35] Among all these metals, palladium has dominated. The first step of these

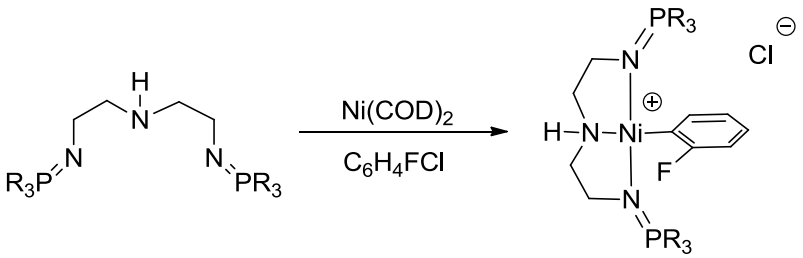


**Scheme 1-18.** C-Cl OA at (NNN)Ni fragment.

reactions is the insertion of a palladium(0) species into a C-halide bond to form a new palladium(II) species. The halide reactivity increases in the order of Cl < Br < I and ArF is generally inert.[35] Most recently, Stephan and coworkers reported the formation of a new (NNN)Ni(Ar)(X) pincer complex from Ni(0) synthons via oxidative addition (Scheme 1-18).[36]

Compared with the extensive study of C-halide oxidative addition at group 10 metal centers, the C-halide oxidative addition on group 9 metals is far less common.[37] Palladium has a stable Pd(0)/Pd(II) oxidation state couple that is normally involved in the oxidative addition reaction, while the group 9 metals have stable M(I)/M(III) (M = Rh, Ir) couple. Our group has reported the thermodynamic C-X bond oxidative addition at (PNP)Ir center to form the (PNP)Ir(Ar)(X).[1b] Ar-X could also oxidatively add to (PNP)Rh (Scheme 1-19).[29b]

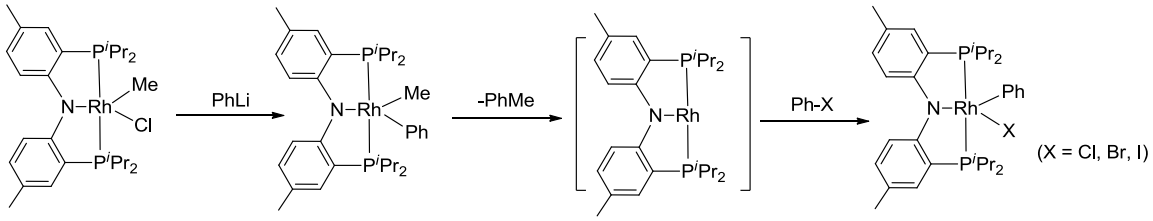


**Scheme 1-19.** C-Cl OA at (PNP)Rh fragment.

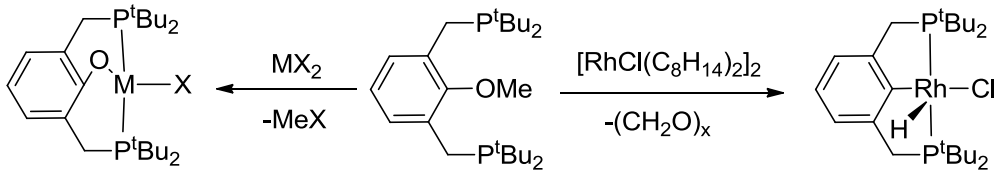


**Scheme 1-20.** C($sp^2$)-O cleavage vs. C($sp^3$)-O cleavage.

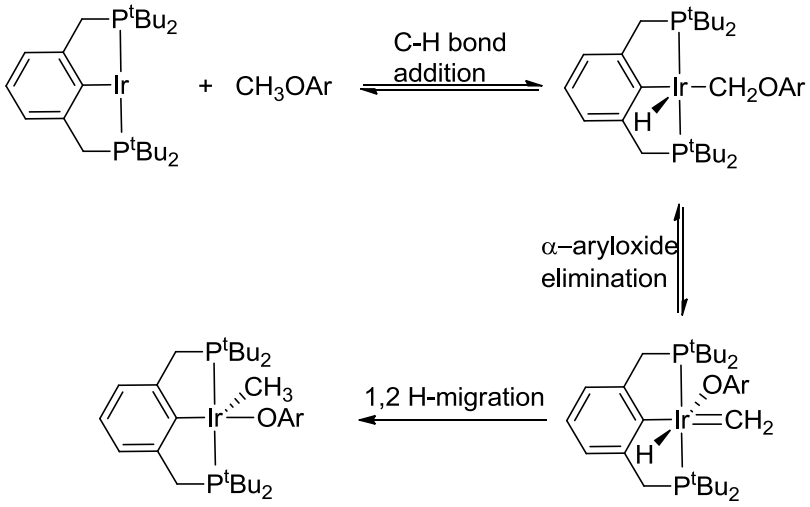


**Scheme 1-21.** C-H activation induced C-O cleavage.

1.4.1.3 C-O bond activation

Strong C-O bond activation is a lot less explored compared with C-H or C-X oxidative addition. Milstein and coworkers have demonstrated that metal insertion into a strong aryl-O bond in aromatic ether was possible by employing the PCP ligand system.[3b] They observed that, although in call cases a $d^8$ metal was used, a nucleophilic metal (Rh(I)) favored direct aryl-O bond activation while electrophilic metals (Pd(II) or Ni(II)) were likely to promote alkyl-O bond cleavage (Scheme 1-20).[38] Another example of intermolecular oxidative addition of a C($sp^3$)-O bond was reported by Tolman and coworkers.[39] Goldman, Chirik, and others have also reported the examples of 'net'C-O oxidative addition that was induced by C-H oxidative addition (Scheme 1-21). Although the chemistry of stoichiometric C-O bond oxidative addition has not been well defined, coupling reactions involving the use of Ar-$O_2$CR or other A-OR electrophiles have been successfully explored with Ni catalysts.[40] The detailed

mechanism for these catalytic reactions is not fully understood but there is sound evidence that suggests that OA of Ar-O bond is part of the catalytic cycle.

1.4.1.4 B-H, B-B activation

The activation of the B-H bond in boranes or B-B bond in diborons by transition metal complexes to give metal-boryls is a key step in a number of catalytic reactions, including the hydroboration of olefins, the borylation of unactivated C-H bonds and the dehydro-coupling of amineboranes.[41] The oxidative addition of either a borane ($HBR_2$) or diboron ($B_2R_4$) to a metal center is enthalpically favored by approximately 10 to 15 kcal/mol.[42] A series of Rh- and Ir-bisboryl complexes have been made by the reaction of [$MCl(PPh_3)_3$] with diboron reagents (Scheme 1-22).[43] Oxidative addition of diboron

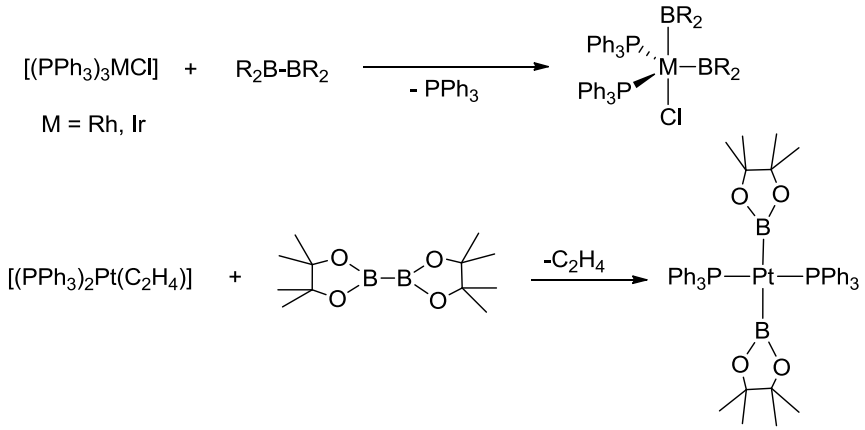


**Scheme 1-22.** B-B OA to Rh/Ir(I) and Pt(0).

to Pt(0) precursors is also common.[44] However, prior to our work, there was no reported example of B-B bond oxidative addition to palladium. Computational studies provide

evidence that oxidative addition of B-B to Pd center is thermodynamically unfavorable.[45] Thus, most palladium-boryl compounds are obtained through OA of B-X bond to Pd.[46]

*1.4.2 Catalytic application*

The design and synthesis of pincer complexes are not just for mere structural interest, but more importantly, for their great applications such as catalysis. Various pincer metal complexes have shown their ability as homogenous catalysts for a number of important reactions. For example, (PCP)Ir$(H)_2$ is a very robust catalyst for alkane dehydrogenation;[47] ($P^OC^OP$)Rh(H)(Cl) is a catalyst precursor for Kumada coupling reactions;[48] the (NCN)Pd complex can catalyze C-H borylation of alkenes;[49] catalytic hydrogenation of carbon dioxide is accomplished by using an Ir(III)-pincer complex,[50] etc. In this section, we are only focused on two types of catalytic reactions: catalytic C-H functionalization and cross coupling reactions.

1.4.2.1 Catalytic C-H functionalization

The interest in C-H activation is motivated by the subsequent C-H functionalization to generate more useful organic molecules. Numerous catalytic C-H functionalization reactions have been reported including dehydrogenation, alkyne dimerization, and borylation of alkenes, et al.

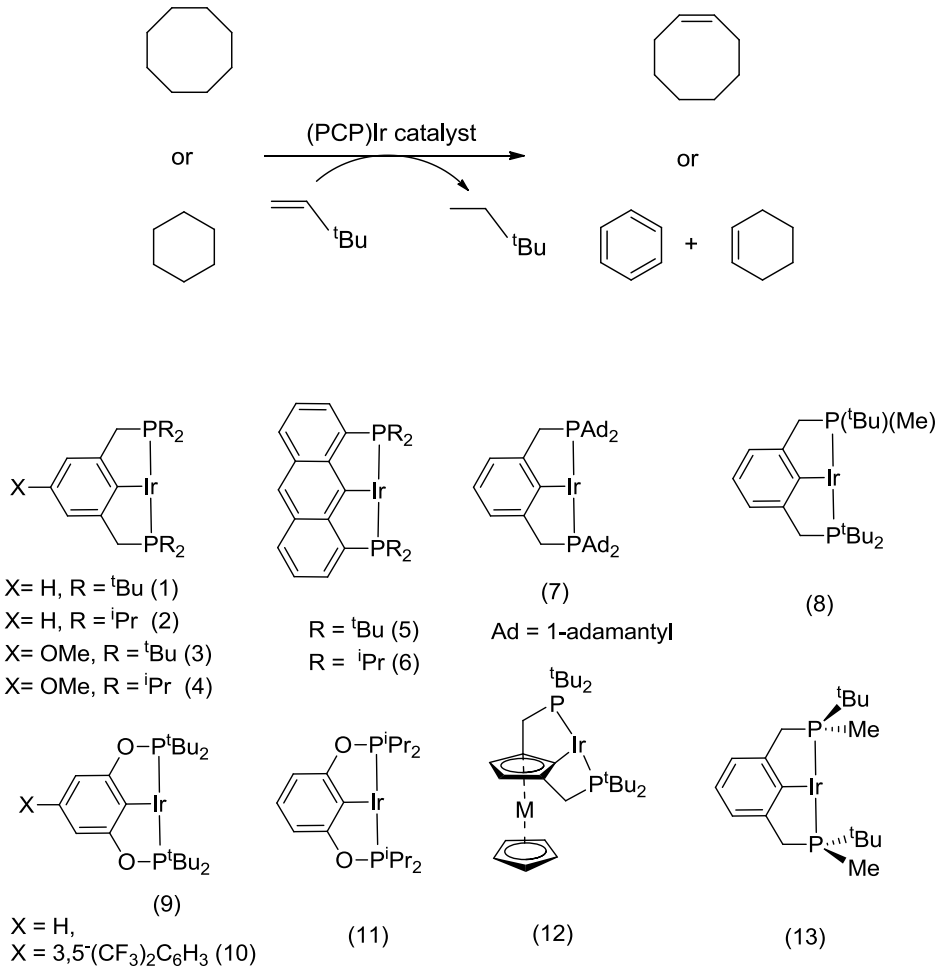


**Scheme 1-23.** Various **"**(PCP)Ir" catalysts for alkane dehydrogenation.

**Dehydrogenation of alkanes by iridium pincer complexes.** The dehydrogenation of alkanes catalyzed by pincer-ligated iridium complexes was first reported by Jensen, Kaska, and coworkers in 1996.[51] Since then, Goldman and others find that the most active catalysts for dehydrogenations are iridium complexes containing 'PCP' pincer ligands (Scheme 1-23).[47] Both transfer dehydrogenation and acceptorless dehydrogenation are accomplished in the PCP iridium system due to the high thermal stability of the catalyst. The mechanism of COA/TBE (COA = cyclooctane; TBE = tert-

butylethylene) transfer dehydrogenation was proposed after the detailed kinetic study of the full catalytic cycle (Scheme 1-24). TBE insertion into the Ir-H bond followed by C-H reductive elimination leads to the formation of the 14-electron intermediate. C-H oxidative addition of alkanes to the Ir(I) and the subsequent β-hydride elimination produces the olefin and regenerates the catalyst. The desired reaction could be inhibited

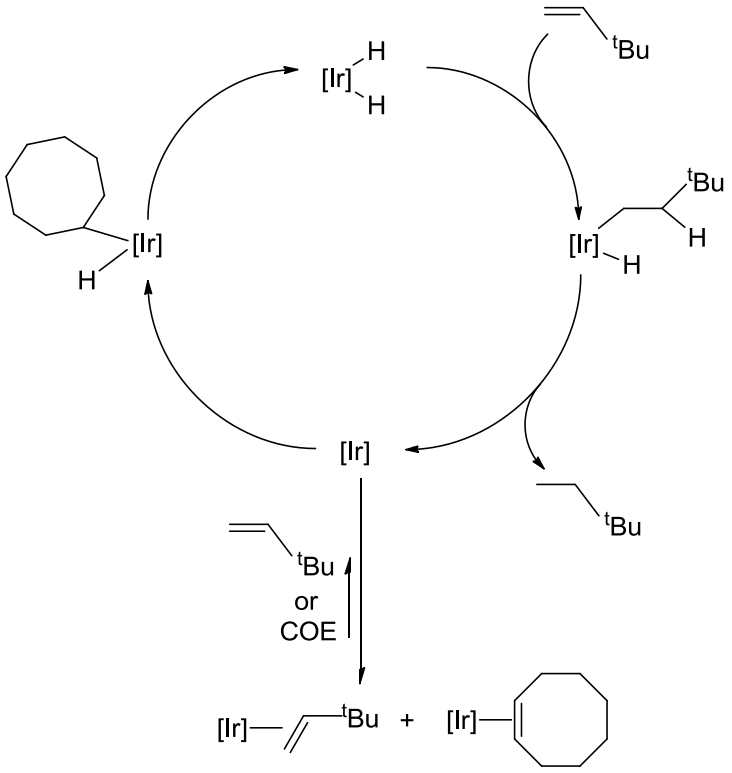


**Scheme 1-24.** Mechanism for COA/TBE transfer dehydrogenation.

by the side reaction — olefin binds to the 14-electron Ir(I) either through π-coordination or through C-H addition. The more facile dehydrogenation of cyclooctane compared

with *n*-alkane is due to weaker binding of the corresponding dehydrogenated product cyclooctene. In the case of acceptorless dehydrogenation, the 14-electron intermediate was generated by thermolytic loss of $H_2$ from the (PCP)Ir$(H)_2$ species, which requires higher temperature and longer reaction times to overcome the high enthalpic barrier.

A wide range of modified PCP pincer ligands with various steric and electronic properties have been explored in order to develop an improved catalyst for alkane dehydrogenation (Scheme 1-23). The most active catalyst among all these iridium pincer complexes for the transfer dehydrogenation of COA are the "$P^OC^OP$" catalysts **9-11** developed by the Brookhart[52] and Jensen[53] groups. The higher activity of catalyst **9** versus **1** results from changes in the resting state and the rate of hydrogen transfer. Catalyst **1** reversibly reacts with TBE to give C-H activation product while catalyst **9** reacts with TBE to form a π-complex. More importantly, the olefin hydrogenation by **9-$H_2$** is much more facile than **1-$H_2$**. The electronic differences for these two compounds are subtle and the pronounced steric difference between these two catalysts is probably the major factor responsible for the reactivity difference. DFT calculations indicated that reactivity differences are attributed to the fact that the iridium center in **9** is less sterically hindered than that in **1**.[54]

**Alkyne dimerization.** Alkyne dimerization is an attractive and atom-economical method of synthesis of conjugated enynes, important building blocks in organic synthesis. Alkyne dimerization is one of the reactions that is well explored, but the chemo- and regioselectivity, as well as the scope of the reactions are still the challenges in this area.[55]

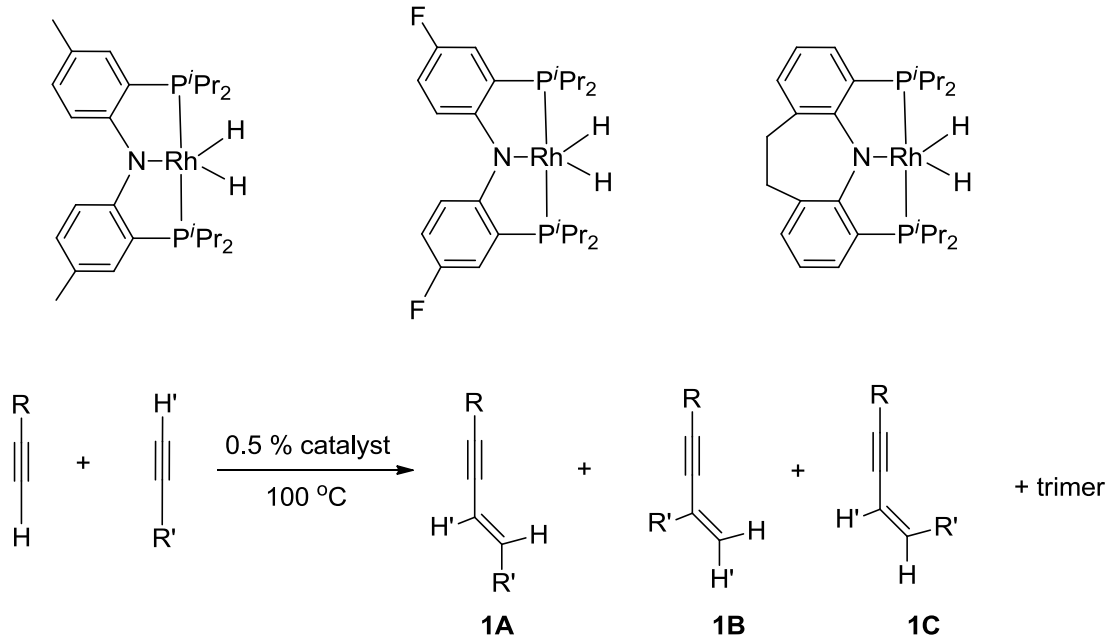


**Scheme 1-25.** (PNP)Rh(H)$_2$ catalyzes terminal alkyne dimerization.

The Ozerov group discovered that each of the three pincer rhodium dihydride complexes in Scheme 1-25 could act as catalysts for dimerization of terminal alkynes.[56] The catalyst bearing "tied" PNP ligand is most active and highly selective for the trans-enyne product. The dimerization proceeded with high selectivity for a variety of 1-alkynes and turnover numbers in excess of 600 were achieved. More importantly, the reaction is compatible with water or even air to some degree, which lanthanide catalysts (also commonly used) cannot tolerate at all.[57]

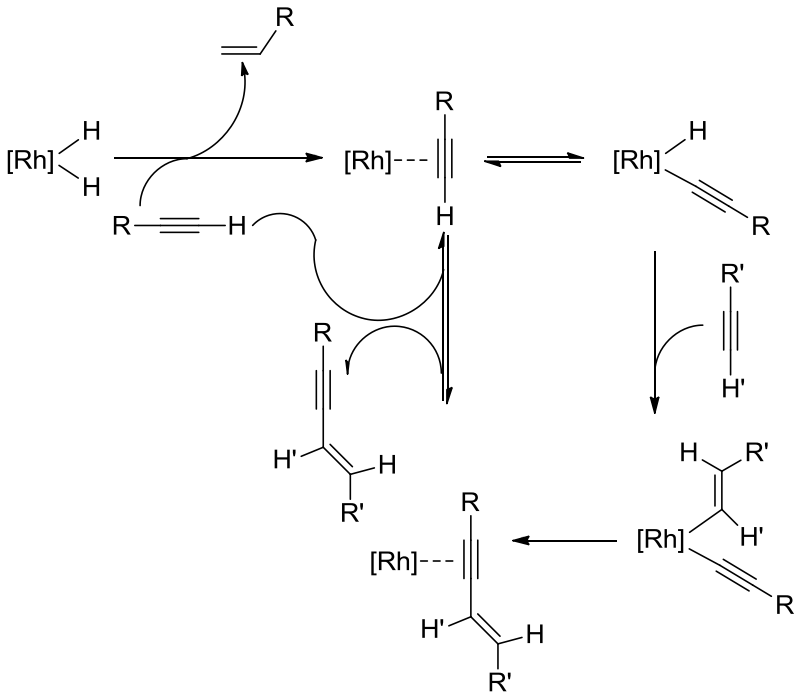


**Scheme 1-26.** Proposed mechanism for (PNP)Rh$(H)_2$ catalyzed terminal alkyne dimerization.

The proposed mechanism of the reaction is shown in Scheme 1-26. One equivalent of alkyne was used to generate the 14-electron (PNP)Rh via the hydrogenation of the alkyne to produce alkene as by-product. C(sp)-H bond oxidative addition of alkyne gave the Rh(III) hydrido-alkynyl complex. 1,2- or 2,1-insertion of the second equivalent alkyne to the Rh-H bond followed by C-C reductive elimination at rhodium gave the product enyne with two possible isomers **1A** and **1B**. Isomer **1C** is not observed in the reaction, which is also consistent with the proposed mechanism. **1C** cannot be produced when insertion of alkyne to the Rh-H bond is involved in the mechanism. The higher selectivity for *trans* isomer **1A** than **1B** can be ascribed to the steric effect. Positioning the non-hydrogen group away from Rh would be preferred for the steric reasons. In

another closely related chemistry, Goldman reported the detained mechanism of alkyne dimerization in (PCP)Ir system.[58] In his chemistry, Goldman found that the 1,2-insertion was reversible and C-C bond reductive elimination from acetylide-vinyl species was disfavored by the substituents on the α carbon of the vinyl group. These observations are consistent with what observed in (PNP)Rh chemistry.

**Alkenes borylation.** C-H borylation reactions are an important emerging field due to the formation of the highly valued organoboronates. Borylation of alkanes, arenes and olefins catalyzed by iridium, rhodium, and ruthenium are all known.[59] Information about the mechanism of the iridium catalyzed borylation of alkanes/arenes has been reported by Hartwig and the reaction went through a Ir(V) intermediate.[60] In 2010, Szabó and coworkers reported an example of a palladium pincer complex catalyzed C-H borylation of alkenes (Scheme 1-27).[49] The borylation proceeded with a high vinylic selectivity. An essential additive for this reaction is to use the hypervalent iodine, which can oxidize the Pd(II) catalyst to Pd(IV). The electron-deficient Pd(IV) underwent facile transmetalation with $B_2pin_2$ to form a Pd-B bond and by-product TFA-Bpin. Insertion of alkene into the Pd-B bond followed by elimination H-TFA produced the corresponding organoboronate. Interestingly, this reaction not only provides an easy access to pinacolboronates but offers the possibility of one-pot Suzuki-Miyaura coupling.

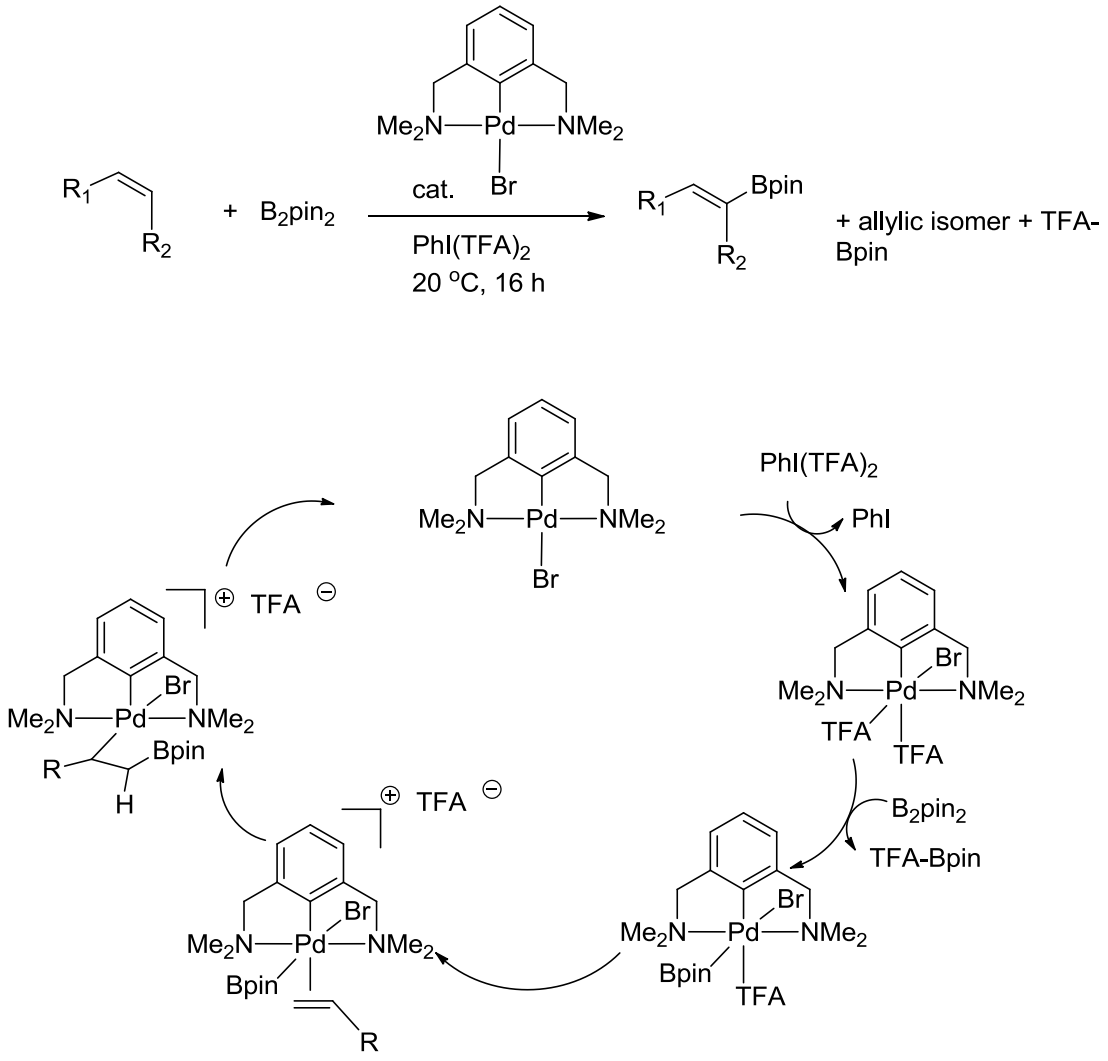


**Scheme 1-27.** Proposed mechanism for C-H borylation of alkenes catalyzed by pincer palladium complex.

1.4.2.2 Cross coupling reactions

Transition metal catalyzed cross coupling reactions to form C-C or C-heteroatom bonds are very important in synthetic chemistry. Negishi, Suzuki and Heck made great contributions on the palladium catalyzed C-C cross coupling reactions and were recognized with the 2010 Noble Prize in chemistry.[61] The coupling of aryl halides with

amines developed by Buchwald and Hartwig has become a standard synthetic method to make aromatic amines.[62] Besides C-C and C-N cross coupling, coupling reactions of C-S and C-O bonds have also been developed.[63]

Palladium is the most frequently used metal in cross coupling reactions. The fundamental first step of cross coupling reactions, Suzuki coupling for example, is the OA of aryl halide or pseudo halide to Pd(0) to form Pd(II).[61] As mentioned before, aryl halide OA to Rh(I) is rare compared with Pd chemistry. The use of a pincer supported Rh(I) complex might be beneficial for C-C or C-heteroatom coupling, because the chelating pincer ligand normally does not allow the phosphine dissociation, which would open another coordination site and result in a mixture of products or the inactivation of the catalyst. Our group has reported the successful stoichiometric Ar-X (X = Cl, Br, I) oxidative addition to (PNP)Rh(I) as well as the clean C-C reductive elimination from (PNP)Rh(Ar)(R), which was generated by transmetalation of (PNP)Rh(Ar)(X) with organolithium or Grignard reagents (Scheme 1-19).[29b] Unfortunately, the catalytic C-C coupling reaction is not successful by using "(PNP)Rh" catalyst. The reason for the failure of the catalytic reaction is not quite clear but might be ascribed to the unclean transmetalation as well as the slow C-C reductive elimination.

Although the catalytic coupling of aryl halides with certain nucleophiles does not work for "(PNP)Rh" catalyst, our group managed to conduct Kumada coupling reactions by coupling between Grignard and aryl iodides catalyzed by "(PCP)Rh".[48] The reaction was much slower or unselective if just employing $[Rh(COD)Cl]_2$ or 1:2 mixture of $[Rh(COD)Cl]_2$ and $Cy_3P$ as catalysts. These control reactions demonstrated the

importance of using pincer supported Rh catalyst. It is possible that the pincer ligand supported Rh is facilitating access to a three-coordinate Rh(I) intermediate, which is essential for OA step. The proposed catalytic cycle is in Scheme 1-28. The proposed intermediacy of OA of aryl halides to ($P^OC^OP$)Rh(I) is supported by the isolation of the oxidative addition product.

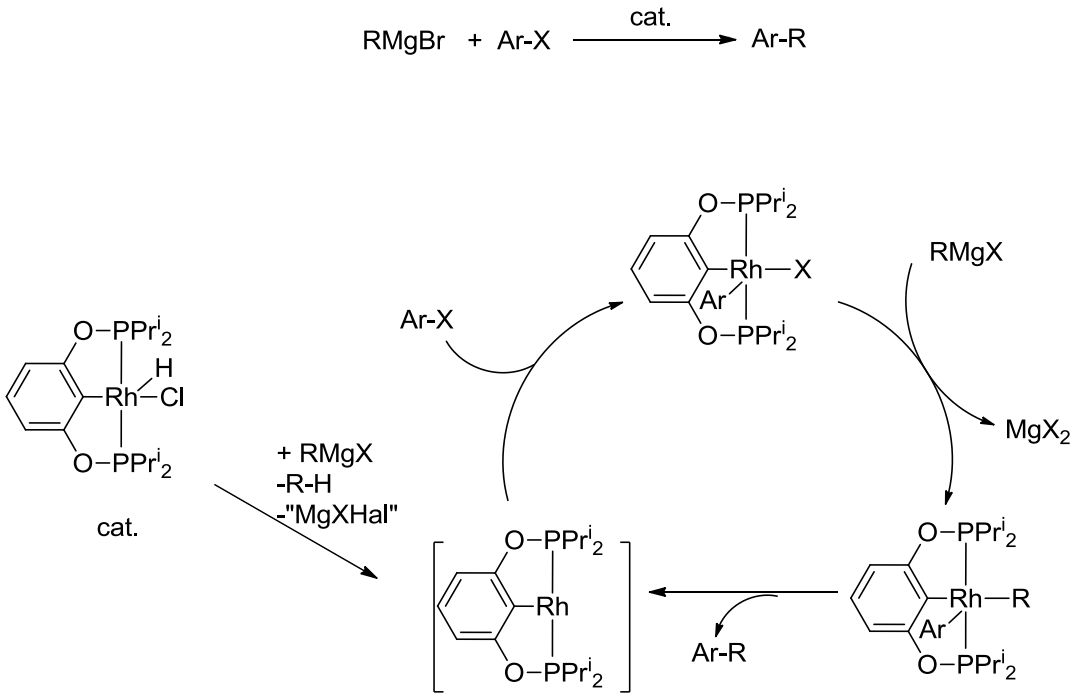


**Scheme 1-28.** Proposed mechanism for "($P^OC^OP$)Rh" catalyzed Kumada C-C cross coupling.

# CHAPTER II

# NET HETEROLYTIC CLEAVAGE OF B-H AND B-B BONDS ACROSS THE N-Pd BOND IN A CATIONIC (PNP)Pd FRAGMENT*

## *2.1 Introduction*

The activation of B-H and B-B bonds by transition metal complexes to give boryls is of great interest to chemists because of its direct relevance to homogeneous catalysis. Transition-metal boryl complexes are important as intermediates in transition-metal-catalyzed hydroboration with boranes, diboration with diboron reagents, as well as borylation of alkanes and arenes.[64-73] Metal-boryl complexes are typically generated through oxidative addition (OA)[74] of boranes or diboron substrates. For example, Marder et al. have reported examples of oxidative addition of borane/diboron compounds to Pt(0),[75] and oxidative addition of B-H and B-B bonds to Rh(I) and Ir (I) is also well known.[71,76]

Classical OA of an X-Y bond (such as B-H or B-B) to the metal center can be contrasted with and complemented by 1,2-addition of an X-Y bond across a metal ligand bond (Scheme 2-1). Both cases necessitate the presence of a filled and of an empty orbital in the metal complex to rupture the X-Y bond and form new bonds to X and Y. For the classical OA, both orbitals are metal-based, whereas for the 1,2-addition, the

---

* Reprinted (parts of this chapter) with permission from "Net Heterolytic Cleavage of B-H and B-B Bonds Across the N-Pd Bond in a Cationic (PNP)Pd Fragment" by Zhu, Y.; Chen, C. H.; Fafard, C. M.; Foxman, B.; Ozerov, O. V., 2011. *Inorg. Chem.*, 50, 7980-7987, Copyright [2011] by American Chemical Society.

ligand orbital contributes a lone pair and the metal an empty orbital. Our group have recently reported[77] 1,2-addition of H-H, alkynyl C-H, and thiolic S-H bonds cross the Pd-N moiety in a cationic, three-coordinate $[(PNP)Pd]^+$ fragment (Scheme 2-2). This 1,2-addition can be viewed as heterolysis of the corresponding H-X bonds.[78] In contrast to most other common examples of complexes undergoing 1,2-addition of non- or weakly polar bonds,[79,80] there is no π-bond in the $[(PNP)Pd]^+$ fragment because the empty and the filled orbital are orthogonal to each other and dimerization is presumably unfavorable on steric grounds. In this sense, $[(PNP)Pd]^+$ resembles the so-called frustrated Lewis pairs (FLPs) recently popularized by Stephan et al.[81]

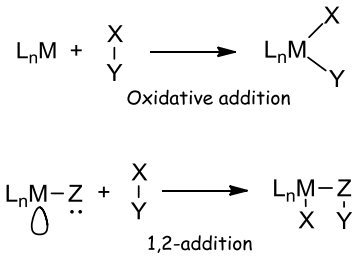


**Scheme 2-1.** Oxidative addition to a metal center and the non-oxidative 1,2-addition.

In this chapter, we describe our investigation of the 1,2-addition of the B-H bond in catecholborane (CatBH) and the B-B bond in bis(catecholate)diboron (CatB-BCat) across the Pd-N moiety in $[(PNP)Pd]^+$. In contrast to our previous report (Scheme 2-2) on net heterolytic cleavage of H-X by $[(PNP)Pd]^+$,[77] here the nitrogen atom is the recipient of X (boron) in net heterolytic cleavage of H-X, not of hydrogen. Addition of

B-H and B-B bonds across metal-oxygen functionalities are rather common. 1,2-addition of B-H across the metal-oxygen bond in oxo-rhenium complexes and peroxo-rhodium complexes has been reported.[82,83] Addition of B-B bonds across late metal alkoxides with release of free alkoxyboron molecule has been used for the synthesis of a

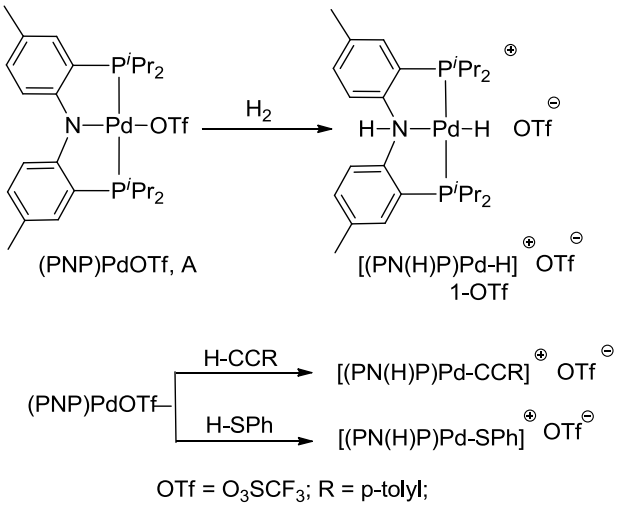


**Scheme 2-2.** Reactions of certain H-X substrates with (PNP)PdOTf.

variety of late metal boryls.[84,85] Another closely related precedent is the very recent report by Clark et al.[86] describing net heterolytic cleavage B-B (and B-H) bonds by a ruthenium center and a pendant oxygen in a Shvo-type[87] system, albeit that does not constitute 1,2-addition (Scheme 2-3). On the other hand, addition of B-B bonds across a metal-nitrogen moiety remains unusual. It is also worth noting that relatively few palladium boryl complexes are known, mainly prepared by oxidative addition of a boron-halogen bond to a Pd center.[46]

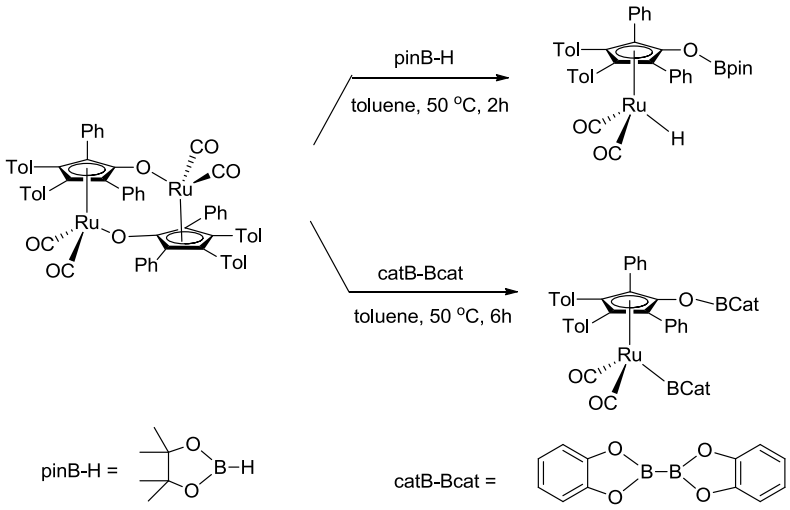


**Scheme 2-3.** Heterolytic cleavage of B-H and B-B bonds by ruthenium dimer.

*Note: Nomenclature of this thesis. All PNP ligands and metal complexes thereof are based upon the diarylamido backbone and will be abbreviated as follows: There are two types of abbreviations. The first is for neutral ligand that is not bound to a metal which is represented as "$^{X}$PN(Z)P$^{R}$". X represents the substituent group that is para to the N, Z represents the group on N and R represents the substituents groups on the phosphines. The second type of abbreviation is for metal complexes, expressed as "($^{X}$PNP$^{R}$)M (N is the anion). Generic "PNP" is used from this point on to represent the anionic PNP array with the diarylamido backbone but without specifying any substituents unless otherwise noted.*

## *2.2 Results and disscussion*

### *2.2.1 Synthesis of [(PNP)Pd]$^+$ synthons **2B** and **2C***

In our previously reported work on the net heterolytic cleavage of H-X bonds in thiols, $H_2$, or an alkyne, (PNP)PdOTf (**2A**) functioned well as a synthon for [(PNP)Pd]$^+$ (Scheme 2-2).[77] Unfortunately, this convenient precursor did not work well in the reaction with the CatB-H substrate, which produced a mixture of unidentified species. Thus we were prompted to turn to more weakly coordinating anions [$BAr^F_4$]$^-$ ($Ar^F$ = 3,5-$(CF_3)_2C_6H_3$) [88, 89] and monocarba-*closo*-dodecaborate [$CB_{11}H_{12}$]$^-$ (also known as "carborane")[90] in place of triflate. Reaction of **2A** with Na[$BAr^F_4$] in THF furnished [(PNP)Pd(THF)]$BAr^F_4$ (**2B**, Scheme 2-4) as a blue solid in 60% isolated yield. An analogous reaction of **2A** with Cs[$CB_{11}H_{12}$] in fluorobenzene yielded (PNP)Pd($CB_{11}H_{12}$) (**2C**, Scheme 2-4) as solid of a different shade of blue in 83% yield. Both **2B** and **2C** were characterized by $^1$H, $^{31}$P, $^{13}$C NMR spectroscopies and elemental analysis. They display apparent $C_{2v}$ symmetry in their room-temperature NMR spectra, as is expected of simple square-planar adducts of [(PNP)Pd]$^+$. We were not able to grow an X-ray quality crystal of **2C**. However, using the same synthetic strategy, we (by Claudia Fafard from Brandeis Univ.) prepared ($^F$PNP)Pd$CB_{11}H_{12}$ (**2$^F$C**, Scheme 2-4), a very similar compound bearing fluorine substituents on the ligand backbone, and obtained its single crystal for an XRD study. The solid-state structure of **2$^F$C** (vide infra) revealed coordination of $CB_{11}H_{12}^-$ to the [($^F$PNP)Pd]$^+$ fragment, and presumably that is the case for **2C**, as well.

Although **2B** and **2C** are adducts of the authentic $[(PNP)Pd]^+$ fragment, the coordination of the THF molecule in **2B** or of the carborane anion in **2C** was sufficiently weak that **2B** and **2C** readily functioned as synthons of $[(PNP)Pd]^+$ in the reactions with B-H, B-B, and H-H bonds described below. We selected two different weakly coordinating anions in order to increase the chances of obtaining X-ray quality crystals containing the cations of interest and of obtaining analytically pure solid products. In the products of net heterolytic splitting , both $[BAr^F{}_4]^-$ and $[CB_{11}H_{12}]^-$ behave as non-coordinating anions.

*2.2.2 Net B-H and B-B heterolytic splitting reactions*

Both **2B** and **2C** readily reacted with 1.0-1.1 equiv. CatB-H (Scheme 2-5), with the reaction complete in 1-3 h as evinced by the evolution of the blue color of **2B** or **2C** into yellow with the formation of the products $[(PN(BCat)P)PdH]BAr^F{}_4$ (**202-$BAr^F{}_4$**) and $[(PN(BCat)P)PdH]CB_{11}H_{12}$ (**202-$CB_{11}H_{12}$**). In both cases, the reaction mixtures also contained small amounts of the $[(PN(H)P)PdH]^+$ (**201-$BAr^F{}_4$** or **201-$CB_{11}H_{12}$**) impurities. Nonetheless, workup allowed isolation of pure **202-$BAr^F{}_4$** in ca. 60% yield while **202-$CB_{11}H_{12}$** was characterized in the presence of **201-$CB_{11}H_{12}$**. $^1H$, $^{31}P$, and $^{13}C$ NMR spectroscopy confirmed the structure and formulation of products **202**. Complex **202-$BAr^F{}_4$** was also characterized by single crystal X-ray diffraction (vide infra) and elemental analysis. It is worth noting that the B-H bond of CatB-H added to the Pd-N bond in the opposite direction compared with the C-H and S-H substrates mentioned above,[77] that is, B added to N while H added to Pd. This is consistent with the reversal of polarity of a B-H bond vs a C-H or an S-H bond.

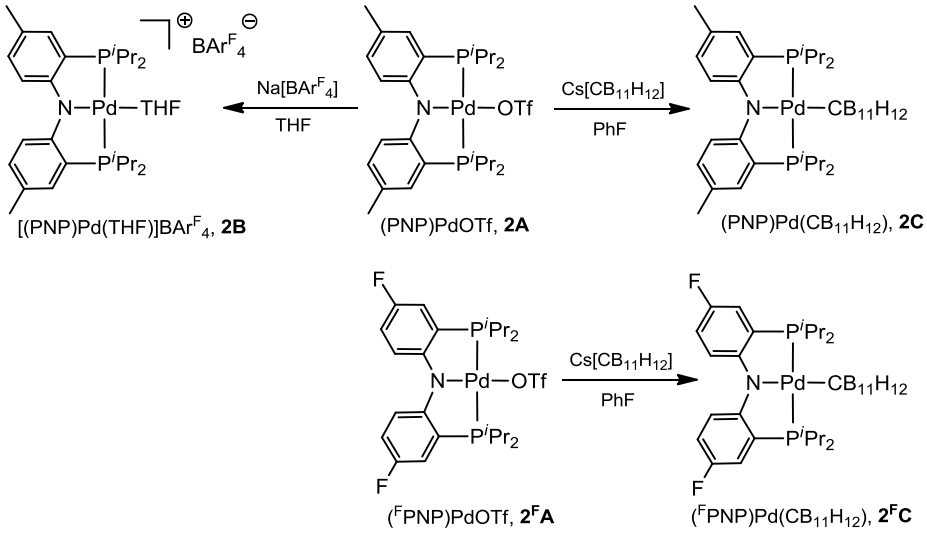


**Scheme 2-4.** Synthesis of compounds **2B**, **2C**, and **2$^F$C**.

The most telling spectroscopic evidence of this regiochemistry in salts of **202** was the Pd-H resonance at δ -12.7 (**202-BAr$^F_4$**) or -12.6 ppm (**202-CB$_{11}$H$_{12}$**) in the $^1$H NMR spectrum. It is also interesting to note that $CB_{11}H_{12}^-$ does not undergo B-H cleavage, which is probably an illustration of the different nature of the B-H bond of in the $CB_{11}H_{12}^-$ cage and in CatB-H, both in the electronic and steric sense.

Analogous reactions of **2B** and **2C** with CatB-BCat proceeded more slowly, requiring >18 h and/or mild heating for completion (Scheme 2-5). The products [(PN(CatB)P)PdBCat]BAr$^F_4$ (**203-BAr$^F_4$**) and [(PN(CatB)P)Pd(BCat)]$CB_{11}H_{12}$ (**203-CB$_{11}$H$_{12}$**) were characterized by $^1$H, $^{31}$P, and $^{13}$C NMR spectroscopy. Like the salts of **202**, both salts of **203** possess $C_s$ symmetry in the NMR spectra at ambient temperature. The NMR spectroscopic signatures of **203-BAr$^F_4$** and **203-CB$_{11}$H$_{12}$** were nearly identical. For example, **203-CB$_{11}$H$_{12}$** gave rise to a $^{31}$P NMR resonance at δ 45.0 ppm,

very similar to **203-BAr$^{F}_{4}$** (44.7 ppm). We did not observe the $^{11}$B signals for **203-BAr$^{F}_{4}$** and **203-CB$_{11}$H$_{12}$** corresponding to the two different BCat groups, even upon cooling to -30 ℃. This was surprising to us because the $^{11}$B NMR resonances of the anions in salts of **203** were easily detected in the same experiments, and because the N-*B* resonance in **202-BAr$^{F}_{4}$** and the Pd-*B* resonance in **204-BAr$^{F}_{4}$** were also readily detected at 21.2 and 37.1 ppm, respectively, in their $^{11}$B{$^{1}$H} NMR spectra. Presumably, the $^{11}$B NMR resonances of the CatB groups in **203-BAr$^{F}_{4}$** and **203-CB$_{11}$H$_{12}$** are substantially broadened, but the origin of this broadening is unclear to us. Nonetheless, the expected $^{1}$H NMR and $^{13}$C NMR resonances for the two distinct CatB groups for **203-BAr$^{F}_{4}$** and **203-CB$_{11}$H$_{12}$** were observed. Compound **203-BAr$^{F}_{4}$** was found to be contaminated with **204-BAr$^{F}_{4}$** and our best attempts at removing this impurity failed. On the other hand, compound **203-CB$_{11}$H$_{12}$** was isolated in a pure solid form, as supported by NMR spectroscopy and elemental analysis data and it was also characterized by single crystal X-ray diffraction (vide infra). **203-BAr$^{F}_{4}$** possesses better solubility in aromatic solvents than **203-CB$_{11}$H$_{12}$**. **203-CB$_{11}$H$_{12}$** is barely soluble in benzene, toluene, or fluorobenzene at room temperature, and precipitated from the toluene reaction mixture. This low solubility is presumably responsible for the fortuitous separation of the likely impurities.

The origin of the formation of salts of **201** in reaction of **2B** and **2C** with CatB-H and of **204** in reactions of **2B** and **2C** with CatB-BCat is not clear. It is likely the result of the protolysis of the N-B bonds in the expected products (see “Hydrolysis” section below).

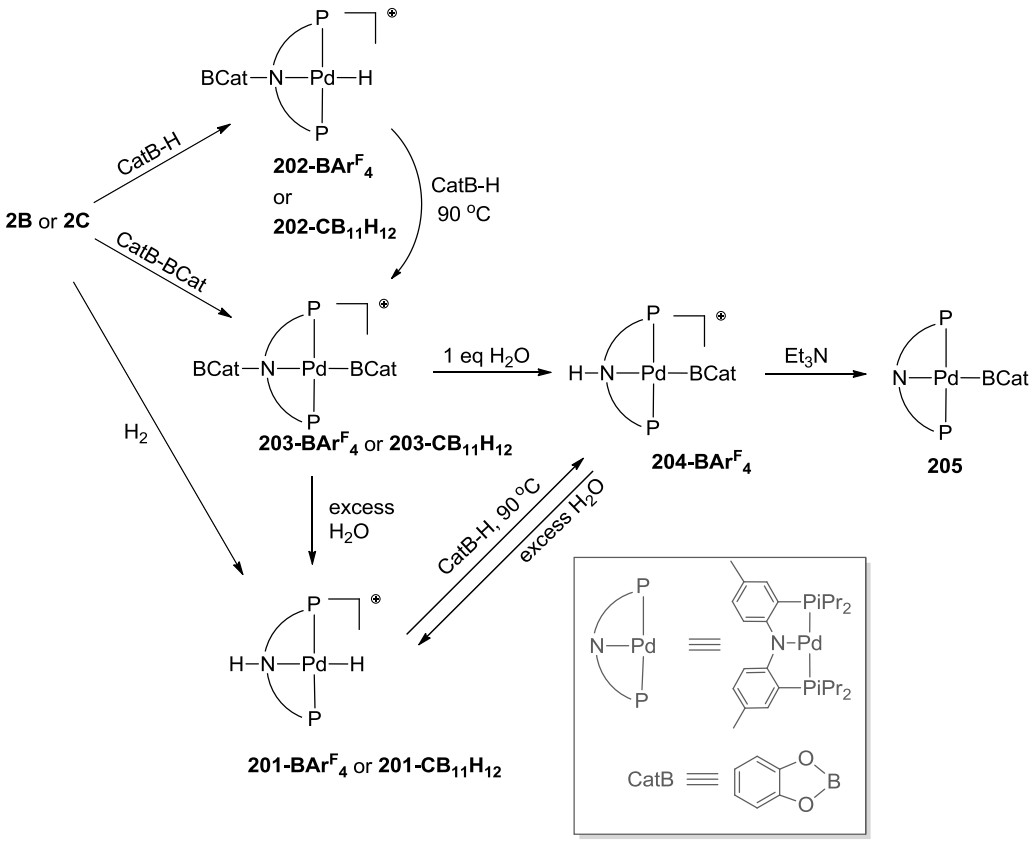


**Scheme 2-5.** Synthesis of compounds **201**-**205** and their interconversion.

The nature of the protic source responsible is at this point unknown. Consistent observation of apparent protolysis products after different drying precautions taken casts doubt (but does not eliminate) the possibility of adventitious water. It is also possible that difficult to remove B-OH impurities in CatB-H and CatB-BCat are the culprit.

*2.2.3 Hydrolysis of B-N and Pd-B bonds*

The B-N and Pd-B bonds in complexes **203-BAr$^F_4$** as well as **203-CB$_{11}$H$_{12}$** were easily hydrolyzed (Scheme 2-5). The hydrolysis of the B-N bond took place more rapidly: reaction of **203-BAr$^F_4$** with 1 equiv. of water produced complex **204-BAr$^F_4$**.

The Pd-B bond was hydrolyzed more slowly, and excess water effected conversion of **203-BAr$^{F}_{4}$** or **203-CB$_{11}$H$_{12}$** to complex **201-BAr$^{F}_{4}$** or **201-CB$_{11}$H$_{12}$**, respectively. Thus, in the course of the hydrolysis, the N-B and Pd-B bonds were converted to the corresponding N-H and Pd-H bonds, with concomitant production of CatBOBCat (Scheme 2-5).[91] The ultimate hydrolysis products **201-BAr$^{F}_{4}$** and **201-CB$_{11}$H$_{12}$** were synthesized independently via reaction of **2B** or **2C** with $H_2$ and characterized by $^{1}$H, $^{13}$C and $^{31}$P NMR spectroscopy (and elemental analysis for **201-BAr$^{F}_{4}$**). These syntheses parallel the previously reported synthesis of **201-OTf** from (PNP)PdOTf and $H_2$.[77] Complexes **201-BAr$^{F}_{4}$** and **201-CB$_{11}$H$_{12}$** have the same cation as **201-OTf** and only differ in the anion. Not surprisingly, they resonated at the same chemical shift (56.3 ppm) in the $^{31}$P NMR spectra and displayed the same number and symmetry of $^{1}$H NMR resonances for the cation. On the other hand, the chemical shifts of the resonances in the

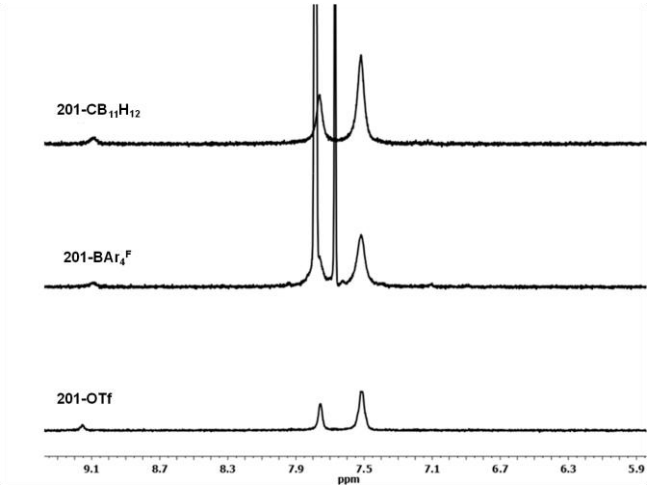


**Figure 2-1.** $^{1}$H NMR spectra of **201-OTf**, **201-BAr$^{F}_{4}$**, **201-CB$_{11}$H$_{12}$** in $CD_2Cl_2$ (only aromatic region shown).

$^1$H NMR spectra in $CD_2Cl_2$ of these three compounds were quite distinct from each other, especially for the N-*H* resonances (δ 8.75, 6.96, 7.07 ppm for **201-OTf**, **201-BAr$^F_4$** and **201-CB$_{11}$H$_{12}$**, respectively).[92] However, the chemical shifts in the $^1$H NMR spectra in the more polar solvent acetone-$d_6$ were only slightly different (δ 9.15, 9.09, 9.08 ppm for the N-*H* resonances for **201-OTf**, **201-BAr$^F_4$** and **201-CB$_{11}$H$_{12}$** respectively) (Figure 2-1). These discrepancies can be rationalized by the notion that triflate, albeit not coordinated to the metal, maintains a closer interaction with the cation in solution than $[BAr^F_4]^-$ or $[CB_{11}H_{12}]^-$.[93] The difference is greater in the less polar solvent ($CD_2Cl_2$) and nearly disappears in acetone. This notion is reinforced by the observation of hydrogen bonding between NH of the cation and the triflate anion in the solid-state structure of **201-OTf**.[77] Most likely, this is the interaction most important for the downfield shift of the NH resonance in solutions of **201-OTf** vs **201-BAr$^F_4$** or **201-CB$_{11}$H$_{12}$**.

The intermediate hydrolysis product **204-BAr$^F_4$** (Scheme 2-5) was isolated in 68% yield from selective reaction of **204-BAr$^F_4$** with 1 equiv. of water, and we were able to obtain single crystals suitable for X-ray diffraction studies (vide infra) using this route. Alternatively, **204-BAr$^F_4$** could be prepared via thermolysis of **201-BAr$^F_4$** with excess CatB-H. Thermolysis with excess CatB-H also served to convert **202-BAr$^F_4$** to **203-BAr$^F_4$**. These reactions converted Pd-H into Pd-BCat (and $H_2$), but did not affect the NH bond in **204-BAr$^F_4$**. **204-BAr$^F_4$** displayed $C_s$ symmetry in its NMR spectra and a single $^{11}$B resonance for the cation (37.1 ppm).

The formation of a metal-boryl bond upon treatment of a metal-hydride with boranes is not without precedent.[94] Dehydrogenative borylation of C-H bonds with $R_2BH$ reagents must also involve conversion of metal hydrides to metal boryls as part of the catalytic cycle.[95] In another study using the PNP ligand, Mindiola reported the formation of the neutral (PNP)NiBCat by treatment of (PNP)NiH with CatB-H.[96] We sought to prepare the analogous neutral (PNP)PdBCat (**205**) by a similar route, but only ca. 30% conversion to **205** was observed after treatment of (PNP)Pd-H with CatB-H at 55 ℃ for two days. Further thermolysis did not lead to complete conversion and some unidentified products began to appear (NMR evidence). On the other hand, addition of a base ($Et_3N$) to the solution of **204-BAr$^F_4$** accomplished deprotonation of **204-BAr$^F_4$** to produce **205**. Complex **205** was only characterized in solution. The characterization data obtained for **205** conform to the proposed palladium boryl neutral structure. Notably, the $^{11}B$ spectrum contained a broad resonance at 45.0 ppm, which is similar to Mindiola's (PNP)NiCat (ca. 47 ppm). Complex **205** gave rise to $C_{2v}$-symmetric NMR spectrum in solution that is typical for (PNP)PdX complexes.

Complexes **204-BAr$^F_4$** and **202-BAr$^F_4$** are isomers. Both can be formally viewed as products of 1,2- vs 2,1-addition of CatB-H to $[(PNP)Pd]^+$, with **202-BAr$^F_4$** having Pd-H and N-B bonds and **204-BAr$^F_4$** having Pd-B and N-H bonds. As mentioned above, only **202-BAr$^F_4$** could in fact be synthesized in this fashion. There was no conversion between these two isomers upon thermolysis of one or the other at 90 ℃. Thus, we were unable to determine which is the more favorable isomer. The lack of interconversion shows that **204-BAr$^F_4$** cannot be an intermediate en route to the formation of **202-BAr$^F_4$**.

### *2.3 Mechanistic considerations*

We have considered the conceivable mechanisms (Scheme 2-6) for the formation of the heterolytic splitting products **202** and **203** (abbreviated as **D** in Scheme 2-6). We assume that $[(PNP)Pd]^+$ is operationally accessible in solution. It seems most likely that the σ-complex[97] **A'** (Scheme 2-6) is formed initially. From it, one could envision either OA to give **B'** followed by B-N RE to produce **D** or a concerted migration of Cat-B to give **D** without an intermediate. The viability of a σ-BB complex with Pd(II) and of a Pd(IV) intermediate **B'** is reinforced by the recent computational investigations by Bo, Peris, and Fernandez.[98]

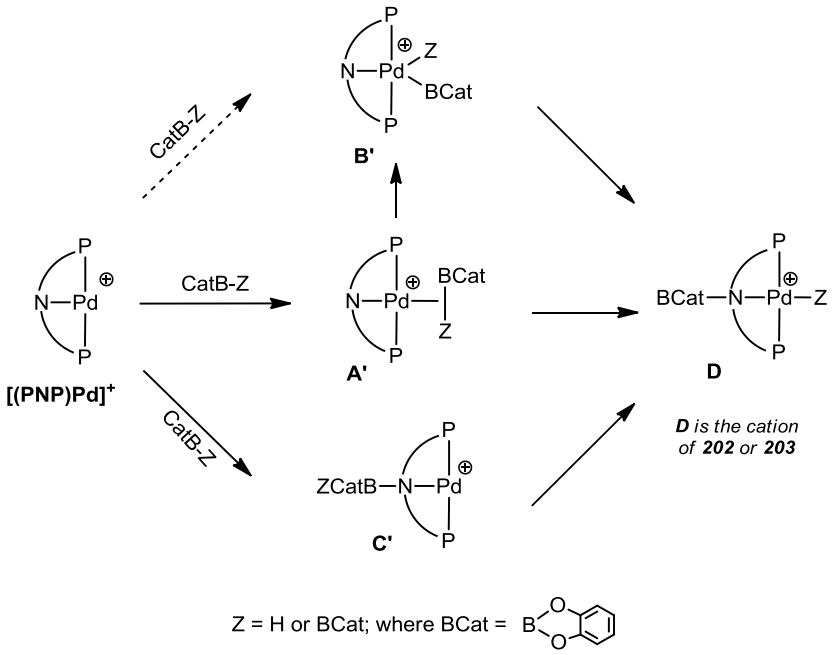


**Scheme 2-6.** Possible mechanisms of heterolytic cleavage of B-H and B-B bonds across Pd-N bond.

The calculations indicated that the addition of CatB-BCat to a three-coordinate, dicationic $[(CNC)Pd]^+$ cation (where CNC is a pyridine/bis(NHC) pincer ligand) was favorable to produce both the σ-BB complex or the Pd(IV) boron-boron OA product, with the σ-BB complex being more stable by ca. 10 kcal/mol and the barrier between the two being small. In our previous work,[77] we considered the mechanism of the heterolytic splitting of $H_2$ by $[(PNP)Pd]^+$. Our DFT calculations there indicated that the dihydride product of H-H OA $[(PNP)Pd(H)_2]^+$ was too high in energy to be an intermediate and that the concerted splitting of H-H (akin to **A'→B'** in Scheme 2-6) possessed a rather high barrier of ca. 28 kcal/mol. Boryl is a more donating ligand than a hydride and it is possible that B-H or B-B OA to $[(PNP)Pd]^+$ (**A'→B'**) and/or the concerted intramolecular transfer of boryl (**A'→C'**) are more accessible. For the $H_2$ splitting, we hypothesized that a likely mechanism involves intermolecular proton transfer from the dihydrogen ligand in $[(PNP)Pd(H_2)]^+$ to N of PNP by an external base (triflate, solvent, possibly adventitious water). However, an analogous transfer of a $CatB^+$ seems a more exotic proposition,[99] especially considering the absence of triflate and the demonstrated deleterious role of water as an impurity.

Another possibility is that the formation of **D** was initiated by an interaction of the Lewis acidic boron center in HBCat /BCat-BCat with the Lewis-baisc N site in PNP to form **C'** (Scheme 2-6). In a subsequent step, formal migration (which could be envisioned intra- or intermolecular) of the hydride or the BCat anion from the four-coordinate boron to the unsaturated Pd center would lead to **D**. A comparable reaction sequence (addition of borane to the heteroatom first) has been proposed for the reaction

of a Rh-peroxo complex with pinacolborane.[83] However, this pathway appears less likely with $[(PNP)Pd]^+$ because the basicity of the N in it should be quite low, while the empty coordination site on Pd is clearly a very reactive functionality.

### *2.4 Solid-state structures of complexes 202-$BAr^F_4$, 203-$CB_{11}H_{12}$, and 204-$BAr^F_4$*[100]

We were able to obtain single crystals of compounds **202-$BAr^F_4$**, **203-$CB_{11}H_{12}$**, and **204-$BAr^F_4$** that were suitable for X-ray diffraction studies. The ORTEP representations of the molecular structures in the solid state are given in Figures 2-2 to 2-4.

In the structures of **202-$BAr^F_4$** (Figure 2-2), **203-$CB_{11}H_{12}$** (Figure 2-3) and **204-$BAr^F_4$** (Figure 2-4), the Pd center adopts a slightly distorted square-planar geometry and all three structures contain a PNP ligand with a central amine nitrogen donor. The Pd-$N_{PNP}$ distances are notably longer in these compounds (2.202(2) Å in **202-$BAr^F_4$**, 2.2517(11) Å in **203-$CB_{11}H_{12}$**, 2.194(3) Å in **204-$BAr^F_4$** than the corresponding distances in the compounds containing the PNP ligand with a central amido, $sp^2$-hybridized nitrogen donor (for example, 2.0072(19) Å in **5**, 2.0258(19) Å in (PNP)PdCl 2.086(4) Å in ($^F$PNP)PdH,[101] and 2.0938(15) Å in ($^F$PNP)PdMe[101]). It is also instructive to analyze how the Pd-N bond length depends on the nature of X and Y in $[(PN(X)P)Pd-Y]^+$. The set of four compounds (X = CatB or H; Y = CatB or H) is completed by considering **201-OTf** (2.160(4) Å)[77] alongside **202-$BAr^F_4$**, **203-$CB_{11}H_{12}$** and **204-$BAr^F_4$** (Table 1). It is apparent that a longer Pd-N bond length results from either X = BCat and Y = BCat. The elongation of the Pd-N bonds may be attributed to the greater *trans*-influence of the boryl ligand than the hydride for Y = BCat,[102] and to the greater steric encumbrance of a boryl-substituted amine for X = BCat.

The boryl moieties (as defined by the O-B-O planes) attached to Pd in complexes **203-$CB_{11}H_{12}$** and **204-$BAr^F_4$** are oriented almost perpendicularly to the Pd coordination plane. Interestingly, the two boryl moieties (B-N and B-Pd) in **203-$CB_{11}H_{12}$** are almost perpendicular to each other, too. Both determined Pd-B bond lengths (1.9879(16) Å in **203-$CB_{11}H_{12}$** and 1.993(4) Å in **204-$BAr^F_4$**) are in the expected range for the palladium boryl complexes. The other bond distances and angles associated with the (PNP)Pd system in **202-$BAr^F_4$**, **203-$CB_{11}H_{12}$** and **204-$BAr^F_4$** are unremarkable. The P-Pd-P angle varies within ca. 157 - 164° and the Pd-P distances in all three compounds are in the 2.26-2.29 Å range.

**Table 1.** Pd-N distances (from XRD studies, in Å) for compounds $[(PN(X)P)Pd\text{-}Y]^+$ (**201-OTf**,[77] **202-$BAr^F_4$**, **203-$CB_{11}H_{12}$**, and **204-$BAr^F_4$**).

| | X = CatB | X = H |
|---|---|---|
| Y = CatB | 2.2517 (11) | 2.202(2) |
| Y = H | 2.194(3) | 2.160(4) |

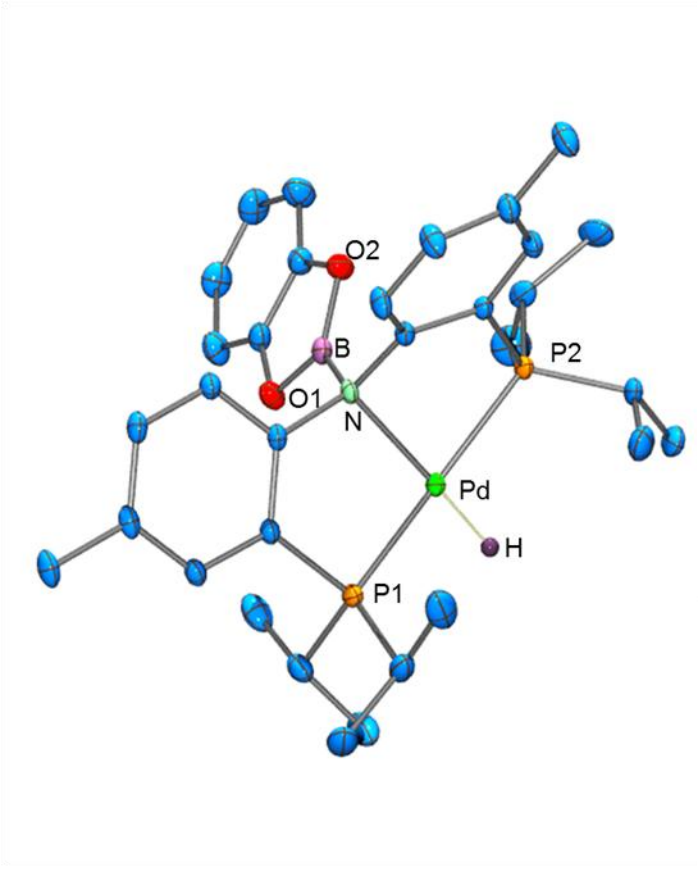


**Figure 2-2.** ORTEP drawing[103] (50% probability ellipsoids) of **202-BAr$^{F}_{4}$**. Only selected atoms are labled. Hydrogen atoms (except Pd-H) and BAr$^{F}_{4}$ anion are omitted for clarity. Selected bond distances (Å) and angles (deg) follow: Pd1-P1, 2.2624(7); Pd1-P2, 2.2838(7); Pd1-N, 2.202(2); Pd1…B1, 2.746(3); Pd1-H, 1.43(4); P1-Pd1-P2, 163.66(3); N-Pd1-H, 175.9(14).

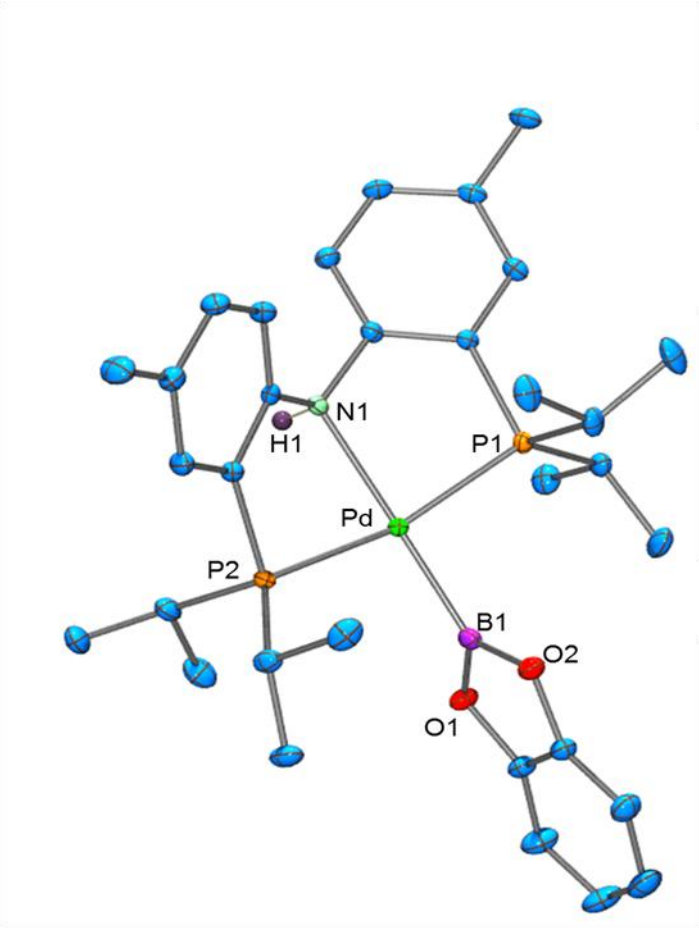


**Figure 2-3.** ORTEP drawing[103] (50% probability ellipsoids) of **204-BAr$^{F}_{4}$**. Only selected atoms are labled. Hydrogen atoms (except H1), BAr$^{F}_{4}$ anion and the cocrystallized molecules of $CH_2Cl_2$ and $H_2O$ are omitted for clarity. Selected bond distances (Å) and angles (deg) follow: Pd-P1, 2.2635(8); Pd1-P2, 2.2859(8); Pd1-N1, 2.194(3); Pd1-B1, 1.993(4); P1-Pd1-P2, 159.94(3); N1-Pd1-B1, 178.45(13).

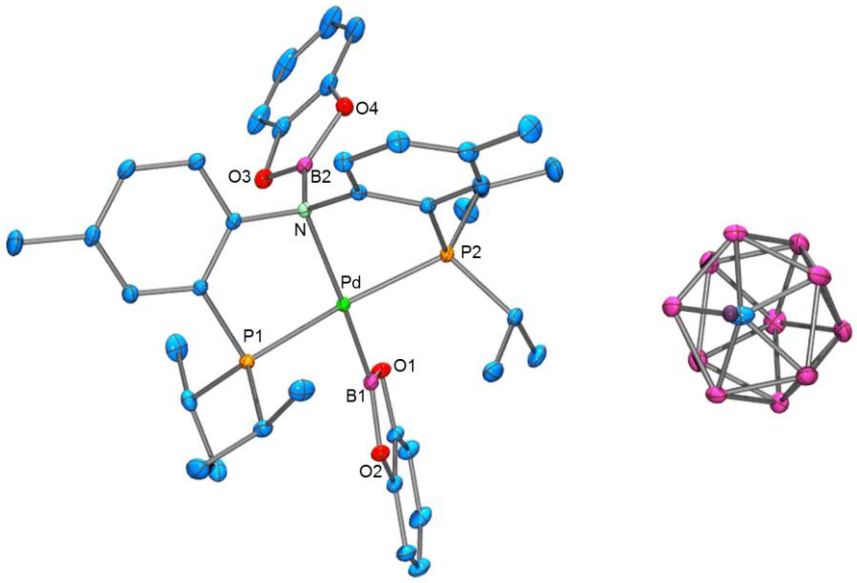


**Figure 2-4.** ORTEP drawing[103] (50% probability ellipsoids) of **203-$CB_{11}H_{12}$**. Only selected atoms are labeled. Hydrogen atoms and the $PhCF_3$ solvent molecule are omitted for clarity. Selected bond distances (Å) and angles (deg) follow: Pd1-P1, 2.2753(4); Pd1-P2, 2.2880(4); Pd1-N, 2.2517(11); Pd1-B1, 1.9879(16); P1-Pd1-P2, 156.521(13); N-Pd1-B1-175.16(5).

### *2.5 Reaction of [(PNP)Ir] fragment with CatB-H, CatB-BCat and CatB-Cl*

In comparison with the $[(PNP)Pd]^+$ fragment, activation of B-H and B-B bonds was also investigated with our (PNP)Ir system. As noted before, oxidative addition of B-X (X = H, B, Cl) bonds to group 9 metals (Rh(I), Ir(I)) is fairly common. Since B-X bonds do 1,2-addition across the Pd-N bond , we were curious to see what their reactivity might be towards (PNP)Ir fragment.

Treatment of $(PNP)Ir(H)_2$ with excess CatB-H (5 eq.) in aromatic solvent leads to ~ 95% formation of $(PNP)Ir(BCat)_2$ (**206**) within minutes and no intermediate was observed by NMR. **206** was isolated and characterized spectroscopically. **206** displays a

singlet at 50.8 ppm by $^{31}P$ NMR and displays $C_{2v}$ symmetry in solution as indicated by $^{1}H$ NMR. Without further experimentation, it is difficult to know exactly how compound **206** was formed.

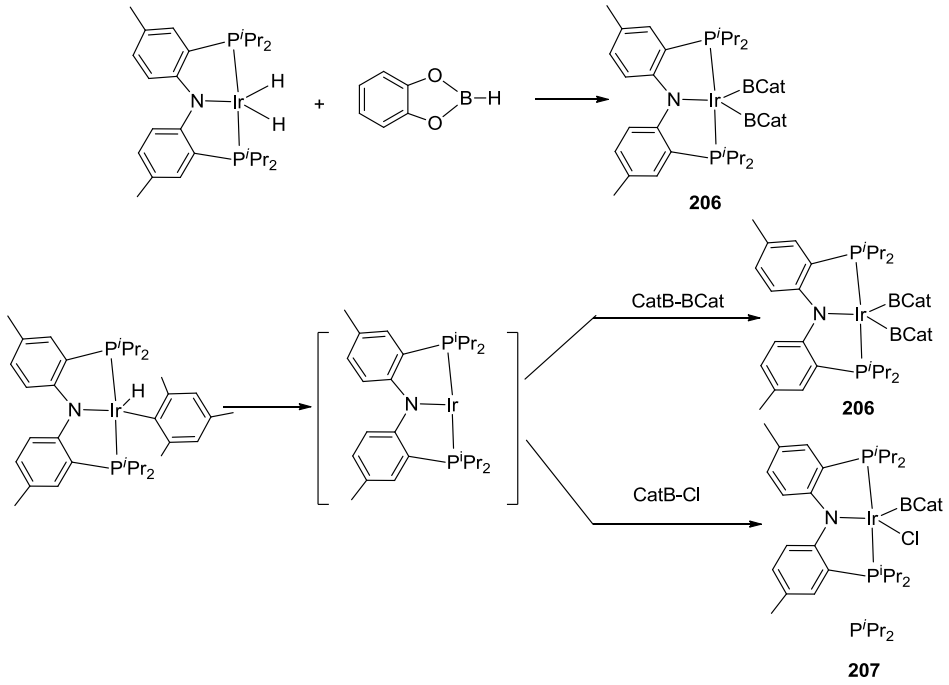


**Scheme 2-7.** Oxidative addition of B-B and B-Cl bonds at (PNP)Ir center.

(PNP)Ir(H)(Mes) (**301**), a useful and interesting molecule that will be discussed more in detail in Chapter III, reacts with CatB-BCat in mesitylene generating compound **206** too (Scheme 2-7). So in [(PNP)]Ir system, B-B bond oxidatively added to Ir(I) center to form Ir(III) bisboryl complex while in the isoelectronic $(PNP)Pd^{+}$ system B-B heterolytically added to Pd-N bond.

Interestingly, we found that not only B-B bonds can do oxidative addition to (PNP)Ir, but B-Cl bond in CatB-Cl as well. Treatment of (PNP)Ir(H)(Mes) (**301**) with CatB-Cl in mesitylene at 80 $^{o}$C for 1 h cleanly produced (PNP)Ir(BCat)(Cl) (**207**). **207** was characterized by NMR spectroscopy in solution. It resonated at 41.1 ppm in the $^{31}$P NMR spectrum and displayed the expected $C_s$ symmetry in its $^{1}$H NMR spectrum.

### *2.6 Conclusion*

In conclusion, we have demonstrated that the $[(PNP)Pd]^+$ fragment is capable of net heterolytic cleavage of the B-H bond in catecholborane and the B-B bond in catecholdiboron. We have isolated and physically characterized cationic palladium hydrides and palladium boryl complexes. The activation of the B-H bond by $[(PNP)Pd]^+$ resulted in the formation of Pd-H and N-B bonds. The addition of a B-B bond across a Pd-N bond to form a palladium boryl complex is unique. It provides another route to palladium boryl complexes and to the cleavage of the B-B bond where oxidative addition of a B-B bond to the palladium center is difficult. Both the N-B and Pd-B bonds are subject to hydrolysis, forming the corresponding N-H and Pd-H bonds. Deprotonation of the partly hydrolyzed product **204-BAr$^{F}_{4}$** by $Et_3N$ gave the neutral palladium boryl complex (PNP)PdBCat. On the other hand, B-B and B-Cl oxidative addition were observed at (PNP)Ir center.

### *2.7 Experimental*

**General considerations.** Unless specified otherwise, all manipulations were performed under an argon atmosphere using standard Schlenk line or glovebox techniques. Ethyl ether, $C_6D_6$, and pentane were dried over Na/K/$Ph_2CO$/18-crown-6,

distilled or vacuum transferred and stored over molecular sieves in an Ar-filled glovebox. Fluorobenzene, catecholborane (CatBH) were dried with and then distilled from $CaH_2$. ($^{F}$PNP)PdOTf,[104] (PNP)PdH,[11b] were prepared according to the published procedures. All other chemicals were used as received from commercial vendors. NMR spectra were recorded on a Varian iNova 300, Varian iNova 400, and Mercury 300 spectrometer. Chemical shifts are reported in δ (ppm). For $^{1}$H and $^{13}$C NMR spectra, the residual solvent peak was used as an internal reference. $^{31}$P NMR spectra were referenced externally using 85% $H_3PO_4$ at δ 0 ppm. $^{19}$F NMR spectra were referenced externally using $CF_3COOH$ at δ -78.5 ppm. $^{11}$B NMR spectra were referenced externally using $BF_3 \cdot Et_2O$ at δ 0 ppm. Elemental analyses were performed by CALI, Inc. (Parsippany, NJ).

**(PNP)PdOTf (2A)**. (PNP)PdH (216 mg, 0.40 mmol) was dissolved in 10 mL $C_6H_6$, followed by the addition of MeOTf (226 μL, 2.0 mmol). The reaction mixture was allowed to stir at room temperature for 2 h. The volatiles were removed under vacuum and the residue was recrystallized from toluene/pentane to give pure solid. Yield: 225 mg, 0.33 mmol, 83%. $^{1}$H NMR ($C_6D_6$): δ 7.50 (d, 2H, *J* = 8 Hz, (PNP)Aryl-*H*), 6.77 (s, 2H, (PNP)Aryl-*H*), 6.60 (d, 2H, *J* = 8 Hz, (PNP)Aryl-*H*), 2.42 (m, 4H, C*H*Me$_2$), 2.02 (6H, Ar-C*H*$_3$), 1.38 (dvt, 12H, CH*Me*$_2$), 1.04 (dvt, 12H, CH*Me*$_2$). $^{13}$C{$^{1}$H} NMR ($C_6D_6$): δ 163.2(t), 132.8, 132.7, 127.3, 117.8, 117.5, 25.2 (m), 20.8, 18.7, 18.0. $^{31}$P{$^{1}$H} NMR ($C_6D_6$): δ 53.6. $^{19}$F NMR ($C_6D_6$): δ -79.2.

**[(PNP)Pd(THF)]BAr$^{F}_{4}$ (2B)**. (PNP)PdOTf (**2A**) (70 mg, 0.10 mmol) was dissolved in 5 mL of cold THF, followed by the addition of Na[BAr$^{F}_{4}$] (88 mg, 0.10 mmol). The

reaction mixture was allowed to stir at room temperature for 1 h. All of the volatiles were removed under vacuum and the residue was dissolved in PhF. The mixture was filtered off Celite and the filtrate was pumped to dryness. The final pure product was obtained after recrystallization from PhF/pentane. Yield: 88 mg, 0.060 mmol, 60%. $^{1}$H NMR ($CD_2Cl_2$): δ 7.73 (s, 8H, $BAr_4$-*H*), 7.58 (s, 4H, $BAr_4$-*H*), 7.28 (d, 2H, *J* = 9 Hz, (PNP)Aryl-*H*), 6.92 (m, 4H, (PNP)Aryl-*H*), 3.95 (m, 4H, O*CH*$_2$), 2.44 (m, 4H, C*H*$Me_2$), 2.23 (s, 6H, Ar-C*H*$_3$), 2.02 (m, 4H, C*H*$_2$), 1.35 (dvt, 12H, CH*Me*$_2$), 1.26 (dvt, 12H, CH*Me*$_2$). $^{13}$C{$^{1}$H} NMR ($CD_2Cl_2$): δ 162.5 (q, *J* = 50 Hz), 162.1(t), 135.4, 133.8, 132.5, 130.6, 129.6 (q, *J* = 234 Hz), 126.5, 123.8, 121.1, 118.1, 77.4, 25.6, 23.0, 20.5, 19.0, 18.1. $^{31}$P{$^{1}$H} NMR ($CD_2Cl_2$): δ 55.5. $^{19}$F NMR ($CD_2Cl_2$): δ -65.7. Elem. An.. Found (Calculated) for $C_{62}H_{60}BNOF_{24}P_2Pd$: C 50.71 (50.65); H 4.18 (4.11); N 0.85 (0.95).

**(PNP)PdCB$_{11}$H$_{12}$ (2C)**. (PNP)PdOTf (**2A**) (34.8 mg, 0.051 mmol) was dissolved in 5 mL PhF. $CsCB_{11}H_{12}$ (17 mg, 0.062 mmol) was added to the solution. The mixture was stirred at RT overnight. The solution was then passed through Celite. The volatiles were removed under vacuum and the resulting solid was recrystallized from PhF/pentane. Yield: 28 mg, 0.041 mmol, 83%. $^{1}$H NMR ($CD_2Cl_2$): δ 7.30 (d, *J* = 8 Hz, 2H, (PNP)Aryl-*H*), 7.05 (br, 2H, (PNP)Aryl-*H*), 6.88 (d, *J* = 8 Hz, 2H, (PNP)Aryl-*H*), 2.80 (m, 4H, C*H*$Me_2$), 2.52-1.50 (br, 12H, $CB_{11}$*H*$_{12}$), 2.21 (s, 6H, Ar-C*H*$_3$), 1.33 (app. q (dvt), *J* = 7.2 Hz, 12H, CH*Me*$_2$)), 1.26 (app. q (dvt), *J* = 7.2 Hz, 12H, CH*Me*$_2$). $^{13}$C{$^{1}$H} NMR ($C_6D_6$): δ 162.1 (t, *J* = 9 Hz, (PNP)Aryl-*C*), 132.9 ((PNP)Aryl-*C*), 132.7 ((PNP)Aryl-*C*), 117.9 ((PNP)Aryl-*C*), 117.6 ((PNP)Aryl-*C*), 117.3 (t, *J* = 6 Hz, (PNP)Aryl-*C*), 54.3, 26.0 (t, *J* = 11 Hz), 20.3, 20.0, 18.4. $^{31}$P{$^{1}$H} NMR ($CD_2Cl_2$): δ

60.0. $^{11}B\{^1H\}$ NMR ($C_6D_6$): δ -9.4, -13.2, -15.2. Elem. An.. Found (Calculated) for $C_{27}H_{52}B_{11}NP_2Pd$: C 47.57 (47.83); H 7.68 (7.73); N 2.10 (2.07).

**($^F$PNP)PdCB$_{11}$H$_{12}$ (2$^F$C)**. ($^F$PNP)PdOTf (**2$^F$A**) (55 mg, 0.079 mmol) was dissolved in 3 mL of fluorobenzene and $CsCB_{11}H_{12}$ (27 mg, 0.097 mmol) was added with stirring. The solution immediately changed from purple to dark blue. After approximately 10 min, the solution was passed through a pad of Celite, the volatiles were removed under vacuum and the residue was washed with pentane. The residue was dried under vacuum. Yield: 37 mg, 0.054 mmol, 68%. $^1H$ NMR ($C_6D_6$): δ 7.22 (m, 2H, Ar-*H*), 6.86 (m, 2H, Ar-*H*), 6.75 (t, *J* = 8 Hz, 2H, Ar-*H*), 3.4-1.4 (br, 12H, $CB_{11}H_{12}$), 2.78 (br, 4H, C*H*Me$_2$), 1.20 (app. q. (dvt), 12H, Hz, CH*Me$_2$*), 1.06 (app. q. (dvt), 12H, Hz, CH*Me$_2$*). $^{31}P\{^1H\}$ NMR ($C_6D_6$): δ 58.5. $^{19}F$ NMR ($C_6D_6$): δ -126.4.

**[(PN(H)P)PdH]BAr$^F_4$ (201-BAr$^F_4$)**. Compound **2B** (36 mg, 0.026 mmol) was dissolved in 0.6 mL of PhF in a J. Young NMR tube. Then 1 atm of $H_2$ was introduced into the tube and the mixture was allowed to stand at room temperature for 30 min until the color changed to colorless. All the volatiles were removed under vacuum. The oily residue was washed with hexanes a few times to obtain an off-white powder. The solid was dried under vacuum. Yield: 28 mg, 0.020 mmol, 77%. $^1H$ NMR ($CD_2Cl_2$): δ 7.69 (s, 8H, BAr$_4$-*H*), 7.53 (s, 4H, BAr$_4$-*H*), 7.37 (m, 4H, (PNP)Aryl-*H*), 7.30 (d, *J* = 6.6 Hz, (PNP)Aryl-*H*), 6.96 (br, 1H, N-*H*), 2.53 (m, 4H, C*H*Me$_2$ ), 2.41 (s, 6H, Ar-*CH$_3$*), 1.34 (app. q (dvt), *J* = 7.2 Hz, 6H, CH*Me$_2$*), 1.13 (app. q (dvt), *J* = 7.2 Hz, 12H, CH*Me$_2$*), 0.91 (app. q (dvt), *J* = 7.2 Hz, 6H, CH*Me$_2$*), -12.5 (br, 1H, Pd-*H*). $^{13}C\{^1H\}$ NMR ($C_6D_6$): δ 162.9 (q, *J* = 50 Hz, BAr$_4$-*C*), 145.5 (t, *J* = 8 Hz, (PNP)Aryl-*C*), 139.3 (t, *J* = 3Hz,

(PNP)Aryl-*C*), 135.3 ($BAr_4$-*C*), 134.2 ((PNP)Aryl-*C*), 133.2 ((PNP)Aryl-*C*), 129.9 (q, *J* = 32 Hz, $BAr_4$-*C*), 125.1 (d, *J* = 272 Hz, $BAr_4$-*C*), 124.8 (t, *J* = 4 Hz, , (PNP)Aryl-*C*), 119.7 ($BAr_4$-*C*), 117.9 (t, *J* = 4 Hz, (PNP)Aryl-*C*), 25.4 (t, *J* = 12 Hz), 23.3 (t, *J* = 13 Hz), 20.3, 19.3 (t, *J* = 4 Hz) , 18.6 (t, *J* = 4 Hz), 18.4, 17.7. $^{31}P\{^1H\}$ NMR ($C_6D_6$): δ 56.4. $^{19}F\{^1H\}$ NMR ($C_6D_6$): δ -63.1. Elem. An.. Found (Calculated) for $C_{58}H_{54}BF_{24}NP_2Pd$: C 49.67 (49.75); H 3.95 (3.89); N 1.71 (0.96).

**[(PN(H)P)PdH]$CB_{11}H_{12}$ (201-$CB_{11}H_{12}$)**. Compound **2A** (104 mg, 0.152 mmol) was dissolved in 6.0 mL of PhF followed by the addition of $CsCB_{11}H_{12}$ (50.0 mg, 0.182 mmol). The reaction mixture was stirred for 4 h and $^{31}P$ NMR analysis indicated full conversion to compound **2C**. The reaction mixture was passed through Celite and the filtrate was transferred to a PTFE-capped flask. $H_2$ was introduced into the flask and the reaction was stirred vigorously for 5 min. The initial blue color disappeared and white precipitate was formed. The precipitate was collected by filtration and washed 3 times with pentane. Yield: 72 mg, 0.106 mmol, 70%. $^1H$ NMR ($CD_2Cl_2$): δ 7.41-7.34 (m, 6H, (PNP)Aryl-*H*), 7.07 (br, 1H, N-*H*), 2.53 (m, 4H, C*H*$Me_2$), 2.43 (s, 6H, Ar-$CH_3$), 2.25~1.39 (m, 12H, $CB_{11}H_{12}$ ), 1.33 (app. q (dvt), *J* = 7.2 Hz, 6H, CH$Me_2$), 1.17 (app. q (dvt), *J* = 7.2 Hz, 12H, CH$Me_2$), 0.92 (app. q (dvt), *J* = 7.2 Hz, 6H, CH$Me_2$), -12.5 (br, 1H, Pd-*H*). $^{31}P\{^1H\}$ NMR ($CD_2Cl_2$): δ 56.3.

**[(PN(BCat)P)Pd(H)]$BAr^F_4$ (202-$BAr^F_4$)**. Compound **2B** (40 mg, 0.029 mmol) was dissolved in about 1 mL of toluene/trifluorotoluene followed by the addition of CatB-H (3.0 μL, 0.029 mmol). The reaction mixture was allowed to stand at room temperature for 1 h and the solution color changed to light yellow. $Et_3N$ (1 μL, 0.007 mmol) was

added to the mixture (to deprotonate and assist in the removal of the traces of **201-BAr$^{F}_{4}$** present). The volatiles were removed under vacuum and the residue was washed with trifluorotoluene/pentane to give white powder after drying under vacuum. Yield: 25 mg, 0.016 mmol, 59%. X-ray quality crystals were obtained by crystalizing the solid in $CH_2Cl_2$/pentane at -35 ℃. $^{1}$H NMR ($C_6D_5Br$): δ 8.20 (s, 8H, $BAr_4$-*H*), 7.58 (s, 4H, $BAr_4$-*H*), 7.26 (m, 4H, (PNP)Aryl-*H*), 7.02 (d, *J* = 8 Hz, 2H, (PNP)Aryl-*H*), 6.72 (br, 4H, catechol-*H*), 2.40 (m, 2H, C*H*Me$_2$), 2.19 (br, 8H, Ar-*CH$_3$* + C*H*Me$_2$ ), 1.92 (m, 2H, C*H*Me$_2$), 1.11 (app. q (dvt), *J* = 7.2 Hz, 6H, CH*Me$_2$*), 0.89 (m, 12H, CH*Me$_2$*), 0.64 (app. q (dvt), *J* = 7.2 Hz, 6H, CH*Me$_2$*), -12.7 (t, *J* = 4.8 Hz, 1H, Pd-*H*). $^{13}$C{$^{1}$H} NMR ($C_6D_6$): δ 162.9 (q, *J* = 50Hz, $BAr_4$-*C*), 147.1 (Catechol-*C*), 145.9 (t, *J* = 8 Hz, (PNP)Aryl-*C*), 139.7 (t, *J* = 3Hz, (PNP)Aryl-*C*), 135.3 ($BAr_4$-*C*), 134.3 ((PNP)Aryl-*C*), 133.5 ((PNP)Aryl-*C*), 129.9 (q, *J* = 34 Hz, $BAr_4$-*C*), 125.1 (d, *J* = 272 Hz, $BAr_4$-*C*), 125.8 (t, *J* = 4 Hz (PNP)Aryl-*C*), 124.4 (Catechol-*C*), 119.7 ($BAr_4$-*C*), 117.9 (t, *J* = 4 Hz, (PNP)Aryl-*C*), 112.7 (Catechol-*C*), 26.4 (t, *J* = 12 Hz), 24.6 (t, *J* = 13 Hz), 20.3 (t, *J* = 3 Hz), 20.2, 19.5 (t, *J* = 4 Hz), 18.9, 18.4. $^{31}$P{$^{1}$H} NMR ($C_6D_6$): δ 53.2. $^{19}$F NMR ($C_6D_6$): δ -63.1. $^{11}$B{$^{1}$H} NMR ($C_6D_6$): δ 21.2 (N-*B*), -6.3 ($BAr_4^F$-*B*). Elem. Anal. Found (calculated) for $C_{64}H_{57}B_2NO_2F_{24}P_2Pd$: C, 50.58 (50.64); H, 3.82 (3.78); N, 0.92 (0.92).

**Thermolysis of 202-BAr$^{F}_{4}$. 202-BAr$^{F}_{4}$** (13 mg, 0.009 mmol) was dissolved in 0.6 mL PhF in a J. Young NMR tube and the solution was heated at 90 ℃ for 15 h. $^{31}$P NMR spectroscopic analysis indicated no observable changes.

**Reaction of 2-BAr$^{F}_{4}$ with HBCat.** Compound **202-BAr$^{F}_{4}$** (10 mg, 0.0060 mmol) was dissolved in 0.6 mL PhF in an NMR tube, followed by the addition of HBCat (4.0

μL, 0.030 mmol). The NMR tube was placed in a 95 ℃ oil bath. After 24 h, $^{31}P\{^{1}H\}$ NMR analysis indicated full conversion to **203-BAr$^{F}_{4}$**.

**[(PN(BCat)P)Pd(H)]CB$_{11}$H$_{12}$ (202-CB$_{11}$H$_{12}$)**. Compound **2C** (35 mg, 0.052 mmol) was dissolved in 0.6 mL of PhF, followed by the addition of CatB-H (5.5 μL, 0.052 mmol). The reaction mixture was allowed to stand at room temperature for 3 h and the solution color changed to light yellow. $^{31}P$ NMR indicated there was ~10% of **201-CB$_{11}$H$_{12}$** besides 90% of **202-CB$_{11}$H$_{12}$** in the reaction mixture. White crystals were formed by carefully layering pentane on top of the PhF solution. However, NMR analysis indicated that these crystals still contain a mixture of both **201-CB$_{11}$H$_{12}$** and **202-CB$_{11}$H$_{12}$**. NMR data for **202-CB$_{11}$H$_{12}$**: $^{1}H$ NMR ($C_6D_6$) (a drop of $CH_2Cl_2$ was added to increase solubility): δ 7.36 (m, 4H, (PNP)Aryl-*H*), 7.18 (br, 2H, (PNP)Aryl-*H*), 6.04 (br, 4H, Catechol-*H*), 2.51 (m, 2H, C*H*Me$_2$), 2.30 (s, 6H, Ar-*CH$_3$*), 2.25 (m, 2H, C*H*Me$_2$), 2.18-1.60 (br, 12H, CB$_{11}$*H$_{12}$*), 1.14 (app. q (dvt), *J* = 8 Hz, 6H, CH*Me$_2$*), 0.95 (m, 12H, CH*Me$_2$*), 0.68 (app. q (dvt), *J* = 8 Hz, 6H, CH*Me$_2$*), -12.6 (t, *J* = 5 Hz, 1H, Pd-*H*). $^{31}P\{^{1}H\}$ NMR ($C_6D_6$): δ 53.3.

**[(PN(BCat)P)Pd(BCat)]BAr$^{F}_{4}$ (203-BAr$^{F}_{4}$)**. Compound **2B** (40 mg, 0.029 mmol) was dissolved in ca. 1 mL of toluene/trifluorotoluene followed by the addition of CatB-BCat (7.0 μL, 0.029 mmol). The reaction mixture was allowed to stir at room temperature for overnight and the solution changed to slightly yellow. $Et_3N$ (1 μL, 0.007 mmol) was added to the mixture (to deprotonate and assist in the removal of the traces of **204-BAr$^{F}_{4}$** present). The volatiles were removed under vacuum and the residue was

washed with trifluorotoluene/pentane to give white powder after drying under vacuum. However, we were not able to get **203-$BAr^F_4$** in analytical pure form. $^1$H NMR analysis indicated the presence of a small amount of [$Et_3NH$]$BAr_4^F$. $^1$H NMR ($C_6D_6$): δ 8.27 (s, 8H, $BAr_4$-*H*), 7.62 (s, 4H, $BAr_4$-*H*), 7.10 (m, 2H, Catechol-*H*), 6.99 (br, 2H, (PNP)Aryl-*H*), 6.96 (m, 2H), 6.81~6.85 (m, 4H), 6.70 (br, 4H), 2.23 (m, 4H, C*H*$Me_2$), 2.03 (s, 6H, Ar-*CH*$_3$), 0.84 (app. q (dvt), *J* = 9 Hz, 6H, CH*Me*$_2$), 0.70 (app. q (dvt), *J* = 8 Hz, 12H, CH*Me*$_2$), 0.52 (app. q (dvt), *J* = 9 Hz, 6H, CH*Me*$_2$)). $^1$H NMR ($CD_2Cl_2$): 7.71 (s, 8H, $BAr_4$-*H*), 7.55 (s, 4H, $BAr_4$-*H*), 7.53 (d, 2H, *J* = 6 Hz, (PNP)Aryl-*H*), 7.488 (br, 2H, (PNP)Aryl-*H*), 7.46 (d, 2H, *J* = 6 Hz, (PNP)Aryl-*H*), 7.22 (m, 2H, Catechol-*H*), 7.12 (m, 4H, Catechol-*H*), 7.06 (m, 2H, Catechol-*H*), 2.81 (m, 2H, C*H*$Me_2$), 2.72 (m, *2*H, C*H*$Me_2$), 2.46 (s, 6H, Ar-*CH*$_3$), 1.11 (m, 18H, CH*Me*$_2$), 0.88 (app. q (dvt), *J* = 9 Hz, 6H, CH*Me*$_2$). $^{13}$C{$^1$H} NMR ($C_6D_6$): δ 162.9 (q, *J* = 50Hz, $BAr_4$-*C*), 148.3(Catechol-*C*), 147.1 (Catechol-*C*), 145.1 (t, *J* = 8 Hz, (PNP)Aryl-*C*), 139.7 (t, *J* = 3Hz, (PNP)Aryl-*C*), 135.3 ($BAr_4$-*C*), 134.5 ((PNP)Aryl-*C*), 133.7 ((PNP)Aryl-*C*), 130.0 (q, *J* = 34 Hz, $BAr_4$-*C*), 123.3 (Catechol-*C*), 125.1 (d, *J* = 272 Hz, $BAr_4$-*C*), 125.8 (t, *J* = 4 Hz, , (PNP)Aryl-*C*), 124.5 (Catechol-*C*), 119.8 ($BAr_4$-*C*), 117.9 (t, *J* = 4 Hz, (PNP)Aryl-*C*), 112.8 (Catechol-*C*), 112.3 (Catechol-*C*), 26.0 (t, *J* = 12 Hz), 24.5 (t, *J* = 13 Hz), 20.3, 19.9, 18.2, 17.5, 17.2. $^{31}$P{$^1$H} NMR ($C_6D_6$): δ 44.7. $^{19}$F NMR ($C_6D_6$): δ -63.2. $^{11}$B{$^1$H} NMR ($C_6D_6$): δ -6.4 ($BAr_4^F$-*B*).

**[(PN(BCat)P)Pd(BCat)]$CB_{11}H_{12}$ (203-$CB_{11}H_{12}$)**. Compound **2C** (62 mg, 0.091 mmol) and CatB-BCat (24 mg, 0.10 mmol) were placed in a PTFE-capped flask together with 3 mL toluene. The reaction mixture was heated at 60 ℃ overnight. The blue

solution changed to yellow-brown the next day and white precipitate was visible at the bottom of the flask. The white precipitate was collected on a glass frit by filtration and was dried under vacuum to fully remove all the solvent volatiles. Yield: 47 mg, 0.051 mmol, 57%. X-Ray quality crystals were obtained by slowly cooling down a hot $PhCF_3$ solution of **203-$CB_{11}H_{12}$**. $^1H$ NMR ($C_6D_6$) (a drop of $CH_2Cl_2$ was added to increase solubility): δ 7.19-7.16 (m, 4H, (PNP)Aryl-*H*), 7.11 (br, 2H, (PNP)Aryl-*H*), 7.04 (m, 2H, Catechol-*H*), 6.82 (m, 2H, Catechol-*H*), 6.78 (br, 4H, Catechol-*H*), 2.40 (m, 4H, C*H*$Me_2$), 2.21 (s, 6H, Ar-$CH_3$), 2.09-1.30 (br, 12H, $CB_{11}H_{12}$), 0.84 (m, 18H, CH$Me_2$), 0.61 (app. q (dvt), *J* = 8 Hz, 6H, CH$Me_2$). $^{13}C\{^1H\}$ NMR ($C_6D_6$) (a drop of $CH_2Cl_2$ was added to increase the solubility): δ 148.3 (Catechol-*C*), 147.2 (Catechol-*C*), 145.1 (t, *J* = 8 Hz, (PNP)Aryl-*C*), 139.9 ((PNP)Aryl-*C*), 134.9 ((PNP)Aryl-*C*), 134.2 ((PNP)Aryl-*C*), 130.1 (t, *J* = 14 Hz, (PNP)Aryl-*C*), 126.3 (t, *J* = 3 Hz, (PNP)Aryl-*C*), 124.4 (Catechol-*C*), 123.0 (Catechol-*C*), 113.0 (Catechol-*C*), 112.3 (Catechol-*C*), 26.3 (t, *J* = 13Hz), 24.8 (t, *J* = 13Hz), 20.9, 20.3, 18.6, 18.0, 17.7, one C for $CB_{11}H_{12}$ anion is missing. $^{31}P\{^1H\}$ NMR ($C_6D_6$) (a drop of $CH_2Cl_2$ was added to increase solubility): δ 45.0. $^{11}B\{^1H\}$ NMR ($C_6D_6$) (a drop of $CH_2Cl_2$ was added to increase solubility): δ -6.6, -12.9, -15.9 ($CB_{11}H_{12}$-*B*). Elem. An.. Found (Calculated) for $C_{39}H_{60}B_{13}NO_4P_2Pd$: C 51.27 (51.15); H 6.69 (6.60); N 1.64 (1.53).

**Hydrolysis of 203-$CB_{11}H_{12}$.** Compound **203-$CB_{11}H_{12}$** (5.0 mg, 0.0060 mmol) was dissolved in 1 mL $PhCF_3$ followed by the addition of 1 μL (excess) of degassed water. Upon addition, $^{31}P\{^1H\}$ NMR analysis indicated 15% of **201-$CB_{11}H_{12}$** and 85% of a

signal at 49.7 ppm (**202-$CB_{11}H_{12}$**). The reaction mixture was fully converted to **201-$CB_{11}H_{12}$** after standing overnight.

**[(PN(H)P)Pd(BCat)]$BAr^F_4$ (204-$BAr^F_4$)**. *Method A.* A solution of 0.015 mmol of **201-$BAr^F_4$** in 0.6 mL PhF in a J. Young tube was treated with catecholborane (8.0 μL, 0.075 mmol) and the reaction mixture was allowed to sit in a 90 ℃ oil bath overnight. $^{31}$P NMR observations revealed quantitative conversion to compound **204-$BAr^F_4$**. The mixture was passed through Celite and the volatiles were removed under vacuum. The oily residue was washed with hexanes three times. X-ray quality crystals were obtained by recrystallizing the off-white solid from $CH_2Cl_2$/hexanes. *Method B*. Compound **203-$BAr^F_4$** (63 mg, 0.039 mmol) was dissolved in ca. 0.6 mL PhF and then treated with degassed water (0.70 μL, 0.039 mmol). After 40 min at room temperature, $^{31}$P NMR observations revealed full conversion to compound **204-$BAr^F_4$**. Volatiles were removed under vacuum. The residue was recrystallized from $CH_2Cl_2$/hexanes and dried completely under vacuum. Yield: 40 mg, 0.026 mmol, 68%. $^1$H NMR ($CD_2Cl_2$): δ 7.71 (s, 8H, $BAr_4$-*H*), 7.54 (s, 4H, $BAr_4$-*H*), 7.37-7.43 (m, 6H, (PNP)Aryl-*H*), 7.23 (m, 2H, Catechol-*H*), 7.06 (m, 2H, Catechol-*H*), 6.89 (br, 1H, N-*H*), 2.71 (m, 2H, C*H*$Me_2$ ), 2.58 (m, 2H, C*H*$Me_2$ ), 2.43 (s, 6H, Ar-*$CH_3$*), 1.20-1.07 (m, 18H, CH*$Me_2$*), 0.92 (app. q (dvt), *J* = 7.2 Hz, 6H, CH*$Me_2$*). $^{13}$C{$^1$H} NMR ($CD_2Cl_2$): δ 162.6 (q, *J* = 50 Hz, $BAr_4$-*C*), 148.9 (Catechol-*C*), 145.2 (t, *J* = 8 Hz, (PNP)Aryl-*C*), 140.1 (t, *J* = 3 Hz, (PNP)Aryl-*C*), 135.4 ($BAr_4$-*C*), 135.2 ((PNP)Aryl-*C*), 134.1 ((PNP)Aryl-*C*), 129.6 (q, *J* = 34 Hz, $BAr_4$-*C*), 125.2 (d, *J* = 272 Hz, $BAr_4$-*C*), 125.7 (t, *J* = 4 Hz, , (PNP)Aryl-*C*), 122.9 (Catechol-*C*), 121.1 ($BAr_4$-*C*), 118.0 (t, *J* = 4 Hz, (PNP)Aryl-*C*), 112.5 (Catechol-*C*), 26.1 (t, *J* =

12 Hz), 24.3 (t, *J* = 13 Hz), 21.1, 19.7, 18.5, 18.4, 17.9. $^{31}P\{^{1}H\}$ NMR ($CD_2Cl_2$): δ 49.8. $^{11}B\{^{1}H\}$ NMR ($CD_2Cl_2$): δ 37.1 (br, Pd-*B*), -6.87 (s, $BAr^{F}{}_{4}$-*B*). Elem. An.. Found (Calculated) for $C_{64}H_{57}B_2NO_2F_{24}P_2Pd$: C 50.31 (50.64); H 3.59 (3.78); N 0.93 (0.92).

**Thermolysis of 204-$BAr^{F}_{4}$. 204-$BAr^{F}_{4}$** (13 mg, 0.009 mmol) was dissolved in 0.6 mL PhF in a J. Young NMR tube and the solution was heated at 90 ℃ for 15 h. $^{31}P$ NMR spectroscopic analysis indicated no observable changes.

**Hydrolysis of 204-$BAr^{F}_{4}$.** Compound **204-$BAr^{F}_{4}$** (12 mg, 0.008 mmol) was dissolved in 1 mL toluene in a NMR tube. Degassed water (1.0 μL, excess) was added. After 4 h, $^{31}P\{^{1}H\}$ NMR analysis indicated ca. 40% conversion to compound **201-$BAr^{F}_{4}$**. It was fully converted to **201-$BAr^{F}_{4}$** after ca. 40 h.

**NMR observation of (PNP)Pd(BCat) (205)** Compound **204-$BAr^{F}_{4}$** (18 mg, 0.012 mmol) was dissolved in 0.6 mL $CD_2Cl_2$ in a NMR tube followed by the addition of $Et_3N$ (5.0 μL, 0.060 mmol). The colorless solution changed to yellow immediately. $^{31}P$ NMR indicated > 90 % conversion to **205**. $^{1}H$ NMR ($CD_2Cl_2$): 7.51 (d, *J* = 9 Hz, 2H, (PNP)Aryl-*H*), 7.16 (m, 2H, Catechol-*H*), 6.96(m, 2H, Catechol-*H*), 6.92 (d, *J* = 8 Hz, 4H, (PNP)Aryl-*H*), 2.40 (m, 4H, C*H*$Me_2$ ), 2.19 (s, 6H, Ar-$CH_3$), 1.01-1.10 (m, 24H, CH$Me_2$). $^{31}P\{^{1}H\}$ NMR ($CD_2Cl_2$): 54.2. $^{1}H$ NMR ($C_6D_6$): 7.90 (d, *J* = 9 Hz, 2H, (PNP)Aryl-*H* ), 7.27 (m, 2H, Catechol-*H*), 6.91 (d, *J* = 9 Hz, 2H, (PNP)Aryl-*H*), 6.85 (m, 4H, overlap of aromatic resonaces), 2.20 (s, 6H, Ar-C$H_3$), 2.14 (m, 4H, C*H*$Me_2$), 1.06 (app. q (dvt), *J* = 8 Hz, 12H, CH$Me_2$), 0.96 (app. q (dvt), *J* = 8 Hz, 12H, CH$Me_2$). $^{13}C\{^{1}H\}$ NMR ($C_6D_6$): 160.7 (t, *J* = 10 Hz, (PNP)Aryl-*C* ), 150.0 (Catechol-*C*), 133.3

((PNP)Aryl-*C*), 132.8 ((PNP)Aryl-*C*), 123.7 (br, (PNP)Aryl-C), 121.7 (Catechol-*C*), 120.9 (t, *J* = 18 Hz, (PNP)Aryl-*C*), 115.2 (t, *J* = 5 Hz, (PNP)Aryl-*C*), 111.6 (Catexhol-*C*), 24.4 (t, *J* = 14 Hz), 20.5, 19.1, 18.0. $^{31}P\{^{1}H\}$ NMR ($C_6D_6$): 54.3. $^{11}B$ NMR ($C_6D_6$): 45.0 (br, Pd-*B*).

In another NMR tube, (PNP)PdH (15 mg, 0.028 mmol) was treated with HBCat (12 μL, 0.072 mmol) in about 0.60 mL of $C_6D_6$ and heated at 55 $^{o}$C. After 12, $^{31}P$ NMR revealed about 15% convertion of (PNP)PdH to (PNP)PdBCat. $H_2$ was also detected by $^{1}H$ NMR. The NMR tube was freeze-pump-thawed twice and put back to 55 $^{o}$C oil bath. After about 48 h, $^{31}P$ NMR revealed only about 28% convertion to (PNP)PdBcat. However, thermolysis of this reaction mixture of longer time at 55 $^{o}$C or at higher temperature (90 $^{o}$C) leads to several unidentified broad signal indicated by $^{31}P$ NMR.

**Synthesis of (PNP)Ir(BCat)$_2$ (206).** *Method A.* (PNP)Ir(H)$_2$ (51 mg, 0.082 mmol) was dissolved in 3 mL PhF followed by the addition of catecholborane (44 μL, 0.41 mmol). The red solution changed to orange within 5 min. The volatiles were removed under vacuum and the residule was recrystalized from PhF/pentane at -35 $^{o}$C. Some orange precipitate was collected the next day. $^{31}P\{^{1}H\}$ NMR ($C_6D_6$): 51.4. $^{1}H$ NMR ($C_6D_6$): 7.60 (d, *J* = 9 Hz, 2H, (PNP)Aryl-*H*), 7.10 (br, 2H, (PNP)Aryl-*H*), 6.96 (m, 4H, CatB), 6.85 (d, *J* = 9 Hz, 2H, (PNP)Aryl-*H*), 6.70 (m, 4H, CatB), 2.94 (m, 4H, C*H*Me$_2$), 2.19 (s, 6H, Ar-C*H*$_3$), 1.45 (app.q (dvt), *J* = 8 Hz, 12H, CH*Me*$_2$), 1.08 (app.q(dvt), *J* = 8 Hz, 12H, CH*Me*$_2$). *Method B.* (PNP)Ir(H)(Mes) (10.0mg, 0.013 mmol) was dissolved in 0.6 mL of mesitylene in a J. Young NMR tube followed by the addition of CatB-Bcat

(5.0, 0.021 mmol). The reaction mixture was heated at 70 $^{o}$C for 1.5 h. The $^{31}$P NMR analysis revealed that it fully converted to compound **206**.

**Synthesis of (PNP)Ir(BCat)(Cl) (207).** (PNP)Ir(H)(Mes) (100 mg, 0.135 mmol) was dissolved in about 3 mL of mesitylene in a flask. CatB-Cl (23.0 mg, 0.148 mmol) was added to the solution. The reaction mixture was heated at 80 $^{o}$C for 1 h. The volatiles were vacuum tranferred to another flask and the left residule was recrystalized from PhF/pentane at -35 $^{o}$C. The purple solid was collected the next day and dried under vacuum. $^{31}$P{$^{1}$H} NMR ($C_6D_6$): 41.3. $^{1}$H NMR ($C_6D_6$): 8.02 (d, *J* = 9 Hz, 2H, (PNP)Aryl-*H*), 6.91 (br, 2H, (PNP)Aryl-*H*), 6.80 (m, 4H, CatB), 6.61 (d, *J* = 9 Hz, 2H, (PNP)Aryl-*H*), 2.87 (m, 2H, C*H*Me$_2$), 2.50 (m, 2H, C*H*Me$_2$), 2.15 (s, 6H, Ar-C*H*$_3$), 1.45 (app.q (dvt), *J* = 8 Hz, 6H, CH*Me*$_2$), 1.15 (app.q (dvt), *J* = 8 Hz, 6H, CH*Me*$_2$), 0.95 (app.q (dvt), *J* = 8 Hz, 6H, CH*Me*$_2$), 0.63 (app.q, *J* = 8 Hz, 6H, CH*Me*$_2$).

**X-Ray data collection, solution, and refinement for 202-BAr$^{F}_{4}$.** All operations were performed on a Bruker-Nonius Kappa Apex2 diffractometer, using graphite-monochromated MoKα radiation. All diffractometer manipulations, including data collection, integration, scaling, and absorption corrections were carried out using the Bruker Apex2 software.[105] Preliminary cell constants were obtained from three sets of 12 frames. Data collection was carried out at 120 K, using a frame time of 15 sec and a detector distance of 60 mm. The optimized strategy used for data collection consisted of six phi and four omega scan sets, with 0.5 ° steps in phi or omega; completeness was 99.0%. A total of 4016 frames were collected. Final cell constants were obtained from the xyz centroids of 9801 reflections after integration.

From the systematic absences and the observed metric constants and intensity statistics, space group *P*-1 was chosen initially; subsequent solution and refinement confirmed the correctness of this choice. Compound **202-BAr$^{F}_{4}$** contained significant disorder, which was resolved successfully. Two-component disorder was described with a constraint that the occupancies of the major and minor components sum to 1.0. Major component disordered atoms were refined by using isotropic displacement parameters, while the atoms involved in the minor component disorder were refined by using isotropic displacement parameters. Atom sets F(22) through F(24) and F(221) through F(241) comprised the major and minor sets, respectively; the major set occupancy was 0.820(6). The ordered non-hydrogen atoms were refined using anisotropic displacement parameters. The hydride ion attached to Pd was located on an electron density difference map and refined using an isotropic displacement parameter; the final Pd-H distance was 1.426(35) Å; other hydrogen atoms were fixed at calculated geometric positions and allowed to ride on the corresponding carbon atoms. The structure was solved using SIR-92,[106] and refined (full-matrix-least squares) using the Oxford University *Crystals for Windows* program.[107] The final least-squares refinement converged to $R_1 = 0.0477$ ($I > 2\sigma(I)$, 14909 data) and $wR_2 = 0.1471$ ($F^2$, 22029 data, 882 parameters).

During the structure solution, electron density difference maps revealed that there was considerable disordered solvent molecules (from history, methylene chloride and/or pentane) in a volume of 654 Å$^3$ per unit cell; the peaks could not be modeled successfully. Thus, the structure factors were modified using the PLATON

SQUEEZE [108] technique, in order to produce a "solvate-free" structure factor set. PLATON reported a total electron density of 104 e- for the cavity, slightly larger than two methylene chloride molecules, with perhaps an additional pentane (110 non-H atom electrons). Use of the SQUEEZE technique resulted in a decrease of ca 4% in *R*. The IUCr CheckCIF routine reported one Alert A and five Alert B issues; these Alerts are related to the disorder issues discussed above.

**X-Ray data collection, solution, and refinement for 203-$CB_{11}H_{12}$.** All operations were performed on a Bruker-Nonius Kappa Apex2 diffractometer, using graphite-monochromated MoKα radiation. All diffractometer manipulations, including data collection, integration, scaling, and absorption corrections were carried out using the Bruker Apex2 software.[105] Preliminary cell constants were obtained from three sets of 12 frames. Data collection was carried out at 120 K, using a frame time of 15 sec and a detector distance of 60 mm. The optimized strategy used for data collection consisted of 5 phi and 4 omega scan sets, with 0.5 ° steps in phi or omega; completeness was 99.9%. A total of 4202 frames were collected. Final cell constants were obtained from the xyz centroids of 9347 reflections after integration.

From the systematic absences, the observed metric constants and intensity statistics, space group *C2/c* was chosen initially; subsequent solution and refinement confirmed the correctness of this choice. The structure was solved using SIR-92,[106] and refined (full-matrix-least squares) using the Oxford University *Crystals for Windows* program.[107] All non-hydrogen atoms were refined using anisotropic displacement parameters; hydrogen atoms were fixed at calculated geometric positions and allowed to ride on the

corresponding carbon atoms. The final least-squares refinement converged to $R_1$ = 0.0286 ($I > 2\sigma(I)$, 14450 data) and $wR_2$ = 0.0741 ($F^2$, 15886 data, 631 parameters).

**X-Ray data collection, solution, and refinement for 204-BAr$^{F}_{4}$.** All operations were performed on a Bruker-Nonius Kappa Apex2 diffractometer, using graphite-monochromated MoKα radiation. All diffractometer manipulations, including data collection, integration, scaling, and absorption corrections were carried out using the Bruker Apex2 software.[105] Preliminary cell constants were obtained from three sets of 12 frames. Data collection was carried out at 120 K, using a frame time of 30 sec and a detector distance of 60 mm. The optimized strategy used for data collection consisted of two phi and five omega scan sets, with 0.5 ° steps in phi or omega; completeness was 99.4%. A total of 2235 frames were collected. Final cell constants were obtained from the xyz centroids of 9849 reflections after integration. From the systematic absences and the observed metric constants and intensity statistics, space group $P2_1/n$ was chosen initially; subsequent solution and refinement confirmed the correctness of this choice. The structure was solved using SIR-92,[106]and refined (full-matrix-least squares) using the Oxford University *Crystals for Windows* program.[107] All ordered non-hydrogen atoms were refined using anisotropic displacement parameters. Compound **204-BAr$^{F}_{4}$** contained significant disorder, which was resolved successfully. In cases where two-component disorder could be resolved (see below) it was described with a constraint that the occupancies of the major and minor components sum to 1.0. Major component disordered atoms were refined by using anisotropic displacement parameters, while minor component atoms were refined using isotropic displacement parameters. The F

atoms of the trifluoromethyl groups associated with carbon atoms C(40), C(55), C(63) and C(64) had major component occupancies of 0.775(8), 0.770(6), 0.831(9) and 0.791(6), respectively. Solvate water and dichloromethane molecules were located during the analysis of the structure. However, it was clear from consideration of atomic contacts that the solvate molecules were not present simultaneously in a single unit cell. Thus, their occupancies were also constrained to sum to 1.0; the occupancy of the dichloromethane solvate was 0.700(3). The ordered non-hydrogen atoms were refined using anisotropic displacement parameters. Hydrogen atoms were fixed at calculated geometric positions and allowed to ride on the corresponding carbon atoms. The final electron-density difference map still contained peaks in the range 1.0 – 2.5 e-/Å$^3$ near the two THF solvate molecules. The final least-squares refinement converged to $R_1$ = 0.0457 ($I > 2\sigma(I)$, 10930 data) and $wR_2$ = 0.1298 ($F^2$, 16624 data, 953 parameters). The IUCr CheckCIF routine reported two Alert B issues; these Alerts are related to the disorder issues discussed above.

# CHAPTER III

# C-H OXIDATIVE ADDITION TO A (PNP)Ir CENTER AND LIGAND-INDUCED REVERSAL OF BENZYL/ARYL SELECTIVITY*

## *3.1 Introduction*

C-H bonds oxidative addition to the transition metals has been an attractive topic to chemists because of the benefit to conduct selective C-H functionalization with unreactive C-H bonds.[109, 110] In 1972, Shilov reported the electrophilic C-H bond activation to Pt(II) (Scheme 3-1).[111] The stoichiometric addition of Pt(IV) to the aqueous solution of Pt(II) and methane finally leads to the production of methanol and methyl chloride. The early examples of C-H bond oxidative addition are all involved in either aryl C-H bonds or intramolecular addition of ligand C-H bonds. In 1982, Bergman and Graham reported the first example of isolation of stable alkyl iridium hydride complexes from the C-H bond oxidative addition of an alkane (Scheme 3-2).[112] Since then, extensive studies of both stoichiometric and catalytic C-H bonds oxidative addition reactions have been reported. The majority of the examples of the metal complexes that underwent C-H oxidative addition are group 7-10 metals containing cyclopentadienyl ligands (Cp) or anionic tridentate ligands, such as tris-pyrazolylborate

*Reprinted (parts of this chapter) with permission from "C-H Oxidative Addition to a (PNP)Ir Center and Ligand Induced Reversal of Benzyl/Aryl Selectivity" by Zhu, Y.; Lei, F.; Chen, C. H.; Finnell, S. R.; Foxman, B.; Ozerov, O. V., 2007. *Organometallics*, 26, 6066-6075, Copyright[2007] by American Chemical Society. "Probing the C−H Activation of Linear and Cyclic Ethers at (PNP)Ir" by Whited, M. T.; Zhu, Y.; Timpa, S. D.; Chen, C. H.; Foxman, B. M.; Ozerov, O. V.; Grubbs, R. H., 2009. *Organometallics*, 28, 4560-4570, Copyright[2009] by American Chemical Society.

(Tp). Such systems have also been used in the mechanistic study to understand mechanisms of C-H activation.[113]

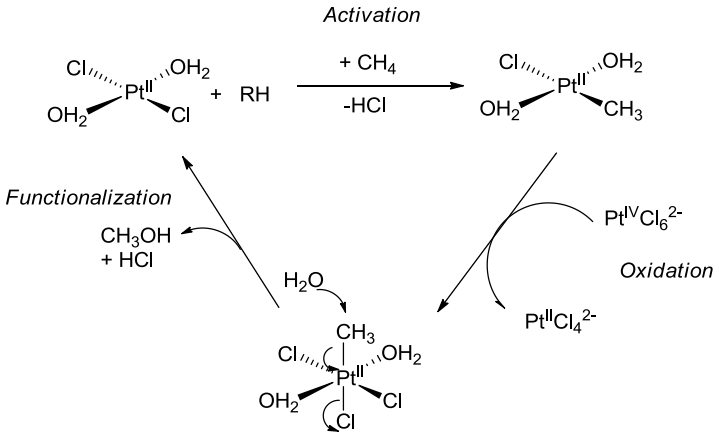


**Scheme 3-1.** Methane C-H bond activation mediated by platinum.

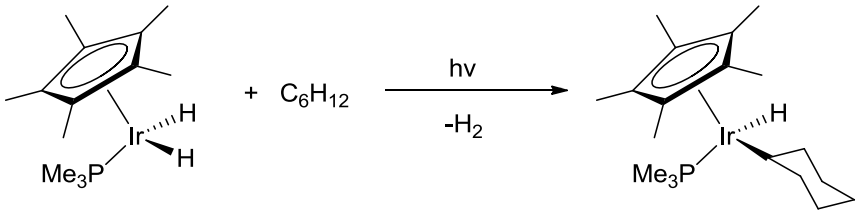


**Scheme 3-2.** Intermolecular alkane C-H oxidative addition by Cp*Ir(III) complex.

Although work by Bergman, Jones, Grahams, and others have demonstrated that there was remarkable selectivity among C-H bonds,[113,114] control and discrimination between activation of aromatic C($sp^2$)-H bonds and aliphatic C($sp^3$)-H bonds, especially benzylic C-H bonds, is still an issue for any substrate containing both. Generally, transition metal systems typically display both the thermodynamic and kinetic preference for the activation of aromatic C-H bonds. The thermodynamic driving force

to activate stronger C-H bonds has been traced to the greater differences in M-C bond strengths compared with the case for C-H bond strengths.[115] Selectivity for a product of benzylic activation may come in cases where (a) formation of an aryl-metal product is sufficiently sterically disfavored,[107-117] (b) the benzylic product is stabilized by $\eta^3$ coordination,[118,119] or (c) in the sense of kinetic selectivity, the reaction proceeds via

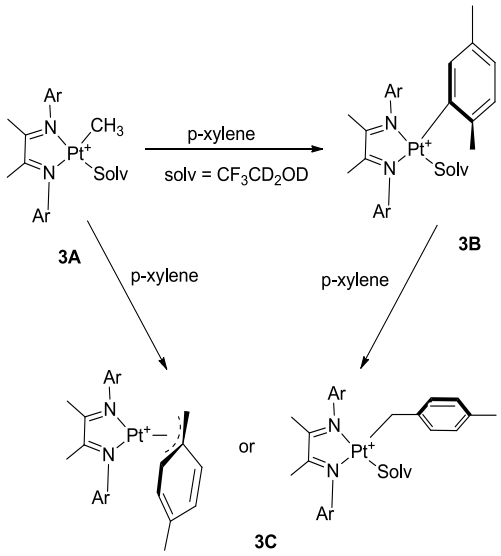


**Scheme 3-3.** Benzylic C-H activation with cationic Pt(II) complexes.

homolysis pathways.[120] Bercaw et al. have reported the kinetic and thermodynamic preferences in aryl vs benzylic C-H bond activation with cationic Pt(II) complexes (Scheme 3-3).[118b] Complex **3A** reacted with mesitylene exclusively to give benzylic C-H activation product. However, *p*-xylene reacted with **3A** to initially give products of both aromatic and benzylic activation. After the starting material was completely consumed,

compound **3C** continued to grow at the expense of compound **3B**. The authors suggested that the thermodynamic preference for benzylic C-H activation appears to result from stabilizing $\eta^3$-bonding species. Eisenberg et al. reported an aryl-to-benzyl rearrangement induced by coordination of ethylene to an Ir(I) center in $(Me_3C_6H_2)Ir(CO)(dppe)$, but the mechanistic details were not fully elucidated.[121]

The interest in C-H activation is motivated by the goal of selective C-H functionalization. Functionalization of arene or alkane C-H bonds has been accomplished by utilizing transition metal complexes. Alkane dehydrogenation to produce olefins catalyzed by (PCP)Ir system[122](Scheme 3-4) is a good example because olefins are the most important feed stocks in chemical industry. Functionalization of

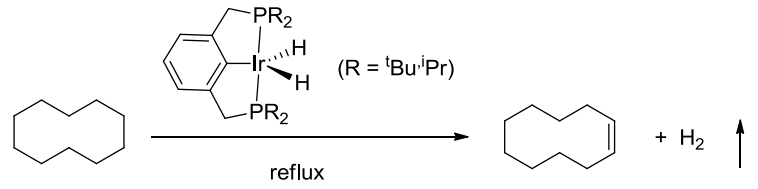


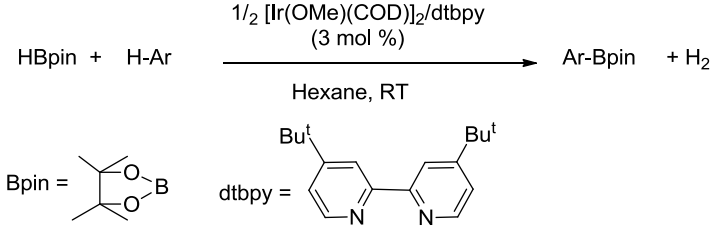


**Scheme 3-4.** Examples of functionalizaiton of alkanes and arenes.

alkanes and arenes with main group reagents, such as borylation[123]and silylation[124], has also been investigated by a few research groups (Scheme 3-4). Our group explored the C-H oxidative addition reactions in the (PNP)Ir system. Previous studies showed that the three-coordinate, $d^8$ iridium intermediate could undergo C-H oxidative addition of arenes like benzene or toluene to form five coordinate Ir(III) complexes. For the substrates of halobenzene (chlorobenzene and bromobenzene), (PNP)Ir system displayed the reactivity of kinetic C-H oxidative addition and thermodynamic C-halide oxidative addition (Scheme 3-5).[1b] In this chapter, an example of ligand-induced reversal aryl/benzyl C-H selectivity in the (PNP)Ir system will be described. The causes of the reversal preference and the mechanism of the transformations will be revealed. Another small project regarding to C-H activation of cyclic ethers by (PNP)Ir will also be described in this chapter.

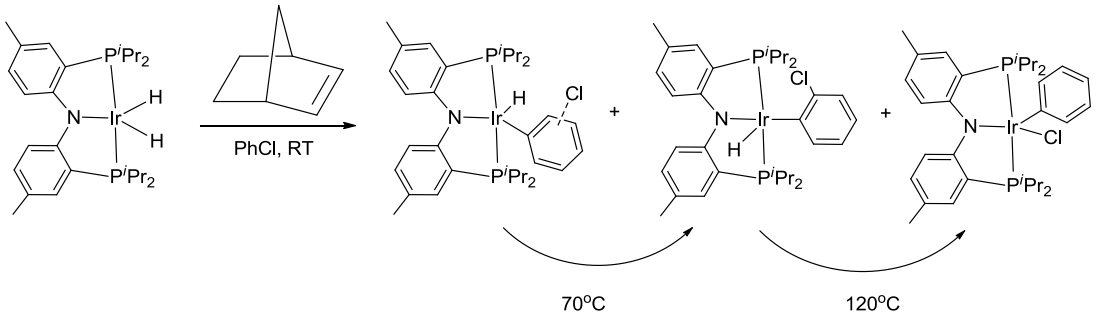


**Scheme 3-5.** Kinetic C-H and thermodynamic C-Cl oxidative addition at (PNP)Ir.

### *3.2 Results and discussion*

*3.2.1 Synthesis of (PNP)Ir(H)(Mes)*

Previous studies by Goldman and others have demonstrated that three-coordinate, 14e (PCP)Ir generated by reacting (PCP)Ir$(H)_2$ with TBE (tert-butylethylene), was a very reactive intermediate that can easily do oxidative addition of C-H bonds in alkanes and arenes.[125] Similar to the (PCP)Ir chemistry, the 14e (PNP)Ir is the key intermediate for the investigation of oxidative addition reactions in our system. Our group found[1b] that the reactive (PNP)Ir intermediate could be generated, although not isolable or even observable by NMR, through the reaction of (PNP)Ir$(H)_2$ with hydrogen acceptor, such as norbornene (NBE) (Scheme 3-6).

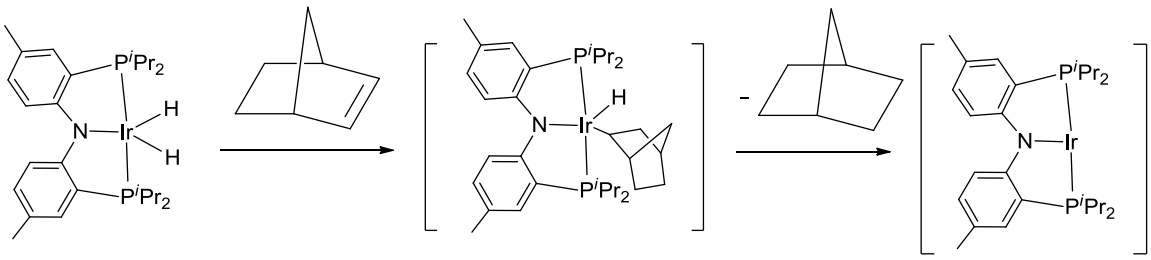


**Scheme 3-6.** The approach to the three-coordinate (PNP)Ir intermediate.

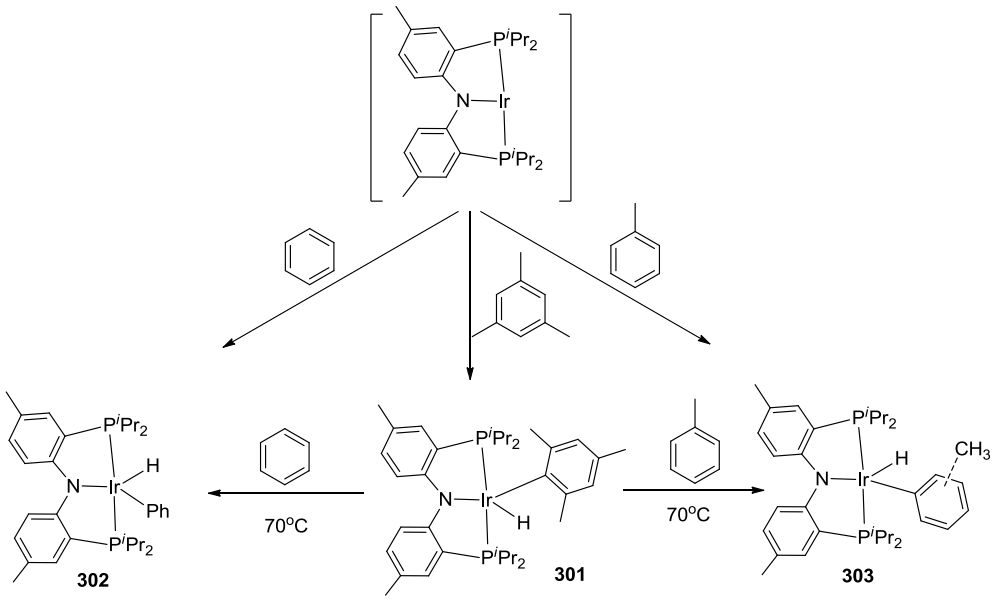


**Scheme 3-7.** Aryl C-H bond oxidative addition at (PNP)Ir fragment.

Dr. Lei Fan has already demonstrated that aryl C-H bonds of arenes like benzene and toluene oxidatively added to (PNP)Ir to form (PNP)Ir(H)(Aryl) complexes (Scheme 3-7).[1b] The aryl C-H bond of a more steric bulky arene, mesitylene, could also add to (PNP)Ir to form (PNP)Ir(H)(Mes) **301**. It is worth mentioning that compound **301** could be obtained with 'one pot' synthesis from the PN(H)P ligand and $[Ir(COD)HCl_2]_2$ with 68% isolated yield as indicated in Scheme 3-8.

*3.2.2 (PNP)Ir(H)(Mes): a good synthon to (PNP)Ir*

Interestingly, thermolysis of **301** in benzene or toluene at 70 ℃ led to the elimination of mesitylene and formation of **302** or **303**, respectively (Scheme 3-7). These results indicated that the C-H addition of mesitylene was reversible. Similar to $(PNP)Ir(H)_2$/norbornene case, **301** can be served as a synthon to 14e (PNP)Ir. This

method opens another door to generate (PNP)Ir where (PNP)Ir$(H)_2$/norbornene method in some cases does not work.

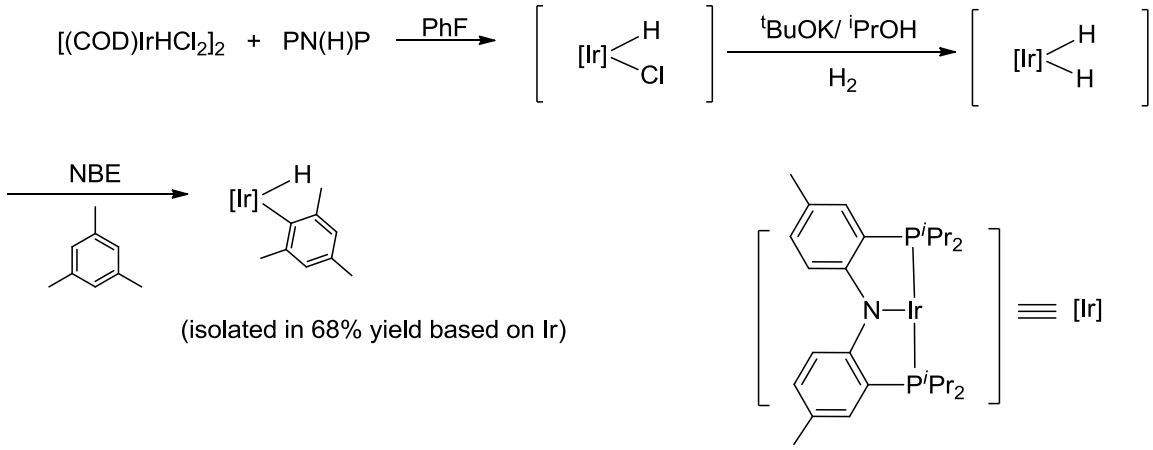


**Scheme 3-8.** 'One pot' synthesis of compound **301**.

*3.2.3 Ligand induced aryl/benzyl C-H oxidative addition*

As shown above, (PNP)Ir has displayed its ability of aromatic C-H oxidative addition reactions. We are very interested in examining the reactivity of (PNP)Ir with heteroatom-containing substrates such as heteroaromatics and ethers. When complex **301** was treated with excess pyridine in $C_6D_6$, the anticipated C-H OA of pyridine did not take place. Instead, an entirely different product **304a** was isolated after 24 h at ambient temperature (Scheme 3-9). Similar products were obtained from the reaction of **301** with $PMe_3$ (**304b**) and thiazole (**304c**). Compounds **304a-c** were fully characterized by NMR spectroscopy. For instance, in **304a**, the Ir-$CH_2$ unit gave rise to characteristic

resonances in the $^{1}H$ ($\delta$ 3.67, br t, $J_{H\text{-}P}$ = 6 Hz) and $^{13}C\{^{1}H\}$ ($\delta$ -6.6, t, $J_{C\text{-}P}$ = 2 Hz) NMR spectra. The hydride resonance in **304b** displayed a large $^{2}J_{H\text{-}P}$ value of 142 Hz for the coupling with the $^{31}P$ nucleus in $PMe_3$, indicative of the *trans* disposition of $PMe_3$ and the hydride. In the solid-state structure[126] of **304c** (Figure 3-1), the N-bound thiazole

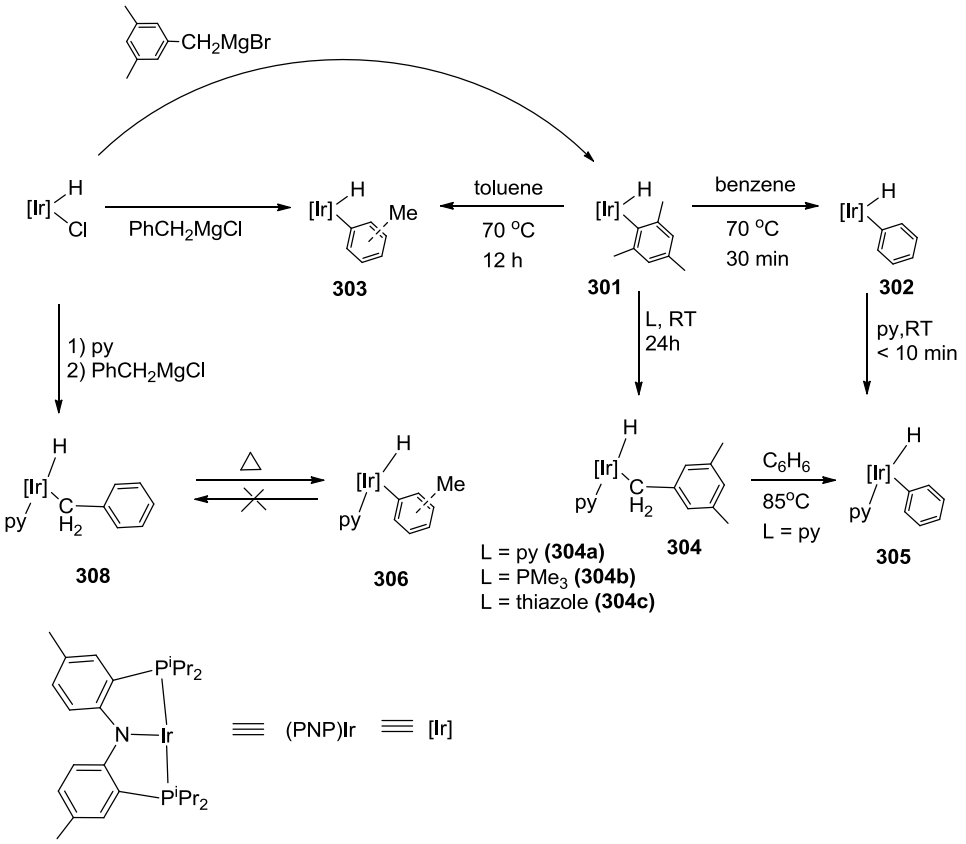


**Scheme 3-9.** Ligand induced benzylic C-H oxidative addition.

ligand is also trans to the hydride. The pyridine ligand in **304a** is most likely *trans* to the hydride as well.

The importance of the steric influence in the aryl to benzyl isomerization was investigated. In contrast to the case for **301**, the less sterically encumbered aryl complexes **302** and **303** readily coordinated pyridine to give **305** and **306**, respectively (Scheme 3-9). Neither **303** nor **306** converted to the corresponding benzyl isomers (PNP)Ir(H)($CH_2$Ph) **307** and **308** upon thermolysis (20 h, 95 ℃). On the other hand, the reverse reactions did proceed: (a) **308** converted to **306** upon thermolysis (complete disappearance of **308** after 70 ℃, 18 h; unidentified products also observed), and (b) an attempted synthesis of **307** from (PNP)Ir(H)(Cl) and Ph$CH_2$MgCl led to **303**.

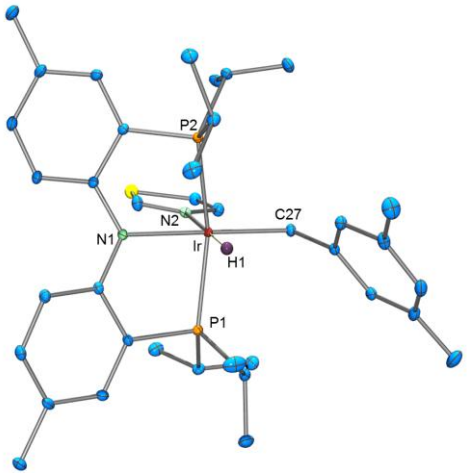


**Figure 3-1.** ORTEP drawing[103] of **304c** (50% thermal ellipsoids). Hydrogen atoms are omitted for clarity except for Ir-H. Selected bond distances (Å) and angles (deg) for **304c**. Ir-P1, 2.2866(7); Ir-P2, 2.3026(7); Ir-N1, 2.137(2); Ir-N2, 2.213(2); Ir-C27, 2.135(3); P1-Ir-P2, 158.33(2); P1-Ir-N1, 82.99(6); P1-Ir-N2, 98.27(6); P2-Ir-N1, 80.56(6); N1-Ir-C27, 179.12(10); P2-Ir-C27, 100.01(8).

Thus, unlike the case for the mesityl/3,5-dimethylbenzyl pair, in the tolyl/benzyl pair, the thermodynamic preference for the aryl isomer exists not only for the five-

coordinate but also for the six-coordinate case. In a sense, the coordination of pyridine (possible to **301** but not **303**) compensates for the ostensibly unfavorable mesityl-to-3,5-dimethylbenzyl isomerization, but the difference in the energies of binding of pyridine to **303** vs **307** does not override the intrinsic unfavorability of tolyl-to-benzyl isomerization. Continued thermolysis of **304a** in $C_6D_6$ led to the production of **305** via activation of the solvent (Scheme 3-9).

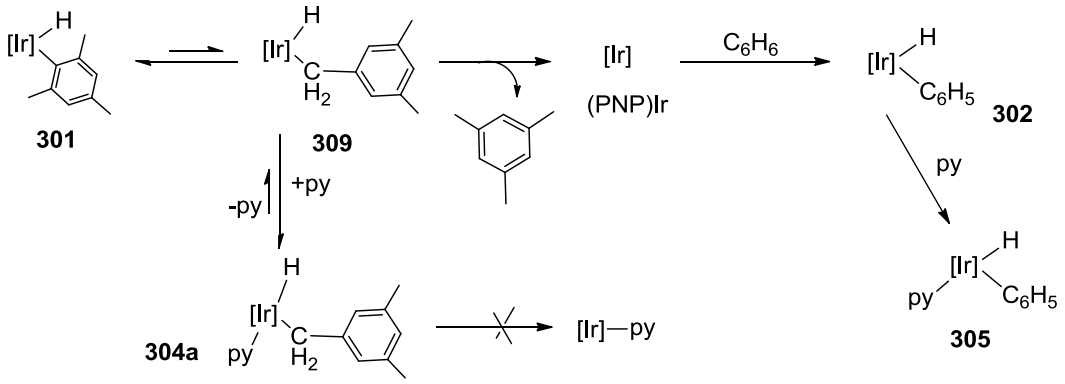


**Scheme 3-10.** Proposed mechanism for transformation of **301** to **304a**, and **304a** to **305**.

*3.2.4 Mechanism for the aryl/benzyl isomerization*

Some kinetic studies were conducted in order to fully understand these transformations. The rate of the transformation of **301** to **304a** in $C_6D_6$ was found to be independent of the concentration of pyridine in the 0.5-2.2 M range. Notably, **301** does not detectably bind pyridine in solution at 22 ℃. This strongly implies that the rate-determining step is the transformation of **301** to its benzylic isomer **309** followed by fast

trapping of the latter by pyridine. An attempt to isolate **309** by treatment of (PNP)IrHCl with 3,5-$Me_2C_6H_3CH_2MgBr$ led to the observation of **301** as the major product (Scheme 3-10). Thus, for the five-coordinate system, the aryl isomer (**301**) is thermodynamically preferred over the benzylic isomer (**309**), although **309** is kinetically accessible. Addition of pyridine, thiazole, or $PMe_3$, however, causes the preference to reverse and favor the benzylic products **304a-c**.[127]

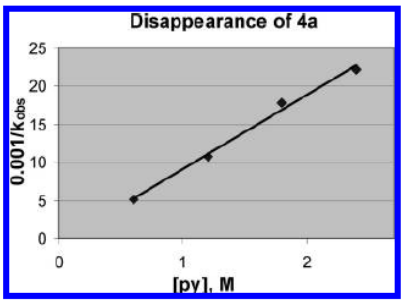


**Figure 3-2.** Rate of disappearance of **304a** as a function of pyridine concentration.

Kinetic studies carried out at 85 ℃ revealed the inverse dependence of the rate of conversion of **304a** to **305** on the concentration of pyridine (Figure 3-2). This is consistent with the dissociation of pyridine from **304a** being necessary for the reaction to proceed (Scheme 3-10). Elimination of mesitylene generates transient (PNP)Ir, which reacts with benzene to give **302**, and the latter is trapped by pyridine to give **305**. A dissociative mechanism for the activation of benzene by **301** is consistent with the previously demonstrated intermediacy of analogous three coordinate Ir fragments (e.g., (PCP)Ir and Milstein's$[(PN^{pyr}P)Ir]^+$)[128,129] in C-H oxidative addition reactions. The lack of direct reductive elimination from the six-coordinate $d^6$ complex **304a** dovetails with

the findings of Goldberg et al. of the necessity of the five-coordinate intermediate for C-X reductive elimination from six-coordinate Pt(IV) $d^6$ complexes.[130] Goldberg et al. investigated the reductive elimination of the methane from $(PH_3)_2Cl_2Pt(CH_3)H$ by computational study. It was found that Pt(IV) complexes almost invariably took place via a pathway involving ligand dissociation before the reductive elimination step. On the other hand, Goldman et al. reported the example of trapping of the reductive-elimination-prone $d^6$ complex (PCP)Ir(H)(Ph) with CO to form a robust six-coordinate CO adduct.[125b] It has also been found that oxidative addition, the reverse process of reductive elimination, is much faster in the three coordinate species than that in the four coordinate species. Halpern showed that $RhCl(PPh_3)_2$, resulting from the loss of a $PPh_3$ ligand from $RhCl(PPh_3)_3$, underwent oxidative addition of $H_2$ at least $10^4$ times faster than $RhCl(PPh_3)_3$.[131]

*3.2.5 C-H oxidative addition of cyclic ethers at (PNP)Ir*

This was a project in collaboration with Prof. Grubbs' group in Caltech. In 2008, Grubbs reported double C-H activation of ethers by (PNP)Ir (Scheme 3-11).[132] In the case of methyl tert-butyl ether, an Ir(I) carbene complex was produced through α,α-dehydrogenation by using excess norbornene as hydrogen acceptor. When reacting with diethyl ether, an Ir(I) vinyl ether adduct was fromed via α,β-dehydrogenation. The versatile reactivity of (PNP)Ir towards different ethers arouse our interest in examining the scope of ether C-H activation. The goal of exploring C-H oxidative addition of ethers was to understand the nature of C-H activation steps and the factors governing selectivity and product distribution. We were focused on the cyclic ethers

(tetrahydrofuran (THF), 1,4-dioxane, tetrahydropyran (THP), and 1,3,5-trioxane) while the Grubbs' group was exploring the linear ethers.

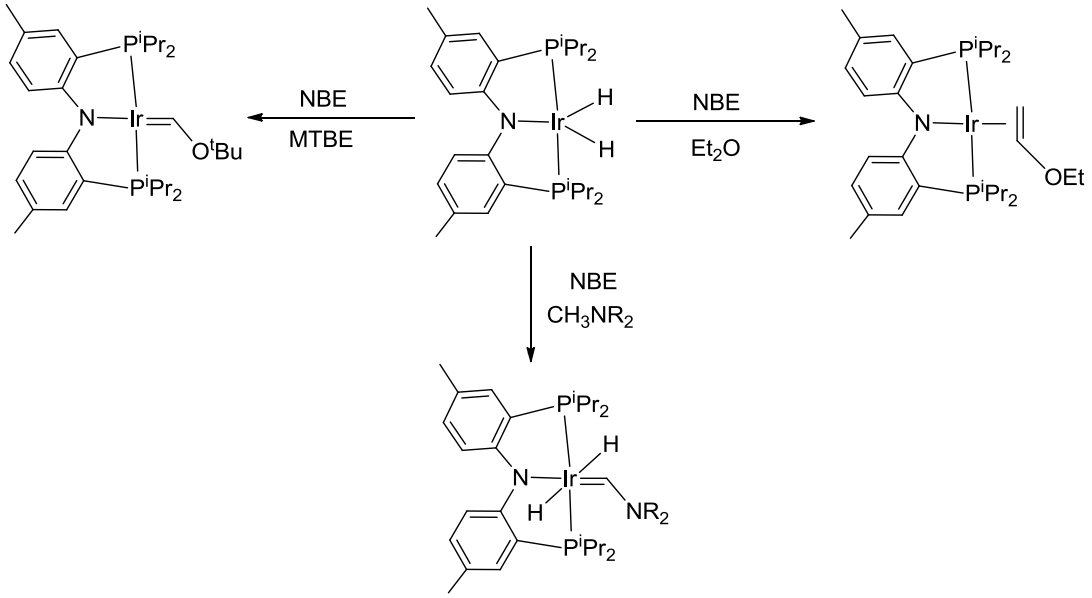


**Scheme 3-11.** C-H activation of ethers and amine at (PNP)Ir center. (by Grubbs' group)

**Reactions with THF.** Reaction of (PNP)$IrH_2$ (**310**) with norbornene (2 equiv) in THF resulted in the immediate appearance of a new species as shown by $^{31}$PNMR (δ 46.7 ppm). This complex could not be cleanly isolated due to slow decomposition to another species, observed at δ 43.1 ppm by $^{31}$P NMR. Thermolysis of the reaction mixture at 60 $^{o}$C for 7 h resulted in complete conversion to the second species. This second species was isolated and identified as the carbene complex derived from α,α-dehydrogenation of THF (Scheme 3-12). Most tellingly, complex **312** displays a diagnostic carbene resonance in its $^{13}$C NMR spectrum (δ 232.6 ppm, t, $J_{P\text{-}C}$ = 11 Hz).

The formation of the carbene complex presumably proceeds by initial C-H bond activation to form the iridium hydride alkyl complex which subsequently rearrange to the hydridocarbene complex by rapid α-hydrogen elimination. Theoretical studies suggest that α-hydrogen migrations can be kinetically favorable if a coordinatively unsaturated species can be accessed.[133]

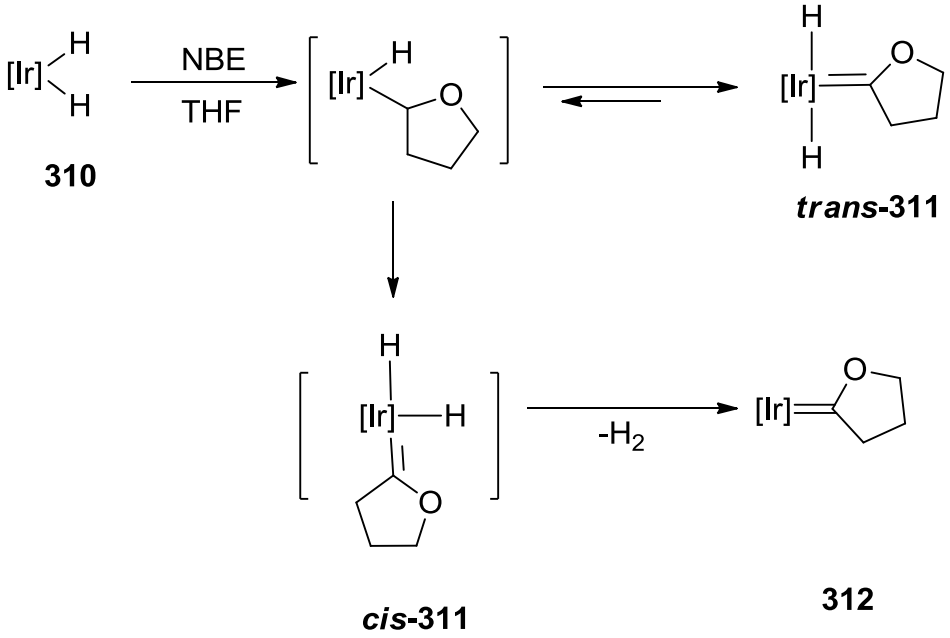


**Scheme 3-12.** Double C-H bond activation of THF: the formation of Ir(I) carbene complex.

The structure of Compound **312**[134] was further confirmed by single-crystal X-ray diffraction (Figure 3-3). Similar to MTBE-derived carbene,[132a] the carbene cants slightly (ca. 20 $^{o}$C out of the square plane) to maximize the push-pull interaction

between the filled pπ amido and empty pπ carbene orbitals. The Ir1-C14 bond distance (1.92 Å) is very similar to that observed in other iridium THF carbene structure.[136]

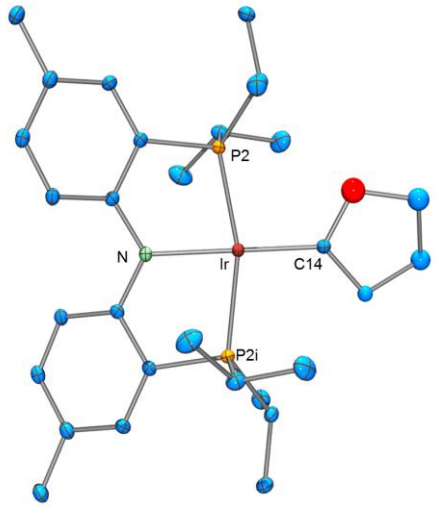


**Figure 3-3.** ORTEP drawing[103] of **312** (50% thermal ellipsoids). Crystal was obtained by Samuel Timpa. Hydrogen atoms are omitted for clarity. Selected bond distances (Å) and angles (deg) for **312**. Ir-P2, 2.2868(8); Ir-N, 2.073(3); Ir-C14, 1.921(4); P2-Ir-P2i, 163.12(4); P2-Ir-N, 81.56(2); P2-Ir-C14, 98.44(2); C14-Ir-N, 179.994.

Although the intermediate leading to compound **312** is not stable enough to be fully characterized, it was accessible via an alternate synthesis. Addition of excess 2,3-dihydrofuran (3 equiv) to a solution of dihydride in benzene-$d_6$ led to quantitative generation of the same intermediate observed in the formation of carbene **312**, which was identified as the trans-dihydrido carbene complex ***trans*-311**, a structural and electronic relative of the trans-dihydrido aminocarbenes previously reported.[132c] ***trans*-311** exhibits $C_{2v}$ symmetry in solution, indicating that rotation about the iridium-carbon

bond is fast on the NMR time scale, as expected on the basis of the similar behavior of the related aminocarbenes.[132b,c] The $^{1}$H NMR spectrum of ***trans*-311** shows a triplet hydride resonance characteristic of such a complex (δ -7.86 ppm, t, $^{2}J_{P\text{-}H}$ = 15 Hz, 2H), as well as a distinctive carbene resonance in its $^{13}$C NMR spectrum (δ 261.2 ppm). In order to lose hydrogen and generate **312**, complex ***trans*-311** must isomerize to place the hydride ligands in a cis configuration to allow for reductive elimination of hydrogen, but a buildup of the cis-dihydrido isomer of ***cis*-311** is not observed. (Note: Compound **312** was synthesized and characterized by Samuel Timpa)

**Reactions with 1,4-dioxane.** Encouraged by the formation of carbene in the double C-H activation of THF reactions, the C-H activation of 1,4-dioxane was explored. Reaction of (PNP)Ir$H_2$ (**310**) with norbornene in 1,4-dioxane resulted in the immediate formation of a new product exhibiting two doublet resonances in its $^{31}$P NMR spectrum

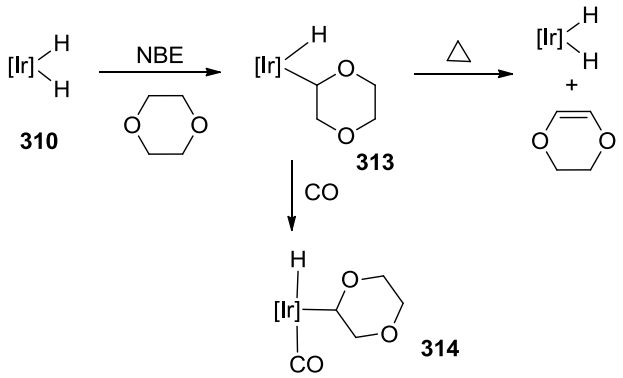


**Scheme 3-13.** C-H activation of 1,4-dioxane with (PNP)Ir fragment.

(δ 46.5 and 43.7 ppm, $^{2}J_{P\text{-}P}$ = 322 Hz). However, direct isolation of this species proved difficult, as complete removal of solvent or thermolysis led to regeneration of starting material **310** with expulsion of 2,3-dihydro-1,4-dioxine. Partial removal of solvent and redissolving the mixture in benzene-$d_6$ allowed characterization of this species by $^{1}$H NMR. The $^{1}$H NMR spectrum revealed a distinct hydride signal at -34.2 ppm (t, $^{2}J_{P\text{-}H}$ = 13 Hz). This upfield hydride resonance is very similar to the hydride chemical shift for compound (PNP)Ir(H)(Ph) (-38 ppm). It seemed most likely that this intermediate was the product of a single C-H oxidative addition of 1,4-dioxane to (PNP)Ir, affording (PNP)Ir(H)(1,4-dioxan-2-yl) **313** (Scheme 3-13).

The further identification for compound **313** was accomplished by a trapping experiment. Goldman has shown that the five-coordinate (PCP)Ir(H)(Ph), which easily undergoes reductive elimination of benzene, may be trapped by addition of CO to afford a stable six-coordinate iridium(III) adduct.[125b] Interestingly, compound **313** could also be trapped with CO to form the stable compound **314**. Compound **314** was isolated and spectroscopically characterized. This complex is structurally related to a previously reported carbonyl adduct of a (PNP)-supported aminoalkyl hydride complex of iridium(III)[132c] and exhibits a diagnostic carbonyl stretch in its infrared absorbance spectrum ($\nu_{CO}$=1980 cm$^{-1}$). The characterization of compound **314** further supported the assignment of compound **313** as the single C-H oxidative addition product of 1,4-dioxane.

**Reactions with THP.** Treatment of (PNP)Ir(H)$_2$ with 4 eq. of norbornene in neat THP resulted in the full consumption of (PNP)Ir(H)$_2$ and the formation of a mixture of

unidentified products as indicated by $^{31}P$ NMR within 10 min. However, after 1 h, $^{31}P$ NMR analysis revealed the formation of (PNP)Ir$(H)_2$ (~70%) and another species at 42.9 ppm (~30%). The reaction mixture was fully converted to this 42.9 ppm species eventually by adding a lot excess norbornene (~ 100 eq.) This compound was isolated analytically pure and characterized by solution multiple nuclear NMR ($^{1}H$, $^{31}P$, $^{13}C$, more detailed information see Experimental Section). Unfortunately, it is still a mysterious compound since we could not come up with a structure that fits all these NMR data. Nonetheless, it is likely that THP participates in a facile transfer dehydrogenation process.

**Reactions with 1,3,5-trioxane.** Reaction with 1,3,5-trioxane is a little bit different from the reactions described above since 1,3,5-trioxane is a solid at the ambient temperature. It is tricky to pick up the reaction solvent. The reactive (PNP)Ir could activate C-H bond of the arene solvent. Using unreactive alkane solvent such as pentane only leads to the formation of Ir(I) norbornene adduct, which is a stable compound and could not regenerate the 14e reactive intermediate in the reaction condition. The reaction was carried out in mesitylene because the solvent activation product (PNP)Ir(H)(Mes) is a synthon to (PNP)Ir too! Treatment of a mesitylene solution of norbornene and 1,3,5-trioxane with solid (PNP)Ir$H_2$ leads to the generation of three products at ambient temperature: the previously characterized (PNP)Ir(H)(Mes) (60%), trans-(PNP)Ir$(H)_2$(CO) (**315**, 15%), and a third unknown species (25%). However, at elevated temperature, all three complexes cleanly convert to trans- (PNP)Ir$(H)_2$(CO) (**315**). This result is not unexpected when considering that 1,3,5-trioxane is a formal trimer of

formaldehyde, with which (PNP)Ir$H_2$ reacts to generate complex **315**. Previous reports have shown that the depolymerization of 1,3,5-trioxane may be promoted by strongly acidic catalysts.[135] In contrast, it seems most likely in this case that a compound derived from C-H activation of 1,3,5-trioxane readily disproportionates to release formaldehyde. One possible mechanism for this transformation is depicted in Scheme 3-14.

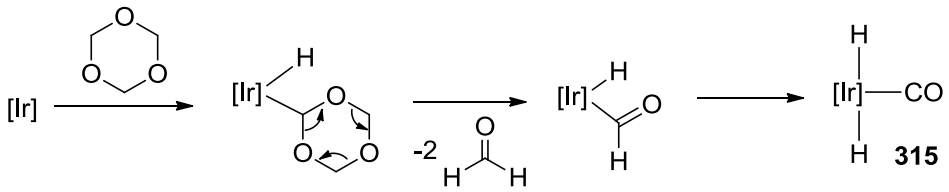


**Scheme3-14.** Possibile mechanism of decarbonylation of 1,3,5-trioxane at (PNP)Ir. center.

Our study together with Grubbs' study have demonstrated that the reaction of (PNP)Ir with ethers is fairly complicated. Different reactivity was observed for four different cyclic ethers. Double C-H activation of THF to form metal carbene complex is not without precedent.[136] It seems that five membered heterocycles often form carbenes much more readily than their six-membered and acyclic counterparts. The studies described above do not allow definitive assignments of rate-limiting steps for each reaction, but they certainly underscore the importance of numerous subtle factors in the thermodynamic stabilization of one isomer relative to another for related substrates at (PNP)Ir.

### *3.3 Conclusion*

This chapter described the C-H activation at (PNP)Ir center. We have demonstrated that the thermodynamic preference for aryl or benzylic C-H oxidative addition may in certain cases depend on the coordination number of the metal center. A higher coordination number favors a less sterically demanding benzylic product instead of the preference for the mesityl isomer for the lower coordination number. We have also presented the C-H activation of cyclic ethers by (PNP)Ir and found that the results were very substrate dependent. These findings highlight the challenge of catalytic functionalization of C-H bonds with ethers by using (PNP)Ir.

### *3.4 Experimental*

**General considerations.** Unless specified otherwise, all manipulations were performed under an argon atmosphere using standard Schlenk line or glove box techniques. Toluene, ethyl ether, and pentane were dried and deoxygenated (by purging) using a solvent purification system by MBraun and stored over molecular sieves in an Ar-filled glove box. $C_6D_6$ and THF were dried over and distilled from Na/K/$Ph_2CO$/18-crown-6 and stored over molecular sieves in an Ar-filled glove box. Fluorobenzene and pyridine were dried with and then distilled from $CaH_2$ and stored over molecular sieves in an Ar-filled glove box. Thiazole and $PMe_3$ were degassed prior to use and stored in an Ar-filled glove box. (PNP)$H_2$ and (PNP)Ir(H)(Cl)[2b] were prepared according to the published procedures. All other chemicals were used as received from commercial vendors. NMR spectra were recorded on a Varian iNova 400 ($^1$H NMR, 399.755 MHz; $^{13}$C NMR, 100.518 MHz; $^{31}$P NMR, 161.822 MHz; $^{19}$F NMR, 376.104 MHz)

spectrometer. For $^{1}H$ and $^{13}C$ NMR spectra, the residual solvent peak was used as an internal reference. $^{31}P$ NMR spectra were referenced externally using 85 % $H_3PO_4$ at 0 ppm. Elemental analyses were performed by CALI, Inc. (Parsippany, NJ).

**(PNP)Ir(H)(Mes) (301).** The following procedure is a modification of the previously reported synthesis. It is a one-sequence synthesis that obviates the unnecessary isolation of various intermediates. $IrCl_3\,4H_2O$ (0.318 g, 0.902 mmol) was added to 10 mL of degassed *i*-PrOH containing 0.45 mL (3.66 mmol) of 1,5-cyclooctadiene. The mixture was refluxed overnight under Ar. Yellow precipitate was found the next day (presumably, $[(COD)IrHCl_2]_2$). The solvent was removed under vacuum and the residue was thoroughly dried in vacuo. The resultant solids were extracted with a minimal amount of PhF followed by the addition of (PNP)H (0.405 g, 0.943 mmol). After stirring for 3 h, a solution of potassium isopropoxide in isopropanol (prepared by adding $KOC(CH_3)_3$ (0.220 g, 1.96 mmol) to 5 mL of degassed *i*-PrOH) was added to this mixture and it was allowed to stir for another 20 min. The solution was then degassed and back-filled with $H_2$ (1 atm, excess) and left stirring overnight. The volatiles were removed in vacuo and the residue was redissolved in ether. The resultant solution was filtered through Celite and the volatiles were removed in vacuo again. The residual solid was redissolved in ether and the resultant solution filtered through a plug of silica gel. The volatiles were removed and the solid residue was thoroughly dried in vacuo, followed by addition of 7.6 mL of mesitylene to get a dark red solution of $(PNP)IrH_2$. Norbornene (127 mg, 1.35 mmol) was added and the mixture was stirred for 20 h to get a dark brown solution which was then filtered through plugs of Celite and silica gel. The

filtrate was collected and the volatiles were removed under vacuum. Recrystallization from pentane gave **301** as a red-brown solid which was >98% pure by NMR. Yield: 455 mg (68% based on Ir).

**Synthesis of 301 from (PNP)Ir(H)(Cl) and $Me_2C_6H_3CH_2MgBr$.** 3,5-$Me_2C_6H_3CH_2Br$ (1g, 5 mmol) was slowly added to Mg (0.36 g, 15 mmol) in ether with vigorous stirring. The reaction mixture was refluxed overnight under Ar. All the volatiles were removed in vacuo and the residue was redissolved in ether and filtered through Celite. The solvent was evaporated under vacuum and the solid was dried to give the crude 3,5-$Me_2C_6H_3CH_2MgBr$. Five milligrams of this solid (0.021 mmol or likely less owing to solvent in the solid Grignard) was added to a solution of (PNP)Ir(H)(Cl) (13 mg, 0.020 mmol) in 0.6 mL of $C_6D_6$ and shaken well. The solution turned dark red immediately. $^{31}P$ NMR analysis indicated that **301** constituted ca. 80% of the reaction mixture.

**Synthesis of (PNP)Ir(H)($C_6H_5$) (302) by thermolysis 301 in $C_6H_6$.** (PNP)Ir(H)(Mes) (**301**) (10 mg, 0.027 mmol) was placed into a J. Young NMR tube. The solid was dissolved in 0.6 mL of $C_6H_6$. The reaction mixture was heated to 70 ℃. In 15 min, **302** (δ 45.7 in the $^{31}P\{1H\}$ NMR spectrum) constituted ca. 85% of the resulting solution ($^{31}P$ NMR evidence) and in 30 min the resonance of **302** was the only one observable by $^{31}P$ NMR. The volatiles were stripped down and the solid was redissolved in $C_6D_6$ for $^{1}H$ NMR characterization. The $^{1}H$ and $^{31}P$ NMR data matched those reported previously.

**Synthesis of (PNP)Ir(D)($C_6D_5$) (302-$d_6$) by thermolysis 301 in $C_6D_6$.** (PNP)Ir(H)(Mes) (**301**) (20 mg, 0.027 mmol) was placed into a J. Young NMR tube. The solid was dissolved in a 0.6 mL of $C_6D_6$. The reaction mixture was heated to 70 $^oC$. In 30 min, the resonance of **302-$d_6$** was the only one observable by $^{31}P$ NMR. Compound **302-$d_6$** was identified on the basis of the absence of the $^1H$ resonances for the Ir-bound hydride and phenyl groups and the $^1H$ NMR and $^{31}P$ NMR spectra that were near-identical to those of **302**. Data for **302-$d_6$**: $^1H$ NMR ($C_6D_6$): δ 7.88 (d, 2H, *J* = 8.8 Hz, PNP-aryl *H*), 6.94 (s, 2H, PNP-aryl *H*), 6.87 (d, 2H, *J* = 8.8 Hz, PNP-aryl *H*), 2.45 (m, 2H, C*H*$Me_2$), 2.24 (m, 2H, C*H*$Me_2$), 2.19 (s, 6H, Ar-$CH_3$), 1.02 (app. q (dvt), 6H, *J* = 8 Hz, CH$Me_2$), 0.95 (m, 12H, CH$Me_2$), 0.90 (app. q (dvt), 6H, *J* = 7.2 Hz, CH$Me_2$). $^{31}P\{^1H\}$ NMR ($C_6D_6$): δ 45.8.

**Synthesis of (PNP)Ir(H)($C_6H_4Me$) (303) by thermolysis 301 in toluene.** (PNP)Ir(H)(Mes) (40 mg, 0.054 mmol) was dissolved in 0.6 mL of toluene in a J. Young tube and heated at 70 $^oC$ for 40 min. In the $^{31}P\{^1H\}$ NMR spectrum, the resonance of **303** at δ 45.3 ppm constituted >95% of the overall $^{31}P$ intensity. The volatiles were removed under vacuum and the residue was dissolved in $C_6D_6$ for $^1H$ NMR characterization. The $^1H$ NMR data are consistent with the presence of two isomers of **303** in approximately 2:1 ratio. The major isomer was readily identified as the meta-isomer, (PNP)Ir(H)(m-$C_6H_4Me$) (**303-m**) based on the characteristic meta-tolyl pattern of the corresponding $^1H$ NMR resonances. The aromatic resonances of the tolyl group of the other isomer were obscured by other aromatic resonances (of the PNP ligand); however two hydride resonances and Me of tolyl resonances were observable. We

tentatively assign the minor isomer as the para-tolyl isomer (PNP)Ir(H)(*p*-$C_6H_4Me$) (**303-p**) based on that the *ortho*-isomer is expected to be disfavored (and not expected to be observed when the *para*-isomer is not!) and on that the likelihood of the four multiplets of the putative *ortho*-tolyl group being completely obscured by a small number of other aromatic resonances is rather small. Data for **303-m** follow. $^1$H NMR ($C_6D_6$): 7.88 (d, 2H, *J* = 8.4 Hz, PNP-aryl *H*), 7.66 (s, 1H, *ortho*-tolyl *H*), 7.06 (t, 1H, *J* = 6.8 Hz, *meta*-tolyl *H*), 6.98 (d, 1H, *J* = 6.8 Hz, tolyl-aryl *H*), 6.94 (s, 2H, PNP-aryl *H*), 6.87 (d, 2H, *J* = 8.4 Hz, PNP-aryl *H*), 6.79 (d, 1H, *J* = 6.8 Hz, tolyl-aryl *H*), 2.46 (m, 2H, C*H*$Me_2$ ), 2.34 (s, 3H, Ar-*CH*$_3$), 2.24 (m, 2H, C*H*$Me_2$ ), 2.19 (s, 6H, Ar-*CH*$_3$), 1.05 (app. q (dvt), 6H, *J* = 8.4 Hz, CH*Me*$_2$), 0.97 (m, 12H, CH*Me*$_2$), 0.91 (app. q (dvt), 6H, *J* = 6.8 Hz, CH*Me*$_2$), -37.4 (br, 1H, Ir-*H*). $^{31}$P{$^1$H} NMR ($C_6D_6$): δ 45.3. Data for **303-p** follow. $^1$H NMR ($C_6D_6$): 7.88 (d, 2H, *J* = 8.4 Hz, PNP-aryl *H*), 7.67 (br, 2H, tolyl-aryl *H*), 7.59 (d, 2H, *J* = 6.8 Hz, tolyl-aryl *H*), 6.94 (s, 2H, PNP-aryl *H*), 6.87 (d, 2H, *J* = 8.4 Hz, PNP-aryl *H*), 2.46 (m, 2H, C*H*$Me_2$ ), 2.30 (s, 3H, Ar-*CH*$_3$), 2.24 (m, 2H, C*H*$Me_2$ ), 2.19 (s, 6H, Ar-*CH*$_3$), 1.05 (app. q (dvt), 6H, *J* = 8.4 Hz, CH*Me*$_2$), 0.97 (m, 12H, CH*Me*$_2$), 0.91 (app. q (dvt), 6H, *J* = 6.8 Hz, CH*Me*$_2$), -37.6 (t, 1H, *J* = 12.8, Ir-*H*). $^{31}$P{1H} NMR ($C_6D_6$): δ 45.3.

**Synthesis of 303 via the reaction of (PNP)(H)(Cl) with $C_6H_5CH_2MgCl$.** (PNP)Ir(H)(Cl) (15 mg, 0.023 mmol) and $C_6H_5CH_2MgCl$ (15 μL of the 1.5 M THF solution, 0.023 mmol) and 0.6 mL $C_6D_6$ were loaded into a J. Young tube. The progress of the reaction at ambient temperature was monitored by $^{31}$P{$^1$H} and $^1$H NMR. In 1 h, **303-m/303-p** constituted ca. 64% of the mixture. After 7 h, **303-m/303-p** constituted ca.

77% of the mixture, that also included 19% of **302-$d_6$** and <4% of other unidentified compounds.

**(PNP)Ir(H)($CH_2$-$C_6H_3(CH_3)_2$)(Py) (304a).** (PNP)Ir(H)(Mes) (**301**) (132 mg, 0.180 mmol) was dissolved in 1 mL of $C_6D_6$ in a Schlenk flask, followed by the addition of pyridine (140 μL, 1.80 mmol). The solution was allowed to stand at room temperature overnight; the color evolved from brown to yellow. The resultant solution was filtered through Celite, the volatiles were removed under vacuum, and the yellow solid residue was recrystallized from ether. Yield: 111 mg, 0.135 mmol, 75%. $^1$H NMR ($C_6D_6$): δ 9.00 (br, 2H, py-*H*), 8.06 (d, 2H, *J* = 8.4 Hz, PNP-aryl *H*), 7.41 (s, 2H, Ar-*H*), 6.95 (s, 2H, Ar-*H*), 6.87 (d, 2H, *J* = 8.4 Hz, PNP-aryl *H*), 6.69 (s, 1H, dimethylbenzyl-aryl *H*), 6.65 (br, 1H, py-*H*), 6.36 (br, 2H, py-*H*), 3.67 (br t, 2H, *J* = 6 Hz, Ir-C*H*$_2$), 2.54 (m, 2H, C*H*Me$_2$), 2.36 (s, 6H, Ar-*CH*$_3$), 2.31 (m, 2H, C*H*Me$_2$), 2.21 (s, 6H, Ar-*CH*$_3$), 1.17 (app. q (dvt), *J* = 7.2 Hz, 6H, CH*Me*$_2$), 1.09 (app. q (dvt), *J* = 6.4 Hz, 12H, CH*Me*$_2$), 0.38 (app. q (dvt), *J* = 6.4 Hz, 6H, CH*Me*$_2$), -22.5 (t, *J* = 16 Hz, Ir-*H*). $^{13}$C{$^1$H} NMR ($C_6D_6$): δ 161.8 (t, *J* = 8 Hz, C-N), 158.1 (aryl-C), 152.9 (br, pyridine-C), 136.2 (pyridine-C), 135.7 (pyridine-C), 132.5 (PNP-aryl C), 131.5 (PNP-aryl C), 129.2 (aryl-C), 125.5 (t, *J* = 21 Hz, PNP-aryl C), 124.4 (aryl-C), 123.9 (PNP-aryl C), 116.4 (t, *J* = 5 Hz, PNP-aryl C), 27.5 (t, *J* = 17 Hz, CHMe$_2$), 26.3 (t, *J* = 12 Hz, CHMe$_2$), 22.2, 21.0, 19.0, 18.9, 18.6, 17.9, -6.6 (t, *J* = 2.3 Hz, Ir-CH$_2$). $^{31}$P{$^1$H} NMR ($C_6D_6$): δ 18.2. Elem. An.. Found (Calculated) for $C_{40}H_{57}N_2P_2Ir$ : C, 58.49 (58.58); H, 7.07 (7.01); N, 3.38 (3.41).

**NMR tube reaction to form 304a under dark. (**PNP)Ir(H)(mesityl) (**301**) (13.2 mg, 0.0180 mmol) was dissolved in 1 mL of $C_6D_6$ in a J. Young tube covered with

aluminum foil, followed by the addition of pyridine (14 μL, 0.180 mmol). This solution was allowed to stand at room temperature for 22 h; the color evolved from brown to yellow. $^{1}$H NMR and $^{31}$P{$^{1}$H} NMR analyses showed that **304a** was formed quantitatively. **(PNP)Ir(H)(CH$_2$-C$_6$H$_3$(CH$_3$)$_2$)(PMe$_3$) (304b).** (PNP)Ir(H)(mesityl) (**301**) (63 mg, 0.090 mmol) was dissolved in 1 mL of $C_6D_6$ in a Schlenk flask, followed by the addition of $PMe_3$ (180 μL, 0.450 mmol). The solution was allowed to stand at room temperature overnight. The solution was allowed to stand at room temperature overnight; the color evolved from brown to yellow. The resultant solution was filtered through Celite, the volatiles were removed under vacuum, and a yellow solid was obtained. Yield: 60 mg, 0.073 mmol, 81%. $^{1}$H NMR ($C_6D_6$): δ 7.66 (d, 2H, *J* = 9.6 Hz, PNP-aryl *H*), 7.10 (br, 4H, Ar-*H*), 6.73 (d, 2H, *J* = 9.6 Hz, PNP-aryl *H*), 6.59 (s, 1H, dimethylbenzyl-aryl *H*), 3.16 (m, 2H, *J* = 8.4 Hz, *J* = 3.6 Hz, Ir-C*H*$_2$), 2.29 (s, 6H, Ar-*CH*$_3$), 2.22 (br, 10H, C*H*Me$_2$ and Ar-*CH*$_3$), 1.22 (m, 18H, CH*Me*$_2$), 1.07 (app. q (dvt), 6H, *J* = 7.6 Hz, CH*Me*$_2$), 0.99 (d, 9H, *J* = 7.2 Hz, P*Me*$_3$), -11.7 (dt, *J* = 20 Hz, *J* = 142 Hz, Ir-*H*). $^{13}$C{$^{1}$H} NMR ($C_6D_6$): δ 160.2 (t, *J* = 9 Hz, C-N), 158.5 (aryl-C), 136.1 (aryl-C), ), 132.3 (aryl-C), 131.6 (PNP-aryl C), 130.0 (PNP-aryl C), 129.3 (t, *J* = 11 Hz, PNP-aryl C), 124.0 (aryl-C), 123.7 (t, *J* = 3.8 Hz, PNP-aryl C), 116.0 (t, *J* = 3.8 Hz, PNP-aryl C), 30.7 (m, $CHMe_2$), 27.4 (t, *J* = 11 Hz, $CHMe_2$), 22.1, 21.0, 20.0, 19.6, 19.0, 18.8, 17.8, 17.6, -18.3(m, Ir-$CH_2$). $^{31}$P{$^{1}$H} NMR ($C_6D_6$): δ 14.3 (d, *J* =17 Hz), -55.1 (t, *J* = 17 Hz). Elem. An.. Found (Calculated) for $C_{38}H_{61}NP_3Ir$: C, 56.01 (55.86); H, 7.56 (7.53); N, 1.71 (1.71).

**(PNP)Ir(H)($CH_2$-$C_6H_3(CH_3)_2$)($C_3H_3NS$) (304c).** (PNP)Ir(H)(Mes) (**301**) (25 mg, 0.033 mmol) was dissolved in 0.6 mL of $C_6D_6$ in a J. Young tube, followed by the addition of thiazole (85 μL, 1.3 mmol). The reaction mixture was heated at 60 $^oC$ for 10 min. The volatiles were removed under vacuum and the residue was recrystallized from ether to get a yellow solid. Yield: 20 mg, 0.024 mmol, (73%). $^1H$ NMR ($C_6D_6$): δ 8.77 (br, 1H, thiazole-H), 8.09 (br, 1H, thiazole-H), 7.96 (d, 2H, *J* = 8.8 Hz, PNP-aryl *H*), 7.36 (s, 2H, Ar-*H*), 6.95 (s, 2H, Ar-*H*), 6.83 (d, 2H, *J* = 8.8 Hz, PNP-aryl *H*), 6.69 (s, 1H, dimethylbenzyl-aryl *H*), 6.18 (s, 1H, thiazole-*H*), 3.64 (br, 2H, Ir-C$H_2$), 2.45 (m, 2H, C*H*$Me_2$), 2.36 (s, 6H, Ar-$CH_3$), 2.27 (m, 2H, C*H*$Me_2$), 2.25 (s, 6H, Ar-$CH_3$), 1.09 (m, 18H, CH$Me_2$), 0.41 (app. q (dvt), 6H, *J* = 6.8 Hz, CH$Me_2$), -22.6 (t, 1H, *J* = 17 Hz, Ir-*H*). $^{31}P\{^1H\}$ NMR ($C_6D_6$): δ 19.5.

**Synthesis of (PNP)Ir(H)($C_6H_5$)(Py) (305) by thermolysis of 304a in $C_6H_6$.** (PNP)Ir(H)($CH_2$-$C_6H_3(CH_3)_2$)(Py) (**304a**) (24.5 mg, 0.0300 mmol) was dissolved in 0.6 mL of $C_6H_6$ in a J. Young tube. Pyridine (24 μL, 0.300 mmol) was added. The reaction mixture placed into a 85 ℃ oil bath. $^{31}P\{^1H\}$ NMR and $^1H$ NMR analysis revealed that **304a** converted to **305** gradually and the conversion was complete after 48 h. The volatiles were removed under vacuum and the yellow solid thus obtained was washed with ether and dried in vacuo to give 18 mg (79%) of **305**. **Synthesis of 305 from 302.** (PNP)Ir(H)(Ph) (**302**) (20 mg, 0.03 mmol) was dissolved in 0.6 mL of $C_6D_6$ in a J. Young NMR tube. Pyridine (10 μL, 0.12 mmol) was added. The brown solution changed to yellow immediately. The volatiles were removed in vacuo and **305** was obtained as a yellow solid. $^1H$ NMR ($C_6D_6$): δ 9.16 (br, 2H, py-H), 8.03 (br, 2H, phenyl-*H*), 7.98 (d,

2H, *J* = 8.8 Hz, PNP-aryl *H*), 7.17 (m, 3H, tolyl-aryl *H*, overlapped with the solvent), 6.91 (s, 2H, PNP-aryl *H*), 6.87 (d, 2H, *J* = 8.4 Hz, PNP-aryl *H*), 6.64 (t, 1H, *J* = 8 Hz, py-*H*), 6.32 (br, 2H, *J* = 6.8 Hz, py-*H*), 2.50 (m, 2H, C*H*$Me_2$), 2.33 (m, 2H, C*H*$Me_2$), 2.18 (s, 6H, Ar-*$CH_3$*), 0.99 (m, 18H, CH*$Me_2$*), 0.68 (app. q (dvt), 6H, *J* = 6.4 Hz, CH*$Me_2$*), -21.6 (t, *J* = 16 Hz, Ir-*H*). $^{13}C\{^1H\}$ NMR ($C_6D_6$): δ 161.6 (t, *J* = 8 Hz, C-N), 154.8 (pyridine-C), 146.9 (Ir-$C_6H_5$), 135.9 (pyridine-C), 135.3 (t, $J_{C-P}$ = 6.1 Hz, Ir-$C_6H_5$-ipso), 132.6 (PNP-aryl C), 131.6 (PNP-aryl C), 126.6 (Ir-$C_6H_5$), 125.8 (t, *J* = 21 Hz, PNP-aryl C), 124.2 (PNP-aryl C), 123.9 (pyridine-C), 120.8 (Ir-$C_6H_5$), 116.9 (t, *J* = 4.6 Hz, PNP-aryl C), 28.8 (t, *J* = 17 Hz, $CHMe_2$), 26.2 (t, *J* = 12 Hz, $CHMe_2$), 21.0, 19.4, 19.3, 18.8, 18.6. $^{31}P\{^1H\}$ NMR ($C_6H_6$): δ 19.4.

**Synthesis of (PNP)Ir(D)($C_6D_5$)(Py) (305-$d_6$) by thermolysis of 304a in $C_6D_6$.** (PNP)Ir(H)($CH_2$-$C_6H_3(CH_3)_2$)(Py) (24.5 mg, 0.0300 mmol) was dissolved in 0.6 mL of $C_6D_6$ in a J. Young tube. Pyridine (24 μL, 0.300 mmol) was added. The reaction mixture was placed into an 85 ℃ oil bath. $^{31}P\{^1H\}$ NMR and $^1H$ NMR analysis revealed that **304a** converted to (PNP)Ir(D)($C_6D_5$)(Py) (**305-$d_6$**) gradually and the conversion was complete after 48 h. The volatiles were removed under vacuum and the resultant yellow solid was washed with ether and dried in vacuo. Yield: 16 mg, 0.021 mmol, 70%. $^1H$ NMR ($C_6D_6$): δ 9.18 (br, 2H, py-*H*), 7.96 (d, 2H, *J* = 8.8 Hz, PNP-aryl *H*), 6.91 (s, 2H, PNP-aryl *H*), 6.87 (d, 2H, *J* = 8.8 Hz, PNP-aryl *H*), 6.63 (t, 1H, *J* = 8 Hz, py-*H*), 6.30 (t, 2H, *J* = 8 Hz, py-*H*), 2.50 (m, 2H, C*H*$Me_2$), 2.34 (m, 2H, C*H*$Me_2$), 2.18 (s, 6H, Ar-*$CH_3$*), 0.99 (m, 18H, CH*$Me_2$*), 0.68 (app. q (dvt), 6H, *J* = 6.8 Hz, CH*$Me_2$*). $^{13}C\{^1H\}$ NMR ($C_6D_6$): δ 161.7 (t, *J* = 9 Hz, C-N), 154.9 (pyridine-C), 146.4 (br, Ir-$C_6D_5$), 135.9

(pyridine-C), 135.0 (t, $J_{C\text{-}P}$ = 5.3 Hz, Ir-$C_6D_5$), 132.6 (PNP-aryl C), 131.6 (PNP-aryl C), 126.3 (br, Ir-$C_6D_5$), 125.8 (t, *J* = 21 Hz, PNP-aryl C), 124.2 (br, PNP-aryl C), 123.9 (pyridine-C), 120.4 (br, Ir-$C_6D_5$), 116.9 (t, *J* = 4.6 Hz, PNP-aryl C), 28.8 (t, *J* = 17 Hz, $CHMe_2$), 26.2 (t, *J* = 12 Hz, $CHMe_2$), 21.0, 19.4, 19.3, 18.8, 18.6. $^{31}P\{^1H\}$ NMR ($C_6D_6$): δ 19.4. Elem. An.. Found (Calculated) for $C_{37}H_{45}D_6NP_2Ir$: C, 56.68 (56.74); H, 7.33 (7.24); N, 3.57 (3.46).

**(PNP)Ir(H)($C_6H_4$Me)(py) (306).** PNP)Ir(H)(Mes) (**301**) (10 mg, 0.014 mmol) was dissolved in 0.6 mL of toluene in a J. Young tube and heated at 70 ℃ for 18 h. $^{31}P$ NMR evidenced the formation of **303** in >95% yield. Pyridine (10 μL, 0.13 mmol) was added to the above solution and the brown solution changed to yellow immediately. Two singlets at δ 19.2 and 19.3 ppm (2:1 ratio) were detected by $^{31}P\{^1H\}$ NMR. The volatiles were removed in vacuo and dissolved in $C_6D_6$ for $^1H$ NMR characterization. A broad resonance at δ 19.5 ppm was evident in $^{31}P$ NMR (presumably two resonances overlapping). The NMR data are consistent with the presence of two isomers of **306** formed by simple addition of pyridine to the in situ-formed **303-m** and **303-p**. The major isomer was identified as (PNP)Ir(H)(m-$C_6H_4$Me)(py) (**306-m**) based on the $^1H$ NMR data. The aromatic resonances of the minor isomer are somewhat obscured. We tentatively assign it as (PNP)Ir(H)(*p*-$C_6H_4$Me) **(306-p)** (see the explanation for the synthesis of **303-m**/**303-p** above). Data for **306-m** follow. $^1H$ NMR ($C_6D_6$): δ 9.21 (br, 2H, py-*H*), 7.96 (d, 2H, *J* = 8.8 Hz, PNP-aryl *H*), 7.92 (s, 1H, *ortho*-tolyl *H*), 7.78 (d, 1H, *J* = 7.6 Hz, tolyl-aryl *H*), 7.10 (t, 1H, *J* = 7.2 Hz, *meta*-tolyl *H*), 7.02 (d, 1H, *J* = 7.6 Hz, tolyl-aryl *H*), 6.92 (s, 2H, PNP-aryl *H*), 6.85 (d, 2H, *J* = 8.4 Hz, PNP-aryl *H*), 6.63

(t, 1H, *J* = 7.2 Hz, py-*H*), 6.32 (t, 2H, *J* = 6.4 Hz, py-*H*), 2.52 (m, 2H, C*H*$Me_2$), 2.40 (s, 3H, Ar-*$CH_3$*), 2.37 (br, 2H, C*H*$Me_2$), 2.18 (s, 6H, Ar-*$CH_3$*), 0.91 (m, 18H, CH*$Me_2$*), 0.68 (app. (dvt), 6H, *J* = 7.2 Hz, CH*$Me_2$*), -21.6 (br, Ir-*H*). $^1$H NMR ($(CD_3)_2CO$): δ 10.23 (br, 2H, py-*H* ), 8.86 (t, 1H, *J* = 7.2 Hz, *meta*-tolyl *H*), 8.76 (s, 1H, *ortho*-tolyl *H*), 8.72 (d, 2H, *J* = 8.4, PNP-aryl *H*), 8.62 (d, 1H, *J* = 7.2 Hz, tolyl-aryl *H*), 8.32 (t, 2H, *J* = 6.8 Hz, py-*H*), 8.09 (s, 2H, PNP-aryl *H*), 7.90 (d, 2H, *J* = 8.4 Hz, PNP-aryl *H*), 7.76 (t, 1H, *J* = 7.2 Hz, py-*H*), 7.61 (d, 1H, *J* = 7.2 Hz, tolyl-aryl *H*), 3.82 (br, 2H, C*H*$Me_2$), 3.58 (br, 2H, C*H*$Me_2$), 3.31 (s, 6H, Ar-*$CH_3$*), 3.27 (s, 3H, Ar-*$CH_3$*), 2.28 (app. (dvt), 6H, *J* = 5.6 Hz, CH*$Me_2$*), 2.11 (app. (dvt), 6H, *J* = 6.8 Hz, CH*$Me_2$*), 2.01 (app. (dvt), 6H, *J* = 6.8 Hz, CH*$Me_2$*), 1.88 (app. (dvt), 6H, *J* = 6.8 Hz, CH*$Me_2$*), -20.8 (br, 1H, Ir-*H*). Partial data for **306-p** follow. $^1$H NMR ($C_6D_6$): δ 2.52 (m, 2H, C*H*$Me_2$), 2.38 (s, 3H, Ar-*$CH_3$*), 2.37 (br, 2H, C*H*$Me_2$), 2.18 (s, 6H, Ar-*$CH_3$*), 0.91 (m, 18H, CH*$Me_2$*), 0.68 (app. (dvt), 6H, *J* = 7.2 Hz, CH*$Me_2$*), -21.6 (br, Ir-*H*).

**Synthesis of (PNP)Ir(H)($CH_2C_6H_5$)(py) (308) and its thermolytic conversion to 306.** (PNP)Ir(H)(Cl) (**307**) (20 mg, 0.030 mmol) was dissolved in 0.6 mL of $C_6H_6$ in a J. Young tube and pyridine (12 μL, 0.15 mmol) was added. $C_6H_5CH_2MgCl$ (30 μL of 1 M solution in ether, 0.030 mmol) was slowly added. The solution changed to orange immediately and was filtered through Celite to remove the insolubles. The volatiles were removed from the filtrate in vacuo and the residue was dissolved in $C_6D_6$ for NMR characterization. When this solution was heated at 70 $^o$C for 18 h, the $^{31}$P NMR and $^1$H NMR analysis indicated that **308** had disappeared and the solution contained a mixture of **306-m**/**306-p** (40% by $^{31}P\{^1H\}$ NMR: δ 19.1, 19.2; $^1$H NMR for hydride signals δ -

21.6), one ma*J*or unidentified compound ($^{31}P\{^{1}H\}$ NMR: δ 43.5 (40%)), and other unidentified compounds (20%). Compound **308** was not isolated and only characterized by NMR spectroscopy in solution. $^{1}H$ NMR ($C_6D_6$): 8.96 (br, 1H, py-*H*), 8.02 (d, 2H, *J* = 8.4 Hz, PNP-aryl *H*), 7.90 (br, 1H, *para*-phenyl *H*), 7.76 (d, 2H, *J* = 7.2 Hz, *ortho*-phenyl *H*), 7.29 (t, 2H, *J* =7.2 Hz, *meta*-phenyl *H*), 6.93 (s, 2H, PNP-aryl *H*), 6.85 (d, 2H, *J* =8.4 Hz, PNP-aryl *H*), 6.72 (br, 2H, py-*H*), 6.39 (br, 2H, py-*H*), 3.73 (t, 2H, *J* = 5.6 Hz, Ir-*CH*$_2$), 2.56 (br, 2H, C*H*Me$_2$), 2.30 (br, 2H, C*H*Me$_2$), 2.20 (s, 6H, Ar-*CH*$_3$), 1.06 (m, 18H, CH*Me*$_2$), 0.40 (app. (dvt), 6H, *J* = 7.2 Hz, CH*Me*$_2$), -22.6 (t, 1H, *J* = 17 Hz, Ir-*H*). $^{31}P\{^{1}H\}$ NMR ($C_6D_6$): δ 18.3.

**Kinetic studies of formation of 304a from 301.** (PNP)Ir(H)(Mes) (**301**) (80.0 mg, 0.108 mmol) was treated with $C_6D_6$ to bring the total volume to 1.60 mL (0.0680 M in Ir). 0.400 mL of this solution was placed into each of four J. Young NMR tubes. 22.0, 44.0, 66.0, 88.0 μL pyridine were added to each tube, respectively. Then $C_6D_6$ was added to bring the volume of solution in each tube to 0.500 mL (resulting [py] = 0.540, 1.08, 1.62, 2.16 M, [Ir] = 0.0540 M). These solutions were stored frozen in liquid $N_2$ until retrieved to perform VT NMR kinetic studies. Temperature was measured before and after each run using the ethylene glycol chemical shift thermometer. Standard deviations for the determination of rate constants were obtained from the linear regression analysis by Microsoft Excel (twice the deviation calculated by Excel). The following values of rate constant at 35 $^{o}$C were found for the rate law below:

d([**301**]) = -k × [**301**] ×dt:

| [py], M | k, $s^{-1}$ |
|---|---|
| 0.54 | $3.41(14)\times10^{-4}$ |
| 1.08 | $3.19(17)\times10^{-4}$ |
| 1.62 | $3.45(17)\times10^{-4}$ |
| 2.16 | $3.08(12)\times10^{-4}$ |

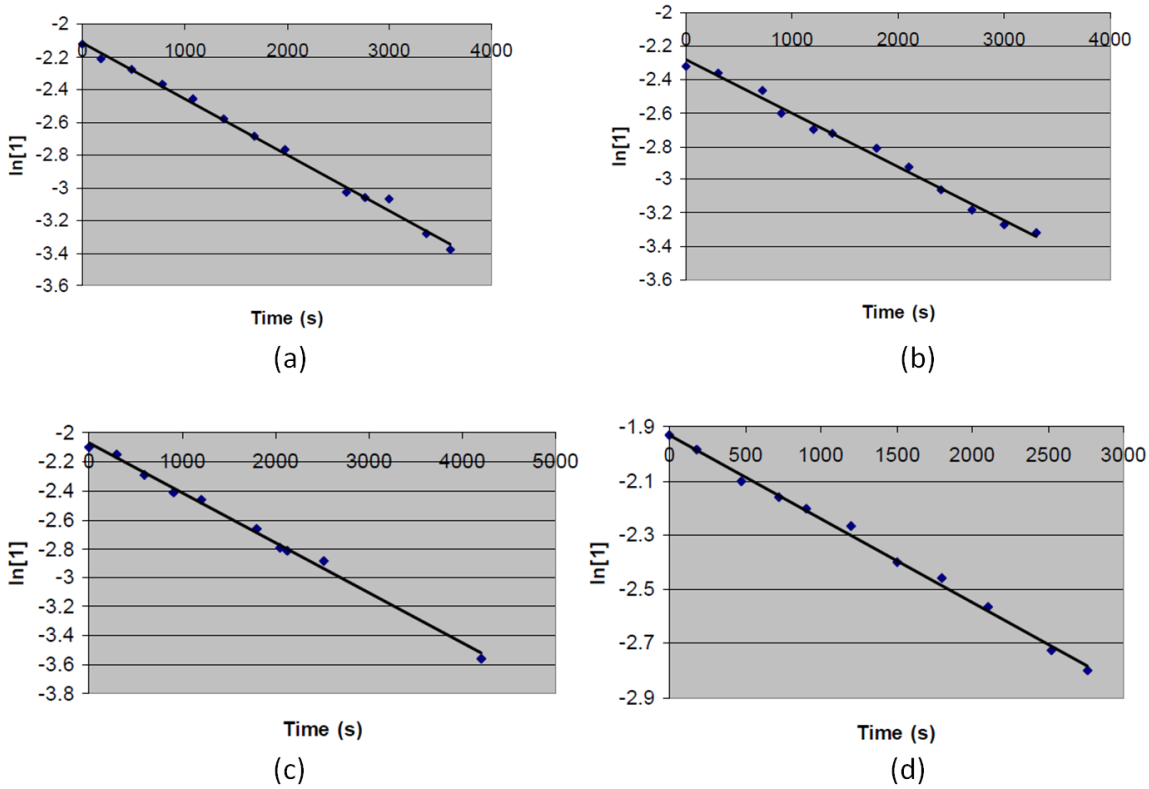


**Figure S1.** Disappearance of **301** as a function of time ((a): [py] = 0.54 M; (b): [py] = 0.54 M; (c): [py] = 1.62 M; (d): [py] = 2.16 M)

**Kinetic studies of conversion of 304a to 302.** Compound **304a** (0.0980 g, 0.120 mmol) was treated with $C_6H_6$ to bring the total volume to 1.60 mL (0.0750 M in Ir).

0.400 mL of this solution was placed into each of four J. Young NMR tubes. 24, 48, 72, 96 μL pyridine were added separately to each tube. Then $C_6H_6$ was added to bring a total volume of 0.500 mL volume (resulting [py] = 0.600, 1.20, 1.80, 2.40 M; [Ir] = 0.0600 M). The four J. Young NMR tubes were simultaneously kept in the same 85 ℃ oil bath. Conversions were measured by periodically rapidly cooling the solutions to ambient temperature and collecting NMR spectra at ca. 22 ℃. The standard deviations were taken to be twice the deviation calculated by the statistical analysis in Microsoft Excel. The following values of rate constant were found at 85 ℃ for the rate law below:

$$d([\mathbf{304a}]) = -kobs \times [(\mathbf{304a})] \times dt:$$

| [py], M | $k_{obs}$, $s^{-1}$ |
|---|---|
| 0.60 | $1.99(3)\times10^{-4}$ |
| 1.20 | $0.93(3)\times10^{-4}$ |
| 1.80 | $0.56(3)\times10^{-4}$ |
| 2.40 | $0.45(3)\times10^{-4}$ |

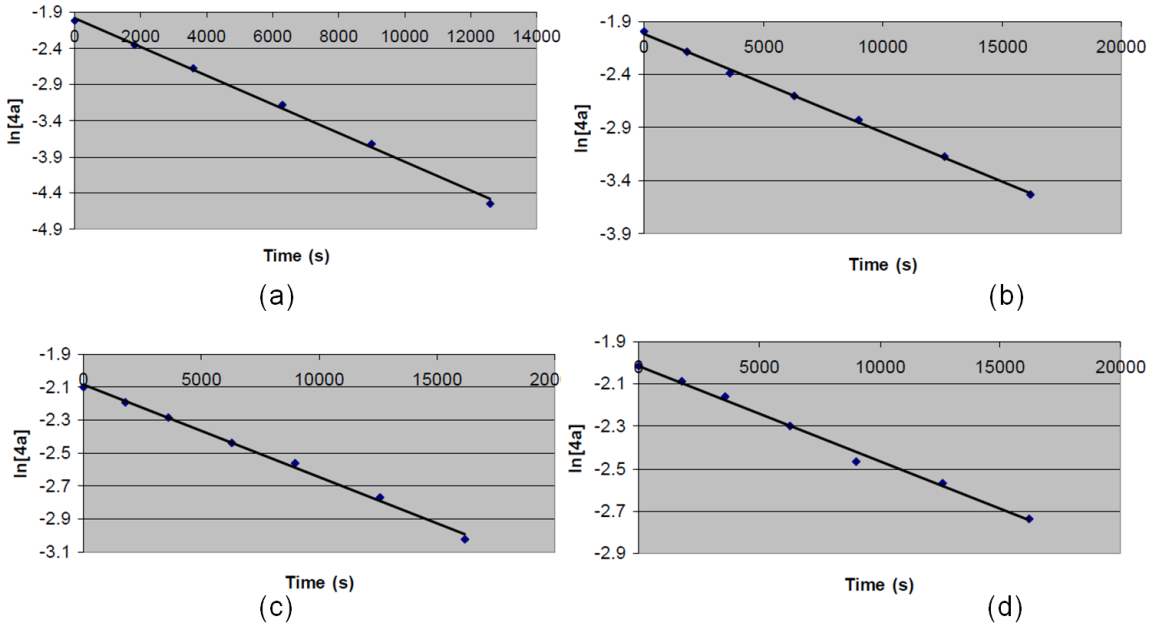


**Figure S2.** Disappearance of **304a** as a function of time ((a): [py] = 0.60 M; (b): [py] = 1.20 M; (c): [py] = 1.80 M; (d): [py] = 2.40 M)

**Synthesis of (PNP)Ir=C($OC_3H_6$) (312).** (PNP)Ir$(H)_2$ (**310**) (76 mg, 0.12 mmol) and norbornene (83 mg, 0.86 mmol) were dissolved in tetrahydrofuran (600 μL) and transferred to a J. Young tube. An immediate color change to brown was accompanied by the appearance of a singlet in the $^{31}P\{^1H\}$ NMR spectrum at δ 46.7 ppm. Thermolysis of the solution (60 ℃, 7 h) resulted in a color change to dark red and ca. 97% conversion to another product at δ 43.1 ppm. The solution was filtered through Celite, and the filtrate was collected.Volatiles were removed in vacuo, and **312** was obtained as a pure solid by slow evaporation of pentane from a concentrated solution at -35 ℃ (21.6 mg, 0.031 mmol, 24%). $^1H$ NMR ($C_6D_6$): δ 7.87 (d, *J* = 8.4 Hz, 2H, Ar-*H*), 7.25 (s, 2H, Ar-*H*), 6.86 (d, *J* = 8.4 Hz, 2H, Ar-*H*), 3.50 (t, $^3J_{H\text{-}H}$ = 6.9 Hz, 2H, $C_3H_6O$), 2.67 (m, 4H,

C*H*($CH_3$)$_2$), 2.29 (s, 6H, Ar-*CH*$_3$), 1.39 (quintet, $^3J_{H\text{-}H}$ = 7.2 Hz, 2H, $C_3H_6O$), 1.30 (dvt, 12H, CH*(CH*$_3$*)*$_2$), 1.24 (dvt, 12H, CH*(CH*$_3$*)*$_2$), 0.39 (t, $^3J_{H\text{-}H}$ =7.5 Hz, 2H, $C_3H_6O$). $^{13}C\{^1H\}$ NMR ($C_6D_6$): δ 232.6 (t, $^2J_{P\text{-}C}$ = 11 Hz, Ir=C), 164.1 (t, *J* = 17 Hz, C-N), 132.5 (PNP-aryl C), 131.2 (PNP-aryl C), 125.3 (PNP-aryl C), 124.7 (PNP-aryl C), 116.4 (PNP-aryl C), 74.6, 60.3, 26.2, 24.2, 20.6, 19.8, 18.7. $^{31}P\{^1H\}$ NMR: δ 42.9 (s). Elem. An.. Found (Calculated) for $C_{30}H_{46}NOP_2Ir$: C, 52.16 (51.98); H, 6.71 (6.66); N, 2.03 (1.90).

**Solution characterization of *trans*-(PNP)Ir(H)$_2$=C(C$_3$H$_6$O) (311-H$_2$).** (PNP)$IrH_2$ (**310**) (39 mg, 0.062 mmol) was dissolved in 0.6 mL of $C_6D_6$ in a J. Young tube followed by the addition of 2,3-dihydrofuran (14 μL, 0.19 mmol). $^{31}P\{^1H\}$NMR spectroscopy showed >97% conversion to 6-$H_2$ (δ 46.7 ppm). $^1H$ NMR ($C_6D_6$): δ 7.78 (d, *J* = 8 Hz, 2H, Ar-*H*), 7.02 (s, 2H, Ar-*H*), 6.73 (d, *J* = 8 Hz, 2H, Ar-*H*), 3.66 (t, $^3J_{H\text{-}H}$ = 6 Hz, 2H, $C_3H_6O$), 2.14-2.24 (m, 10H, Ar-*CH*$_3$ and -C*H*($CH_3$)$_2$), 1.02-1.22 (m, 28H, CH*(CH*$_3$*)*$_2$ and $C_3H_6O$), -7.86 (t, $^3J_{P\text{-}H}$ = 15 Hz, 2H, Ir-*H*). $^{13}C\{^1H\}$ NMR ($C_6D_6$): δ 261.2 (br, Ir=C), 161.9 (t, *J* = 9 Hz, C-N), 130.7 (PNP-aryl C), 124.7 (t, *J* = 25 Hz, PNP-aryl C), 122.8 (t, *J* = 24 Hz, PNP-aryl C), 115.6 (t, *J* = 4 Hz, PNP-aryl C), 79.7, 65.4, 26.4 (t, *J* = 16 Hz), 23.7, 20.6, 18.9, 18.6. $^{31}P\{^1H\}$ NMR: δ 46.7 (s). $^1H$ NMR ($CD_2Cl_2$): δ 7.29 (d, *J* = 8 Hz, 2H, Ar-H), 6.89 (s, 2H, Ar-H), 6.65 (d, *J* = 8 Hz, 2H, Ar-H), 4.41 (t, *J* = 7 Hz, 2H, $C_3H_6O$), 2.62 (t, *J* = 8 Hz, 2H, $C_3H_6O$), 2.33 (m, 4H, $CH(CH_3)_2$), 2.18 (s, 6H, Ar-$CH_3$), 1.80 (m, 2H, $C_3H_6O$), 1.10 (m, 24H, $CH(CH_3)_2$), -8.58 (t, *J* = 15 Hz, 2H, Ir-H). $^{31}P\{^1H\}$ NMR ($CD_2Cl_2$): δ 46.7 (s).

**Solution Characterization of (PNP)Ir(H)(1,4-dioxan-2-yl) (313).** (PNP)$IrH_2$ (**310**) (14.8 mg, 0.024 mmol) was combined with norbornene (14 mg, 0.14 mmol) in a J. Young tube and dissolved in 0.6 mL of 1,4-dioxane. $^{31}P$ NMR of the sample immediately displayed two doublets and an unidentified compound with a singlet at 42.9 ppm (ca. 15% by $^{31}P$ NMR). The volatiles were partially removed and the residues redissolved in $C_6D_6$. $^{31}P$ NMR in $C_6D_6$ showed the same percentage of a singlet at 41.9 ppm (ca. 15%) and two doublets representing **313** together with some amount of (PNP)$IrH_2$. $^{1}H$ NMR($C_6D_6$): δ 7.75 (m, 2H, Ar-*H*), 7.02 (d, *J* = 6 Hz, 1H, Ar-*H*), 6.97 (d, *J* = 6 Hz, 1H, Ar-*H*), 6.83 (d, *J* = 8 Hz, 2H, Ar-*H*), 5.65 (m, 1H, $C_4H_7O$), 4.02 (m, 2H, $C_4H_7O$), 3.80 (m, 2H, $C_4H_7O$), 3.74 (d, *J* = 10 Hz, 1H), 3.52 (d, *J* = 11 Hz, 1H), -34.2 (t, $^{3}J_{P\text{-}H}$ =13 Hz, 1H). All other protons of **313** were obscured by an unknown compound and traces of (PNP)$IrH_2$. $^{31}P\{^{1}H\}$ NMR: δ 46.5 (d, *J* = 322 Hz), 43.7 (d, *J* = 322 Hz). Thermolysis of **313** in 1, 4-dioxane leads to the transformation back to (PNP)$IrH_2$. Removal of solvent in vacuo also regenerates (PNP)$IrH_2$.

**Synthesis of (PNP)Ir(H)(1,4-dioxan-2-yl)(CO) (314).** (PNP)$IrH_2$ (**310**) (53 mg, 0.085 mmol) was combined with norbornene (26 mg, 0.26 mmol) in a J. Young tube and dissolved in 0.6 mL of 1,4-dioxane. A $^{31}P$ NMR spectrum of the sample immediately revealed two doublets and an unidentified compound with a singlet at 42.9 ppm (ca. 15% by $^{31}P$ NMR). The solution was frozen and the headspace evacuated and backfilled with carbon monoxide (1 atm). As the solution thawed, a gradual change in color from brown to yellow was observed, and $^{31}P$ NMR spectroscopy showed that the mixture contained 80% **314**. The volatiles were removed under vacuum, and the residue was crystallized in

toluene/pentane to obtain analytically pure **314** (26 mg, 0.035 mmol, 43%). $^{1}$H NMR($C_6D_6$): δ 7.64 (d, *J* = 8 Hz, 2H, Ar-*H*), 6.95 (s, 1H, Ar-*H*), 6.82 (s, 1H, Ar-*H*), 6.71 (t, *J* = 8 Hz, 2H, Ar-*H*), 5.27 (m, 1H, $C_4H_7O$), 3.94 (m, 2H, $C_4H_7O$), 3.78 (m, 2H, $C_4H_7O$), 3.68 (d, $^{3}J_{H-H}$ = 8 Hz, 1H), 3.54 (d, $^{3}J_{H-H}$ = 9 Hz, 1H, $C_4H_7O$), 2.43 (m, 1H, $CH(CH_3)_2$), 2.37 (m, 2H, $CH(CH_3)_2$), 2.19 (s, 3H, Ar-$CH_3$), 2.16 (s, 3H, Ar-$CH_3$), 2.07 (m, 1H, $CH(CH_3)_2$), 1.36 (q, $^{3}J_{H-H}$ = 8 Hz, 3H, $CH(CH_3)_2$),1.20 (q, $^{3}J_{H-H}$ = 8 Hz, 9H, $CH(CH_3)_2$), 1.12 (q, $^{3}J_{H-H}$ = 8 Hz, 9H, $CH(CH_3)_2$), 0.91 (q, $^{3}J_{H-H}$ = 8 Hz, 3H, $CH(CH_3)_2$), -8.34 (t, $^{3}J_{P-H}$ = 17 Hz, 1H, Ir-*H*). $^{13}C\{^{1}H\}$ NMR ($C_6D_6$): δ 179.7 (t, $^{2}J_{P-C}$ = 5 Hz), 161.1 (t, *J* = 8 Hz, C-N), 160.9 (t, *J* = 8 Hz,CN), 131.7 (PNP-aryl C), 131.5 (PNP-aryl C), 130.7 (PNP-aryl C), 130.6 (PNP-aryl C), 124.4 (t, *J* = 6 Hz, PNP-aryl C), 124.1 (t, *J* = 3 Hz, PNP-aryl C), 124.0 (t, *J* = 3 Hz, PNP-aryl C), 123.1 (t, *J* = 6 Hz, PNP-aryl C), 115.8 (t, *J* = 4 Hz, PNP-aryl C), 115.2 (t, *J* =4 Hz, PNP-aryl C), 81.6, 70.5, 67.1, 51.8 (t, *J* =2 Hz), 26.6 (t, *J* =16 Hz), 26.5, 25.9 (t, *J* =15 Hz), 25.8, 20.5, 20.4, 18.7, 18.4, 18.2, 18.0, 17.6, 17.5, 17.1, 17.0. $^{31}P\{^{1}H\}$ NMR: δ 28.6 (s). IR ($cm^{-1}$) ν(CO): 1980. Elem. An.. Found (Calculated) for $C_{31}H_{48}NO_3P_2Ir$: C, 50.53 (50.69); H, 6.57 (6.54); N, 1.90 (1.85).

**Synthesis of *trans*-(PNP)Ir(H)$_2$(CO) (315)** from 1,3,5-trioxane. (PNP)Ir$H_2$ (**310**) (16.5 mg, 0.026 mmol) was placed in a J. Young tube followed by the addition of a mesitylene solution of 1,3,5-trioxane (33 mg, 0.36 mmol) and norbornene (5 mg, 0.053 mmol). $^{31}P\{^{1}H\}$ NMR spectroscopy showed instantaneous generation of a reaction mixture containing 60% of the known compound (PNP)Ir(H)(Mes),(**301**) 15% of the trans-(PNP)Ir(H)$_2$(CO) (**315**) and 25% of an unidentified compound (42.1 ppm). The reaction mixture was heated at 85 $^{o}$C for 30 min, after which time $^{31}$P and $^{1}$H NMR

showed quantitative generation of *trans*-(PNP)Ir(H)$_2$(CO) (**315**) from all three intermediates.

**X-Ray data collection, solution, and refinement for 304c.** All operations were performed on a Bruker-Nonius Kappa Apex2 diffractometer, using graphite-monochromated MoKα radiation. All diffractometer manipulations, including data collection, integration, scaling, and absorption corrections were carried out using the Bruker Apex2 software.[105] Preliminary cell constants were obtained from three sets of 12 frames. Data collection was carried out at 120 K, using a frame time of 10 sec and a detector distance of 60 mm. The optimized strategy used for data collection consisted of seven phi and two omega scan sets, with 0.5 ° steps in phi or omega; completeness was 99.1%. A total of 4961 frames were collected. Final cell constants were obtained from the xyz centroids of 9594 reflections after integration.

From the lack of systematic absences, the observed metric constants and intensity statistics, space group $P2_1/n$ was chosen initially; subsequent solution and refinement confirmed the correctness of this choice. The structures were solved using SIR-92,[106] and refined (full-matrix-least squares) using the Oxford University Crystals for Windows program.[107] All ordered non-hydrogen atoms were refined using anisotropic displacement parameters; the hydride ion attached to Ir was refined using an isotropic displacement parameter. Hydrogen atoms attached to carbon atoms were fixed at calculated geometric positions and allowed to ride on the corresponding carbon atoms.

The crystal structure of **304c** contained disorder of the thiazole moiety, which was resolved successfully. The two-component disorder was described with a constraint that

the occupancies of the major and minor components sum to 1.0. Both major and minor component atoms were refined by using isotropic displacement parameters. Atoms S(1) and C(38) were disordered via an approximate reflection plane passing through Ir(1), N(2) and the midpoint of the C(38)-S(1) bond. However, the disorder is not statistical: the occupancy of the major component is 0.779(4). The final least-squares refinement converged to $R_1 = 0.0223$ ($I > 2\sigma(I)$, 8478 data) and $wR_2 = 0.0591$ ($F^2$, 10804 data, 397 parameters).

**X-Ray data collection, solution, and refinement for 312.** All operations were performed on a Bruker-Nonius Kappa Apex2 diffractometer, using graphite-monochromated MoKα radiation. All diffractometer manipulations, including data collection, integration, scaling, and absorption corrections were carried out using the Bruker Apex2 software.[105] Preliminary cell constants were obtained from three sets of 12 frames. Data collection was carried out at 120 K, using a frame time of 10 sec and a detector distance of 60 mm. A total of 3173 frames were collected. Final cell constants were obtained from the xyz centroids of 9725 reflections after integration.

From the lack of systematic absences, the observed metric constants and intensity statistics, space group *Pbca* was chosen initially; subsequent solution and refinement confirmed the correctness of this choice. The structures were solved using SIR-92,[106] and refined (full-matrix-least squares) using the Oxford University Crystals for Windows program.[107] All ordered non-hydrogen atoms were refined using anisotropic displacement parameters. Hydrogen atoms attached to carbon atoms were fixed at calculated geometric positions and allowed to ride on the corresponding carbon atoms.

The carbene ring was placed such that the O atom was in the 2-position (as established from spectroscopic evidence). The carbene ring lies on a crystallographic 2-fold axis containing the Ir and C14 atoms, and thus the O and C atoms must be disordered in the 2- and 5-positions. Beyond this expected disorder, it was noted that the oxygen atom (O1) and the carbon atom in the 5-position (C15) are not strictly related by the crystallographic 2 axis; further, the atoms in the 3- and 4- positions (C17, C16) are also not related by the 2-fold axis. In the final model the occupancies of atoms O1, C15, C16, and C17 were fixed at 0.5 and refined by using isotropic displacement parameters. In addition, both angular and distance restraints were made to various atoms on the ring, with an angular restraint for C14-O1-C17 of 110.0(5) ° and distance restraints of C15 to C16, C17 to O1, C14 to C15, C16 to C17, and C14 to O1 of 1.500, 1.490, 1.400, 1.480, and 1.350 (with esd's of 0.005), respectively.

# CHAPTER IV

# C-H AND C-O OXIDATIVE ADDITION IN REACTIONS OF ARYL CARBOXYLATES WITH (PNP)Rh FRAGMENT*

## *4.1 Introduction*

Catalytic transformations of aryl halides that rely on the oxidative addition (OA) of $C_{Aryl}$-halogen bond to a Ni(0) or Pd(0) center are among the most explored, useful, and celebrated reactions in chemistry.[137,138] The ability to perform similar reactions using Ar-$O_2$CR ($O_2$CR = carboxylate, carbamate, carbonate) instead of Ar-Hal is an attractive expansion because Ar-$O_2$CR substrates are easily prepared from phenols (Ar-OH). Phenols are available through routes and in environments not always easily duplicated with aryl halides. In addition, Ar-$O_2$CR groups may provide avenues for directing functionalization of the arene ring that are not accessible with aryl halides.[139]

Coupling reactions of Ar-$O_2$CR and even other Ar-OR′ electrophiles have been successfully explored with Ni catalysts.[140-142] The interest in the use of Ar-$O_2$CR has increased significantly in the last few years, with reports on Suzuki-Miyaura coupling by Garg,[143] Nakamura,[144] Shi,[145] and Snieckus[143a, 146] and on aromatic amination by Chatani[147] using aryl pivalates and carbamates. There is sound evidence indicating that $C_{Aryl}$-$O_2$CR OA is part of the catalytic cycle in these reactions,[143,147, 148] however,

*[Zhu, Y.; Smith, D. A.; Herbert, D. E.; Gatard, S.; Ozerov, O. V. *Chem. Commun.* **2012**, *48*, 218.]-Reproduced (parts of this chapter) by permission of The Royal Society of Chemistry

authentic, well-defined $C_{Aryl}$-$O_2CR$ OA as an individual reaction has not been studied experimentally.[149]

Our group has been exploring[150,20,29b] oxidative addition reactions of aryl halides with the T-shaped $d^8$ (PNP)Rh species **406** (Scheme 4-1). The (PNP)Rh fragment **406** participates in reactions similar to those of $L_nM^0$ (M = Pd, Ni), despite possessing a different geometry and a different d-electron configuration. Recently, we have also explored catalysis of the arylation of aryl halides with a closely related ($P^OC^OP$)Rh fragment.[48] We became interested in whether such a Rh fragment can also undergo $C_{Aryl}$-$O_2CR$ OA and here we disclose our results showing that it is indeed possible with (PNP)Rh.

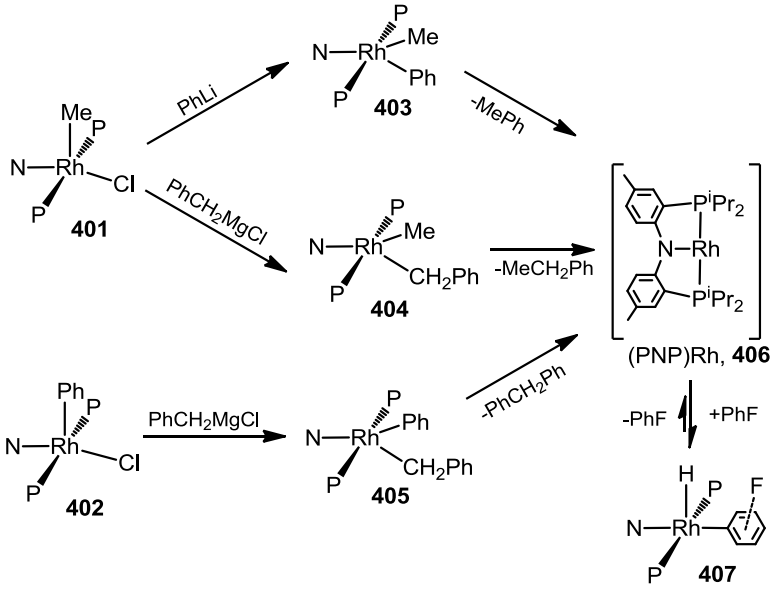


**Scheme 4-1.** Synthesis of various precursors to (PNP)Rh (**406**).

### *4.2 Results and discussion*

*4.2.1 Synthesis of the synthons for (PNP)Rh*

The key fragment **406** cannot be isolated or observed because of its high reactivity.[150] We have devised two ways to access it in solution: a) either by irreversible C-C reductive elimination (RE) or b) by reversible dissociation from a place holder ligand.[150] It is more convenient (although not always necessary) to have access to an isolable precursor to **406**. For (a), the C-C RE in (PNP)Rh(Ph)(Me) (**403**), reported previously,[29b] conveniently generates **406** from (PNP)Rh(Me)(Cl) (**401**),[2b] however it occurs too rapidly for isolation and storage of pure **403**. C-C RE in (PNP)Rh(Me)($CH_2$Ph) (**404**) and (PNP)Rh(Ph)($CH_2$Ph) (**405**) proceeded more slowly

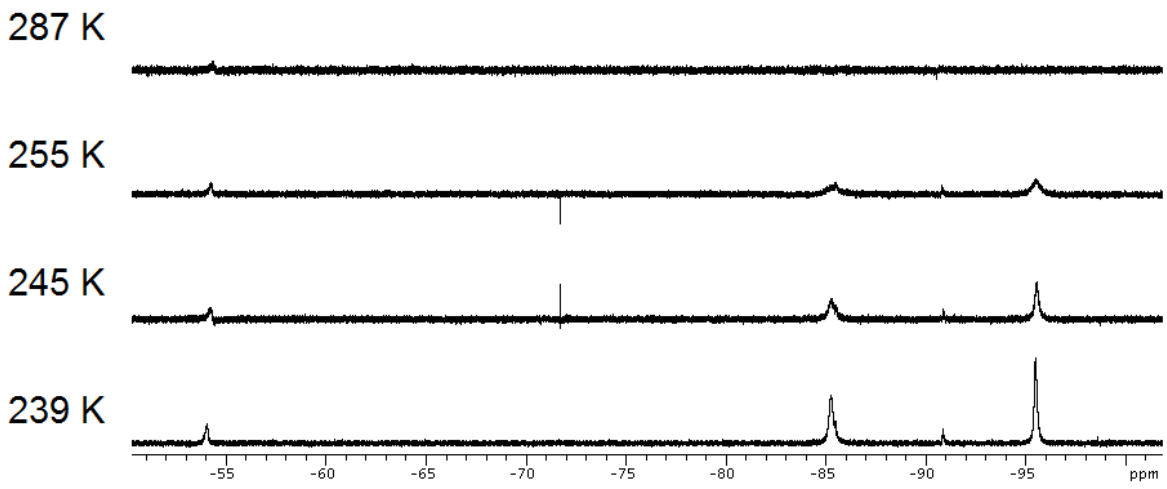


**Figure 4-1.** Variable temperature $^{19}$F NMR spectra of **407** in PhF.

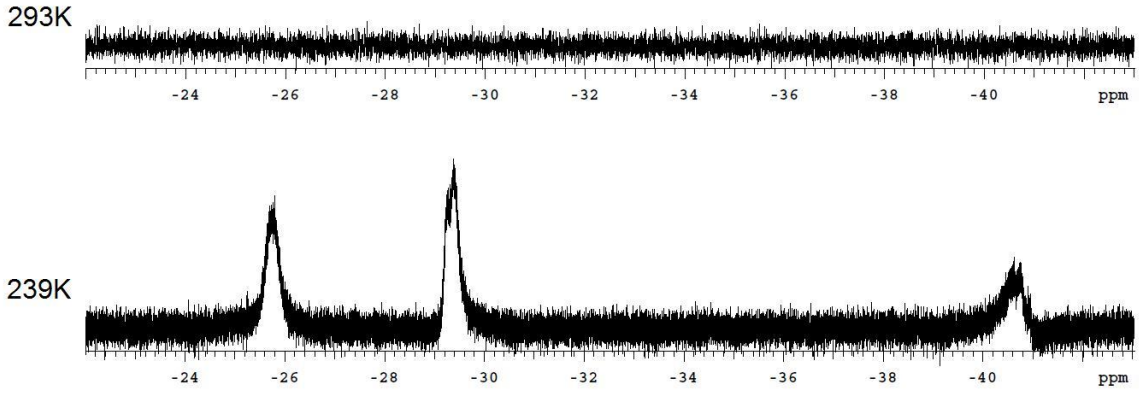


**Figure 4-2.** Variable temperature $^{1}$H NMR spectra of **407** in PhF (Referenced to trace poly(dimethylsiloxane) as 0 ppm and only hydride region shown).

and we were able to isolate **405** as a pure solid from (PNP)Rh(Ph)(Cl) (**402**) (Scheme 4-1).

For (b), the weakest practical adduct of (PNP)Rh would be one with the solvent. Given that we typically use aromatic solvents for our studies, an arene adduct was an appealing target. Thermolysis of **403** in fluorobenzene resulted in the formation of a product that in the pure isolated form analyzed correctly for the empirical formula of "(PNP)Rh(PhF)" (**407**, Scheme 4-1). In solution at near ambient temperature, **407** is only stable in PhF as solvent. It gave rise to a single $^{31}$P NMR resonance at 20 ℃ at 52.4 ppm (d, $J_{P\text{-}Rh}$ = 113 Hz) while no identifiable $^{19}$F NMR or upfield hydride $^{1}$H NMR resonance could be detected for **407** at 20 ℃. However, upon cooling to -34 ℃, a few $^{19}$F NMR resonances in the -50 to -95 ppm range and a few broad $^{1}$H NMR resonances

in the -25 to -41 ppm range were detected (Figure 4-1, 4-2). The paucity of the available data precluded conclusive identification of the species in solution, but it seems most likely that a rapid equilibrium between various isomers (including rotamers) of (PNP)Rh(H)($C_6H_4F$) takes place, perhaps also involving a π-complex of PhF. This analysis is consistent with the observed average $J_{P\text{-}Rh}$ = 113 Hz, that is indicative of trivalent Rh in the PNP framework and is similar to the $J_{P\text{-}Rh}$ values of other C-H OA products reported here and elsewhere.[150] Caulton et al. reported that the ground state of ($^{Si}$PNP)Rh (where $^{Si}$PNP = ($^{t}Bu_2PCH_2SiMe_2)_2N$) is an intramolecular C-H OA product that exists in equilibrium with a phenyl/hydrido "adduct" in benzene solution.[151] The X-ray structural determination on a crystal of **407** (Figure 4-3) revealed a fluorophenyl/hydride structure. The substitutional disorder of the fluorophenyl group in the crystal (50% F *syn* with Rh-H, 50% *anti*) is consistent with the notion of rotamers of close energy. No C-F OA was observed after thermolysis at 95 ℃ for 18 h in neat PhF.

*4.2.2 Reaction of (PNP)Rh with $PhO_2CPh$ and $MeO_2CPh$*

We selected several Ar-$O_2$CR substrates for our study and monitored their reaction with **405** (Scheme 4-2A) under mild thermolysis (60 ℃, 2-3 h) by NMR spectroscopy in situ. These thermolytic conditions were needed to complete the C-C reductive elimination in **405**; the reaction of the presumed **406** so generated with the substrate was much faster as no intermediates were observed. We were able to use (PNP)Rh precursors other than **405** for these syntheses, as shown in Scheme 4-2B.

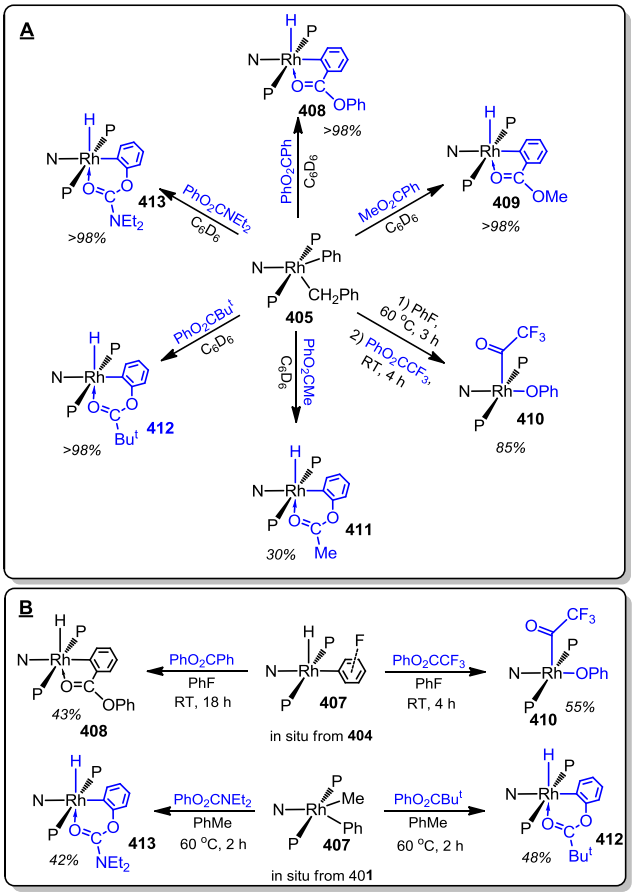


**Scheme 4-2. A** (top): Reactions of **405** under mild thermolysis (60 ℃, 2-3 h) with various esters (1.1-3 equiv per Rh). **B** (bottom): Preparative isolation of compounds **408**, **410**, **412**, and **413**.

The reaction of **405** with phenyl benzoate and, for comparison also with methyl benzoate, resulted in complete conversion to the C-H OA products **408** and **409**, respectively. The C-H OA took place exclusively at the *ortho*-position of the benzoate Ph ring. Harsher thermolysis (100 ℃, 18 h) of **408** or **409** did not result in any further transformations. Our group recently described[150] analogous *ortho*-C-H OA[152] taking place in nitroarenes and arenecarboxylic acid esters. The *ortho*-O chelated C-H OA

products share common diagnostic spectroscopic features. For example, **408** gave rise to a $^{1}$H NMR hydride resonance at δ -19.9 ppm as well as a $^{13}$C{$^{1}$H} resonance at 181.0 ppm for the Rh-bound carbon, both of which manifested themselves as doublets of triplets ($J_{H\text{-}Rh}$ = 35 Hz, $J_{H\text{-}P}$ = 14 Hz; $J_{C\text{-}Rh}$ = 28 Hz, $J_{C\text{-}P}$ = 10 Hz). A single crystal X-ray diffraction study confirmed the structure of **408** (Figure 4-4). As expected, the carbonyl oxygen is coordinated to Rh, completing the d$^{6}$ Rh(III) octahedral coordination sphere.

*4.2.3 Reaction of (PNP)Rh with $PhO_2CCF_3$*

In terms of its basicity and leaving group ability in organic chemistry, trifluoroacetate is probably the most "halide-like" of carboxylates.[153] We wondered if phenyl trifluoroacetate might also be the most "aryl halide-like" in OA reactivity. However, the reaction of in-situ generated **407** with it resulted in the acyl-oxygen OA main product **410**, with no evidence for either aryl-oxygen OA or C-H OA (Scheme 4-2A). The diagnostic $^{13}$C NMR resonance for the Rh-bound acyl carbon at 191.9 ppm was observed as a doublet of triplets in the $^{13}$C{$^{19}$F,$^{1}$H} NMR spectrum with $J_{C\text{-}Rh}$ = 44 Hz and $J_{C\text{-}P}$ = 9 Hz. IR spectroscopic analysis revealed a carbonyl stretching band at 1701 cm$^{-1}$. We have also prepared (PNP)Rh($COCF_3$)(I) by OPh/I metathesis of **410** with $Me_3$Si-I in situ and $Me_3$SiOPh was observed by $^{1}$H NMR spectrum. (PNP)Rh($COCF_3$)(I) gave rise to a $^{13}$C{$^{1}$H} multiplet at 192 ppm and a $\nu_{CO}$ = 1693 cm$^{-1}$. These data are similar to other examples of trifluoroacetyl complexes of Rh as well as Pd/Pt/Ir.[154-156] Extended thermolysis of **410** led to a mixture of products that included (PNP)Rh($CF_3$)(CO)(OPh)[157] and the previously reported (PNP)Rh(CO),[56] indicating CO

deinsertion as the major pathway of reaction for **410**, typical for late metal trifluoroacetyl compounds.[158]

*4.2.4 Reaction of (PNP)Rh with $PhO_2CCH_3$*

We also tested phenyl acetate in the reaction with **405** (Scheme 4-2). A mixture of products was obtained, one of which we tentatively identified as **411** based on the solution NMR spectroscopic data. The presence of (PNP)Rh(CO)[56] in the initial mixture and its increasing prominence upon further thermolysis indicated that the formation of **411** is reversible (unlike **408** and **409**) and that decarbonylation was taking place. The decarbonylation of $PhO_2CMe$ likely takes place through intermediates analogous to those in the reactions of $PhO_2CCF_3$.

*4.2.5 Reaction of (PNP)Rh with $PhO_2C^tBu$ and $PhO_2CNEt_2$*

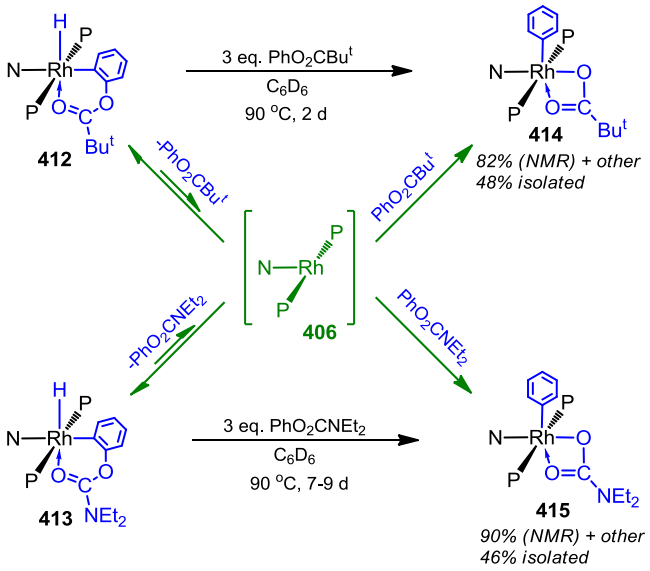


**Scheme 4-3.** Formation of the aryl-oxygen OA products upon thermolysis at 90 ℃. The proposed mechanistic path is shown in green.

Finally, we turned to $PhO_2CBu^t$ and $PhO_2CNEt_2$ as substrates, noting that aryl pivalates and carbamates were successfully used in Ni-catalyzed coupling reactions.[143,148] Mild thermolysis of **405** in the presence of $PhO_2CBu^t$ and $PhO_2CNEt_2$ resulted in the quantitative formation of compounds **412** and **413**, respectively (Scheme 4-2A). The diagnostic NMR spectroscopic features for **412** and **413** were the $^1$H NMR hydride resonances (δ -19.41 (**412**), -19.53 (**413**) ppm) as well as the $^{13}C\{^1H\}$ resonances for the Rh-bound carbons (δ 139.9 (**412**) and 141.7 (**413**) ppm), all of which were observed as doublets of triplets ($J_{H\text{-}Rh}$ = 31 Hz, $J_{H\text{-}P}$ = 14 Hz for both; $J_{C\text{-}Rh}$ = 30 or 29 Hz, $J_{C\text{-}P}$ = 10 or 9 Hz for **412** and **413**, respectively). The immediate coordination environment about Rh is the same for **408**/**409** and **412**/**413**; the difference is in that the $\kappa^2$-*C*,*O* chelate forms a five-membered ring in **408**/**409** and a six-membered ring in **412**/**413**.

Thermolysis at 90 ℃ of **412** (2 d) and **413** (9 d) resulted in the conversion to the $C_{Aryl}$-O OA products **414** and **415**, respectively (Scheme 4-3). Isolation of analytically pure **414** and **415** was accomplished in 46-48% unoptimized yields. The conversion of **412**/**413** to **414**/**415** was also studied in situ by NMR spectroscopy with an internal integration standard. Interestingly, it was found that the yield of **414**/**415** was only ca. 50% if pure samples of **408**/**409** were thermolyzed in $C_6D_6$ to 100% conversion. The yield of **414**/**415** increased to 82-90% when the thermolysis was carried out in the presence of 3 equiv of $PhO_2CBu^t$ or $PhO_2CNEt_2$, respectively. The remainder of the fully consumed **412**/**413** gave rise to a mixture of unidentified products. We hypothesize that the reaction path from **412**/**413** to **414**/**415** involves intermediate liberation of

$PhO_2CBu^t$ or $PhO_2CNEt_2$ by C-H RE and an attack of **406** on the $C_{aryl}$-O bond in the free substrate. In the absence of added extra substrate, the substrate concentration in solution is low and **406** may undergo unselective and irreversible attack on itself. The notion of intermediate liberation of $PhO_2CBu^t$ or $PhO_2CNEt_2$ is consistent with the observation of a mixture of **414** and **415** when **412** is thermolyzed in the presence of $PhO_2CNEt_2$ or **413** in the presence of $PhO_2CBu^t$.[159]

Concerted RE from a six-coordinate $d^6$ metal center typically requires prior dissociation of one of the ligands.[160] In the case of **412**/**413**, this would necessitate dissociation of the O-donor as the first step. The longer time needed for the conversion of **413** is likely a reflection of the stronger donor power of the carbonyl oxygen in carbamate.

***4.3 Solid-state structures of compounds 407, 408 and 415***[161]

Three Rh compounds, **407**, **408** and **415** were isolated for X-ray diffraction study. The structure of **407** can be described as square pyramidal with the hydride ligand trans to the apical site. The hydride ligand was located by XRD. The P-Rh-P angle is 160.58(4)°, typical for PNP complexes. The orientation of fluorine in fluorophenyl group is disordered in the crystal structure of **407** (50% F *syn* with Rh-H, 50% *anti*) and this is consistent with the notion of rotamers of close energy.

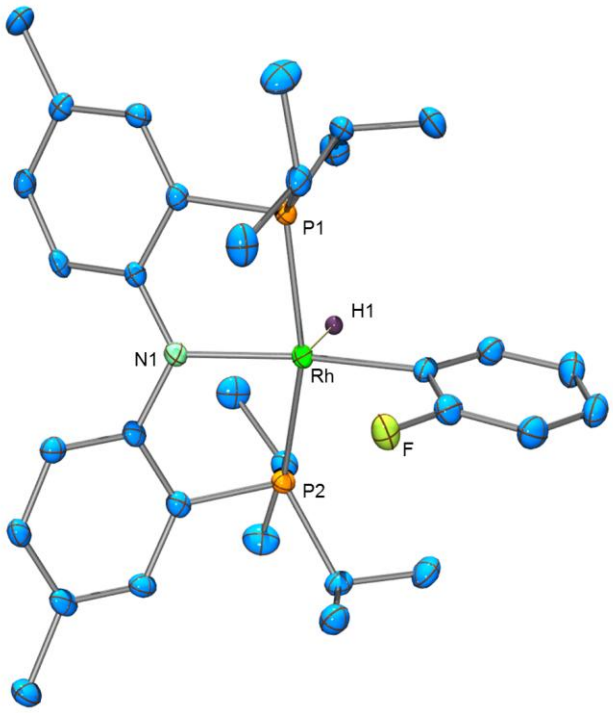


**Figure 4-3.** ORTEP drawing[103] of **407** (50% thermal ellipsoids). Crystal was obtained by Dan Smith. Hydrogen atoms (except Rh-H) and disorder of the fluorophenyl group are omitted for clarity. Selected bond distances (Å) and angles (deg) for **407**: Rh1-P1, 2.2695(17); Rh1-P2, 2.2847(19); Rh1-N1, 2.059(4); Rh1-C33, 2.024(4); P1-Rh1-P2, 160.58(4); C33-Rh1-N1, 168.78(16); P2-Rh1-N1, 81.68(12).

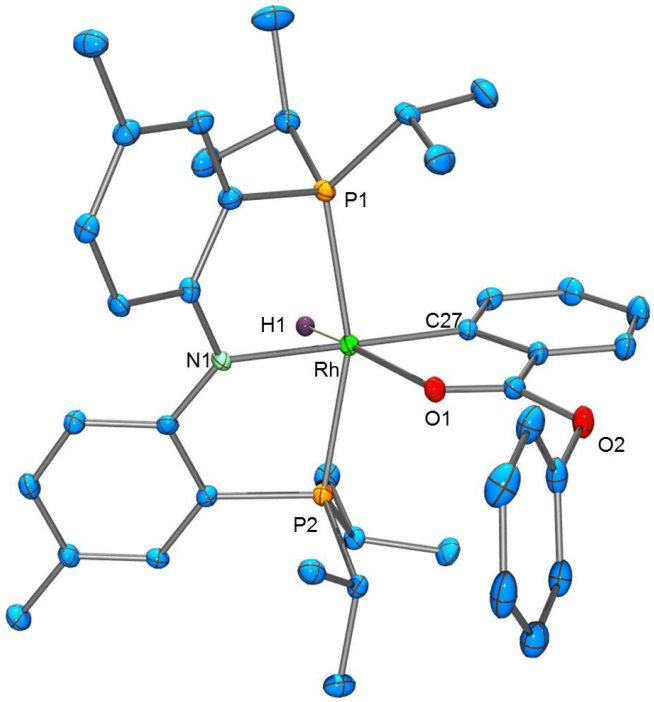


**Figure 4-4.** ORTEP drawing[103] of **408** (50% thermal ellipsoids). Hydrogen atoms (except Rh-H) are omitted for clarity. Selected bond distances (Å) and angles (deg) for **408**: Rh1-P1, 2.301(4); Rh1-P2, 2.291(4); Rh1-N1, 2.128(5); Rh1-C27, 2.017(5); Rh1-O1, 2.264(4); Rh1-H1, 1.46 (5); P1-Rh1-P2, 160.40(7); C27-Rh1-N1, 177.78(17); P2-Rh1-N1, 80.18(10); C27-Rh1-O1 78.9(2); P1-Rh1-H1 87(2).

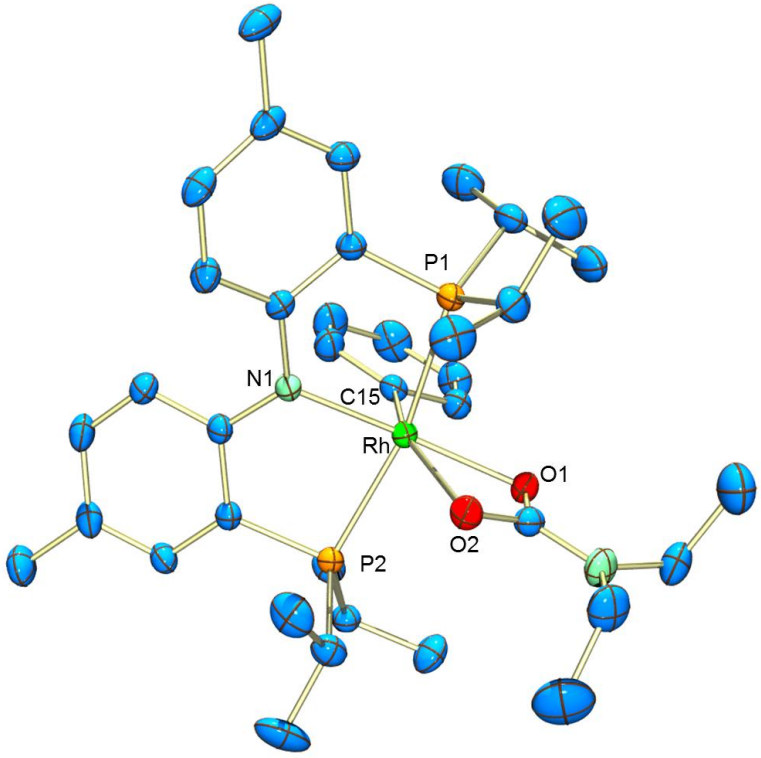


**Figure 4-5.** ORTEP drawing[103] of **415** (30% thermal ellipsoids). Hydrogen atoms are omitted for clarity. Selected bond distances (Å) and angles (deg) for **415**: Rh1-P1, 2.3061(13); Rh1-P2, 2.3215(12); Rh1-N1, 2.044(2); Rh1-C15, 2.016(3); Rh1-O1, 2.107(2); Rh1-O2, 2.279 (2); P1-Rh1-P2, 165.87(3); C15-Rh1-N1, 91.24(11); P2-Rh1-N1, 82.45(7); O2-Rh1-O1 59.78(7); P1-Rh1-O1 94.76(6); N1-Rh1-O1, 171.44(8); C15-Rh1-O2, 157.08(10).

The geometry of the six-coordinate compound **408** can be described as distorted octahedron. The hydride ligand was located by XRD study. The strong trans influence hydride was trans to the oxygen. The hydride resonated at -19.9 ppm in $^{1}$H NMR wasconsistent with the observation that the coordination of the sixth ligand would make the hydride shift downfield compared with the hydride trans to empty site in square pyramidal complexes. As shown in Figure 4-4, the *ortho*-C-H bond activation product

was formed due to the chelating effect to form the stable five membered ring.[152] The C-H activation of benzyl ring instead of phenyl ring can probably be ascribed to the formation of more stable five membered ring than the six membered ring.

The solid-state structure of **415** was established in a single crystal X-ray diffraction study (Figure 4-5). The environment about Rh is distorted octahedral, with the acute bite angle of the $\kappa^2$-carbamate being the major source of deviation. The two Rh-O bond lengths differ by ca. 0.17 Å and the N1-Rh1-O1 angle of 171.44(8)° is closer to linearity than the C15-Rh1-O2 angle of 157.08(10)°. This is consistent with the bond to O *trans* to N (weak *trans*-influence) being stronger than to O trans to Ph (strong *trans*-influence). The Rh-C bond lengths in the structures of **407**, **408**, and **415** are very similar (2.016(3) – 2.024(4) Å). The other angles and distances in the Rh coordination spheres are generally unremarkable.

***4.4 Attempted C-C cross coupling reactions catalyzed by (PNP)Rh system***

Coupling reactions of Ar-$O_2$CR with nucleophiles have shown success with nickel catalysts. We are interested to examine whether similar reactions would be accomplished in a well defined (PNP)Rh system. As described above, our (PNP)Rh fragment can successfully oxidative add Ph-O bond in $PhO_2CBu^t$ and $PhO_2CNEt_2$ especially in the presence of excess substrate. However, these two reactions are very slow (several days at 90 $^oC$). We tested the coupling reactions of $PhO_2CBu^t$ with *p*-F-$C_6H_4B(OH)_2$ catalyzed by (PNP)Rh(Ph)(OC(O)$Bu^t$). Not too surprisingly, we did not observe the catalytic conversion in this reaction.

Although (PNP)Rh(Ph)(OC(O)Bu$^t$) is not a good catalyst to couple $PhO_2CBu^t$ with *p*-F-$C_6H_4B(OH)_2$, we do observe catalytic coupling of PhOTf with *p*-F-$C_6H_4B(OH)_2$ by using (PNP)Rh(Ph)(OTf) (**416**) as the catalyst (eq.1). Aryl triflates are valuable starting materials for C-C bond formation because of their stability and greater availability from phenols. Compound **416** was synthesized through the oxidative addition of Ph-O to (PNP)Rh intermediate. It is encouraging that the (PNP)Rh system can indeed conduct catalytic C-C coupling reaction but the results are not satisfied. The best conversion was 75%, with 45% yield of the desired coupling product and fluorobenzene as by-product.

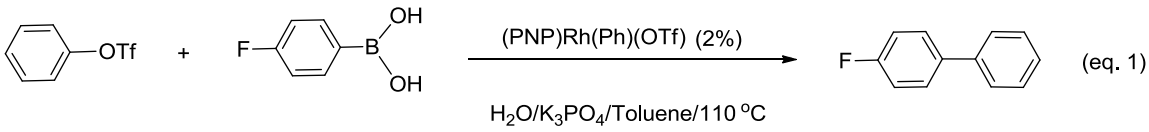

(eq. 1)

### *4.5 Conclusion*

In conclusion, the outcome of the reaction of the (PNP)Rh fragment with Ph-$O_2$CR substrates is strongly dependent on the nature of R. It appears that a bulky and/or more electron-donating R group helps block the undesirable $C_{acyl}$-O OA and channel the reaction towards $C_{aryl}$-O OA. The competition between $C_{acyl}$-O OA and $C_{aryl}$-O OA has been recognized before in the chemistry of Ni.[143a,148] Our findings here also highlight C-H OA as another potential side reaction and illustrate that pivalate and carbamate may be particularly suitable for pursuing $C_{aryl}$-O OA reactions regardless of the metal involved.

We hope that the insight from this study with a well-defined (PNP)Rh fragment will help design and understand other systems as well.

### *4.6 Experimental*

**General Considerations.** Unless specified otherwise, all manipulations were performed under an argon atmosphere using standard Schlenk line or glovebox techniques. Ethyl ether, $C_6D_6$, and pentane were dried over Na/K/$Ph_2CO$/18-crown-6, distilled or vacuum transferred and stored over molecular sieves in an Ar-filled glovebox. Fluorobenzene was dried with and then distilled from $CaH_2$. (PNP)Rh(Me)(Cl),[2b] (PNP)Rh(Ph)(Cl),[29b] (PNP)Rh($S^iPr_2$),[150] $PhO_2CBu^t$, [162] $PhO_2CNEt_2$[163] were prepared according to the published procedures. All other chemicals were used as received from commercial vendors (PhLi, 1.8 M/$Bu_2O$; BnMgCl, 1.0 M/$Et_2O$; MeMgCl, 3.0 M/THF). NMR spectra were recorded on a Varian iNova 300, Varian iNova 400, and Mercury 300 spectrometer. Chemical shifts are reported in δ (ppm). For $^1H$ and $^{13}C$ NMR spectra, the residual solvent peak was used as an internal reference. $^{31}P$ NMR spectra were referenced externally using 85% $H_3PO_4$ at δ 0 ppm. $^{19}F$ NMR spectra were referenced externally using $CF_3COOH$ at δ -78.5 ppm. Elemental analyses were performed by CALI, Inc. (Parsippany, NJ).

**Synthesis of precursors to (PNP)Rh (406).**

**(PNP)Rh(Me)(Ph) (403). 401** (15 mg, 0.026 mmol) was treated with PhLi (15 μL, 0.026 mmol) in $C_6D_6$ in a J. Young NMR tube. After 10 min, $^{31}P\{^1H\}$ NMR spectroscopic analysis revealed complete disappearance of the starting material and only the doublet for **403** was detected (35.9 ppm, $J$ = 118 Hz). Complex **403** is unstable and

thus was only characterized in situ in solution. Selected NMR spectroscopic data collected at the early stage of the reaction (10 min after the addition of PhLi) fit our previously reported data for complex **403.**[29b]

**(PNP)Rh(Me)($CH_2Ph$)** (**404**). **401** (15 mg, 0.026 mmol) was treated with $PhCH_2MgCl$ (26 μL, 0.026 mmol) in $C_6D_6$ in a J. Young NMR tube. After 10 min, $^{31}P\{^1H\}$ NMR spectroscopic analysis revealed complete disappearance of the starting material and only the doublet for **404** was detected (32.2 ppm, $J$ = 120 Hz). $^1H$ NMR spectroscopic analysis revealed >98% conversion of (PNP)Rh(Me)(Cl) to (PNP)Rh(Me)($CH_2Ph$) by using TMS as an internal integration standard. Complex **404** was not stable enough for isolation in pure solid form, and thus was only characterized in situ in solution. NMR data collected at the early stage of the reaction (10 min after the addition of BnMgCl). $^{31}P\{^1H\}$NMR ($C_6D_6$): δ 32.2 (d, $J$ = 120 Hz). $^1H$ NMR ($C_6D_6$): δ 7.84 (d, $J$ = 8 Hz, 2H, (PNP)Aryl-*H*), 7.50 (d, $J$ = 8 Hz, 2H, Bn-*H*), 7.09 (d, $J$ = 8 Hz, 2H, Bn-*H*), 7.01 (t, $J$ = 6 Hz,1H, Bn-*H*), 6.92 (br, 2H, (PNP)Aryl-*H*), 6.86 (d, $J$ = 8 Hz, 2H, (PNP)Aryl-*H*), 3.56 (td, $J$ = 6, 3 Hz, 2H, Bn-*H*), 2.36 (m, 2H, C*H*$Me_2$), 2.22 (s, 6H, Ar-C*H*$_3$), 2.16 (m, 2H, C*H*$Me_2$), 1.57 (td, $J$ = 6, 2 Hz, 3H, Rh-C*H*$_3$), 1.26 (app. q(dvt), $J$ = 7 Hz, 6H, CH*Me*$_2$), 1.05 (app. q(dvt), $J$ = 7 Hz, 6H, CH*Me*$_2$), 0.94 (app. q(dvt), $J$ = 7 Hz, 6H, CH*Me*$_2$), 0.72 (app. q(dvt), $J$ = 7 Hz, 6H, CH*Me*$_2$).

**(PNP)Rh(Ph)($CH_2Ph$) (405). 402** (82 mg, 0.13 mmol) was treated with BnMgCl (140 μL, 0.14 mmol) in PhF. After 10 min, the reaction mixture was passed through Celite and silica. The volatiles were removed under vacuum. The residue was dissolved in pentane and placed in a -35 ℃ freezer. The green precipitate was collected the next

day and dried in vacuum. Yield: 64 mg, 0.10 mmol, 72%. $^{31}$P NMR{$^{1}$H} ($C_6D_6$): δ 34.2 (d, *J* = 121 Hz). $^{1}$H NMR ($C_6D_6$): δ 8.01 (d, *J* = 8 Hz, 2H), 7.64 (d, *J* = 7 Hz, 2H), 7.47 (d, *J* = 8 Hz, 2H), 7.14 (m, 2H, overlapping with $C_6D_6$), 7.03 (d, *J* = 7 Hz, 1H), 6.96 (d, *J* = 6 Hz, 2H), 6.94 (br, 2H), 6.91 (d, *J* = 5 Hz, 2H), 6.87 (t, *J* = 7 H, 1H), 4.16 (q, *J* = 4 Hz, Rh-C*H*$_2$), 2.21 (m, 8H, Ar-C*H*$_3$+C*H*Me$_2$), 1.75 (m, 2H, C*H*Me$_2$), 0.90 (m, 12H, CH*Me*$_2$), 0.82 (app. q(dvt), *J* = 7 Hz, 6H, CH*Me*$_2$), 0.71 (app. q(dvt), *J* = 7 Hz, 6H, CH*Me*$_2$). $^{13}$C{$^{1}$H} NMR ($C_6D_6$): δ 160.7 (vt, *J* = 9 Hz, *C*-N), 151.5, 151.4, 150.8 (dt, *J* = 34, 10 Hz, Rh-*C*), 136.7, 133.3, 131.9, 129.7, 128.5, 126.5, 125.1, 124.3 (vt, *J* = 3 Hz), 122.1, 121.9 (vt, *J* = 18 Hz), 117.1 (t, *J* = 5 Hz), 25.0 (vt, *J* = 11 Hz), 24.5 (vt, *J* = 10 Hz), 21.2 (dt, *J* = 29, 5 Hz, Rh-*C*H$_2$), 20.6, 19.4, 19.1, 18.8, 18.5.

**(PNP)Rh($C_6H_5F$) (407).** To a stirred solution of $C_6H_5F$ (3 mL) of **402** (25 mg, 0.039 mmol) was added MeMgCl (13 μL, 0.039 mmol). After 5 minutes the solution was filtered through Celite, the volatile components removed *in vacuo* and $C_6H_5F$ (1 mL) added. After standing for 24 h a color change was noted for the solution from dark green to brown and removal of the volatile components gave an orange-brown solid (16.9 mg, 0.027 mmol, 69 %). Brown block-like crystals suitable for an X-ray diffraction study were grown by slow evaporation of a solution prepared by the method above but using $PhCH_2MgCl$ (39 μL, 0.039 mmol) as the transmetallation reagent. $^{1}$H NMR ($C_6H_5F$, 239 K) δ: -25.71, -29.31, -40.68 (all br), referenced to trace poly(dimethylsiloxane) grease as 0 ppm. $^{19}$F NMR ($C_6H_5F$, 255 K) δ: -54.03 (br), -85.29 (br, overlapping) -85.50 (br, overlapping), -90.85 (br), -95.50 (br). $^{31}$P{$^{1}$H} NMR ($C_6H_5F$, 293 K) δ: 52.4 (d, *J* = 113 Hz). Elem. An.. Found (Calculated) for $C_{32}H_{45}NFP_2Rh$: C 61.08 (61.24); H 7.16 (7.23).

**Thermolysis of 407. 407** (10 mg, 0.016 mmol) was dissolved in 0.6 mL PhF in a J. Young NMR tube and was heated at 95 $^{o}$C for 18 h. $^{31}$P NMR spectroscopic analysis indicated no observable changes.

**Reactions with $PhO_2CPh$.**

**(PNP)Rh(H)($C_6H_4COOC_6H_5$) (408). 401** (41 mg, 0.070 mmol) was dissolved in 1 mL of PhF followed by the addition of $PhCH_2MgCl$ (78 μL, 0.078 mmol). The mixture was passed through Celite and silica gel after stirring at ambient temperature for 10 min. The volatiles were removed under vacuum. The residue was redissolved in about 0.6 mL of PhF and heated at 60 ℃ for 3 h. The green solution gradually turned brown. $^{31}P\{^{1}H\}$ NMR spectroscopic analysis indicated full conversion to **407**. $PhO_2CPh$ (13 mg, 0.065 mmol) was added to the solution and the reaction mixture was left at room temperature for overnight. The brown color of the solution changed to green-yellow. The volatiles were removed under vacuum and the residue was recrystallized from PhF/pentane at -35 ℃ to produce a yellow solid. Yield: 21 mg, 0.029 mmol, 43%. $^{31}P\{^{1}H\}$NMR ($C_6D_6$): δ 52.6 (d, *J* = 110 Hz). $^{1}$H NMR ($C_6D_6$): δ 8.12 (d, *J* = 8 Hz, 1H), 7.94 (d, *J* = 7 Hz, 1H), 7.70 (d, *J* = 8 Hz, 2H), 7.09 (d, *J* = 7 Hz, 2H), 7.05 (t, *J* = 2 Hz, 1H), 6.80-6.93 (m, 5H), 6.73 (m, 3H), 2.16 (s, 6H), 2.07 (m, 4H), 1.09 (app. q(dvt), *J* = 8 Hz, 6H), 0.94 (m, 12H), 0.85 (app. q(dvt), *J* = 8 Hz, 6H), -19.9 (dt, *J* = 35 Hz, *J* = 14 Hz, 1H). $^{13}C\{^{1}H\}$NMR ($C_6D_6$): δ 181.0 (dt, *J* = 28, 10 Hz, Rh-*C*), 173.7 (C=O), 161.1 (vt, *J* = 9 Hz, C-N), 151.4 (C-O), 144.6, 133.6, 131.8, 131.1, 130.2, 129.5, 126.0, 122.8 (vt, *J* = 4 Hz), 122.3 (vt, J = 20 Hz), 121.5, 120.6, 115.9 (vt, *J* = 5 Hz), 115.6, 25.3 (vt, *J* = 12 Hz),

24.1 (vt, *J* = 11 Hz), 20.6, 18.3, 17.8 (two signals overlapping), 17.7. Elem. An.. Found (Calculated) for $C_{39}H_{50}NO_2P_2Rh$: C 64.11 (64.20); H 6.84 (6.91).

**Thermolysis of complex 408.** Complex **408** (10 mg, 0.014 mmol) was dissolved in 0.6 mL $C_6D_6$ in a J. Young NMR tube and was heated at 100 ℃ for 18 h. Both $^{31}P$ and $^{1}H$ NMR spectroscopic analyses indicated no observable changes.

**NMR tube synthesis of 408 from 405. 405** (10 mg, 0.014 mmol) and $C_6H_5OC(O)C_6H_5$ (3.0 mg, 0.015 mmol) were dissolved in 0.60 mL of $C_6D_6$ in a J. Young NMR tube. The reaction mixture was placed in a 60 ℃ oil bath for 100 min. $^{1}H$ NMR spectroscopic analysis indicated >98% conversion to **408** by using $(Me_3Si)_2O$ as an internal integration standard.

**Reactions with $MeO_2CPh$.**

**(PNP)Rh(H)($C_6H_4COOCH_3$) (409). 401** (30 mg, 0.052 mmol) was dissolved in about 0.6 mL of PhF followed by the addition of PhLi (31 μL, 0.057 mmol). The reaction mixture was stirred for about 10 min and passed through Celite and silica. The volatiles were removed under vacuum. The residue was redissolved in about 0.6 mL of PhF and heated at 60 ℃ for 3 h. The green solution gradually turned brown. $^{31}P\{^{1}H\}$ NMR spectroscopic analysis indicated full conversion to **407**. $MeO_2CPh$ (9.0 μL, 0.068 mmol) was added to the solution and the reaction mixture was left at room temperature overnight. The brown color of the solution changed to green-yellow. The volatiles were removed under vacuum. The residue was redissolved in $C_6D_6$. **409** was not isolated and only characterized in solution by NMR spectroscopy. $^{31}P\{^{1}H\}$ NMR ($C_6D_6$): δ 52.1 (d, *J*

= 110 Hz). $^{1}$H NMR ($C_6D_6$): δ 7.91 (d, *J* = 7 Hz, 1H), 7.83 (m, 3H), 7.04 (t, *J* = 6 Hz, 1H), 6.91 (br, 2H), 6.85 (m, 3H), 3.32 (s, 3H), 2.22 (s, 6H), 2.09 (m, 2H), 2.00 (m, 2H), 1.08 (app. q(dvt), *J* = 8 Hz, 6H), 0.94 (app. q(dvt), *J* = 8 Hz, 6H), 0.88 (m, 12H), -19.5 (dt, *J* = 35 Hz, *J* = 14 Hz, 1H). Thermolysis of complex **409** at 100 ℃ for 18 h did not lead to any observable changes by NMR spectroscopy.

**NMR tube synthesis of 409 from 405. 405** (10 mg, 0.014 mmol) and $MeO_2CPh$ (4.0 μL, 0.030 mmol) were dissolved in 0.60 mL of $C_6D_6$ in a J. Young NMR tube. The reaction mixture was placed in a 60 ℃ oil bath for 100 min. $^{1}$H NMR spectroscopic analysis indicated >98% conversion to **409** by using $(Me_3Si)_2O$ as internal standard .

**Reactions with $PhO_2CCF_3$.**

**(PNP)Rh(OPh)(C(O)$CF_3$) (410). 401** (119 mg, 0.205 mmol) was dissolved in 3 mL of PhF followed by the addition of BnMgCl (225 μL, 0.225 mmol). The mixture was passed through Celite and silica after stirring at ambient temperature for 10 min. The volatiles were removed under vacuum. The residue was redissolved in about 3 mL of PhF and heated at 60 ℃ oil bath for 3 h. $^{31}$P{$^{1}$H} NMR spectroscopic analysis indicated full conversion to **407**. After that, $PhO_2CCF_3$ (305 μL, 2.05 mmol) was added to the solution and the reaction mixture was left at ambient temperature for 4 h. The volatiles were removed under vacuum and the residue was recrystallized from PhF/pentane at -35 ℃ to give a green solid. Yield: 81 mg, 0.112 mmol, 55%. $^{31}$P{$^{1}$H} NMR ($C_6D_6$): δ 50.4 (d, *J* = 110 Hz). $^{1}$H NMR ($C_6D_6$): δ 7.46 (d, *J* = 8 Hz, 2H), 7.16-7.20 (m, 2H), 6.81 (s, 1H), 6.77 (d, *J* = 5 Hz, 2H), 6.67-6.74 (m, 4 Hz), 2.28 (m, 4H), 2.09 (s, 6H), 1.28 (app.

q(dvt), *J* = 8 Hz, 6H), 0.94 (app. q(dvt), *J* = 8 Hz, 6H), 0.84 (m, 12H). $^{13}C\{^{19}F, ^{1}H\}$ NMR ($C_6D_6$): δ 191.9 (dt, $J_{C\text{-}Rh}$ = 44 Hz, $J_{C\text{-}P}$ = 9 Hz, *C*=O), 172.9, 159.9 (t, *J* = 9 Hz, N-*C*), 132.7, 132.0, 131.2, 129.2, 126.1, 120.3, 118.1, 115.1, 105.6, 25.6 (br), 23.8 (br), 20.5, 18.0, 17.4, 16.8. $^{19}F$ NMR ($C_6D_6$): δ -66.9. IR (solid): 1701 $cm^{-1}$. Elem. An.. Found (Calculated) for $C_{34}H_{45}NO_2F_3P_2Rh$: C 56.72 (56.59); H 6.46 (6.29); N 1.90 (1.94).

**NMR tube synthesis of 410. 405** (10 mg, 0.014 mmol) was dissolved in 0.6 mL of PhF in a J. Young NMR tube. A capillary with a $PPh_3$ solution as standard was inserted in the same NMR tube. The reaction mixture was placed in a 60 ℃ oil bath for 3 h. $^{31}P\{^{1}H\}$ NMR indicated complete conversion to **407**. After that, $PhO_2CCF_3$ (21 μL, 0.14 mmol) was added to the solution and the reaction mixture was left at ambient temperature for 4 h. $^{31}P\{^{1}H\}$ NMR spectroscopic analysis indicated 85% conversion to product **510** and 15% of an unidentified product (singlet at δ 30.6 ppm).

**NMR tube synthesis of (PNP)Rh(I)(C(O)$CF_3$). 410** (11 mg, 0.015 mmol) was treated with $Me_3SiI$ (7.0 μL, 0.045 mmol) in a J. Young NMR tube in 0.60 mL of $C_6D_6$. After 1 h at room temperature, $^{31}P\{^{1}H\}$ NMR spectroscopic analysis indicated >97% conversion to (PNP)Rh(I)(C(O)$CF_3$). No NMR detectable changes were observed after overnight. $^{1}H$ NMR ($C_6D_6$): δ 7.57 (d, *J* = 8 Hz, 2H), 6.80 (br, 2H), 6.76 (d, *J* = 8 Hz, 2H), 2.69 (m, 2H), 2.39 (m, 2H), 2.09 (s, 6H), 1.37 (app. q(dvt), *J* = 8 Hz, 6H), 1.17 (app. q(dvt), *J* = 8 Hz, 6H), 1.06 (app. q(dvt), *J* = 8 Hz, 6H), 0.99 (app. q(dvt), *J* = 8 Hz, 6H). $^{13}C\{^{1}H\}$ NMR ($C_6D_6$): δ 192.5~191.5 (m, *C*=O), 160.0 9 (vt, *J* = 9 Hz, N-*C*), 132.7, 132.1, 126.8, 119.6 (vt, *J* = 19 Hz), 118.6, 103.3 (q, *J* = 301 Hz), 25.9 (vt, *J* = 12 Hz),

25.3 (vt, $J$ = 12 Hz), 20.5, 19.0, 181., 17.8, 17.7. $^{31}P\{^{1}H\}$ NMR ($C_6D_6$): δ 51 (d(br), $J$ = 100 Hz). $^{19}F$ NMR ($C_6D_6$): δ -68.9. IR ($C_6D_6$): 1693 $cm^{-1}$.

In another J. Young NMR tube, **410** (11 mg, 0.015 mmol) was treated with $Me_3SiI$ (7.0 μL, 0.045 mmol) in 0.60 mL of $CDCl_3$. After 1h at room temperature, $^{31}P\{^{1}H\}$ NMR analysis indicated >97% conversion to (PNP)Rh(I)($C(O)CF_3$). $^{1}H$ NMR ($CDCl_3$): 7.45 (d, $J$ = 8 Hz, 2H), 6.98 (br, 2H), 6.92(d, $J$ = 9 Hz, 2H), 2.98 (m, 2H), 2.74 (m, 2H), 2.26 (s, 6H), 1.44 (app. q(dvt), $J$ = 8 Hz, 6H), 1.29 (app. q(dvt), $J$ = 8 Hz, 6H), 1.16 (app. q(dvt), $J$ = 8 Hz, 12H). $Me_3SiOPh$ was also observed by NMR, matching the data from a literature source.[164]

**Thermolysis of complex 410.** In a J. Young NMR tube, **410** (10 mg, 0.014 mmol) was dissolved in about 0.6 mL of $C_6D_6$ and placed in a 60 ℃ oil bath for 15 h. Based on $^{31}P$ NMR spectroscopic analysis, (PNP)Rh(CO) (~20%) was observed together with another new broad doublet at δ 57.0 ppm ($J$ = 88 Hz) (~70%) and a broad signal δ 53 ppm . Interestingly, free $PhO_2CCF_3$ (-75.5 ppm) was detected by $^{19}F$ NMR spectroscopy. A quartet δ 3.5 ppm ($J$ = 11 Hz) together with another small signal at ca. -4 ppm were also observed by $^{19}F$ NMR. Although the Rh complexes are unidentified in this reaction, the formation of (PNP)Rh(CO) as well as the apparent quartet in the $^{19}F$ NMR spectrum (Rh-$CF_3$) suggest that CO deinserted from the acyl complex. The IR spectrum of this mixture revealed two CO stretching bands (2062 and 1942 $cm^{-1}$). We have not been able to isolate analytically pure compounds from this reaction mixture. We tentatively assign the signal δ 57.0 ppm observed by $^{31}P$ NMR to complex (PNP)Rh($CF_3$)(CO)(OPh) (IR: 2062 $cm^{-1}$).

**Reactions with $PhO_2CCH_3$.**

**Reaction with $PhO_2CCH_3$. 401** (15 mg, 0.026 mmol) was dissolved in about 0.6 mL of PhF, followed by the addition of PhLi (15 μL, 0.027 mmol). The reaction mixture was stirred for about 10 min and passed through Celite and silica. The volatiles were removed under vacuum. The residue was redissolved in about 0.6 mL of PhF and heated at 60 ℃ for 3 h. The green solution turned to brown gradually. $^{31}P\{^1H\}$ NMR indicated full conversion to **407**. $PhO_2CCH_3$ (5.0 μL, 0.039 mmol ) was added to the solution and the reaction mixture was allowed to stand at room temperature. After 2 h, $^{31}P\{^1H\}$ NMR spectroscopic analysis revealed two doublets δ 49.9 ppm ($J$ = 108 Hz) (57%) and 47.1 ppm ($J$ = 131 Hz) (43%). Unfortunately, we were not able to isolate pure compounds out of this reaction mixture. Due to the similarity in the $^{31}P\{^1H\}$ NMR (δ 49.9 ppm ($J$ = 108 Hz)) and the Rh-*H* $^1H$ NMR signals (δ -19.6 ppm (dt, $J$ = 33, 12 Hz)) to compounds **408** and **409**, we tentatively assigned the $^{31}P$ signal δ 49.9 ppm ($J$ = 108 Hz) to the compound **411**.

**NMR tube reaction of 405 with $PhO_2CCH_3$. 405** (15 mg, 0.021 mmol) and $PhO_2CCH_3$ (3.0 μL, 0.025 mmol ) were dissolved in 0.60 mL of $C_6D_6$ in a J. Young NMR tube. The reaction mixture was heated at 60 $^oC$ for 100 min. $^{31}P\{^1H\}$ NMR spectroscopic analysis revealed the formation of (PNP)Rh(CO) (30%), the possible C-H activation product **411** (30%) and two other unidentified species (40%). Continued thermolysis of this reaction mixture at 95 $^oC$ for 2 days resulted in (PNP)Rh(CO) as the only observable compound by $^{31}P$ NMR. However, $^1H$ NMR spectroscopic analysis revealed that (PNP)Rh(CO) can only account for ~50% percent of the total

organometallic Rh by using $(Me_3Si)_2O$ as internal standard. Free ethane was also observed by $^1H$ NMR.

**Reactions with $PhO_2CBu^t$.**

**(PNP)Rh(H)($C_6H_4O(O)CCMe_3$) (412). 401** (138 mg, 0.238 mmol) was dissolved in 1 mL of toluene followed by the addition of PhLi (138 μL, 0.248 mmol). The mixture was passed through Celite and silica after stirring at ambient temperature for 10 min. The volatiles were removed under vacuum. The residue was redissolved in about 3 mL of toluene. $PhO_2CBu^t$ (47 μL, 0.26 mmol) was added to the solution and the reaction mixture was heated at 60 ℃ for 100 min. The volatiles were removed under vacuum and the residue was recrystallized from toluene/pentane at -35 ℃. Yield: 73 mg, 0.103 mmol, 45%. $^{31}P\{^1H\}$ NMR ($C_6D_6$): δ 50.4 (d, *J* = 110 Hz). $^1H$ NMR ($C_6D_6$): 7.76 (d, *J* = 8 Hz, (PNP)Aryl-*H*), 7.67 (d, *J* = 6 Hz, 1H), 6.90 (br, 2H, (PNP)Aryl-*H*), 6.79-6.86 (m, 5H), 2.21 (s, 6H, Ar-C*H*$_3$), 2.15 (m, 4H, C*H*$Me_2$), 1.10 (app. q(dvt), 6H, *J* = 7 Hz, CH*Me*$_2$), 1.01 (m, 15H, CH*Me*$_2$ + C*Me*$_3$), 0.91 (m, 12H, CH*Me*$_2$), -19.41(dt, *J* = 31 Hz, 14 Hz, 1H). $^{13}C\{^1H\}$ NMR ($C_6D_6$): δ 177.3, 160.7 (vt, *J* = 10 Hz, *C*-N), 155.5, 149.0, 139.9 (dt, *J* = 29 Hz, 9 Hz, ipso-*C*), 131.6, 131.2, 123.9, 123.2 (vt, *J* = 10 Hz), 122.5 (vt, *J* = 3 Hz), 122.2, 116.1, 115.7 (t, *J* = 5 Hz), 39.9, 26.7, 25.2 (vt, *J* = 14 Hz), 24.6 (vt, *J* = 9 Hz), 20.7, 18.3, 18.2, 17.9. Elem. An.. Found (Calculated) for $C_{37}H_{54}NO_2P_2Rh$: C 62.49 (62.62); H 7.61 (7.67).

**NMR tube synthesis of 412. 405** (10 mg, 0.014 mmol) and $PhO_2CBu^t$ (3.5 μL, 0.015 mmol) were dissolved in 0.60 mL of $C_6D_6$ in a J. Young NMR tube. The reaction

mixture was placed in a 60 ℃ oil bath for 100 min. $^{1}$H NMR spectroscopic analysis indicated >98% conversion to complex **412** by using $(Me_3Si)_2O$ as internal standard.

**(PNP)Rh($C_6H_5$)(OC(O)C$Me_3$) (414). 412** (40 mg, 0.056 mmol) and $PhO_2CBu^t$ (30 μL, 0.16 mmol) were dissolved in about 0.6 mL $C_6D_6$ in a sealed NMR tube and the NMR tube was heated in a 90 ℃ oil bath. The yellow-greenish solution changed to red gradually. After 53 h, $^{31}$P NMR spectroscopic analysis revealed complete consumption of **412** and the appearance of a new dominant doublet of **414**. The reaction mixture was passed through Celite. The volatiles were removed under vacuum and the residue was recrystalized from toluene/pentane at -35 ℃. Yield: 19 mg, 0.027 mmol, 48%. $^{31}$P{$^{1}$H} NMR ($C_6D_6$): δ 40.0 (d, *J* = 107 Hz). $^{1}$H ($C_6D_6$): δ 8.08 (d, *J* = 8 Hz, 1H), 7.92 (d, *J* = 9 Hz, 2H), 6.68-6.99 (m, 8H), 2.47 (m, 2H), 2.24 (m, 2H), 2.12 (s, 6H), 1.35 (s, 9H), 1.22 (app. q(dvt), *J* = 8 Hz, 6H), 1.15 (app. q(dvt), *J* = 8 Hz, 6H), 1.07 (app. q(dvt), *J* = 8 Hz, 6H), 0.40 (app. q(dvt), *J* = 8 Hz, 6H). $^{13}$C{$^{1}$H} NMR ($C_6D_6$): δ 189.2 (C=O), 161.3 (t, *J* = 10 Hz, *C*-N), 138.7 (dt, *J* = 29 Hz, 9 Hz, ipso-*C*), 136.0, 132.5, 131.5, 127.3, 125.4 (vt, *J* = 3 Hz), 123.0, 119.0, 118.8 (vt, *J* = 6 Hz), 118.7, 118.5, 39.3, 30.0, 24.1 (vt, *J* = 11 Hz), 23.5 (vt, *J* = 12 Hz), 20.5, 19.2, 17.6, 17.5, 17.3. Elem. An.. Found (Calculated) for $C_{37}H_{54}NO_2P_2Rh$: C 62.61 (62.62); H 7.77 (7.67).

**NMR tube thermolysis of 412 in the absence of $PhO_2CBu^t$. 412** (10 mg, 0.014 mmol) was dissolved in about 0.6 mL $C_6D_6$ in a sealed NMR tube and heated in a 90 ℃ oil bath for two days. $^{31}$P{$^{1}$H} NMR spectroscopic analysis revealed that there are several other unidentified species in the reaction mixture in addition to **414** (50%).

**NMR tube thermolysis of 412 in the presence of excess $PhO_2CBu^t$.** The NMR sample of complex **412** generated from the reaction of **405** with $PhO_2CBu^t$, as described above, was treated with 3 equiv of $PhO_2CBu^t$. The reaction mixture was heated at 90 ℃ for 2 d. $^{31}P$ NMR spectroscopic analysis indicated disappearance of the C-H activation product **412** and the formation of one doublet corresponding the C-O activation product **414**. However, the $^1H$ NMR spectroscopic analysis indicated only ca. 82% formation of the desired product. Some small amounts of impurities remain unidentified.

**NMR tube thermolysis of 412 in the presence of excess $PhO_2CNEt_2$. 412** (10 mg, 0.014 mmol) and $PhO_2CNEt_2$ (10 μL, 0.060mmol) were dissolved in about 0.6 mL $C_6D_6$ in a sealed NMR tube and heated in a 90 ℃ oil bath. After 5 d, $^1H$ NMR spectroscopic analysis indicated the formation of compounds **414** and **415** in a ca. 1:2 ratio.

**Reactions with $PhO_2CNEt_2$.**

**(PNP)Rh(H)($C_6H_4O(O)CNEt_2$) (413). 401** (57 mg, 0.098 mmol) was dissolved in 1 mL of toluene followed by the addition of PhLi (57 μL, 0.10 mmol). The mixture was passed through Celite and silica after stirring at ambient temperature for 10 min. The volatiles were removed under vacuum. The residue was redissolved in about 3 mL of toluene. $PhO_2CNEt_2$ (22 μL, 0.12 mmol) was added to the solution and the reaction mixture was heated at 60 ℃ for 100 min. The volatiles were removed under vacuum and the residue was recrystallized from pentane/hexamethyldisiloxane at -35 ℃. Yield: 30 mg, 0.041 mmol, 42%. $^{31}P\{^1H\}$ NMR ($C_6D_6$): δ 49.7 (d, $J$ = 111 Hz). $^1H$ ($C_6D_6$): 7.80 (d, $J$ = 8 Hz, 2H, (PNP)Aryl-*H*), 7.77 (br, 1H), 6.95 (br, 2H, (PNP)Aryl-*H*), 6.92 (d, $J$ = 8

Hz, 1H), 6.89 (d, *J* = 3 Hz, 1H), 6.86 (d, *J* = 8 Hz, 2H, (PNP)Aryl-*H*), 6.77 (d, *J* = 7 Hz, 1H, (PNP)Aryl-*H*), 2.93 (q, *J* = 7 Hz, 2H, C*H*$_2$CH$_3$), 2.79(q, *J* = 7 Hz, 2H, C*H*$_2$CH$_3$), 2.34 (m, 2H, C*H*Me$_2$), 2.23 (s, 6H, Ar-C*H*$_3$), 2.18 (m, 2H, C*H*Me$_2$), 1.15 (app. q(dvt), *J* = 8 Hz, 6H, CH*Me*$_2$), 1.03 (m, 18H, CH*Me*$_2$), 0.84 (t, *J* = 6 Hz, 3H, CH$_2$C*H*$_3$), 0.57 (t, *J* = 6 Hz, 3H, CH$_2$C*H*$_3$), -19.53 (dt, *J* = 31 Hz, 14 Hz, 1H, Rh-*H*). $^{13}$C{$^1$H} NMR (C$_6$D$_6$): δ 160.9 (vt, *J* = 8 Hz, *C*-N), 155.7, 155.1, 148.5, 141.7 (dt, *J* = 30 Hz, 10 Hz), 131.5, 131.4, 123.6 (vt, *J* = 20 Hz), 123.4, 122.2 (vt, *J* = 3 Hz), 122.0, 115.9, 115.6 (vt, *J* = 6 Hz), 41.9, 25.1 (vt, *J* = 10 Hz), 24.9 (vt, *J* = 10 Hz), 20.7, 18.2, 17.9, 14.0, 13.2. Elem. An.. Found (Calculated) for $C_{37}H_{55}N_2O_2P_2Rh$: C 61.25 (61.32); H 7.58 (7.65); N 3.81 (3.87).

**NMR tube synthesis of 413. 405** (10 mg, 0.014 mmol) and PhO$_2$CNEt$_2$ (4.0 μL, 0.015 mmol) were dissolved in 0.60 mL of C$_6$D$_6$ in a J. Young NMR tube. The reaction mixture was placed in a 60 ℃ oil bath for 100 min. $^1$H NMR spectroscopic analysis indicated >98% conversion to complex **413** by using (Me$_3$Si)$_2$O as an internal integration standard.

**(PNP)Rh(C$_6$H$_5$)(OC(O)NEt$_2$) (415). 413** (48 mg, 0.066 mmol) and PhO$_2$CNEt$_2$ (37 μL, 0.20 mmol) were dissolved in about 0.6 mL C$_6$D$_6$ in a sealed NMR tube and the NMR tube was heated in a 90 ℃ oil bath. The yellow-greenish solution changed to red gradually. After 9 d, the $^{31}$P NMR spectroscopic analysis showed complete consumption of **413** and the appearance of a new dominant doublet of **415**. The reaction mixture was passed through Celite. The volatiles were removed under vacuum and the residue was recrystalized from pentane/hexamethyldisiloxane at -35 ℃. Yield: 22 mg, 0.030 mmol,

46%. $^{31}P\{^{1}H\}$ NMR ($C_6D_6$): δ 39.9 (d, *J* = 108 Hz). $^{1}H$ NMR ($C_6D_6$): δ8.10 (d, *J* = 9 Hz, 1H), 7.88 (d, *J* = 8 Hz, 2H, (PNP)Aryl-*H*), 7.01 (d, *J* = 7 Hz, 2H), 6.87 (m, 3H), 6.82 (d, *J* = 8 Hz, 1H), 6.78 (br, 1H), 6.75 (br, 1H), 3.32 (q, *J* = 7 Hz, 2H, C*H*$_2$CH$_3$), 3.24 (q, *J* = 7 Hz, 2H, C*H*$_2$CH$_3$), 2.52 (m, 2H, C*H*Me$_2$), 2.20 (m, 2H, C*H*Me$_2$), 2.14 (s, 6H, Ar-CH$_3$), 1.34 (app. q(dvt), *J* = 8 Hz, 6H, CH*Me*$_2$), 1.01-1.21 (m, 18H), 0.55 (app. q(dvt), *J* = 8 Hz, 6H, CH*Me*$_2$). $^{13}C\{^{1}H\}$ NMR ($C_6D_6$): δ 165.1 (*C*=O), 161.1 (vt, *J* = 9 Hz, *C*-N), 140.2 (dt, *J* = 34 Hz, 9 Hz), 136.5, 133.7, 132.3, 131.3, 127.1, 125.4, 125.0 (vt, *J* = 3 Hz), 122.8, 120.2 (vt, *J* = 20 Hz), 118.7 (t, *J* = 5 Hz), 40.4, 40.3, 24.6 (vt, *J* = 10 Hz), 24.0 (vt, *J* = 11 Hz), 20.5, 19.2, 18.2, 17.9, 17.6, 14.8, 14.6. Elem. An.. Found (Calculated) for $C_{37}H_{55}N_2O_2P_2Rh$: C 61.35 (61.32); H 7.78 (7.65); N 3.79 (3.87).

**NMR tube thermolysis of 413 in the absence of $PhO_2CNEt_2$. 413** (10 mg, 0.015 mmol) was dissolved in about 0.6 mL $C_6D_6$ in a sealed NMR tube and heated in a 90 ℃ oil bath for 7 days. $^{31}P\{^{1}H\}$ NMR spectroscopic analysis revealed that there were several unidentified species in the reaction mixture in addition to **415** (50%). It is worth noting that the by-products observed by this reaction are similar to the by-products observed in the thermolysis of **412** in the absence of phenyl pivalate.

**NMR tube thermolysis of 413 in the presence of excess $PhO_2CNEt_2$.** The NMR sample of complex **413** generated from reaction of **405** with $PhO_2CNEt_2$as described above was treated with excess (10 eq) of $PhO_2CNEt_2$. The reaction mixture was heated at 90 ℃ for 9 d. $^{31}P$ NMR spectroscopic analysis indicated disappearance of the C-H activation product **413** and the formation of one doublet corresponding the C-O activation product **415**. However, the $^{1}H$ NMR spectroscopic analysis indicated only ca.

90% formation of the desired product. Some small amounts of impurities remian unidentified.

**NMR tube thermolysis of 413 in the presence of excess $PhO_2CBu^t$. 413** (10 mg, 0.015 mmol) together with $PhO_2CBu^t$ (11μL, 0.060 mmol) were dissolved in about 0.6 mL $C_6D_6$ in a sealed NMR tube and heated in a 90 ℃ oil bath. After 5 d, $^1$H NMR spectroscopic analysis indicated >98% conversion to compounds **414** and **415** in a ca. 5:2 ratio.

**Reactions with PhOTf.**

**(PNP)Rh(Ph)(OTf) (416).** (PNP)Rh($SPr^i_2$) (200.0 mg, 0.31 mmol) was treated with phenyl triflate (55.2 μL, 0.34 mmol) in fluorobenzene (5 mL) in a Teflon stoppered gas tight round bottom flask. After 1.5 h at 80 ℃, (PNP)Rh(Ph)(OTf) was the major compound observed by $^{31}P\{^1H\}$ NMR (another minor doublet at 57.4 ppm, $J$ = 128 Hz). Then, the resultant solution was filtered through Celite. The filtrate was evaporated to dryness to yield to a green residue. Then, this residue was dissolved in pentane and placed in the freezer at -35 ℃ to afford (PNP)Rh(Ph)(OTf) by precipitation. Yield: 0.146 g, 0.192 mmol, 62 %. $^1$H NMR ($C_6D_6$): δ 7.84 (d, 2H, 8 Hz, Ar-*H* of PNP), 7.81 (br d, 1H, $C_6H_5$), 6.78 (s, 2H, Ar-*H* of PNP), 6.74 (br, 1H, $C_6H_5$), 6.71 (d, 2H, $J$ = 8 Hz, Ar-*H* of PNP), 6.63 (t, 1H, $J_{H-H}$ = 8 Hz, $C_6H_5$), 6.61 (t, 1H, $J_{H-H}$ = 8 Hz, $C_6H_5$), 6.41 (t, 1H, $J_{H-H}$ = 7 Hz, $C_6H_5$), 3.45 (m, 2H, C*H*$Me_2$), 2.18 (m, 2H, C*H*$Me_2$), 2.06 (s, 6H, Ar-C$H_3$ of PNP), 1.04 (app. quartet (dvt), 6H, $J$ = 8 Hz, CH$Me_2$), 0.90 (app. quartet (dvt), 6H, $J$ = 8 Hz, CH$Me_2$), 0.98 (app. quartet (dvt), 6H, $J$ = 8 Hz, CH$Me_2$), 0.18 (app. quartet (dvt),

6H, $J$ = 8 Hz, CH*Me*$_2$). $^{13}C\{^1H\}$ NMR ($C_6D_6$): δ 161.5 (vt, 10 Hz, *C*-N), 139.3 (dt, $J_{C\text{-}P}$ = 9 Hz, $J_{C\text{-}Rh}$ = 38 Hz, *i*-$C_6H_5$), 133.6 (br, $C_6H_5$), 132.3, 131.8, 130.7 (br, $C_6H_5$), 130.0 (s, $C_6H_5$), 126.6(t, $J$ = 3 Hz) 124.3 (s, $C_6H_5$), 121.2 (s, *p*-$C_6H_5$), 119.8 (t, $J$ = 5 Hz), 116.8 (t, $J$ = 18 Hz), 27.1 (t, $J$ = 9 Hz), 24.8 (t, 9 Hz), 20.3, 19.3, 17.8, 15.4 (four s (two are overlapping at 19.3 ppm)), 1.2 (s, Rh-*C*$H_3$). $^{31}P\{^1H\}$ NMR ($C_6D_6$): δ 40.3 (d, $J$ = 106 Hz). $^{19}F\{^1H\}$ NMR ($C_6D_6$): δ -79.9.

**X-Ray data collection, solution, and refinement for 407.** A brown, multi-faceted crystal of suitable size (0.3 x 0.1 x 0.1 mm) and quality was selected from a representative sample of crystals of the same habit using an optical microscope, mounted onto a nylon loop and placed in a cold stream of nitrogen (110 K). Low-temperature X-ray data were obtained on a Bruker APEXII CCD based diffractometer (Mo sealed X-ray tube, Kα = 0.71073 Å). All diffractometer manipulations, including data collection, integration and scaling were carried out using the Bruker APEXII software.[105] An absorption correction was applied using SADABS.[165] The space group was determined on the basis of systematic absences and intensity statistics and the structure was solved by direct methods and refined by full-matrix least squares on $F^2$. The structure was solved in the monoclinic $P2_1/c$ space group using XS[166] (incorporated in SHELXTL). No obvious missed symmetry was reported by PLATON.[108] All non-hydrogen atoms were refined with anisotropic thermal parameters. Hydrogen atoms were placed in idealized positions and refined using riding model with the exception of the hydrogen bound to rhodium which was located from the difference map. The structure was refined (weighted least squares refinement on $F^2$) and the final least-squares refinement

converged to $R_1$ = 0.0537 ($I > 2\sigma(I)$, 4907) and w$R_2$ = 0.1322 ($F^2$, 32901 data, 357 parameters). The fluorine atom on the fluorobenzene residue was found to reside with equal occupancy on C(34) and C(35) and was refined as such.

**X-Ray data collection, solution, and refinement for 408.** An orange block (0.10 x 0.09 x 0.07 mm) was selected from a representative sample of crystals of the same habit using an optical microscope, mounted onto a nylon loop and placed in a cold stream of nitrogen (110 K). Low-temperature X-ray data were obtained on a Bruker APEXII CCD based diffractometer (Mo sealed X-ray tube, Kα = 0.71073 Å). All diffractometer manipulations, including data collection, integration and scaling were carried out using the Bruker APEXII software.[105] An absorption correction was applied using SADABS.[165] The space group was determined on the basis of systematic absences and intensity statistics and the structure was solved in the monoclinic space group $P2_1/c$ by direct methods using XS[166] (incorporated in SHELXTL). and refined by full-matrix least squares on $F^2$. No obvious missed symmetry was reported by PLATON.[108] All non-hydrogen atoms were refined with anisotropic thermal parameters. Hydrogen atoms were placed in idealized positions and refined using riding model with the exception of the hydrogen bound to rhodium which was located from the difference map. The structure was refined (weighted least squares refinement on $F^2$) and the final least-squares refinement converged to $R_1$ = 0.0596 ($I > 2\sigma(I)$, 8357 data) and w$R_2$ = 0.1602 ($F^2$, 38554 data, 420 parameters).

**X-Ray data collection, solution, and refinement for 415.** A brown, multi-faceted crystal of suitable size (0.25 x 0.05 x 0.03 mm) and quality was selected from a

representative sample of crystals of the same habit using an optical microscope and mounted onto a nylon loop. Due to a fault with the cryostream, room-temperature X-ray data were obtained on a Bruker APEXII CCD based diffractometer (Mo sealed X-ray tube, Kα = 0.71073 Å). All diffractometer manipulations, including data collection, integration and scaling were carried out using the Bruker APEXII software.[105] An absorption correction was applied using SADABS.[165] The space group was determined on the basis of systematic absences and intensity statistics and the structure was solved by direct methods and refined by full-matrix least squares on $F^2$. The structure was solved in the monoclinic $P2_1/n$ space group using XS[166] (incorporated in SHELXTL). No obvious missed symmetry was reported by PLATON.[108] All non-hydrogen atoms were refined with anisotropic thermal parameters. Hydrogen atoms were placed in idealized positions and refined using riding model. The structure was refined (weighted least squares refinement on $F^2$) and the final least squares refinement converged to $R_1$ = 0.0397 ($I > 2\sigma(I)$, 8517 data) and w$R_2$ = 0.1045 ($F^2$, 40598 data, 410 parameters).

# CHAPTER V

# SYNTHESIS, CHARACTERIZATION, AND REACTIVITY OF A RHODIUM DIFLUOROCARBENE COMPLEX SUPPORTED BY PNP PINCER LIGAND

## *5.1 Introduction*

Transition metal carbene metal complexes are of great interest to organometallic chemists due to their role in a wide variety of catalytic reactions.[167] The importance of olefin metathesis reactions as well as of metal carbene complexes as olefin metathesis catalysts— was recognized with the awarding of the Nobel Prize in Chemistry in 2005 to Chauvin, Grubbs, and Schrock.

Among the metal carbene complexes, difluorocarbene complexes are relatively rare. One of the general ways to produce the difluorocarbene complexes is via fluoride abstraction from the trifluoromethyl ligand by a Lewis acid.[168] Examples to generate metal difluorocarbene through α-fluorine elimination are also known.[169]

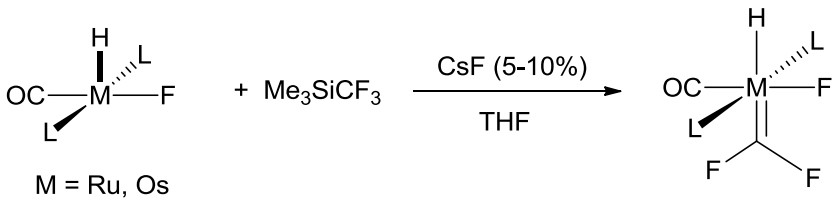


**Scheme 5-1.** Caulton's example of generating difluorocarbene metal complexes.

$Me_3SiCF_3$ has been exploited in organic chemistry as a convenient $CF_3$ transfer reagent.[170] On the other hand, not until 2000 Caulton et al applied it to organometallic synthesis.[169b] Caulton reported the reaction of $Me_3SiCF_3$ with $MHF(CO)L_2$ (M = Ru, Os) in the presence of a catalytic amount of $F^-$ (CsF) to give the difluorocarbene complexes $MHF(CF_2)(CO)L_2$ (Scheme 5-1). The authors proposed that in the presence of $F^-$, $Me_3SiCF_3$ exchanged $CF_3$ group with fluoride of $MHF(CO)L_2$ to give $Me_3SiF$ and fluorocarbene complexes $MHF(CF_2)(CO)L_2$ via α-fluorine migration. In 2001, Grubbs and coworkers reported a unique example of metathesis of 1,1-difluoroethylene with a ruthenium carbene complex to generate the ruthenium difluorocarbene (Scheme 5-2).[171]

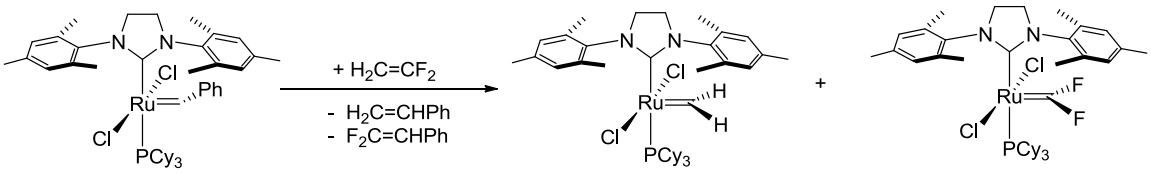


**Scheme 5-2.** Grubbs' example of making difluorocarbene complex through metathesis.

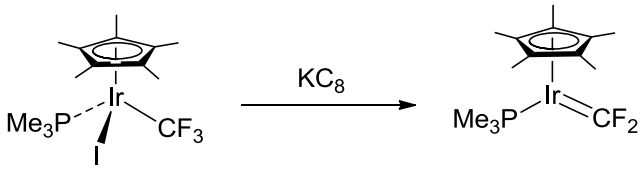


**Scheme 5-3.** Generation of a difluorocarbene complex through the reduction method by Hughes.

More recently, Hughes et al. reported a new reductive methodology to reduce perfluoroalkyl iridium metal complexes to perfluoroalkylidene by using $KC_8$ (Scheme 5-3). [172] Although difluorocarbene metal complexes are approachable by different synthetic routes, their reactivity is less studied and limited to exploration of their nucleophilic vs electrophilic character.

In this chapter, the synthesis and characterization of a PNP pincer ligated rhodium(I) difluorocarbene complex will be described and its reactivity towards electrophilic silylium cation will also be discussed.

### *5.2 Results and discussion*

#### *5.2.1 Synthesis and characterization of (PNP)Rh(=$CF_2$)*

A small amount of (~5 % by $^{31}$P NMR spectrum) of (PNP)Rh(=$CF_2$) (**501**) was first observed in the thermolysis of (PNP)Rh($COCF_3$)(OPh) (**410**) as described in Chapter 4. The mechanism of the formation of carbene complex is still unclear; however, **501** could

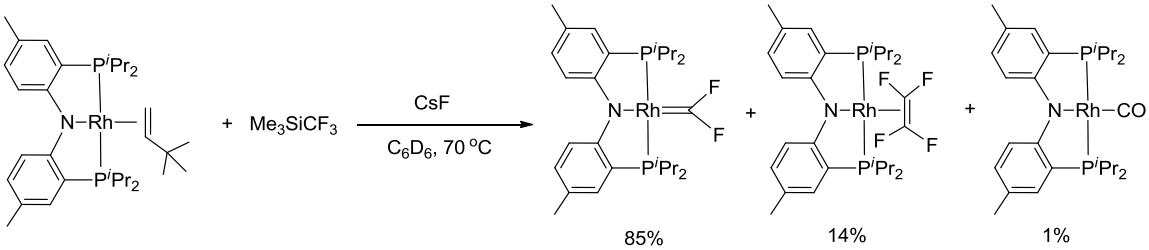


**Scheme 5-4.** Synthesis of (PNP)Rh(=$CF_2$).

be synthesized independently by reacting (PNP)Rh(TBE) (TBE = *tert*-butylethylene) with $Me_3SiCF_3$ in the presence of CsF. It is worth mentioning that there is no reaction between (PNP)Rh(TBE) and $Me_3SiCF_3$ in the absence of CsF. The reaction produced **501** (85%) along with (PNP)Rh($C_2F_4$) (**502**) (14%) and the previously reported (PNP)Rh(CO)[56] (1%) (Scheme 5-4). No PNP-containing intermediates were observed during the reaction.

Both **501** and **502** have been characterized spectrospically and by X-ray single crystal studies. **501** displays $C_{2v}$ symmetry in solution at room temperature as indicated by $^1$H NMR spectroscopy. Its $^{31}P\{^1H\}$ NMR signal is a doublet of triplets due to the coupling to rhodium and two fluorine nuclei (δ 53.7 ppm, $J_{Rh-P}$ = 146 Hz, $J_{F-P}$ = 30 Hz). The $^{19}$F NMR signal was found at δ 95.4 ppm as a doublet of triplets as well, with $J_{Rh-F}$ = 49 Hz and $J_{F-P}$ = 30 Hz. This low field $^{19}$F NMR chemical shift is characteristic of fluorocarbene metal complexes, which normally resonate in the δ 80-200 ppm region.[158] The carbene carbon resonance appears at low field as a doublet of triplets of triplets with a large $^1J_{C-F}$ coupling constant (δ 206.3 ppm, $J_{Rh-C}$ = 85 Hz, $J_{C-P}$ = 12 Hz, $J_{C-F}$ = 454 Hz). For compound **502**, the most distinctive NMR spectral features are the $^{31}P\{^1H\}$ NMR doublet of quintets resonance at δ 52.3 ppm ($J_{Rh-P}$ = 137 Hz, $J_{F-P}$ = 23 Hz) and the $^{19}$F NMR resonance at δ -100.8 ppm (broad). Compound **502** was not isolated in an analytically pure form due to its low fractional content in the reaction mixture, however, a 'lucky' crystal was grown and **502** was characterized by X-ray single crystal diffraction in the solid state.

The formation of **501** is not fully understood. Apparently, the presence of the $F^-$ source (CsF) is very important in this reaction. It has been demonstrated that the catalytic fluoride reacts with $Me_3SiCF_3$ to form either $Me_3Si(CF_3)_2^-$ or $Me_3Si(CF_3)(F)^-$ anions depending on the amount of $F^-$ used.[173] It is likely that formation of the anion increased the nucleophilicity of $CF_3$ which can attack the rhodium center. α-Fluoride abstraction leads to the observed fluorocarbene species (Scheme 5-5 (A)).

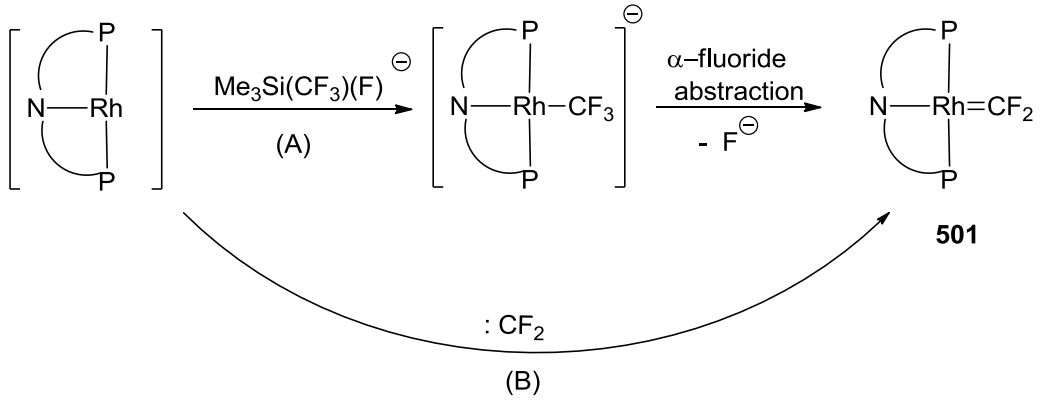


**Scheme 5-5.** Possible pathways for the formation of **501**.

The rhodium(I) diflurocarbene could also be formed by trapping free $:CF_2$ carbene with three-coordinate (PNP)Rh which was generated through the dissociation of TBE in solution (Scheme 5-5 (B)). The decomposition of trifluoromethane anion to difluorocarbene and a fluoride anion has been recognized before.[174] The formation of **502** might imply that free $:CF_2$ was generated and reacted with **501** to form the side product. On the other hand, we could not rule out the possibility that **502** might be formed through the dimerization of free carbene to give $CF_2=CF_2$, which could then be

trapped by the metal. However, no free $CF_2$=$CF_2$ was observed by $^{19}F$ NMR. The reaction of adventitious water with fluorocarbene metal complex to give the corresponding carbonyl complex is known[158] and is possibly responsible for the formation of (PNP)Rh(CO).

*5.2.2 Solid-state structures of compounds **501** and **502***[175]

Like most rhodium four-coordinate $d^8$ complexes, **501** adopts an approximately square planar geometry at the rhodium center with N1-Rh1-C1 of 171.39(15) ° and P1-Rh1-P2 of 162.14(4) ° (Figure 5-1). The Rh-C1 double bond distance of 1.821(4) Å is the same as that in $(PPh_3)_2Rh(CF_2)(F)$ (1.820(3) Å) published by Grushin et al.[176] The two C-F distances are only slightly different from each other and are within the range of the C-F bond distance in other difluorocarbene complexes.[172] The F1-Rh1-F2 angle is 100.8(3) °, which is also very similar to the corresponding one in $(PPh_3)_2Rh(CF_2)(F)$ (100.0(2) °). All other metrics relating to the PNP ligand are unremarkable.

The solid state structure of **502** is shown in Figure 5-2. The $C_2F_4$ ligand is symmetrically bonded to the rhodium. The four F atoms are coplanar with each other and are bent away from the metal center with C14 being displaced 0.453 Å from that plane towards rhodium. The C=C double bond distance of 1.354(7) Å is significantly shorter than its value in other structures which ranges from 1.37 Å to 1.44 Å.[177] The C-

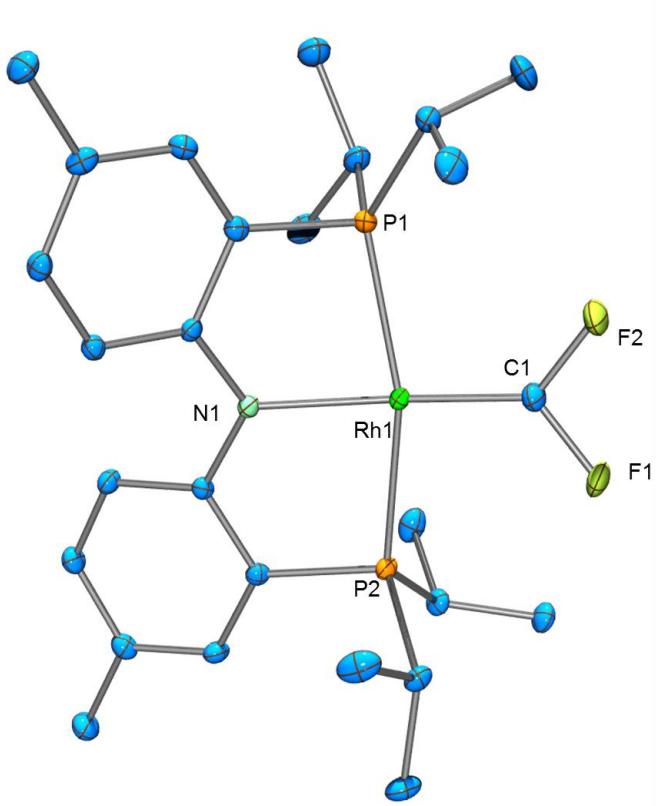


**Figure 5-1.** ORTEP drawing[103] of **501** (50% thermal ellipsoids). Hydrogen atoms are omitted for clarity. Selected bond distances (Å) and angles (deg) for **501**: Rh1-C1, 1.821(4); Rh1-N1, 2.043(3); Rh1-P1, 2.3033(12); Rh1-P2, 2.3012(11); C1-F1, 1.335 (4), C1-F2, 1.348 (5); P1-Rh1-P2, 162.14 (4); N1-Rh1-C1, 171.39 (15); F2-C1-F1, 100.8(3); Rh1-C1-F2, 130.1(3); Rh1-C1-F1, 128.6.

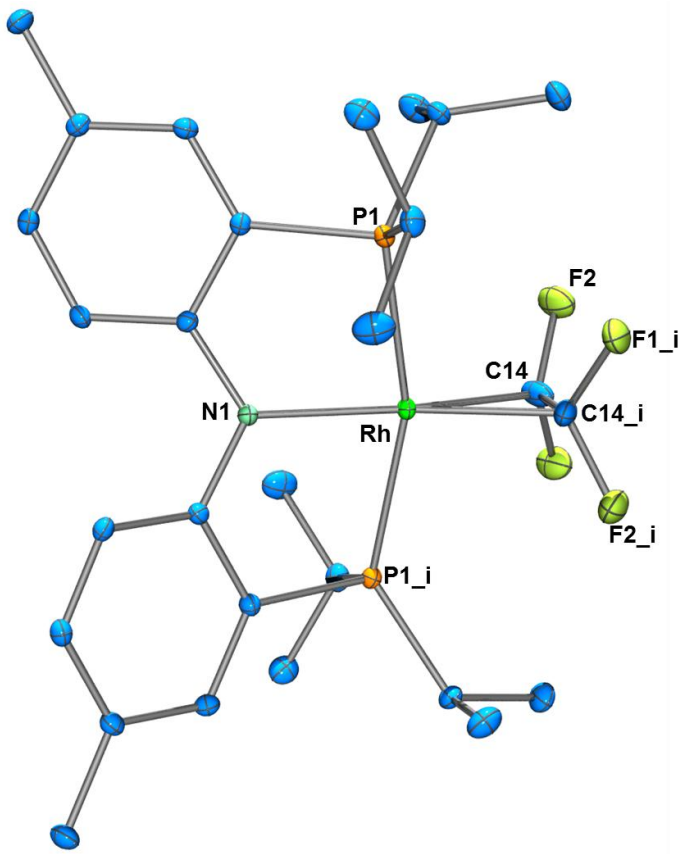


**Figure 5-2.** ORTEP drawing[103] of **502** (50% thermal ellipsoids). Hydrogen atoms are omitted for clarity. Selected bond distances (Å) and angles (deg) for **502**: Rh1-C14, 2.006(3); Rh1-N1, 2.054(3); Rh1-P1, 2.3309(11); C14-F1, 1.378(3), C14-F2, 1.361(3); C14-C14_i, 1.354(7); P1-Rh1-P1_i, 161.57(3); C14-Rh-C14_i, 39.4(2); C14-Rh-N1, 160.28(10).

C distance in uncoordinated $C_2F_4$ is 1.313 (35) Å.[178] The slightly elongated C-C distance in **502** indicates there is only moderate back donation from metal center to π* orbital of the olefin. The Rh-C14 bond distance of 2.006(3) Å is similar to the corresponding one in complexes $[(PPh_3)_2]Rh(C_2F_4)Cl$ (2.01 Å) [179] and $(C_5H_5)Rh(C_2F_4)(C_2H_4)$ (2.024(2) Å).[177c]

*5.2.3 Reactivity of compound **501***

**Reaction with nucleophiles.** Compound **501** is stable in common solvents such as benzene, toluene or pentane. Previously reported difluorocarbene complexes exhibited both electrophilic and nucleophilic reactivity at carbene carbon center.[158] The difluorocarbene complex can be attacked by nucleophiles such as $LiBHEt_3$. The attempt to make (PNP)Rh(=$CH_2$) carbene complex by reacting **501** with $LiBHEt_3$ failed and the previously reported complex (PNP)Rh($C_2H_4$)[150] was formed instead (Scheme 5-6).

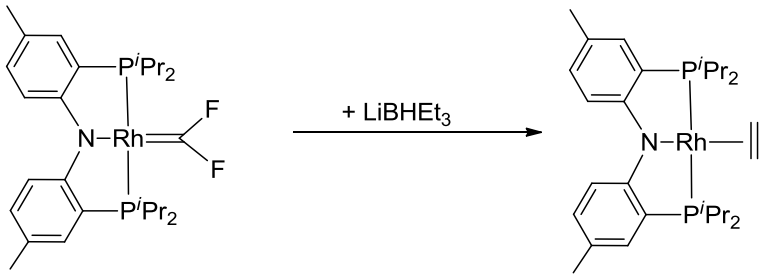


**Scheme 5-6.** Reaction of **501** with $LiBHEt_3$.

**Attempts to make a fluorocarbyne complex.** Halocarbyne metal complexes are especially rare. In 2006, the Hughes group reported the first terminal fluorocarbyne complex that was prepared via two electron reduction of the corresponding metal (Mo) trifluoromethyl complex (Scheme 5-7).[180] Since then, no other terminal fluorocarbyne complexes have been reported until very recently. The same group published a series of group 6 (Cr, Mo, W) metal fluorocarbyne complexes that are obtained by a similar way as they obtained the first example.[172b] With compound **501** in hand and noting that $CF^+$

is isoelectronic with CO, it was very appealing to see if we could break one of the C-F bonds in the carbene complex to form the terminal fluorocarbyne rhodium complex.

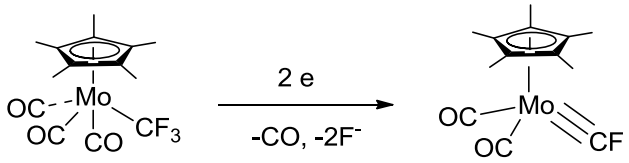


**Scheme 5-7.** Formation of terminal fluorocarbyne through 2e reduction.

By using silylium catalysis, our group accomplished hydrodefluorination of aliphatic C-F bonds.[181] The key element of that process is the use of the highly electrophilic silylium cation[182] to break the strong C-F bond by abstracting fluoride. Inspired by the success of the hydrodefluorination reaction, we wanted to abstract the fluoride from the difluorocarbene with a silylium cation (Scheme 5-8).[183] Reaction of compound **501** with 1 eq. of $^{i}Pr_3Si^{+}(B(C_6F_5)_4)^{-}\cdot C_7H_8$ in *ortho*-dichlorobenzene (ODCB) led to an immediate color change from red to bluish. $^{31}P$ NMR analysis indicated the disappearance of the carbene complex with the formation of a new doublet of douplets resonating at δ 89.4 ppm with $J_{Rh\text{-}P}$ = 106 Hz and $J_{F\text{-}P}$ = 12 Hz. Other than the $^{19}F$ resonance observed for $^{i}Pr_3SiF$ and the anion, the only other observed $^{19}F$ NMR resonance appeared as a doublet of triplets at the downfield chemical shift of δ 65.3 with $J_{Rh\text{-}F}$ = 136 Hz and $J_{P\text{-}F}$ = 12 Hz. This downfield chemical shift is in the range of the known group 6 metal terminal fluorocarbyne complexes (50—90 ppm).[172] Notably, the $^{2}J_{Rh\text{-}F}$ (136 Hz) is much larger than that in the (PNP)Rh(=$CF_2$) (49 Hz). Interestingly, the $^{2}J_{W\text{-}F}$ (133 Hz) in compound

$Cp^*W(CO)_2(CF)$ is also much larger than in its corresponding precursor $Cp^*W(CO)_3(CF_3)$ (43 Hz).[172b]

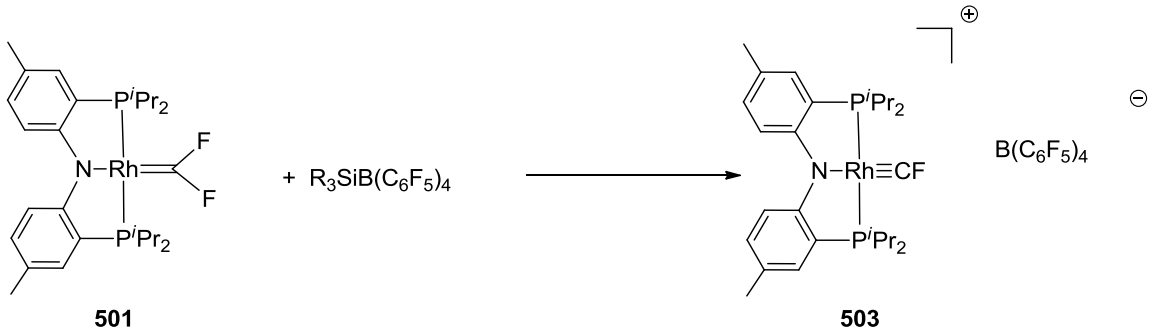


**501** **503**

**Scheme 5-8.** Possible reaction route to make terminal rhodium fluorocarbyne complex.

The $^1H$ NMR spectroscopic analysis of a mixture of ODCB/$C_6D_6$ indicated that this new compound adopted $C_{2v}$ symmetry at room temperature on the NMR timescale. Based on this NMR evidence, we tentatively assigned this new complex as the terminal fluorocarbyne complex $[(PNP)Rh(\equiv CF)]^+(B(C_6F_5)_4)^-$ (**503**) although so far we have not been able to observe the diagnostic carbyne resonance by $^{13}C\{^1H\}$ NMR spectroscopy due to the poor solubility of this cationic species. It is worth mentioning that the use of triisopropylsilylium generated in situ from the $Ph_3C^+$ salt and the silane did not affect the reaction result and similar NMR features were observed. Using other weakly coordinating anions as partners to the silylium cation appears necessary in order to increase the solubility of the new compound or to help get X-ray quality crystals.

### *5.3 Conclusion*

In this chapter, we described the synthesis of a PNP pincer supported Rh(I) difluorocarbene complex (PNP)Rh(=$CF_2$) (**501**) through the reaction of (PNP)Rh(TBE) with $Me_3SiCF_3$ in the presence of CsF. This rhodium carbene complex was fully characterized by NMR spectroscopy and X-ray crystal study. The side product (PNP)Rh($C_2F_4$) (**502**) generated in this reaction was also characterized spectroscopically and by X-ray crystal diffraction. Reaction of the rhodium difluorocarbene complex with a silylium cation resulted in a new compound which we tentatively assigned as the cationic terminal fluorocarbyne species [(PNP)Rh(≡CF)]$^+$($B(C_6F_5)_4$)$^-$ (**503**). However, more characterization is needed in order to fully confirm the proposed structure.

### *5.4 Experimental*

**General considerations.** Unless specified otherwise, all manipulations were performed under an argon atmosphere using standard Schlenk line or glove box techniques. Toluene, ethyl ether, and pentane were dried and deoxygenated (by purging) using a solvent purification system by MBraun and stored over molecular sieves in an Ar-filled glove box. $C_6D_6$ and THF were dried over and distilled from Na/K/$Ph_2CO$/18-crown-6 and stored over molecular sieves in an Ar-filled glove box. Fluorobenzene and pyridine were dried with and then distilled from $CaH_2$ and stored over molecular sieves in an Ar-filled glove box. $Me_3SiCF_3$ was degassed prior to use and stored in an Ar-filled glove box. CsF was grounded and dried at 130 $^oC$ under vacuum for 2 days. (PNP)Rh(TBE) was prepared according to the published procedures.[20] $^iPr_3SiB(C_6F_5)_4$ $C_7H_8$ was prepared similarly to the literature procedures.[184] All other

chemicals were used as received from commercial vendors. NMR spectra were recorded on a Varian iNova 400 ($^{1}$H NMR, 399.755 MHz; $^{13}$C NMR, 100.518 MHz; $^{31}$P NMR, 161.822 MHz; $^{19}$F NMR, 376.104 MHz) spectrometer. For $^{1}$H and $^{13}$C NMR spectra, the residual solvent peak was used as an internal reference. $^{31}$P NMR spectra were referenced externally using 85 % $H_3PO_4$ at 0 ppm. Elemental analyses were performed by CALI, Inc. (Parsippany, NJ).

**Syntesis of (PNP)Rh(=CF$_2$) (501).** (PNP)Rh(TBE) (105 mg, 0.170 mmol), $Me_3SiCF_3$ (50.0 μL, 0.340 mmol) and CsF (25.0 mg, 0.170 mmol) were placed in a Teflon flask in about 3 mL $C_6D_6$. The reaction mixture was stirred vigorously and heated at 70 $^{o}$C for 6 days. NMR analysis revealed the presence of 85% of **501** and 14% of **502** together with 1% of (PNP)Rh(CO). The reaction was passed through Celite. The volatiles were removed under vacuum and the residue was extracted with pentane. The pentane solution was passed through Celite again. The volatiles were removed under vacuum. The residue was dissolved in isooctane and placed in the freezer at -35 $^{o}$C. Small amount of precipitate was formed the next day. The solution was filtered through Celite. The volatiles were removed and dried under vacuum. NMR analysis indicated > 98% purity of **501**. Yield, 51.0 mg, 0.088 mmol, 52% $^{1}$H NMR ($C_6D_6$): δ 7.66 (d, $J$ = 8 Hz, 2H, (PNP)Aryl-*H*), 7.10 (br, 2H, (PNP)Aryl-*H*), 6.80 (d, $J$ = 8 Hz, 2H, (PNP)Aryl-*H*), 2.43 (m, 4H, C*H*($CH_3$)$_2$), 2.19 (s, 6H, Ar-C*H*$_3$), 1.27 (app.q., $J$ = 8 Hz, 12 H, CH(C*H*$_3$)$_2$), 1.13 (app.q., $J$ = 8 Hz, 12 H, CH(C*H*$_3$)$_2$). $^{31}$P{$^{1}$H}NMR ($C_6D_6$) : 53.7 (dt, $J_{Rh-P}$ = 146 Hz, $J_{F-P}$ = 30 Hz). $^{19}$F NMR ($C_6D_6$): 95.6 (dt, $J_{Rh-F}$ = 49 Hz, $J_{P-F}$ = 30 Hz). $^{13}$C{$^{1}$H}NMR ($C_6D_6$): 206.3 (dtt, $J_{Rh-C}$ = 85 Hz, $J_{C-P}$ = 12 Hz, $J_{C-F}$ = 454 Hz), 162.3 (t, $J$

= 11 Hz), 132.4, 131.9, 125.8 (t, *J* = 3 Hz), 122.3 (t, *J* = 18 Hz), 116.1 (t, *J* = 3 Hz), 25.4 (t, *J* = 11 Hz), 20.5, 19.3 (t, *J* = 3 Hz), 18.5. Elem. An.. Found (Calculated) for $C_{27}H_{40}NF_2P_2Rh$: C 55.81 (55.77); H 6.96 (6.93); N 2.35 (2.41).

**NMR observation of the formation of (PNP)Rh($C_2F_4$) (502).** Compound **502** was observed in the process of generating **501** as described above. $^1$H NMR ($C_6D_6$): δ 7.43 (d, *J* = 8 Hz, 2H, (PNP)Aryl-*H*), 6.81 (br, 2H, (PNP)Aryl-*H*), 6.74 (d, *J* = 8 Hz, 2H, (PNP)Aryl-*H*), 2.30 (m, 4H, C*H*($CH_3$)$_2$), 2.13 (s, 6H, Ar-C*H*$_3$), 1.27 (app.q., *J* = 8 Hz, 12 H, CH(C*H*$_3$)$_2$), 0.97 (app.q., *J* = 8 Hz, 12 H, CH(C*H*$_3$)$_2$). $^{31}$P{$^1$H}NMR ($C_6D_6$) : 53.7 (dqui., $J_{Rh-P}$ = 137 Hz, $J_{F-P}$ = 23 Hz). $^{19}$F NMR ($C_6D_6$): -100.8 (br).

**Reaction of 501 with $LiBHEt_3$.** Compound **501** (10.0 mg, 0.017 mmol) was dissolved in about 0.6 mL $C_6D_6$ in a J Young tube followed by the addition of $LiBHEt_3$ (34.0 μL, 1.0M/toluene). After 30 min, NMR analysis revealed the complete formation of the previously reported compound (PNP)Rh($C_2H_4$).

**Reaction of 501 with triisopropylsilylium salt.** Compound **501** (10.0 mg, 0.017 mmol) was dissolved in about 0.5 mL of *ortho*-dichlorobenzene followed by the addition of $^i$Pr$_3$SiB($C_6F_5$)$_4$ $C_7H_8$ in a J. Young NMR tube.. The red solution changed from red to blue-greenish within a few minutes. $^{31}$P NMR analysis indicated the disappearance of **501** with the formation of a new doublet of doublet. $^i$Pr$_3$SiF was produced according to the $^{19}$F NMR spectrum. A new doublet of triplets at the lower field region was also present in $^{19}$F NMR spectrum. The reaction solution was transferred from the NMR tube to a flask. About 5 mL of pentane was added to the flask and the solution was stirred vigorously for a few minutes to get the blue-greenish oily stuff at the bottom. The liquid

was decanted and the oily precipitate was dissolved in a mixture of ODCB/$C_6D_6$. $^1$H NMR ($C_6D_6$/ODCB) (Due to the use of ODCB, the aromatic region is only selectively reported): δ 6.78 (brt, *J* = 4 Hz, 2H, (PNP)Aryl-*H*), 6.73 (d, *J* = 9 Hz, 2H, (PNP)Aryl-*H*), 2.15 (m, 4H, C*H*($CH_3$)$_2$), 2.12 (s, 6H, Ar-C*H*$_3$), 0.88 (app.q. *J* = 8 Hz, 12H, CH(C*H*$_3$)$_2$), 0.75 (app.q. *J* = 8 Hz, 12H, CH(C*H*$_3$)$_2$). $^{31}$P{$^1$H} NMR ($C_6D_6$/ODCB): 89.6 (dd, $J_{Rh-P}$ = 106 Hz, $J_{F-P}$ = 12 Hz). $^{19}$F NMR ($C_6D_6$/ODCB): 65.3 (dt, $J_{Rh-F}$ = 136 Hz, $J_{P-F}$ = 12 Hz).

**X-Ray data collection, solution, and refinement for 501.** A red block crystal of suitable size (0.30 x 0.21 x 0.15 mm) was selected from a representative sample of crystals of the same habit using an optical microscope, mounted onto a nylon loop and placed in a cold stream of nitrogen (110 K). Low temperature X-ray data were obtained on a Bruker APEXII CCD based diffractometer (Mo sealed X-ray tube, Kα = 0.71073 Å). All diffractometer manipulations, including data collection, integration and scaling were carried out using the Bruker APEXII software.[105] An absorption correction was applied using SADABS.[165] The space group was determined on the basis of systematic absences and intensity statistics and the structure was solved by direct methods and refined by full-matrix least squares on $F^2$. The structure was solved in the monoclinic *Pna*2$_1$ space group using XS[166] (incorporated in SHELXTL). No obvious missed symmetry was reported by PLATON.[108] All non-hydrogen atoms were refined with anisotropic thermal parameters. Hydrogen atoms were placed in idealized positions and refined using riding model. The structure was refined (weighted least squares refinement on $F^2$) and the final least squares refinement converged to $R_1$ = 0.0357 ($I > 2\sigma(I)$, 6606 data) and w$R_2$ = 0.0751 ($F^2$, 30909 data, 298 parameters).

**X-Ray data collection, solution, and refinement for 502.** A red block crystal of suitable size (0.17 x 0.14 x 0.11 mm) was selected from a representative sample of crystals of the same habit using an optical microscope, mounted onto a nylon loop and placed in a cold stream of nitrogen (110 K). Low temperature X-ray data were obtained on a Bruker APEXII CCD based diffractometer (Mo sealed X-ray tube, Kα = 0.71073 Å). All diffractometer manipulations, including data collection, integration and scaling were carried out using the Bruker APEXII software.[105] An absorption correction was applied using SADABS.[165] The space group was determined on the basis of systematic absences and intensity statistics and the structure was solved by direct methods and refined by full-matrix least squares on $F^2$. The structure was solved in the monoclinic $C2/c$ space group using XS[166] (incorporated in SHELXTL). No obvious missed symmetry was reported by PLATON.[108] All non-hydrogen atoms were refined with anisotropic thermal parameters. Hydrogen atoms were placed in idealized positions and refined using riding model. The structure was refined (weighted least squares refinement on $F^2$) and the final least squares refinement converged to $R_1$ = 0.0293 ($I > 2\sigma(I)$, 2775 data) and w$R_2$ = 0.0862 ($F^2$, 3031 data, 169 parameters).

# CHAPTER VI

# SYNTHESIS OF PYRROLYL SUBSTITUTED PNP PINCER LIGANDS AND THE CORRESPONDING RHODIUM COMPLEXES

## *6.1 Introduction*

The Ozerov group has a history of working with 'PNP' pincer ligands. Beautiful work has been achieved at ($^{Me}$PNP$^{iPr}$)Rh system and some has been discussed in the previous chapters. Some of these results highlight the potential of (PNP)Rh system for use in cross-coupling catalysis. Transition metal catalyzed C-C and C-heteroatom cross couplings present important tools in modern synthesis. Well-established cross couplings include the Kumada-Corriu coupling, Heck olefination, Suzuki coupling, Stille coupling, Negishi coupling, Sonogashira coupling, Tsuji-Trost reaction, and Buchwald-Hartwig amination.[185] They are usually conducted with Pd or Ni catalysts, where aryl halide and pseudo halide are common substrates.[186] The Sames group has successfully incorporated oxidative addition (OA) to Rh in the catalytic direct C-arylation of indoles and pyrroles (Scheme 6-1).[37] In addition to that, quite a few examples of OA of Ar-Hal to Rh(I) complexes have been published in the recent years.[187] Oxidative addition (OA) of the carbon-halogen bond to the metal center is a key step in metal catalyzed coupling reactions while C-C or C-heteroatom reductive elimination (RE) normally involves in the catalytic cycle as the last step to form the coupling products.

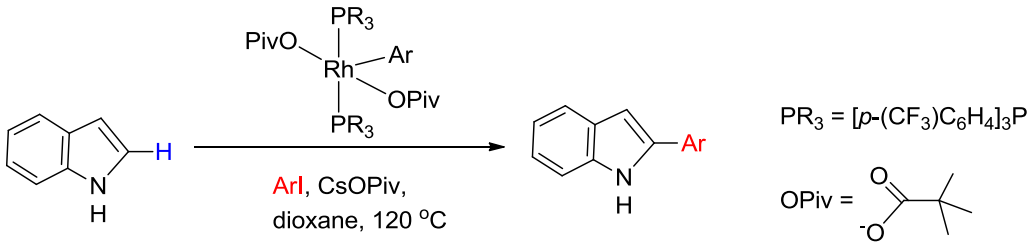


**Scheme 6-1.** C-arylation of indoles catalyzed by rhodium complex.

In 2006, we reported the ability of ($^{Me}$PNP$^{iPr}$)Rh system to undergo OA with unactivated aryl halides (Br and Cl) to Rh(I) and also to perform C-C RE from Rh(III).[29b] These reactions were observed to occur at ambient temperature, were well defined and easy to study mechanistically. Although we have examined all these

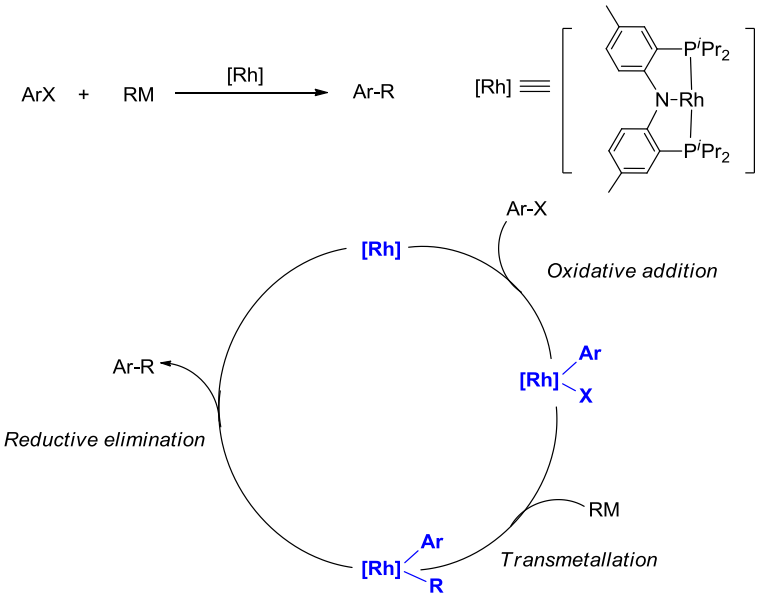


**Scheme 6-2.** Proposed C-C cross coupling reactions catalyzed by "(PNP)Rh".

stoichiometric reactions, we have not been able to accomplish the catalytic coupling reactions as proposed in Scheme 6-2. Several problems arise when the reaction is performed catalytically, leading to less than ideal results with the present system.

Firstly, our three coordinated ($^{Me}PNP^{iPr}$)Rh is a very reactive intermediate and it is non-innocent toward some polar solvents (e.g. $Et_2O$) or some transmetallation reagents.[150] For example, Dr. Gatard found ($^{Me}PNP^{iPr}$)Rh reacted with $Ph_2Zn$, presumably forming product ($^{Me}PNP^{iPr}$)Rh(Ph)(ZnPh), which did not undergo further reaction with aryl halide.[188] Secondly, the C-C RE at ($^{Me}PNP^{iPr}$)Rh(R)(R') is slow. Kinetic studies have shown $t_{1/2}$ = 7 min at 40 $^{o}$C for eliminating Ph-Ph and $t_{1/2}$ = 17 min at 40 $^{o}$C for eliminating Ph-Me.

In this chapter, we will cover the synthesis of the first π-accepting PNP ligand bearing pyrrolyl substituents. The π-accepting ability of tris(N-pyrrolyl)-phosphine $P(pryl)_3$ was found to fit the following trend: fluoroalkyl phosphines > $P(pryl)_3 \approx P(C_6F_5)_3$ > $P(OPh)_3$.[189] It is logical to think that in the $^{Me}PNP^{pryl}$ system, back donation from the metal to the pincer ligand will decrease the electron density on the metal center which would result in different properties and applications compared with the $^{Me}PNP^{iPr}$ system. Other than $^{Me}PNP^{pryl}$, this chapter will also disclose the approach of other $^{Me}PNP^{R}$ pincer ligands derived from their pyrrolyl analogue. We hoped that this novel ligand system would lead to some interesting reactivity and in this chapter we will disclose our findings by making a series of complexes containing ($^{Me}PNP^{pryl}$)Rh fragment and examing their reactivity.

## *6.2 Results and discussion*

### *6.2.1 Ligand Synthesis*

#### 6.2.1.1 Synthesis of $^{Me}$PN(P)P$^{pryl}$

Although PNP ligands with a variety of electron-donating phosphine substituents have been synthesized by our former group members as well as others, electron-withdrawing substituents have not been introduced so far. The synthesis of the PNP ligand bearing pyrrolyl groups on phosphorus was inspired by the work of Milstein[190,191], Moley and Petersen.[189] Moloy and Petersen demonstrated that *N*-pyrrolyl phosphines possess exceptional electron-accepting properties. A series of resonance structures (Scheme 6-3) can be drawn for the pyrrolyl phosphine ligands that suggest the N-pyrrolyl phosphine should be relatively weak σ-donors and good π-acceptors. In 2005, the Milstein group reported the synthesis of PCP pincer ligand with pyrrolyl on the phosphorus atoms and its coordination chemistry with rhodium.[190] Due to the strong π-accepting ability of the ligand, formation of the first stable $d^8$ $ML_5$ PCP-based complexes was observed.

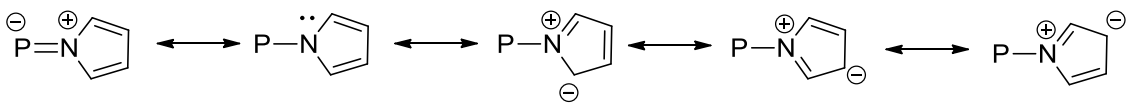

**Scheme 6-3.** Resonance structures of pyrrolyl substituted phosphine.

We were first interested in making the pyrrolyl substituted ligand with a methyl group bound to the center nitrogen $^{Me}$PN(Me)P$^{pryl}$, because we have found the N-Me

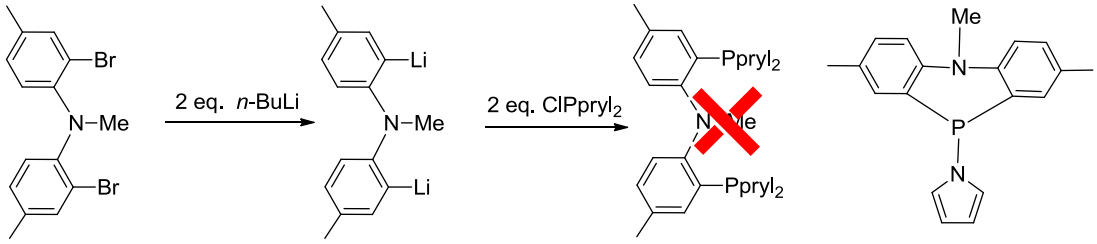


**6A** **601**

**Scheme 6-4.** Synthesis of **601**.

bond in $^{Me}$PN(Me)$^{iPr}$ can oxidatively add to rhodium center to make a useful ($^{Me}$PNP$^{iPr}$)Rh(Me)(Cl) metal precursor.[2b] We hoped that $^{Me}$PN(Me)P$^{pryl}$ would undergo analogous reactivity with rhodium. Synthesis of the $^{Me}$PN(Me)P$^{pryl}$ ligand was first tested with the similar method as making $^{Me}$PN(Me)P$^{iPr}$. However, treatment of compound N-methylated dibromoarylamine (**6A**) with 2 eq. of *n*-BuLi and followed by the addition of 2 eq. of ClPpryl$_2$ led to a mixture products (Scheme 6-4). We were able to recrystallize and isolate the major product as compound **601**. The formation of **601** is likely due to the good leaving ability of pyrrolyl group and the P-N bond undergoing nucleophilic attack by the aryl lithium to form the cyclized product.

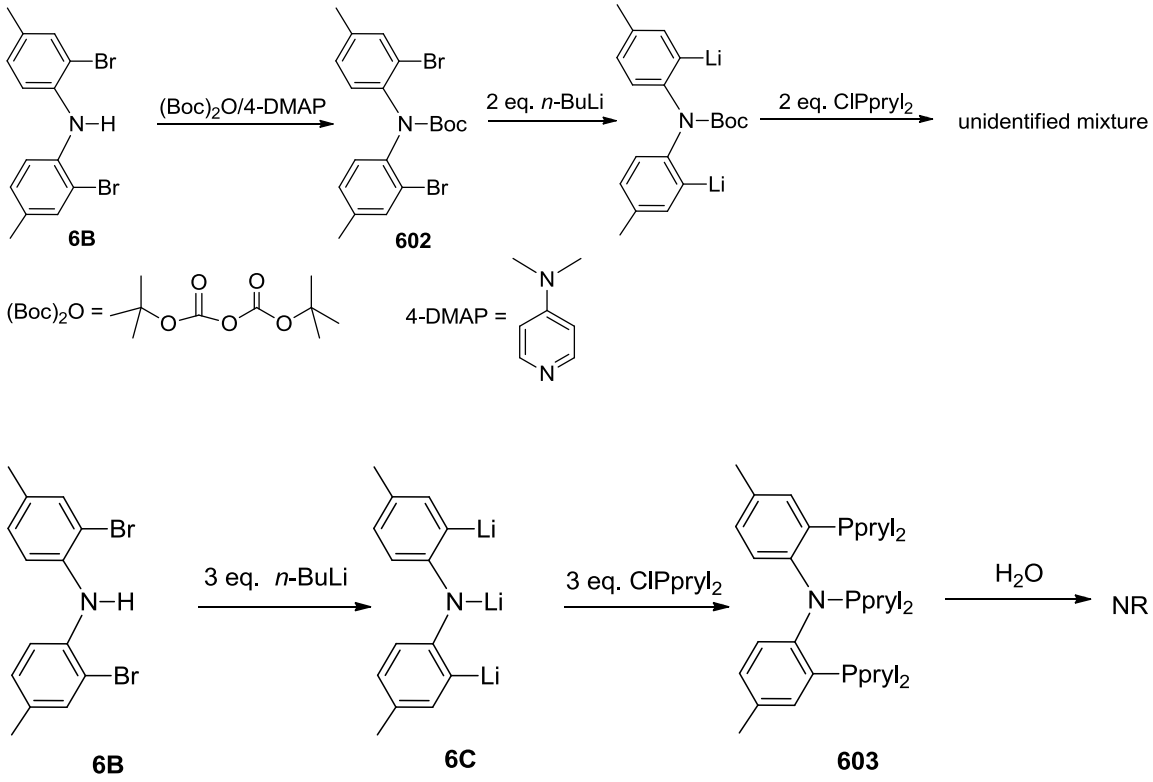


**Scheme 6-5.** Synthesis of **603**.

In order to circumvent this cyclization problem, we tried to install relatively large protecting groups on the nitrogen center. We first tried Boc (*tert*-butyloxycarbonyl). Treatment of the dibromodiarylamine presursor (**6B**) with $(Boc)_2O$ in the presence of base led to formation of **602**. Clean Li/Br exchange was obtained after reacting **602** with 2 eq. *n*-BuLi at -78 $^{o}$C in $Et_2O$. However, a mixture of three products was formed after the addition of 2 eq. $ClPpryl_2$ as indicated by the $^{31}P$ NMR spectrum. Unfortunately, we were not able to isolate a single product from this mixture (Scheme 6-5). Another method we tried was to make a central N-P bond by taking advantage of its ability to

undergo hydrolysis to form the N-H bond. Trilithium salt (**6C**), generated from deprotonation of N-H bond and double lithium bromine exchange, was added to 3 eq. of $ClPpryl_2$. After stirring at room temperature overnight, $^{31}P$ NMR analysis revealed that compound **603** was the major product in the reaction mixture ($^{31}P$ NMR (ppm): δ 63.9 (d, 2P, $J_{P\text{-}P}$ = 49 Hz, *P*-Aryl), 85.5 (t, 1P, $J_{P\text{-}P}$ = 49 Hz, *P*-N)) (Scheme 6-5). We were able to isolate **603** in 42% yield. Compound **603** is air stable and soluble in aromatic solvents such as benzene and toluene. It is insoluble in alkanes such as pentane and hexanes. The solubility in diethyl ether is also poor.

6.2.1.2 Synthesis of $PN(Li)P^{pryl}$ and $PN(H)P^{pryl}$

With compound **603** in hand, we hoped to break the central N-P bond through protolysis. The $PN(H)P^{Ph}$ ligand was made through this route by our former group member Lei Fan. There are seven N-P bonds in **603** and we were aiming at selectively breaking the central N-P bond. However, in contrast to the facile solvolysis of the N-P bond of most alkylaminophosphines by protic reagents, it was found that **603** was very stable towards water and alcohols. None of the seven N-P bonds could be hydrolyzed even in the presence of excess aqueous HCl at elevated temperature. The inertness of the N-P bond in pyrrolylphosphine is probably due to the involvement of the lone pair in the π-electron sextet of the heterocyclic ring preventing electrophilic attack of the nitriogen. The stability of central N-P bond towards water may be attributed to the reduced basicity of nitrogen due to the N→P π bonding effect.

Interestingly, the central N-P bond could be selectively attacked by $LiNMe_2$. Treatment of compound **603** with $LiNMe_2$ (1.3 eq.) in THF led to the formation of the

lithium salt **604** as the major product with the concomitant production of $P(NMe_2)(pryl)_2$ ($^{31}P$ NMR (ppm): δ 79.6 (br)). The amount of $LiNMe_2$ added to the reaction is crucial, because excess $LiNMe_2$ would attack the $P\text{-}N_{pyrrolyl}$ bonds. The lithium salt of the $^{Me}PNP^{pryl}$ ligand was isolated in 58% yield. There are two THF molecules binding to the lithium center based on the integrations of the $^1H$ NMR spectrum (Scheme 6-6).

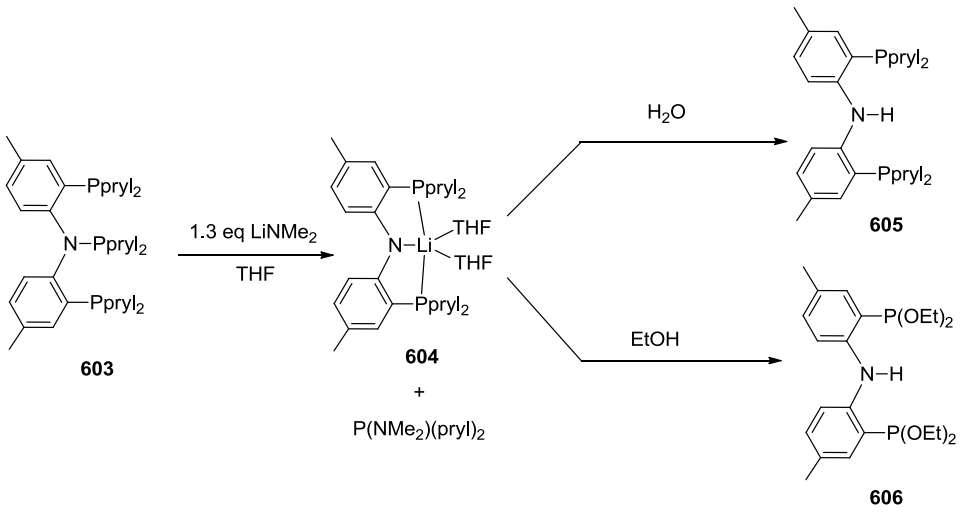


**Scheme 6-6.** Hydrolysis/alcoholysis of **604**.

Hydrolysis of this lithium salt with water led to the formation of the ligand $^{Me}PN(H)P^{pryl}$ (**605**). Most astonishingly, $^{Me}PN(H)P^{OEt}$ (**606**) was produced after addition of EtOH to $^{Me}PN(Li)P^{pryl}$ (**604**) (Scheme 6-6). The different reactivity of $^{Me}PN(P)P^{pryl}$ and $^{Me}PN(Li)P^{pryl}$ with alcohol seems surprising, but could be related to the basicity of the reaction mixture. In the $^{Me}PN(Li)P^{pryl}$ reaction, the system is more basic and there is also LiOEt present which served as a better nucleophile than EtOH in the $^{Me}PN(P)P^{pryl}$

system. It was also worth noting that the reaction of $^{Me}PN(Li)P^{pryl}$ (**604**) with MeOH was messy and gave multitude of unidentified products.

6.2.1.3 Synthesis of $^{Me}PN(H)P^{R}$

As noted above, the N-P bond underwent nucleophilic attack by $LiNMe_2$. We were also interested to determine the reactivity of **603** with other nucleophiles such as organolithium reagents, organozinc reagents or Grignard reagents.

The attempts to selectively break central N-P bond with organozinc or Grignard reagents all met with failure. No reaction took place after the addition of $Me_2Zn$ or MeMgCl to compound **603**. $^{31}P$ NMR data only suggested the presence of the starting material.

Organolithium reagents, on the other hand, did attack the N-P bonds. Addition of 1 eq. *n*-BuLi to **603** in ether only led to about ~15% conversion of the starting material with the formation of two new products as indicated by the $^{31}P$ NMR spectrum. The integration ratio of these two resonances in $^{31}$ P NMR was 2:1. These two compounds were identified as $^{Me}PN(Li)P^{Bu}$ . ($^{31}P$ NMR (ppm): δ -39.7 (br)) and P(*n*-Bu)$_3$ ($^{31}P$ NMR (ppm): δ -31.3 (s), which is consistent with the literature reported data[192]). The reaction did not go to completion until the addition of 7 eq. *n*-BuLi. Other than the two signals detected by $^{31}P$ NMR, no other intermediate was observed upon the addition of excess *n*-BuLi. Similar reactions were also done at lower temperature (-78 $^{o}$C and -20 $^{o}$C) and achieved the same result. These reactions indicate that *n*-BuLi can attack the P-N bond but, unlike $LiNMe_2$, it breakes all seven P-N bonds in the molecule. Hydrolysis of

$^{Me}$PN(Li)P$^{Bu}$ generated compound $^{Me}$PN(H)P$^{Bu}$ (**607**) which was characterized by solution NMR.

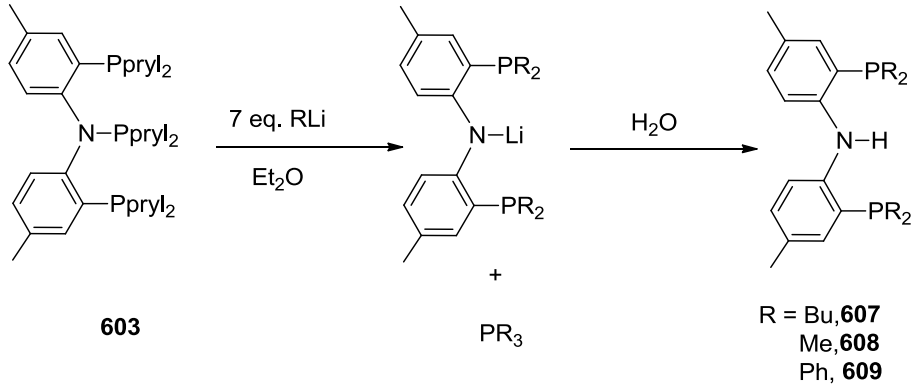


**Scheme 6-7.** Nucleophilic attack upon **603** by organolithium reagents.

Similarly, treatment of **603** with 7 eq. MeLi or PhLi led to the full conversion of the starting material to $^{Me}$PN(Li)P$^{Me}$ and $^{Me}$N(Li)P$^{Ph}$ (Scheme 6-7). No intermediate was observed even when only deficient amounts of lithium reagents was added. Hydrolysis of the lithium salts generated the N-H version of the ligand $^{Me}$PN(H)P$^{Me}$ (**608**) and $^{Me}$PN(H)P$^{Ph}$ (**609**).

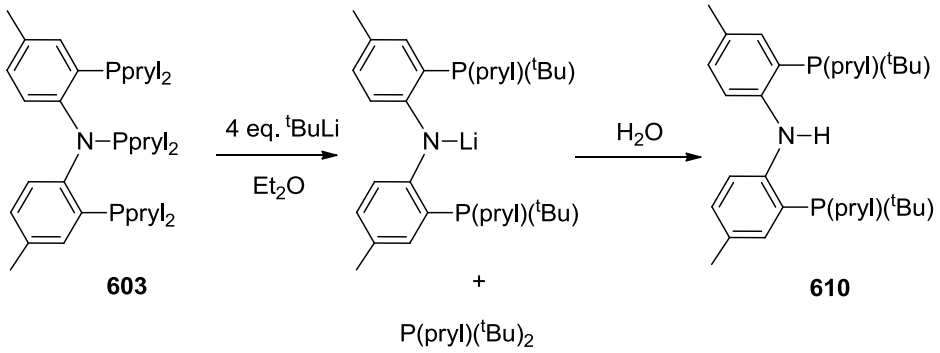


**Scheme 6-8.** Reaction of **603** with $^{t}$BuLi.

The synthesis of $^{Me}$PN(H)P$^{Ph}$ ligand has already been published via different route[193], but $^{Me}$PN(H)P$^{Me}$ ligand is new. The $^{Me}$PN(H)P$^{Me}$ is special because it has the least bulky dialkyl-phosphine donor sites, which could endow the corresponding metal complexes with possible unusual reactivity. It is possible to synthesize the $^{Me}$PN(H)P$^{Me}$ ligand by the regular synthesis method as we did for $^{Me}$PN(H)P$^{iPr}$, but it involves in the use of $ClPMe_2$ which is pyrophoric and not easily commercially available.

We were also very interested in making the $^{Me}$PN(H)P$^{tBu}$ ligand considering that the bulky substituent on phosphines (cone angle of P($^{t}$Bu)$_3$: 182 °) might lead to some interesting reactivity. The bulky pincer ligand may allow stabilization of some very reactive species. For example, the Caulton group was able to synthesize the T-shaped (PNP)M complexes, M = Fe, Co, Ni, PNP = $[(^{t}Bu_2PCH_2SiMe_2)_2N]^{-1}$ by using Fryzuk type PNP ligand.[194] In another example, Brookhart et al. reported the NMR characterization of a σ-methane Rh(I) complex supported by P$^{O}$N$^{O}$P ligand, (P$^{O}$N$^{O}$P) = 2,6-$(^{t}Bu_2PO)_2C_5H_3N$. It was found that the σ-methane complex was at lower energy than the methyl hydride complex for that system, which allowed spectroscopic

characterization of the methane complex.[195] Inspired and encouraged by the formation of $^{Me}$PN(H)P$^{R}$ (R = Me, Bu, Ph), we attempted to make $^{Me}$PN(H)P$^{tBu}$ from $^{Me}$PN(P)P$^{pryl}$. Treatment of 4 eq. of $^{t}$BuLi with compound **603** in $Et_2O$ led to the formation of two major products (δ 62.3(br), 92.3 (s)) as well as a few other minor products as indicated by $^{31}$P NMR (Scheme 6-8). Adding another 3 eq. of $^{t}$BuLi to the reaction mixture did not give further reaction. Hydrolysis of this reaction with EtOH led to the appearance of two singlets δ 55.3 and 53.8 ppm as revealed by $^{31}$P NMR spectroscopy. Because the reaction is not very clean, we could not isolate and fully characterize the major product. Based on the $^{31}$P NMR data, we propose that the stectrically imposing $^{t}$Bu can only substitute one pyrrolyl group on each phosphine, leading to formation of the tentatively assigned compound **610**. The by-product resonated δ 92.3 ppm in the $^{31}$P{$^{1}$H} NMR spectrum is consistent with the reported $^{31}$P NMR chemical shift for P($^{t}$Bu)$_2$(pryl).[196]

*6.2.2 Synthesis of Rhodium complexes supported by ligand **603***

6.2.2.1 N-P cleavage by metal complex

The central N-P bond in **603** can not only be attacked by strong nucleophiles such as organolithium reagents or lithium amide, but it can also be cleaved in a reaction with a transition metal center. Reaction of **603** with [Rh(COD)Cl]$_2$ followed by the addition of $Me_2Zn$ cleanly forms compound ($^{Me}$PNP$^{pryl}$)Rh(P(pryl)$_2$Me) **611** (Scheme 6-9). **611** was fully characterized using solution NMR techniques. It displayed $C_{2v}$ symmetry in solution at room temperature on the NMR time scale.

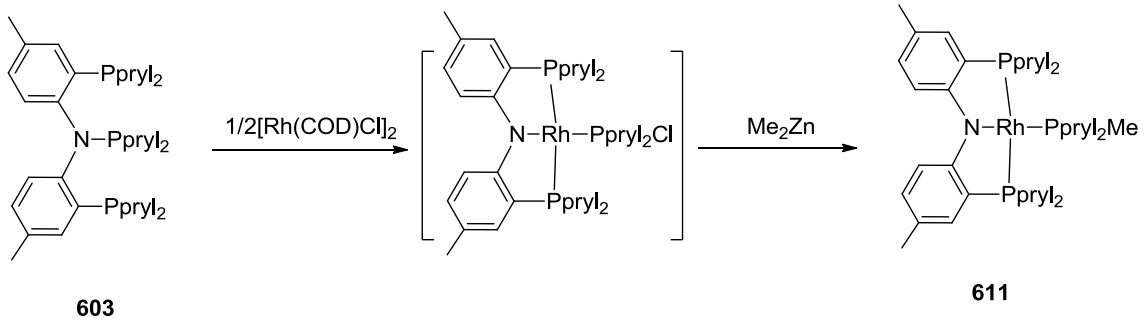


**Scheme 6-9.** Synthesis of **611** through N-P cleavage.

The solid state structure[197] of **611** was confirmed by X-ray diffraction (Figure 6-1). The environment of the four-coordinate $d^8$ Rh(I) can be described as distorted square planar. The pincer P-Rh distances are unremarkable and very similar to the corresponding ones found in ($^{Me}$PNP$^{iPr}$)Rh complexes. The N1-Rh-P3 angle (177.65(5) °) only slightly deviates from linearity, but the P1-Rh-P2 is merely 156.51(2) °.

Treatment of **611** with 1 atm of CO resulted in the formation of ($^{Me}$PNP$^{pryl}$)Rh(CO) **(612)** ($^{31}$P NMR (ppm): δ 110.7 ($J_{Rh-P}$ = 178 Hz)) and the free phosphine Ppryl$_2$Me ($^{31}$P NMR (ppm): δ 80.2) as indicated by $^{31}$P NMR (Scheme 6-10). Interestingly, this reaction is reversible. Under vacuum, CO dissociated from **612** and the reaction shifted back to the formation of **611**. A reasonable explanation for these observations is that due to the electron withdrawing property of the pincer ligand, there is less back donation from the rhodium to CO which makes CO substitution reversible. The IR stretching frequency of the carbonyl in **612** is 1995 cm$^{-1}$ in $C_6D_6$, which is shifted 50 cm$^{-1}$ compared with the corresponding one in ($^{Me}$PNP$^{iPr}$)Rh(CO) (1945 cm$^{-1}$).[56] The increased CO stretching frequency strongly implies that the rhodium center in

($^{Me}$PNP$^{pryl}$)Rh fragment is more electron deficient than it is in the ($^{Me}$PNP$^{iPr}$)Rh fragment.

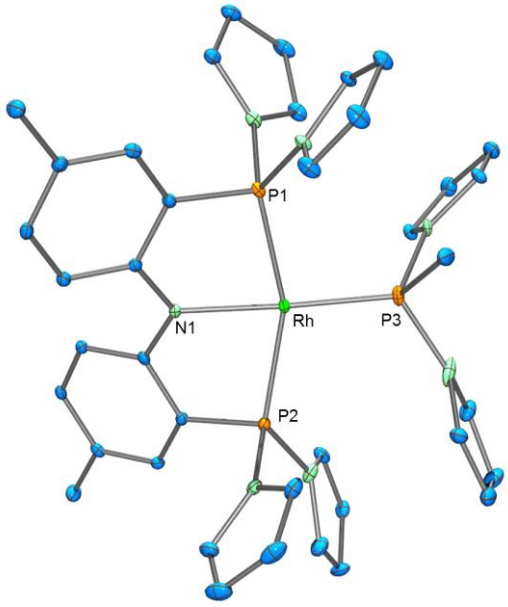


**Figure 6-1.** ORTEP drawing[103] of **611** (50% thermal ellipsoids). Hydrogen atoms and disorder of the pyrrolyl groups are omitted for clarity. Selected bond distances (Å) and angles (deg) for **611**: Rh-P1, 2.2696(10); Rh-P2, 2.2655(10); Rh-N1, 2.1015(19); Rh-P3, 2.2020(10); P1-Rh-P2, 156.51(2); P3-Rh-N1, 177.65(5); P2-Rh-N1, 78.03(6).

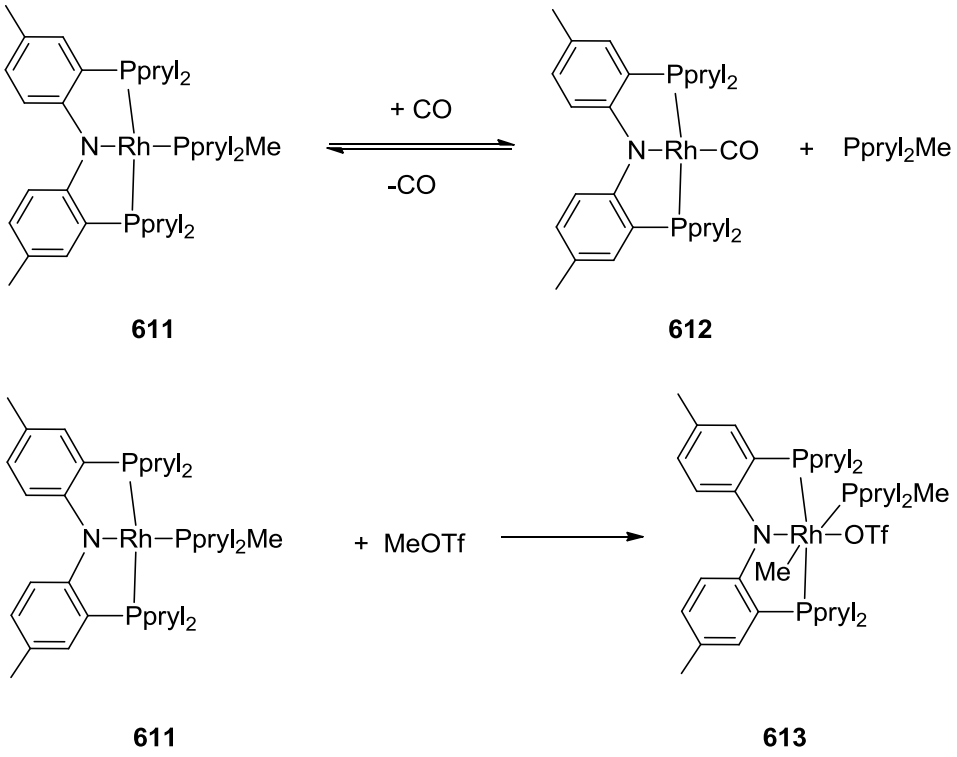


**Scheme 6-10.** Synthesis of **612** and **613.**

Compound **613** was obtained by adding 3 eq. MeOTf to **611.** Excess amount of MeOTf did not precipitate the ancillary phosphine ligand as its phosphonium salt (Scheme 6-10). **613** was characterized by multi-nuclear solution NMR. The $^{31}P\{^{1}H\}$ NMR spectrum of **613** exhibits a dd at δ 109.7 ppm ($J_{Rh\text{-}P}$ = 132 Hz, $J_{P\text{-}P}$ = 37 Hz, 2P) and a dt at δ 100.2 ppm ($J_{Rh\text{-}P}$ = 142 Hz, $J_{P\text{-}P}$ = 37 Hz, 1P). The dt observed by $^{1}H$ NMR spectroscopy at δ 0.59 ppm ($J_{Rh\text{-}H}$ = 2 Hz, $J_{P\text{-}H}$ = 6 Hz) is consistent with the formation of a Rh-$CH_3$ bond.

6.2.2.2 Synthesis of ($^{Me}$PNP$^{pryl}$)Rh(COD) complex

Four-coordinate Rh(I) complexes ($^{Me}$PNP$^{pryl}$)Rh(L) are attractive molecules to synthesize especially for those compounds where L is bound to Rh very weakly and can dissociate in solution to generate the reactive 14 e ($^{Me}$PNP$^{pryl}$)Rh intermediate. Our former group member Dr. Gatard[150] synthesized a variety of ($^{Me}$PNP$^{iPr}$)Rh-L complexes (where L = organic sulfide or sulfoxide, dinitrogen, or *tert*butylethylene) by trapping transient ($^{Me}$PNP$^{iPr}$)Rh in situ. Equilibrium studies established the relative affinity of the ($^{Me}$PNP$^{iPr}$)Rh fragment for various L in the following order (of decreasing affinity): $Ph_2SO$ > $SBu^n_2$ > SPhMe > dibenzothiophene > $SPh_2$ > benzothiophene > $SPr^i_2$> thiophene ≈$SBu^tMe$ > $SBu^s_2$ ≈ $H_2C$=$CHCMe_3$ >> $SBu^t_2$. More importantly, it was found that both ($^{Me}$PNP$^{iPr}$)Rh($SPr^i_2$) and ($^{Me}$PNP$^{iPr}$)Rh($H_2C$=$CHCMe_3$) were good starting precursors to generate ($^{Me}$PNP$^{iPr}$)Rh fragment and do further OA reactions.

($^{Me}$PNP$^{pryl}$)Rh(COD) (**614**) complex was quantitatively synthesized and isolated as an orange solid via the transmetalation of ($^{Me}$PN(Li)P$^{pryl}$) with $[Rh(COD)Cl]_2$ (Scheme 6-11). **614** was characterized by solution NMR techniques. $^{31}$P NMR spectrum displays a doublet at δ 117.5 ppm with $J_{Rh-P}$ = 170 Hz. The olefinic resonances of the coordinated COD appear at 4.13 and 3.77 ppm in the $^1$H NMR spectrum, which is the typical region for olefin complexes.

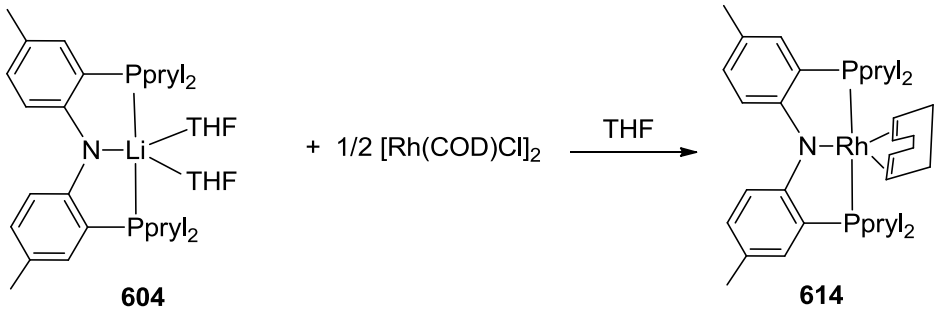


**Scheme 6-11.** Synthesis of **614**.

**Reaction of ($^{Me}$PNP$^{pryl}$)Rh(COD) with MeI**. Oxidative addition of methyl iodide to a $d^8$ metal center is well known. For example, the reaction of MeI with $[M(CO)I_2]^-$ (M = Rh, Ir) is a key step in the homogeneous catalytic carbonylation of methanol.[198] The reaction of ($^{Me}$PNP$^{pryl}$)Rh(COD) with excess methyl iodide in $C_6D_6$ at 50 $^oC$ led to the formation of a new product with the formula ($^{Me}$PNP$^{pryl}$)Rh(Me)(I)($ICH_3$) (**615a**) and the release of free COD as indicated by solution NMR spectroscopy (Scheme 6-12). A doublet resonated at δ 101.6 ppm with $J_{Rh\text{-}P}$ = 139 Hz appeared in the $^{31}$P NMR spectrum. This relatively small Rh-P coupling constant is consistent with the formation of a Rh(III) species. More importantly, a triplet at δ 1.69 ppm with $J_{P\text{-}H}$ = 7 Hz was present in the $^1$H NMR spectrum indicating the formation of Rh-$CH_3$ bond. However, we believe that this is a six-coordinate compound in solution. We tried to work up this reaction by removing the solvent as well as the excess MeI under vacuum. The residue was redissolved in $C_6D_6$. Interestingly, a new doublet shifted from 101.6 to 105.4 ppm with $J_{Rh\text{-}P}$ = 145 Hz was detected by $^{31}$P NMR. A new doublet of triplets at δ 1.41 ppm ($J_{P\text{-}H}$ = 7 Hz) corresponding to Rh-$CH_3$ was also present in the $^1$H NMR spectrum. We

propose that this new species was an iodide bridged dimer [($^{Me}$PNP$^{pryl}$)Rh(Me)(I)]$_2$ (**615b**). Compound ($^{Me}$PNP$^{pryl}$)Rh(Me)(I)($ICH_3$) (**615a**) was reformed by adding excess MeI to the solution of **615b**.

The origins of the formation of compounds **615a** and **615b** were probably a combination of both steric and electronic factors. Pyrrolyl substituted phosphine is less bulky than the isopropyl substituted phosphine (the calculated cone angle for P(pyrrolyl)$_3$ is 145° while that for P$^i$Pr$_3$ is 160°). The smaller ligand renders its metal complex with enough room to coordinate to the sixth ligand. On the other hand, the π-accepting property of the $^{Me}$PNP$^{pryl}$ ligand also makes the metal center less electron rich than the corresponding $^{Me}$PNP$^{iPr}$ supported metal center. The coordination of the sixth ligand compensates for the relatatively electron poor metal center. These two factors might account for the difficulty isolating five-coordinated Rh(III) species in the [($^{Me}$PNP$^{pryl}$)Rh] system.

Compound ($^{Me}$PNP$^{pryl}$)Rh(Me)(OAc) (**616**) was obtained quantitatively through salt metathesis of [($^{Me}$PNP$^{pryl}$)Rh(Me)(I)]$_2$ with 1 eq. AgOAc. Although we have not characterized **616** by X-ray crystal diffraction, it is likely that the acetate binds to rhodium in the $\eta^2$-fashion to form the 18 e six-coordinate Rh(III) compound due to the reasons described above.

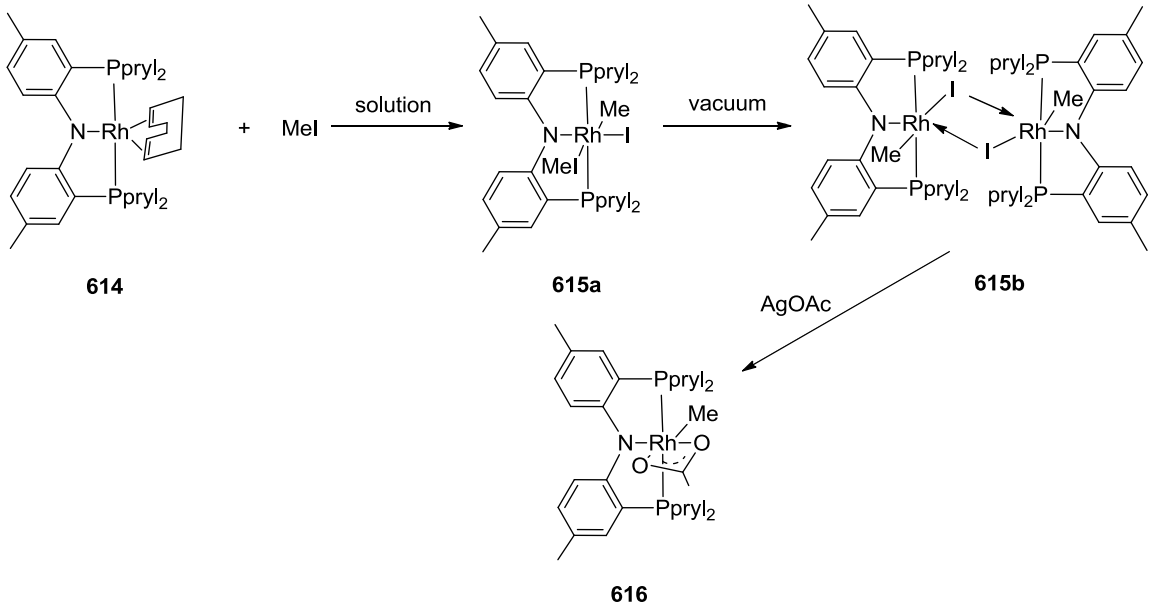


**Scheme 6-12.** Synthesis of **615** and **616**.

6.2.2.3 Synthesis of ($^{Me}$PNP$^{pryl}$)Rh(HSiEt$_3$) and ($^{Me}$PNP$^{pryl}$)Rh(S$^i$Pr$_2$) complexes

Treatment of **616** with triethylsilane in $C_6D_6$ at room temperature resulted in the release of triethylsilylacetate as well as methane as indicated by $^1$H NMR (Scheme 6-13). A new doublet resonated at δ 111.8 ppm with the $J_{Rh-P}$ = 184 Hz was observed by $^{31}$P NMR. A doublet of triplets at δ = -13.2 ppm with $J_{Rh-H}$ = 25 Hz and $J_{P-H}$ = 13 Hz was detected by $^1$H NMR. More importantly, this up-field hydride signal displayed a $J_{Si-H}$ value of 35 Hz in the $^1$H{$^{31}$P}NMR spectrum indicating the interaction between the silicon and hydrogen. We assigned the new complex as a silane σ-complex ($^{Me}$PNP$^{pryl}$)Rh(η$^2$-HSiEt$_3$) (**617**). Generally, nonclassical silane complexes display a $J_{Si-H}$

coupling constant of 20 Hz up to 200 Hz, while classic silyl hydride complexes typically exhibit $J_{Si\text{-}H}$ values of 10 Hz.[199] It is worth noting that to the best of our knowledge, no mononuclear Rh(I) silane σ-complex has been reported in the literature so far. Most of

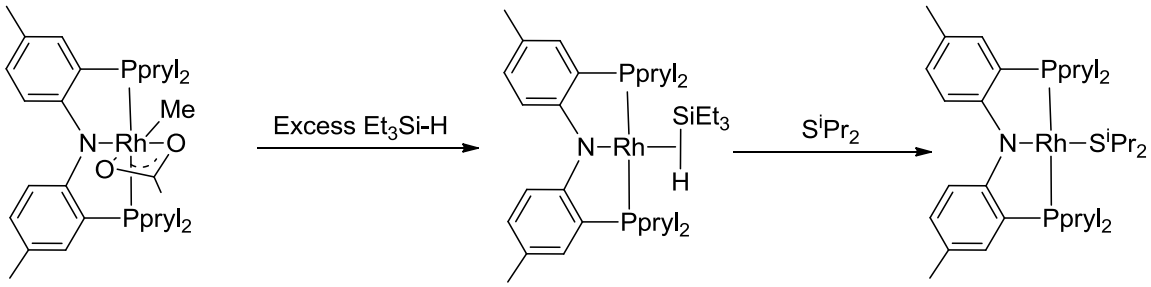


**616** **617** **618**

**Scheme 6-13.** Synthesis of **617** and **618**.

the group 9 silane σ-complexes are cationic M(III) compounds. For example, the Brookhart group reported the characterization of a series of cationic Rh(III) nonclassical silane complexes by the addition of silanes to cationic Rh(III) precursors.[200] The lack of oxidative addition of triethylsilane also illustrates the electron deficient nature of the ligand system.

Compound **617** can be cleanly converted to ($^{Me}$PNP$^{pryl}$)Rh(S$^{i}$Pr$_2$) (**618**) in the presence of excess S$^{i}$Pr$_2$ at room temperature within 5 hours. Free Et$_3$SiH was also observed by $^1$H NMR. Compound **618** displayed $C_{2v}$ symmetry by NMR at room temperature. A single doublet $^{31}$P NMR resonance was observed at δ 106.5 ppm with $J_{Rh\text{-}P}$ = 198 Hz.

6.2.2.4 Aryl-halide oxidative addition at ($^{Me}$PNP$^{pryl}$)Rh center

Ar-X (X = I or Br) can oxidatively add to ($^{Me}$PNP$^{pryl}$)Rh(I) fragment to form the corresponding Rh(III) species. Reaction of ($^{Me}$PNP$^{pryl}$)Rh(S$^{i}$Pr$_2$) (**618**) or compound **614** with PhI or PhBr in $C_6D_6$ at 70 $^{o}$C did not lead to the desired OA product ($^{Me}$PNP$^{pryl}$)Rh(Ph)(X). Monitoring the reaction by $^{1}$H NMR revealed the disappearance of the starting material and the release of the free S$^{i}$Pr$_2$. However, a few broad signals were obtained in the $^{31}$P NMR spectrum and we could not identify the products from the mixture. It is likely that one or some of the pyrrolyl substituents on the phosphine ligand was activated by the metal as four broad signals in the 5~6 ppm region were observed by $^{1}$H NMR spectroscopy. The five-coordinate ($^{Me}$PNP$^{pryl}$)Rh(Ph)(X) is probably difficult to achieve due to the steric and electronic nature of ($^{Me}$PNP$^{pryl}$)Rh system as described above. Not surprisingly, the reaction of ($^{Me}$PNP$^{pryl}$)Rh(S$^{i}$Pr$_2$) with PhX in the presence of a donor ligand "L" such as acetonitrile proceeded cleanly to form the six-coordinate ($^{Me}$PNP$^{pryl}$)Rh(Ph)(X)(L) compounds (**619**, **620**, **621**, Scheme 6-14). Ph-I oxidatively added to the Rh(I) center faster than Ph-Br (2 h at 70 ℃ vs 2 d at 90 ℃). Unfortunately, no Ph-Cl or Ph-OTf OA was observed under the similar reaction conditions. In comparison, ($^{Me}$PNP$^{iPr}$)Rh(Ph)(Cl) and ($^{Me}$PNP$^{iPr}$)Rh(Ph)(OTf) can cleanly be produced through the OA of PhCl and PhOTf to ($^{Me}$PNP$^{iPr}$)Rh that is generated through the dissociation of S$^{i}$Pr$_2$ from ($^{Me}$PNP$^{iPr}$)Rh(S$^{i}$Pr$_2$). The rate of OA probably depends on the rate of $^{i}$Pr$_2$S dissociation, and that would be affected by both sterics and electronics. Both electronic and steric factors indicate that the dissociation of $^{i}$Pr$_2$S should be more

difficult in compound **618** than in ($^{Me}$PNP$^{iPr}$)Rh(S$^{i}$Pr$_2$). It could also be that the Ph-Cl OA to (PNP-pryl)Rh is not more favorable than the binding of $^{i}$Pr$_2$S.

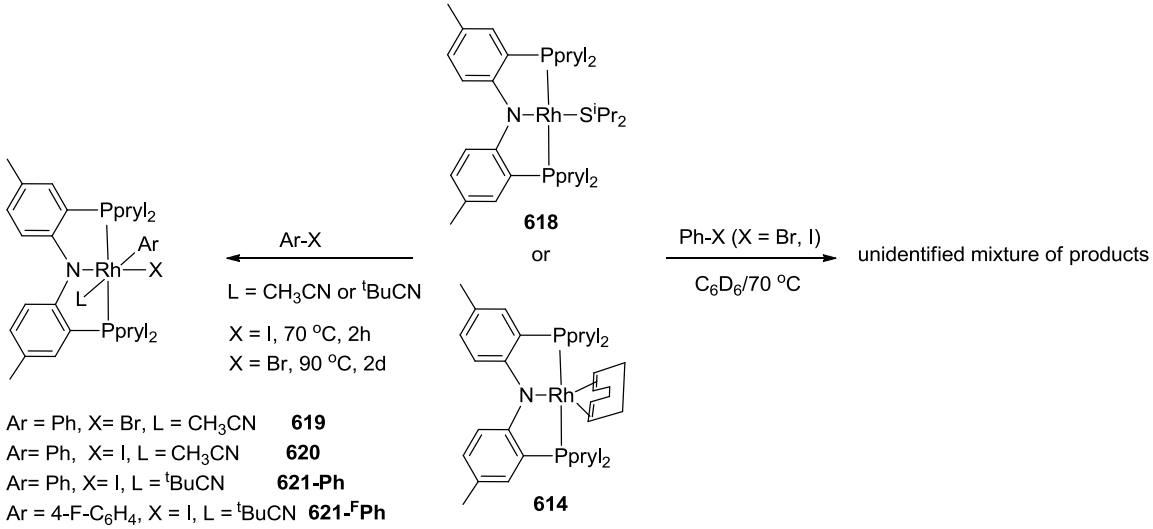


**Scheme 6-14.** Ar-X OA at ($^{Me}$PNP$^{pryl}$)Rh in the presence of external donor ligand.

6.2.2.5 Synthesis of ($^{Me}$PNP$^{pryl}$)Rh(Ph)(OAc) and ($^{Me}$PNP$^{pryl}$)Rh(Ph)(OTf)(NC$^{t}$Bu)

Although Ar-I and Ar-Br can oxidatively add to rhodium to make a Rh-I or Rh-Br bond, we are more interested in installing harder and better leaving groups such as triflate to the rhodium, which can later facilitate the installation of other ligands onto the metal center. Similar to ($^{Me}$PNP$^{pryl}$)Rh(Me)(OAc), compound ($^{Me}$PNP$^{pryl}$)Rh(Ph)(OAc) (**622**) was synthesized through the salt metathesis of ($^{Me}$PNP$^{pryl}$)Rh(Ph)(I)(L) with AgOAc (Scheme 6-15). The $\eta^2$ coordination mode of the acetate group completes the sixth coordination site and forms the coordination saturated 18 e Rh(III) compound.

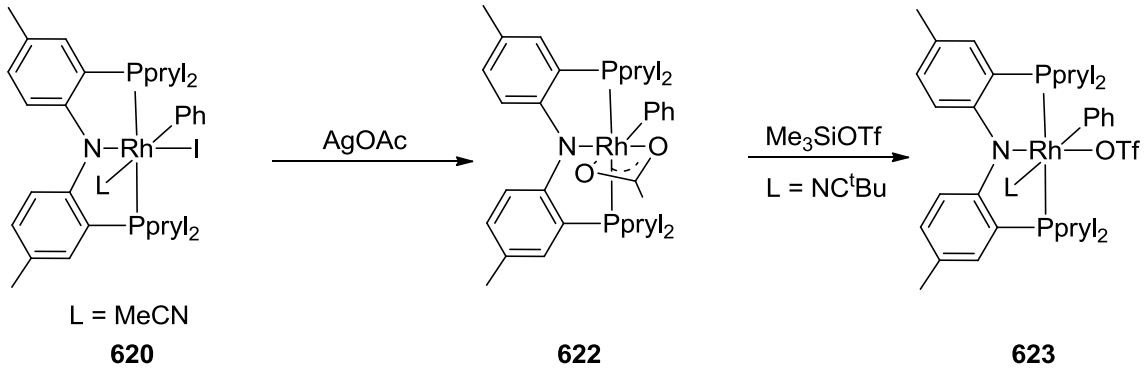


**Scheme 6-15.** Synthesis of **622** and **623** through metathesis.

($^{Me}$PNP$^{pryl}$)Rh(Ph)(OTf) is an attractive molecule to synthesize because OTf is a good leaving group and our group has already demonstrated its versatile reactivity in other systems. One of the common routes to generate metal-triflate is by reacting metal-acetate/chloride with a trialkylsilyl triflate. However, no reaction was observed between ($^{Me}$PNP$^{pryl}$)Rh(Ph)(OAc) and excess $Me_3SiOTf$ in $C_6D_6$ at room temperature. Interestingly, ($^{Me}$PNP$^{pryl}$)Rh(Ph)(OAc) reacted with $Me_3SiOTf$ immediately in the presence of an external donor ligand such as NC$^t$Bu (Scheme 6-15). With fast workup, the six-coordinate ($^{Me}$PNP$^{pryl}$)Rh(Ph)(OTf)(NC$^t$Bu) (**623**) could be isolated as a red-purple solid. Compound **623** was characterized by solution NMR. Five different aromatic resonances were observed for the phenyl ring bound to Rh in $^1$H NMR indicating the slow rotation of the Rh-Ph bond on the NMR time scale. A distinctive doublet of triplets was also detected at δ 140.3 ppm corresponding to the *ipso*-C bound to Rh in $^{13}$C{$^1$H} NMR. A singlet resonanced at δ -78.3 ppm (relatively down field compared to free triflate anion) by $^{19}$F NMR also indicated that the OTf is bound to the

rhodium center. Compound **623** is not stable in solution. The $C_6D_6$ solution of **623** decomposed to form two unidentified products at room temperature after 24 h or 50 $^oC$ after 3 h.

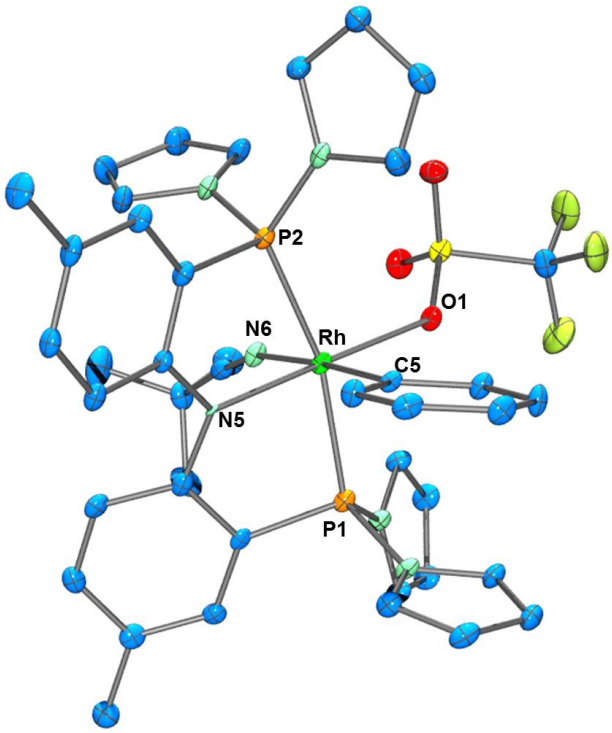


**Figure 6-2.** ORTEP drawing[103] of **623** (50% thermal ellipsoids). Hydrogen atoms are omitted for clarity. Selected bond distances (Å) and angles (deg) for **623**: Rh-P1, 2.304(2); Rh-P2, 2.277(2); Rh-O1, 2.135(5); Rh-N5, 2.023(6); Rh-N6, 2.146(6); Rh-C5, 2.062(7); P1-Rh-P2, 164.46(7); O1-Rh-N5, 177.1 (2); C5-Rh-N6, 175.9(3).

The structure[197] of **623** was further confirmed by X-ray crystal diffraction (Figure 6-2). The six coordinate rhodium adopts the octahedral geometry with the phenyl group trans to NC$^t$Bu. The P-Rh-P angle is 164.46 °which is similar to what is observed in six coordinate ($^{Me}$PNP$^{iPr}$)Rh complexes.[161]

6.2.2.6 Activation of $Ph_2Zn$ by ($^{Me}PNP^{pryl}$)Rh

One reason the C-C cross coupling reaction catalyzed by (PNP)Rh does not work very well is that the transmetalation reagent is not innocent towards the 14 e (PNP)Rh intermediate. For example, the Zn-Ph bond in $Ph_2Zn$ can be activated by ($^{Me}PNP^{pryl}$)Rh.

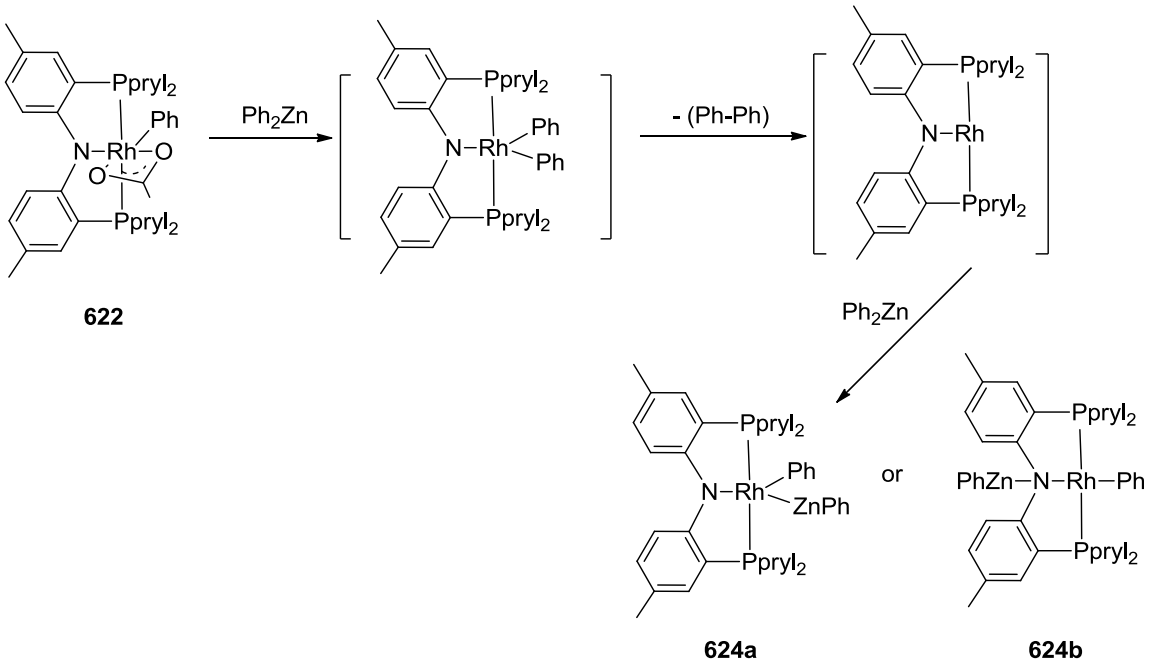


**Scheme 6-16.** Ph-Zn bond activation by ($^{Me}PNP^{pryl}$)Rh.

Reaction of ($^{Me}PNP^{pryl}$)Rh(Ph)(OAc) with 2 eq. $Ph_2Zn$ at room temperature in $C_6D_6$ or $CD_2Cl_2$ led to an immediate color change from red to green. Within 10 min, $^{31}P$ NMR analysis indicates complete disappearance of the starting material and the formation of two new products resonating at δ 112.4 ppm ($J_{Rh-P}$ = 173 Hz) (~82%) and 100.6 ppm ($J_{Rh-P}$ = 107 Hz) (~18%). After 1 h, only a single compound δ 112.4 ppm was observed by $^{31}P$ NMR. It is likely that compound **622** reacts with the organozinc transmetallation

reagent to form ($^{Me}$PNP$^{pryl}$)Rh(Ph)(Ph) ($^{31}$PNMR: δ 100.6 ppm ($J_{Rh-P}$ = 107 Hz)) which is unstable and undergoes C-C reductive elimination to generate the three coordinate ($^{Me}$PNP$^{pryl}$)Rh intermediate. The expected Ph-Ph by-product was observed by $^{1}$H NMR spectroscopy. The Zn-Ph bond of $Ph_2Zn$ was activated by ($^{Me}$PNP$^{pryl}$)Rh and resulted in the formation of a rhodium-zinc adduct. The product has not been fully characterized yet. We tentatively assigned it as a Zn-Ph oxidative addition product ($^{Me}$PNP$^{pryl}$)Rh(Ph)(ZnPh) (**624a**) The other possibility is instead of doing Zn-Ph oxidative addition, Zn-Ph does 1,2-addition reaction adding across the Rh-N bond to form the product ($^{Me}$PN(ZnPh)P$^{pryl}$)Rh(Ph) (**624b**) (Scheme 6-16). Unfortunately, we cannot differentiate these two structures based on NMR techniques. Due to the poor solubility of the compound, no X-ray crystal structure has been obtained. Zn-C bond oxidative addition to Rh(I) is not without precedent. Goldberg reported an example of the formation of (PNP)*Rh($ZnCH_3$)($CH_3$)(OTf) ((PNP)* = 2,6-bis(di-*tert*-butylphosphinomethyl)pyridine) by reacting (PNP)*Rh(OTf) with dimethylzinc. [201] Compound **624** did not react further with aryl halide, which is direct evidence for catalytic inhibition in the catalytic cycle.

*6.2.3 Examination of the C-O reductive elimination in (MePNPpryl)Rh system*

One of our goals for the utilization of the new ($^{Me}$PNP$^{pryl}$)Rh system is to study the reductive elimination (C-C, C-N, C-O etc) at rhodium center by taking advantage of the relatively electron poor nature of the metal center in contrast to the ($^{Me}$PNP$^{iPr}$)Rh system. The formation of C-C and C-N bonds is well studied by other systems, especially the palladium catalyzed C-C and C-N cross coupling reactions.[185] C-O RE from

palladium(IV) and platinum(IV) centers to form carboxylates has also been developed.[202] Palladium catalyzed C-O bond formation has emerged as an effective method for the construction of ethers from aryl halides and phenols or alcohols.[203] C-C reductive elimination was studied at five coordinate ($^{Me}$PNP$^{iPr}$)Rh(R)(R') by Dr. Gatard in our group. The reductive elimination of R-R' was clean and quantitative. However, the C-N and C-O bonds elimination has not been accomplished yet by the ($^{Me}$PNP$^{iPr}$)Rh system.

**Examination of C-O RE at ($^{Me}$PNP$^{pryl}$)Rh(Ph)(OPh)(NC$^{t}$Bu).** Reductive elimination proceeds faster at a five-coordinate $d^6$ metal center than the corresponding six-coordinate one.[33,130] Unfortunately, so far only six-coordinate ($^{Me}$PNP$^{pryl}$)Rh complexes have been synthesized and all the attempts to make the five-coordinate ($^{Me}$PNP$^{pryl}$)Rh complexes have been unsuccessful.

Reaction of compound **623** with excess NaOPh in PhF at room temperature for 4 h led to the formation of two new products as indicated by $^{31}$P NMR spectroscopy. Two different $^{t}$BuCN signals were also observed by $^{1}$H NMR. These two products could not be separated by recrystalization. We tentatively assigned them as the two geometric isomers of compound ($^{Me}$PNP$^{pryl}$)Rh(Ph)(OPh)(NC$^{t}$Bu) (**625**). Compound **625** was thermolyzed in the presence of Ph-I in $C_6D_6$ at 70 $^{o}$C for ~17 h. $^{31}$P NMR analysis revealed the formation of ($^{Me}$PNP$^{pryl}$)Rh(Ph)(I)(NC$^{t}$Bu) in > 95% yield (Scheme 6-17).

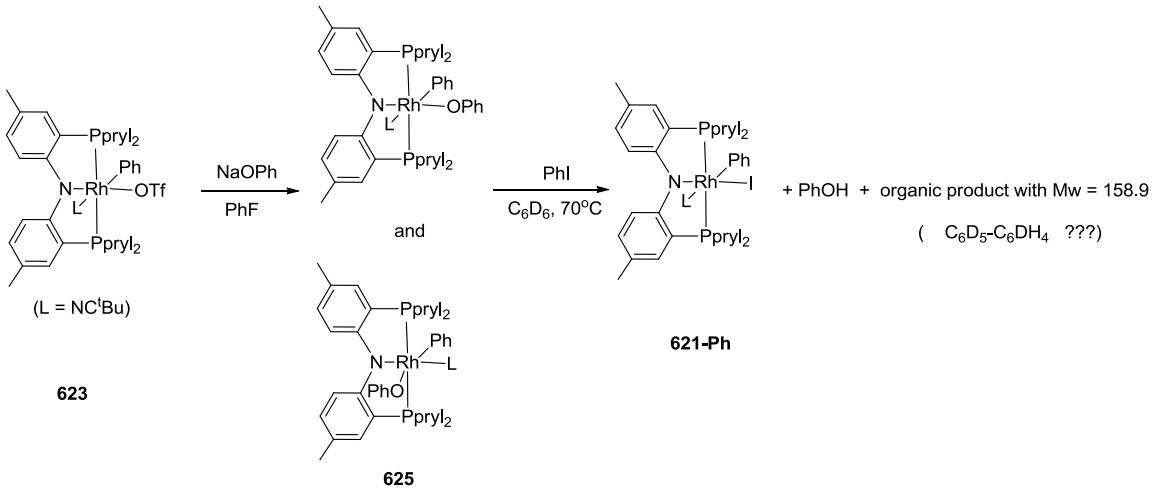


**Scheme 6-17.** Thermolysis of **623** and NaOPh in the presence of PhI in $C_6D_6$.

Interestingly, no C-O RE product (PhO-Ph) was detected by NMR or mass spectroscopy. Instead, PhOH was observed in the $^1$H NMR spectrum and another product with molecular weight of 158.9 was detected in the mass spectrum. Similarly, the organic products PhOH and $C_6H_5$-$C_6H_5$ were observed when thermolysis of the reaction in $C_6H_6$ instead of $C_6D_6$.

We investigated the reaction further in order to understand the reaction process. Both ($^{Me}$PNP$^{pryl}$)Rh(Ph)(I)(NC$^t$Bu) and ($^{Me}$PNP$^{pryl}$)Rh(4-F-$C_6H_4$)(I)(NC$^t$Bu) were found when ($^{Me}$PNP$^{pryl}$)Rh(Ph)(OPh)(NC$^t$Bu) was thermolyzed in the presence of 4-F-$C_6H_4$I. Moreover, the organic compounds PhOH, $C_6H_5$-$C_6H_5$, and $C_6H_5$-$C_6H_4$F as well as small amount of PhO$C_6H_4$F and $(C_6H_4F)_2$ were detected by GC/MS.

Without further study, it is difficult to fully understand the mechanism of these reactions. However, with the observation of the formation of PhO-H and **621**, one can perceive several possible reaction pathways.

One of the possible reaction pathways is shown in Scheme 6-18. Dissociation of the pivalonitrile from **625** led to the formation of the five-coordinated intermediate **6A'**. Solvent $C_6H_6$ came in and C-H activation generated PhO-H and the rhodium biphenyl species **6C'**. C-C RE formed biphenyl and generated the transient three-coordinated intermediate **6E'**. OA of PhI followed by the coordination of pivalonitrile eventually led to the finally observed **621-Ph**.

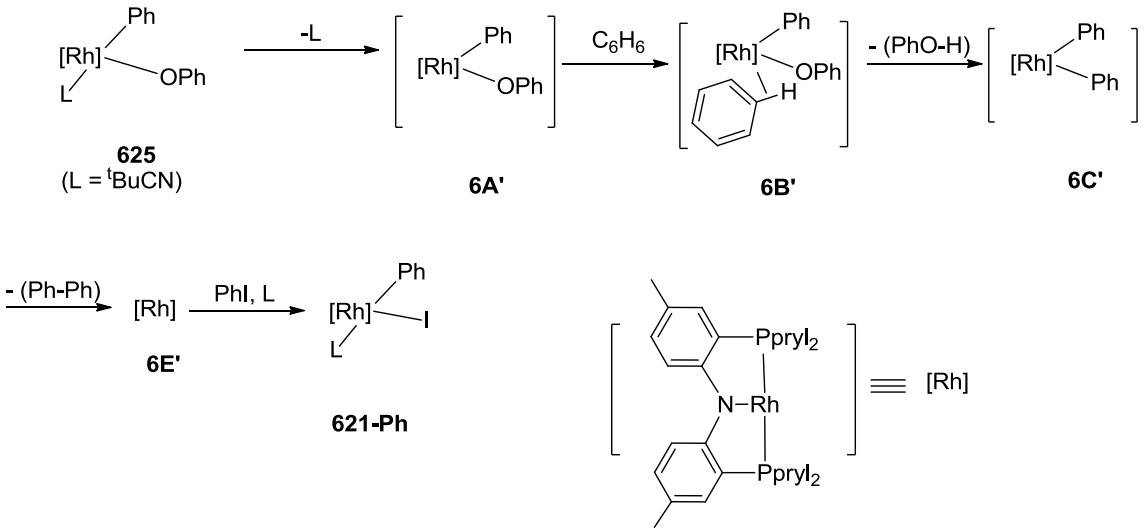


**Scheme 6-18.** The transformation via C-H activation of benzene solvent.

The reaction pathway as described in Scheme 6-18 fits the experimental data when the reaction was done in $C_6H_6$. However, it disagrees with the data while the reaction

was done in $C_6D_6$. C-D bond in $C_6D_6$ was activated and PhO-D should be observed if the reaction followed the pathway in Scheme 6-18. In reality, only PhO-H was formed even the reaction was done in $C_6D_6$.

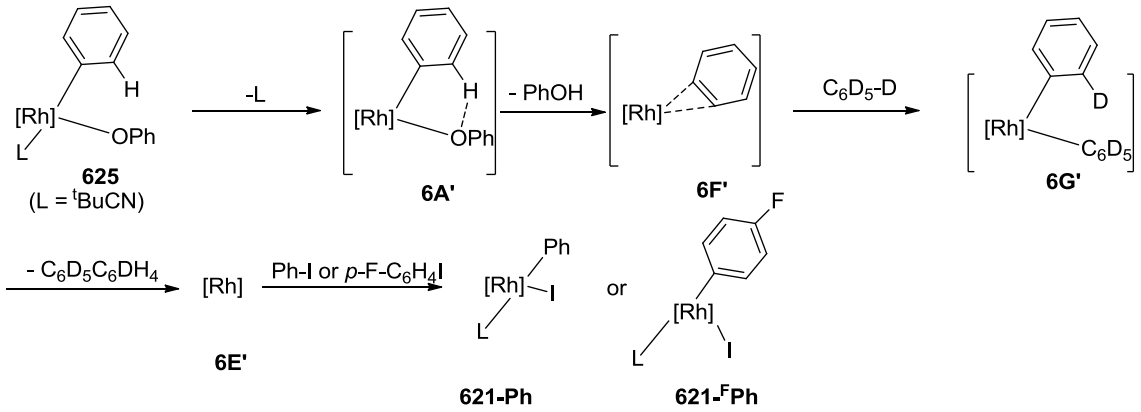


**Scheme 6-19.** The transformation via a benzyne intermediate.

The second reaction pathway one can think of is via a benzyne intermediate. A Rh-benzyne intermediate (**6F'**) was possibly generated due to the β-H abstraction for the formation of PhO-H (Scheme 6-19). In the presence of benzene as solvent, the benzyne intermediate affected the C-H (or C-D) bond activation of the solvent, forming the rhodium bis-aryl complex (**6G'**) which underwent fast C-C reductive elimination to release the biphenyl. The C-H activation mediated by a metal-benzyne complex is not without precedence.[204] Aryl iodide oxidatively added to the transient three-coordinate rhodium (**6E'**) and was trapped by the nitrile to generate the observed rhodium (III) compound. This reaction pathway fits the observed formation of PhO-H no matter the reaction was done in $C_6H_6$ or $C_6D_6$. Based on this reaction process, the GC/MS

observed product should be $C_6D_5$-$C_6DH_4$ with the molecular weight of 160 when the reaction was done in $C_6D_6$. However, only a product with the molecular weight of 158.9 was observed. So this reaction route is inconsistent with the GC/MS experimental data.

It is also likely that the C-H bond activation of pyrrolyl ligand was involved during the transformation. The intermediate **6H'** might be accessible through the interaction of C-H bond from pyrrolyl ligand with **6A'**. After the release of PhO-H and followed by C-D

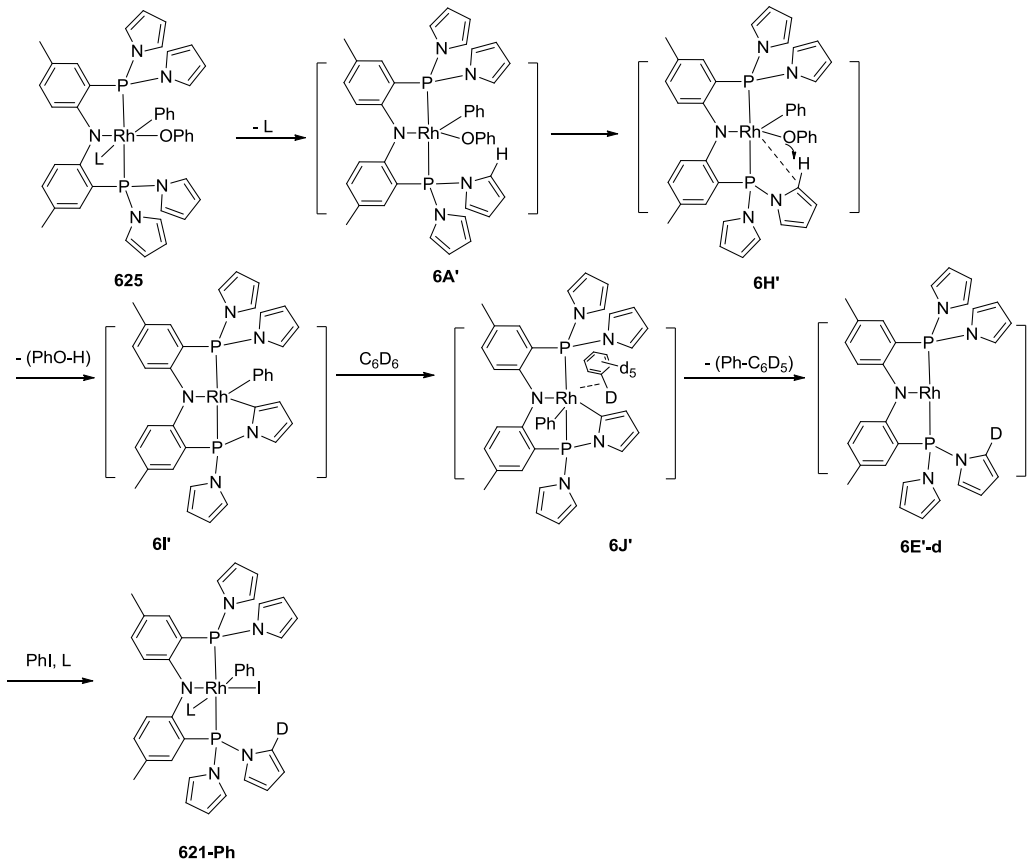


**Scheme 6-20.** The transformation via a pyrrolyl C-H bond activation.

bond activation, an intermediate similar to **6J'** as shown in Scheme 6-20 was possibly formed. Elimination of Ph-$C_6D_5$ and migration of deuterium to the pyrrolyl ligand regenerated the transient **6E'-d**. This pathway fits the experimental data we have obtained so far, including the formation of PhO-H as well as the formation of Ph-$C_6D_5$ as interoperated from GC/MS. However, more data need to be obtained in order to fully support this pathway.

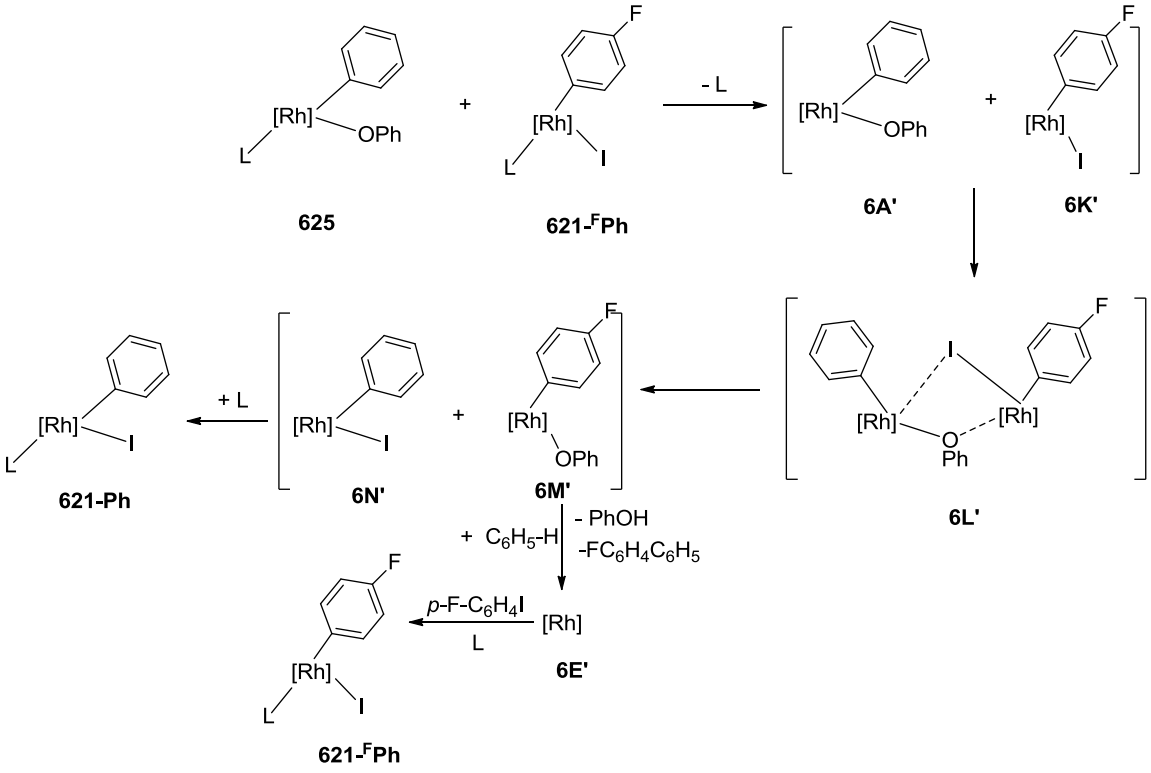


**Scheme 6-21.** I/OPh exchange via the intermediacy of the dirhodium complex.

The reaction became more complicated when it is done in $C_6H_6$ and in the presence of *p*-fluoro-phenyliodide. Both ($^{Me}$PNP$^{pryl}$)Rh(Ph)(I)(NC$^t$Bu) (**621-Ph**) and ($^{Me}$PNP$^{pryl}$)Rh(*p*-F-$C_6H_4$)(I)(NC$^t$Bu) (**621-$^F$Ph**) were formed. We propose that the formation of both **621-Ph** and **621-$^F$Ph** is due to I/OPh exchange between **625** and **621-$^F$Ph**, probably via the intermediacy of the dirhodium complex **6L'** as shown in Scheme 6-21.

***6.3 Conclusion***

In summary, we have synthesized a new π-accepting PNP ligand bearing pyrrolyl substituent. Other PNP ligands with different substituent on the phosphorous atoms have also been synthesized by reacting $^{Me}$PNP$^{pryl}$ with organolithium reagents. A PNP ligand with ethoxy groups on the phosphorus has also been successfully achieved. This study develops a completely new method to synthesize PNP ligands with different electronic and steric properties.

We have also synthesized several Rh(I) complexes supported by $^{Me}$PNP$^{pryl}$ ligand via N-P cleavage, direct transmetalation, or ligand substitution. Six-coordinate Rh(III) has been obtained through oxidative addition of aryl-halide to rhodium. However, in comparison to ($^{Me}$PNP$^{iPr}$)Rh system, no five-coordinate ($^{Me}$PNP$^{pryl}$)Rh(III) species has been obtained and this is probably due to both steric and electronic factors. One of our goals for exploring this new ligand system is to examine the RE reactions at rhodium center. The lack of isolation of five-coordinate ($^{Me}$PNP$^{pryl}$)Rh(III) species precludes the direct comparison of the rate of C-C reductive elimination reactions between ($^{Me}$PNP$^{iPr}$)Rh and ($^{Me}$PNP$^{pryl}$)Rh systems. On the other hand, we studied the C-O

reductive elimination at ($^{Me}$PNP$^{pryl}$)Rh(III) center. Unfortunately, no C-O RE product was observed and further examination indicated that benzene C-H activation might be involved in these transformations.

### *6.4 Experimental*

**General Considerations.** Unless specified otherwise, all manipulations were performed under an argon atmosphere using standard Schlenk line or glovebox techniques. Ethyl ether, $C_6D_6$, and pentane were dried over Na/K/$Ph_2CO$/18-crown-6, distilled or vacuum transferred and stored over molecular sieves in an Ar-filled glovebox. Fluorobenzene was dried with and then distilled from $CaH_2$. $[Rh(COD)Cl]_2$,[205] $ClPpryl_2$[206] were prepared according to the published procedures. All other chemicals were used as received from commercial vendors (PhLi, 1.8 M/$Bu_2O$; *n*-BnLi, 2.5 M/hexanes; MeMgCl, 3.0 M/THF; $Me_2Zn$, 1.0 M/Heptane). NMR spectra were recorded on a Varian iNova 300, Varian iNova 400, and Mercury 300 spectrometer. Chemical shifts are reported in δ (ppm). For $^1$H and $^{13}$C NMR spectra, the residual solvent peak was used as an internal reference. $^{31}$P NMR spectra were referenced externally using 85% $H_3PO_4$ at δ 0 ppm. $^{19}$F NMR spectra were referenced externally using $CF_3COOH$ at δ -78.5 ppm. Elemental analyses were performed by CALI, Inc. (Parsippany, NJ).

**Synthesis of 601.** Under Ar, *n*-BuLi (1.09 mL, 2.72 mmol) was slowly added to a solution of *N*-methyl-bis(2-bromo-4-methylphenyl)amine (500 mg, 1.362 mmol) at 0 $^oC$. The reaction mixture was warmed to room temperature and stirred for 1 h, and then it was cooled down to -100 $^oC$. $ClPpryl_2$ (430 μL, 2.66 mmol) was added to it. The

reaction mixture was warmed up to room temperature and stirred overnight. A yellow solution with white precipitate was formed the next day. The volatiles were removed under vacuum and the residue was extracted with toluene. The solution was passed through Celite and silica. The volatiles of the filtration were removed and recrystallization of the residue from ether afforded **601** as white solid. Yield, 160 mg, 1.04 mmol, 38.4%. $^{31}P\{^{1}H\}$ NMR ($C_6D_6$): δ 8.1. $^{1}H$ NMR ($C_6D_6$): δ 7.54 (dd, *J* = 12 Hz, *J* = 2 Hz, 2H), 7.00 (dd, *J* = 8 Hz, *J* = 2 Hz, 2H), 6.90 (m, 2H), 6.65 (d, *J* = 8 Hz, 2H), 6.25 (m, 2H), 2.94 (s, 3H), 2.01(s, 6H).

**Synthesis of 602**. Bis(2-bromo-4-methylphenyl)amine (567 mg, 1.60 mmol), $(Boc)_2O$ (553 μL, 2.40 mmol), 4-DMAP (40.0 mg, 0.32 mmol) were dissolved in about 10 mL of THF. The reaction mixture was refluxed in THF for about 40 h. $^{1}H$ NMR indicated there was only about ~ 50% conversion of the starting material. The volatiles were removed under vacuum and the residue was extracted with ether. The ether solution was passed through Celite and silica. The volatiles of the filtration were removed and the residue was washed with pentane for 3 times (3 x 5 mL) to get the white solid. $^{1}H$ NMR ($C_6D_6$):δ 7.45 (d, *J* = 8 Hz, 2H), 7.24 (br, 2H), 6.58 (d, *J* = 8 Hz, 2H), 1.75 (s, 6H), 1.50 (s, 9H).

**Synthesis of 603.** Bis(2-bromo-4-methylphenyl)amine (1.18 g, 3.36 mmol) was dissolved in about 50 mL of ether. *n*-BuLi (4.16 mL, 10.4 mmol) was slowly added to the solution. The reaction mixture was stirred at room temperature for 2 h and then slowly added to a flask containing ClPpryl (1.68 mL, 10.4 mmol) in an ice bath. The color immediately changed to red. The reaction was stirred at room temperature for

overnight. Slightly yellow solution together with white precipitate was formed the next day. The volatiles were removed under vacuum and the residue was dissolved in toluene. The solution was passed through Celite and silica. The volatiles from the filtration were removed and the oily residue was washed with pentane to afford white power. The solid power was dried under vacuum. Yield, 966 mg, 1.41 mmol, 42.1%. $^{31}P\{^{1}H\}$ NMR ($C_6D_6$): δ 63.9 (d, 2P, $J_{P\text{-}P}$ = 49 Hz, *P*-Aryl), 85.5 (t, 1P, $J_{P\text{-}P}$ = 49 Hz, *P*-N). $^{1}H$ NMR($C_6D_6$): δ 6.70 – 6.60 (m, 10 H), 6.56 (m, 8 H), 6.26 (m, 4H), 6.20 (m. 8H), 1.81 (s, 6H). $^{13}C\{^{1}H\}(C_6D_6)$:δ 145.5 (q, $J_{P\text{-}C}$ = 13 Hz), 136.9, 133.4, 132.8 (t, *J* = 10 Hz), 132.6, 128.8 (dt, *J* = 10 Hz, *J* = 5 Hz), 124.2 (t, *J* = 7 Hz), 123.7 (d, *J* = 15 Hz), 112.6 (d, *J* = 5 Hz), 112.4.

**Synthesis of 604.** Compound **603** (143 mg, 0.209 mmol) was dissolved in about 3 mL of THF followed by the addition of $LiNMe_2$ (12.0 mg, 0.231 mmol ). The solution color changed to yellow immediately. $^{31}P$ NMR analysis revealed that compound **604** was the major product together with the formation of $Ppryl_2(NMe_2)$. There were also a few other signals observed by $^{31}P$ NMR spectroscopy, presumably due to the products of the unselective cleavage of P-N bonds from the ligand back bone. The volatiles were removed under vacuum and the residue was recrystallized from THF/pentane to get yellow powder. The solid was washed with pentane 3 times and dried under vacuum. Yield, 80.0 mg, 0.12 mmol, 57.1%. $^{31}P\{^{1}H\}$ NMR ($C_6D_6$): δ 75.2. $^{1}H$ NMR ($C_6D_6$): δ 7.00 (d, *J* = 6 Hz, 2H), 6.92 (m, 2H), 6.85 (m, 8H), 6.77 (d, *J* = 6 Hz, 2H), 6.34 (m, 8H), 3.35 (m, 8H), 2.03 (s, 6H), 1.23 (m, 8H).

**Synthesis of 605.** Compound **603** (665 mg, 0.973 mmol) was dissolved in about 6 mL of THF followed by the addition of $LiNMe_2$ (52.0 mg, 1.07 mmol ). The solution color changed to yellow immediately. $^{31}P$ NMR analysis revealed that compound **604** was the major product together with the formation of $Ppryl_2(NMe_2)$. There were also a few other signals observed by $^{31}P$ NMR, presumably due to the products of the unselective cleavage of P-N bonds from the ligand back bone. The reaction mixture was taken out of the glovebox and excess degassed water was added to it. The yellow solution changed to colorless within a few minutes. The volatiles were removed under vacuum and the residue was dissolved in toluene. The solution was passed through Celite and silica. Remove the volatiles from the filtration and recrystalize the residue from pentane gave compound **605** as air stable white solid. Yield, 253 mg, 0.53 mmol, 50%. $^{31}P\{^1H\}$ NMR ($C_6D_6$): δ 66.1. $^1H$ NMR ($C_6D_6$): δ 6.78 (m, 12H), 6.55 (d, *J* = 5 Hz, 2H), 6.28 (m, 8H), 4.97 (br, 1H), 1.90 (s, 6H). $^{13}C\{^1H\}$ NMR ($C_6D_6$): δ 144.1 (d, *J* = 22 Hz), 132.8, 132.7, 131.4 (d, *J* = 5 Hz), 124.4 (d, *J* = 14 Hz), 121.4, 112.9 (d, *J* = 4 Hz) (one aromatic 'C' is either missing or overlapped with other aromatic resonances) 20.7.

**Synthesis of 606.** Compound **604** (50.0 mg, 0.074 mmol) was dissolved in about 2 mL of THF followed by the addition of degassed EtOH (100 μL, excess). The yellow solution changed to colorless within minutes. $^{31}P$ NMR analysis indicated the disappearance of the starting material and the formation of a new product with > 95% purity. The volatiles were removed under vacuum. The residue was extracted with toluene and the solution was passed through Celite. The volatiles were removed under

vacuum. Recrystallization was attempted from several different solvents, however, we could not isolate compound **606** as a solid form. $^{31}P\{^{1}H\}$ NMR ($C_6D_6$): δ 155.6. $^{1}H$ NMR ($C_6D_6$): δ 7.73 (d, *J* = 7 Hz, 2H), 7.71 (br, 1H), 7.26 (dd, *J* = 8 Hz, *J* = 3 Hz, 2H), 6.91 (d, *J* = 8 Hz, 2H), 3.86 (m, 8H), 2.17 (s, 6H), 1.17 (t, *J* = 8H, 12H). $^{13}C\{^{1}H\}$ NMR ($C_6D_6$): δ 144.4 (d, *J* = 17 Hz),132.1 (d, *J* = 17 Hz), 131.9, 130.0 (d, *J* = 4 Hz), 129.8, 119.6, 62.6 (d, *J* = 10 Hz), 20.8, 17.2 (d, *J* = 5 Hz).

**NMR observation of 607.** Compound **603** (15.0 mg, 0.022 mmol) was charged with 0.6 mL of $Et_2O$ in a J Young NMR tube followed by the addition of *n*-BuLi (61.0 μL, 0.154 mmol). The solution turned to yellow immediately. $^{31}P$ NMR analysis indicated the formation of P(*n*-Bu)$_3$ (-31.3 ppm) and a new signal at δ -39.9 ppm. Excess degassed EtOH was added to the reaction mixture and the yellow solution changed to colorless immediately. The solution was passed through Celite and silica. The volatiles were removed under vacuum. The sample was redissloved in $C_6D_6$ for NMR analysis. $^{31}P\{^{1}H\}$ NMR ($C_6D_6$): δ -45.9. $^{1}H$ NMR ($C_6D_6$): δ 8.07 (t, *J* = 8 Hz, 1H), 7.35 (d, *J* = 8 Hz, 2H), 7.29 (br, 2H), 6.91 (d, *J* = 8 Hz, 2H), 2.18 (s, 6H), 1.70-1.66 (m, 8H), 1.46-1.32 (m, 16H), 0.80 (t, *J* = 7H, 12H).

**NMR observation of 608.** Compound **603** (15.0 mg, 0.022 mmol) was charged with 0.6 mL of $Et_2O$ in a J. Young NMR tube followed by the addition of MeLi (102 μL, 0.154 mmol). The solution turned to yellow immediately. $^{31}P$ NMR analysis indicated the formation of $PMe_3$ (-61.3 ppm) and a new signal at δ -62.6 ppm. Excess degassed EtOH was added to the reaction mixture and the yellow solution changed to colorless immediately. The solution was passed through Celite and silica. The volatiles were

removed under vacuum. The sample was redissolved in $C_6D_6$ for NMR analysis. $^{31}P\{^1H\}$ NMR ($C_6D_6$): δ -63.3. $^1H$ NMR ($C_6D_6$): δ 7.50 (t, *J* = 8 Hz, 1H), 7.23 (d, *J* = 8 Hz, 2H), 7.15 (br, 2H), 6.89 (d, *J* = 8 Hz, 2H), 2.17 (s, 6H), 1.10 (br, 12H).

**NMR observation of 609.** Compound **603** (15.0 mg, 0.022 mmol) was charged with 0.6 mL of $Et_2O$ in a J Young NMR tube followed by the addition of PhLi (84.0 μL, 0.154 mmol). The solution turned to yellow immediately. $^{31}P$ NMR analysis indicated the formation of $PPh_3$ (-4.4 ppm) and a new signal at δ -14.9 ppm. Excess degassed EtOH was added to the reaction mixture and the yellow solution changed to colorless immediately. The solution was passed through Celite and silica. The volatiles were removed under vacuum. Both $^{31}P$ and $^1H$ NMR data are consistent with the published NMR data for $^{Me}P(H)P^{Ph}$.

**Synthesis of 611.** Compound **603** (50.0 mg, 0.073 mmol) was dissolved in about 2 mL of PhF followed by the addition of $[Rh(COD)Cl]_2$ (16.5 mg, 0.066 mmol Rh). $^{31}P$ NMR analysis revealed the disappearance of the ligand and the appearance of a few new signals which we have not been able to fully characterize. $Me_2Zn$ (37.0 μL, 0.037 mmol) was added to the reaction mixture and the reaction was left at room temperature for overnight. The solution was passed through Celite and silica. The volatiles were removed under vacuum and the residue was washed with pentane and dried under vacuum to get red solid as compound **611**. The X-ray quality crystal was obtained by crystallizing from PhF/pentane at -35 $^oC$. $^{31}P\{^1H\}$ NMR ($C_6D_6$): δ 112.6 (d, *J* = 190 Hz). $^1H$ NMR ($C_6D_6$): δ 7.45 (d, *J* = 8 Hz, 2H), 6.86 (br, 2H), 6.71 (br, 8H), 6.65(d, *J* = 8 Hz, 2H), 6.57 (br, 4H), 6.20 (br, 8H), 6.15 (br, 4H), 1.89 (s, 6H), 1.31 (br, 3H).

$^{13}C\{^{1}H\}$ NMR ($C_6D_6$): δ 159.9 (t), 135.4, 131.0, 126.4 (br), 123.9, 122.9 (d, $J$ = 5 Hz), 116.8 (t, $J$ = 5 Hz), 116.7 (t, $J$ = 5 Hz), 113.2, 112.5 (d, $J$ = 5 Hz), 23.7 (t, $J_{C\text{-}P} = J_{C\text{-}Rh}$ = 15 Hz), 20.1.

**NMR observation of 612.** Compound **611** (15.0 mg, 0.019 mmol) was dissolved in 0.6 mL $C_6D_6$ in a J. Young NMR tube and charged with 1 atm of CO. The red solution became orange within minutes. $^{31}P$ NMR analysis revealed the complete disappearance of the starting material and the formation of the free phosphine $Ppryl_2Me$ (δ 80.2 ppm) as well as the new doublet resonated at δ 110.7 ppm. However, removal of the volatiles under vacuum and redissolve the residue in $C_6D_6$ converted the product back to compound **611** as indicated by both $^{1}H$ and $^{31}P$ NMR. Solution NMR characterization for **612**: $^{31}P\{^{1}H\}$ NMR ($C_6D_6$): δ 110.7 (d, $J$ = 178 Hz). $^{1}H$ NMR ($C_6D_6$): δ 7.40 (dt, $J$ = 9 Hz, $J$ = 3 Hz, 2H), 7.15 (t, $J$ = 4 Hz, 2H), 6.93 (m, 8H), 6.64 (d, $J$ = 9 Hz, 2H), 6.23 (m, 8H), 1.87 (s, 6H).

**Synthesis of 613.** Compound **611** (45.0 mg, 0.056 mmol) was dissolved in about 2 mL of PhF followed by the addition of MeOTf (20.0 μL, 0.177 mmol Rh). The reaction mixture was left at room temperature overnight. The solution was passed through Celite the next day. The volatiles were removed under vacuum and the residue was washed with pentane to get a red solid. Yield, 50.0 mg, 0.052 mmol, 92%. $^{31}P\{^{1}H\}$ NMR ($C_6D_6$): δ 109.7 (dd, $J_{Rh\text{-}P}$ = 132 Hz, $J_{P\text{-}P}$ = 37 Hz, 2P), 100.2 (dt, $J_{Rh\text{-}P}$ = 142 Hz, $J_{P\text{-}P}$ = 37 Hz, 1P) $^{1}H$ NMR ($C_6D_6$): δ 7.84 (dt, $J$ = 9 Hz, $J$ = 3 Hz, 2H), 7.33 (br, 4H), 6.84 (t, $J$ = 6 Hz, 2H), 7.77 (d, $J$ = 9 Hz, 2H), 6.56 (br, 4H), 6.30 (br, 4H), 6.12 (br, 8H), 6.06 (br,

4H), 1.85 (s, 6H), 1.28 (d, $J$ = 6 Hz, 3H), 0.59 (dt, $J_{Rh-H}$ = 2 Hz, $J_{P-H}$ = 6 Hz, 3H). $^{19}F$ NMR ($C_6D_6$): δ -78.1.

**Synthesis of 614.** Compound **604** (80.0 mg, 0.12 mmol) was dissolved in about 2 mL of THF followed by the addition of $[Rh(COD)Cl]_2$ (29.0 mg, 0.12 mmol Rh). The yellow solution changed to orange immediately. After 30 min, the volatiles were removed under vacuum. The residue was extracted with toluene and passed through Celite. The volatiles from the filtrate were removed under vacuum again to get a yellow-orange residue. The residue was washed with pentane three times to get a yellow powder. Yield, 73 mg, 0.10 mmol, 83%. $^1H$ NMR ($C_6D_6$): δ 7.49 (br, 2H, (PNP)Aryl-*H*), 7.20 (dt, $J$ = 8 Hz, $J$ = 2 Hz, 2H, (PNP)Aryl-*H*), 6.93 (s, 4H, pryl-*H*), 6.88 (s, 4H, pryl-*H*), 6.65 (dd, $J$ = 8 Hz, $J$ = 2 Hz, 2H, (PNP)Aryl-*H*), 6.41 (s, 4H, pryl-*H*), 6.15 (s, 4H, pryl-*H*), 4.13 (br. 2H, COD-*H*), 3.77 (br, 2H, COD-*H*), 2.02 (m, 2H, COD-*H*), 1.96 (s, 6H, Ar-C*H*$_3$), 1.60 (m, 2H, COD-*H*), 1.41 (m, 2H, COD-*H*), 1.24 (m, 2H, COD-*H*). $^{31}P\{^1H\}$ NMR ($C_6D_6$): δ 117.4 (d, $J$ = 169 Hz).

**Synthesis of 615.** Compound **614** (54.0 mg, 0.074 mmol) was treated with MeI (18 μL, 0.29 mmol) in about 0.6 mL of $C_6D_6$. The reaction mixture was heated at 50 $^oC$ for 22 h. $^{31}P$ NMR analysis indicated the disappearance of the starting material and the formation of compound **615a**. Solution NMR data for **615a** $^1H$ NMR ($C_6D_6$): δ 7.60 (d, $J$ = 9 Hz, 2H, (PNP)Aryl-*H*), 7.58 (s, 4H, pryl-*H*), 7.35 (br, 2H, (PNP)Aryl-*H*), 7.23 (s, 4H, pryl-*H*), 6.66 (d, $J$ = 9 Hz, 2H, (PNP)Aryl-*H*), 6.23 (s, 6H, pryl-*H*), 1.89 (s, 6H, Ar-C*H*$_3$), 1.69 (t, $J$ = 7 Hz, 3H, Rh-C*H*$_3$), 1.39 (s, 3H, C*H*$_3$I, overlapping with free $CH_3I$). $^{31}P\{^1H\}$ NMR: δ 101.6 (d, $J$ =139 Hz). The excess $CH_3I$ and other volatiles were

removed under vacuum and the residue was washed with pentane to get the red powder of **615b**. Yield, 34.0 mg, 0.045 mmol, 61%. $^{1}$H NMR ($C_6D_6$): δ 7.61 (br, 6H, (PNP)Aryl-*H* + pryl-*H*), 7.24 (br, 2H, (PNP)Aryl-*H*), 6.95 (br, 4H, pryl-*H*), 6.71 (d, *J* = 8 Hz, 2H, (PNP)Aryl-*H*), 6.22 (s, 4H, pryl-*H*), 6.13 (br, 4H, pryl-*H*), 1.89 (s, 6H, Ar-C*H*$_3$), 1.41 (t, *J* = 7 Hz, 3H, Rh-C*H*$_3$). $^{31}$P{$^{1}$H} NMR: δ 105.4 (d, *J* =145 Hz).

**Synthesis of 616.** Compound **615b** (444 mg, 0.58 mmol) was treated with AgOAc (97.0 mg, 0.58 mmol) in 5 mL of toluene and stirred at room temperature for overnight. The reaction mixture was passed through Celite. The volatiles were removed under vacuum. The residue was recrystallized from toluene/pentane at -35 $^{o}$C to get red crystals. Yield, 283 mg, 0.41 mmol, 70.2%. $^{1}$H NMR ($C_6D_6$): δ 7.61 (dt, *J* = 9 Hz, *J* = 4 Hz, 2H, (PNP)Aryl-*H*), 7.30 (br, 4H, pryl-*H*), 7.22 (t, *J* = 4 Hz, 2H, (PNP)Aryl-*H*), 6.94 (br, 4H, pryl-*H*), 6.65 (dd, *J* = 8 Hz, *J* = 2 Hz, 2H, (PNP)Aryl-*H*), 6.28 (br, 8H, pryl-*H*), 1.86 (s, 6H, Ar-C*H*$_3$), 1.53 (s, 3H, C*H*$_3$CO$_2$), 1.05 (td, *J* = 6 Hz, *J* = 2 Hz, 3H, Rh-*Me*) $^{31}$P{$^{1}$H} NMR ($C_6D_6$): δ 103.7 (d, *J* = 142 Hz).

**Synthesis of 617.** Compound **616** (24.0 mg, 0.034 mmol) was dissolved in about 0.6 mL of $C_6D_6$ in a J. Young NMR tube. $Et_3SiH$ (11.2 μL, 0.068 mmol) was added to the solution. The solution was left at room temperature for 5 h. The volatiles were removed under vacuum and the residue was washed with cold pentane twice. $^{1}$H NMR ($C_6D_6$): δ 7.55 (dt, *J* = 8 Hz, *J* = 2 Hz, 2H, (PNP)Aryl-*H*), 7.09 (br, 10H, (PNP)Aryl-*H* + pryl-*H*), 6.89 (dd, *J* = 8 Hz, *J* = 2 H, (PNP)Aryl-*H*), 6.26 (s, 8H, pryl-*H*), 1.90 (s, 6H, Ar-C*H*$_3$), 0.99 (t, *J* = 8 Hz, 9H, C*H*$_3$CH$_2$), 0.44 (q, *J* = 8 Hz, 6H, CH$_3$C*H*$_2$), -13.2 (dt, *J* = 25 Hz, *J* = 13 Hz, 1H, Si-*H*). Hydride region for $^{1}$H{$^{31}$P}NMR ($C_6D_6$): δ -13.2 (d, $J_{Rh-H}$ = 25 Hz,

$J_{Si-H}$ = 35 Hz). $^{13}C\{^1H\}$NMR ($C_6D_6$): δ 160.5 (t, *J* = 16 Hz), 135.6, 131.6, 127.1 (t, *J* = 4 Hz), 124.7 (t, *J* = 4 Hz), 124.4 (t, *J* = 26 Hz), 116.6 (t, *J* = 7 Hz), 113.5 (t, *J* = 3 Hz). 20.0, 10.7 (br), 10.1. $^{31}P\{^1H\}$NMR ($C_6D_6$): δ 111.8 (d, *J* = 184 Hz).

**Synthesis of 618.** Compound **616** (100 mg, 0.143 mmol) was dissolved in about 5 mL of toluene followed by the addition of $Et_3SiH$ (70.0 μL, 0.430 mmol) and $^iPr_2S$ (145 μL, 1.00 mmol). The reaction mixture was left at room temperature overnight. The reaction mixture was passed through Celite and silica the next day. The volatiles were removed under vacuum. The residue was recrystallized from PhF/pentane at -35 $^oC$ to get the red powder. Yield, 85.0 mg, 0.115 mmol, 80.1%. $^1H$ NMR ($C_6D_6$): δ 7.44 (dt, *J* = 8 Hz, *J* = 2 Hz, 2H, (PNP)Aryl-*H*), 7.24 (br, 10H, (PNP)Aryl-*H* + pryl-*H*), 6.63 (dd, *J* = 8 Hz, *J* = 2 H, (PNP)Aryl-*H*), 6.30 (br, 8H, pryl-*H*), 2.04 (sep. 2H, C*H*$(CH_3)_2$), 1.98 (s, 6H, Ar-C$H_3$), 0.92 (d, *J* = 6 Hz, 12H, CH(C$H_3$)$_2$). $^{31}P\{^1H\}$ NMR ($C_6D_6$): δ 106.5 (d, *J* = 198 Hz).

**Solution characterization of 619.** Compound **618** (15.0 mg, 0.020 mmol) and PhBr (5.0 μL, 0.047 mmol) were dissolved in about 0.6 mL of $CH_3CN$ in a J. Young tube and heated at 90 $^oC$ for 2 days. The $^{31}P$ NMR analysis revealed the disappearance of the starting material and the formation of a new product. Some red precipitate forms when the solution was cooled to room temperature. The liquid was decanted and the solid was washed with pentane three times to get the pure sample of **619**. $^1H$ NMR ($C_6D_6$): δ 7.85 (d, *J* = 8 Hz, 2H, (PNP)Aryl-*H*), 7.70 (s, 4H, pryl-*H*), 7.30 (br, 2H, (PNP)Aryl-*H*), 6.74 (d, *J* = 8 Hz, 2H, (PNP)Aryl-*H*), 6.71 (t, *J* = 9 Hz, 1H, phenyl-*H*), 6.60 (br, 2H, phenyl-*H*), 6.53 (s, 4H, pyrl-*H*), 6.25 (s, 4H, pryl-*H*), 6.03 (s, 4H, pryl-*H*), 1.85 (s, 6H, Ar-C$H_3$),

0.21 (br, 3H , NCC*H*$_3$) (2 H from the phenyl group is missing from proton NMR spectrum at room temperature.). $^{31}P\{^1H\}$NMR ($C_6D_6$): 98.1 (d, *J* = 135 Hz).

**Synthesis of 620.** Compound **614** (138 mg, 0.186 mmol) and PhI (42.0 μL, 0.372 mmol) were dissolved in about 4 mL of $CH_3CN$. The mixture was heated at 70 $^oC$ for 2 h. Red crystals crashed out from the solution. These crystals were collected on a frit and dried under vacuum. Yield, 116 mg, 0.268 mmol, 72%. $^1H$ NMR ($C_6D_6$): δ 7.85 (d, *J* = 8 Hz, 2H, (PNP)Aryl-*H*), 7.59 (s, 4H, pryl-*H*), 7.28 (br, 2H, (PNP)Aryl-*H*), 6.74 (d, *J* = 8 Hz, 2H, (PNP)Aryl-*H*), 6.69 (t, *J* = 9 Hz, 1H, phenyl-*H*), 6.67 (s, 4H, pyrl-*H*), 6.56 (t, *J* = 9 Hz, 2H, phenyl-*H*), 6.24 (s, 4H, pryl-*H*), 6.05 (s, 4H, pryl-*H*), 1.85 (s, 6H, Ar-C*H*$_3$), 0.29 (s, 3H , NCC*H*$_3$). $^{31}P\{^1H\}$NMR ($C_6D_6$): 100.3 (d, *J* = 137 Hz). $^1H$ NMR ($CD_2Cl_2$): 7.84 (dt, *J* = 8 Hz, *J* = 2 Hz, 2H, (PNP)Aryl-*H*), 7.25 (s, 4H, pryl-*H*), 7.19 (t, *J* = 2 Hz, 2H, (PNP)Aryl-*H*), 7.10 (dd, *J* = 8 Hz, *J*= 2 Hz, 2H, (PNP)Aryl-*H*), 6.53 (t, *J* = 9 Hz, 1H, phenyl-*H*), 6.35 (s, 4H, pyrl-*H*), 6.33 (s, 4H, pyrl-*H*), 6.27 (t, *J* = 9 Hz, 2H, phenyl-*H*), 6.01 (s, 4H, pyrl-*H*), 2.23 (s, 6H, Ar-C*H*$_3$), 1.66 (s, 3H, NCC*H*$_3$). (2 H from the phenyl group is missing from proton NMR spectrum at room temperature.) $^{13}C\{^1H\}$($CD_2Cl_2$): 159.8 (t, *J* = 15 Hz), 140.0 (dt, *J* = 27 Hz, *J* = 10 Hz), 135.2, 133.3, 128.1 (t, J = 4 Hz), 126.9, 125.7, 124.9, 122.9, 120.0 (t, *J* = 28 Hz),119.0 (t, *J* = 9 Hz), 112.3 (t, *J* = 3 Hz), 112.2 (t, *J* = 3 Hz), 20.3, 2.8. (one C signal from the phenyl group is missing by $^{13}C\{^1H\}$ NMR at room temperature)

**Solution characterization of 621.** Compound **618** (15.0 mg, 0.020 mmol) and PhI (5.0 μL, 0.045 mmol) were dissolved in about 0.6 mL of $C_6D_6$ in the presence of excess NC$^t$Bu in a J. Young tube and heated at 70 $^oC$ for 2 h. $^{31}P$ NMR and $^1H$ NMR analysis

revealed the disappearance of the starting material and the formation of a new product corresponding to compound **621-Ph**. $^{1}$H NMR ($C_6D_6$): δ 8.25 (br, 1H, phenyl-*H*), 7.75 (d, *J* = 8 Hz, 2H, (PNP)Aryl-*H*), 7.67 (s, 4H, pryl-*H*), 7.17 (br, 2H, (PNP)Aryl-*H*), 6.91 (br, 1H, phenyl-*H*), 6.73 (d, *J* = 8 Hz, 2H, (PNP)Aryl-*H*), 6.66 (t, *J* = 9 Hz, 1H, phenyl-*H*), 6.53 (s, 4H, pyrl-*H*), 6.49 (br, 2H, phenyl-*H*), 6.30 (s, 4H, pryl-*H*), 6.00 (s, 4H, pryl-*H*), 1.84 (s, 6H, Ar-C*H*$_3$), 0.44 (br, 9H , NC(C*H*$_3$)$_3$). $^{31}$P{$^{1}$H}NMR ($C_6D_6$): 100.9 (d, *J* = 137 Hz).

**Synthesis of 622.** Compound **620** (84.0 mg, 0.097 mmol) and AgOAc (18 mg, 0.108 mmol) were dissolved in about 3 mL toluene. The reaction mixture was stirred at room temperature for overnight. The reaction mixture was passed through Celite. The volatiles were removed under vacuum. The residue was recrystallized from toluene/pentane at -35 $^{o}$C to get a red powder. Yield, 55.0 mg, 0.072 mmol, 75%. $^{1}$H NMR ($C_6D_6$): δ.7.58 (dt, *J* = 8 Hz, *J* = 2 Hz, 2H, (PNP)Aryl-*H*), 7.23 (d, *J* = 8 Hz, 1H, phenyl-*H*), 7.10-7.13 (br, 6H, (PNP)Aryl-*H* + pryl-*H*), 6.72 (m, 2H, phenyl-*H*), 6.60 (dd, *J* = 8 Hz, *J* = 2 Hz, 2H, (PNP)Aryl-*H*), 6.57 (br, 1H, phenyl-*H*), 6.52 (s, 4H, pryl-*H*), 6.49 (t, *J* = 8 Hz, 1H, phenyl-*H*), 6.26 (s, 4H, pryl-*H*), 6.03 (s, 4H, pryl-*H*), 1.82 (s, 6H, Ar-C*H*$_3$), 1.66 (s, 3H, C*H*$_3$CO$_2$). $^{13}$C{$^{1}$H} NMR ($C_6D_6$): δ 187.4, 160.3 (t, *J* = 14 Hz), 140.5 (dt, *J* = 30 Hz, *J* = 10 Hz), 134.9, 134,5, 131.5, 130.9, 129.3, 127.2, 125.6, 124.5 (t, *J* = 3 Hz), 124.4 (t, *J* = 4 Hz), 123.7, 120.5 (t, *J* = 28 Hz), 119.3 (t, *J* = 6 Hz), 113.4 (t, *J* = 3 Hz), 112.9 (t, *J* = 3 Hz), 22.3, 20.0. $^{31}$P{$^{1}$H} NMR ($C_6D_6$): δ. 100.7 (d, *J* = 142 Hz).

**Synthesis of 623.** Compound **622** (70.0 mg, 0.092 mmol) was dissolved in about 1 mL of toluene followed by the addition $Me_3SiOTf$ (50.0 μL, 0.276 mmol). NMR analysis indicated that there was no reaction. However, the color changed to purple immediately by adding excess $CH_3CN$ to the solution. The volatiles were removed under vacuum immediately. The residue was recrystallized from toluene/pentane at -35 $^oC$ to get a red-purple powder. Yield, 68.0 mg, 0.073 mmol, 80 %. $^1H$ NMR ($C_6D_6$): δ 7.61 (s, 4H, pryl-*H*), 7.54 (br, 3H, (PNP)Aryl-*H*+ phenyl-*H*), 7.07 (br, 2H, (PNP)Aryl-*H*), 6.79 (t, *J* = 7 Hz, 1H, phenyl-*H*), 6.71 (t, J = 7 Hz, 1H, phenyl-*H*), 6.65 (br, 1H, phenyl-*H*), 6.61 (d, *J* = 8 Hz, 2H, (PNP)Aryl-*H*), 6.49 (t, *J* = 7 Hz, phenyl-*H*), 6.39 (s, 4H, pryl-*H*), 6.33 (s, 4H, pryl-*H*), 5.99 (s, 4H, pryl-*H*), 1.78 (s, 6H, Ar-C*H*$_3$), 0.65 (s, 9H, C(C*H*$_3$)$_3$). $^{13}C\{^1H\}$ NMR ($C_6D_6$): δ 158.9 (t, J = 15 Hz), 140.3 (dt, J = 28 Hz, J = 8 Hz), 134.6, 134.5, 133.7, 132.0, 130.1, 128.3, 127.5, 125.5 (t, J = 3 Hz), 124.4 (t, J = 2 Hz), 124.2, 122.6 (t, J = 30 Hz), 119.5 (q, J = 319 Hz), 119.1 (t, J = 7 Hz), 113.4 (t, J = 2 Hz), 113.1 (t, J = 3 Hz), 29.1, 26.7, 19.9. $^{31}P\{^1H\}$ NMR ($C_6D_6$): δ. 98.0 (d, *J* = 137 Hz). $^{19}F$ NMR ($C_6D_6$): δ -78.3.

**Solution characterization of 624.** Compound **622** (9.0 mg, 0.012 mmol) and $Ph_2Zn$ (4.6 mg, 0.024 mmol) were mixed in about 0.6 mL of $CD_2Cl_2$ in a J. Young NMR tube. The color changed to green within minutes. After 10 min, $^{31}P$ NMR analysis revealed the disappearance of the starting material and the formation of two new products at δ 100.6 (d, *J* = 107 Hz) (18%) and 112.4 (d, *J* = 173 Hz) (82%). After 1 h, only the product resonated at δ 112.4 (d, *J* = 173 Hz) was observed by $^{31}P$ NMR. The formation of biphenyl was confirmed by $^1H$ NMR. The volatiles were removed under vacuum and

the green powder was washed with pentane three times. $^{1}$H NMR ($CD_2Cl_2$): δ 7.50 (dt, *J* = 8 Hz, *J* = 3 Hz), 7.08-6.98 (m, 8H), 6.94 (br, 10H), 6.86 (t, *J* = 9 Hz, 2H), 6.75 (d, *J* = 9 Hz, 2H), 6.39 (br, 8 H), 2.17 (s, 6H). $^{31}$P{$^{1}$H}NMR ($CD_2Cl_2$): δ 112.4 (d, *J* = 173 Hz).

**Reaction of 623 with NaOPh in the presence of PhI in $C_6D_6$.** Compound **623** (10.0 mg, 0.011 mmol) and NaOPh (5.0 mg, 0.043 mol) were stirred in about 1 mL PhF for 4 h. $^{31}$P NMR analysis indicated the disappearance of **623** and the formation of two new products. The reaction mixture was passed through Celite and the volatiles were removed under vacuum. The residue was redissolved in about 0.6 mL $C_6D_6$ and 3.0 μL of PhI was adding to the $C_6D_6$ solution. The solution was transferred to a J. Young NMR tube and heated at 70 $^{o}$C for 17 h. Only compound **621-Ph** was observed as the rhodium complex as shown by $^{31}$P NMR spectrum. Ph-OH was observed by $^{1}$H NMR spectroscopy. The GC/MS analysis indicated the presence of a compound with the molecular weight of 158.9, which is corresponding to the MW of $C_6D_5$-$C_6H_5$.

**Reaction of 623 with NaOPh in the presence of 4-F-$C_6H_4$I in $C_6H_6$.** Compound **623** (10.0 mg, 0.011 mmol) and NaOPh (5.0 mg, 0.043 mol) were stirred in about 1 mL PhF for 4 h. $^{31}$P NMR analysis indicated the disappearance of **623** and the formation of two new products. The reaction mixture was passed through Celite and the volatiles were removed under vacuum. The residue was redissolved in about 0.6 mL $C_6H_6$ and 3.0 μL of 4-F-$C_6H_4$I was adding to the $C_6H_6$ solution. The solution was transferred to a J. Young NMR tube and heated at 70 $^{o}$C for 17 h. Compound **621-Ph** and **621-$^{F}$Ph** were observed as the rhodium complexes as shown by $^{31}$P NMR spectrum. Ph-OH was observed by $^{1}$H NMR spectroscopy. GC/MS indicated compound *para*-F-$C_6H_4C_6H_5$ as

the major organic product. Compounds $(FC_6H_4)_2$ and $(C_6H_5)_2$ were also detected by GC/MS.

**X-Ray data collection, solution, and refinement for 611.** A red crystal of suitable size and quality (0.40 x 0.04 x 0.03 mm) was selected from a representative sample of crystals of the same habit using an optical microscope, mounted onto a nylon loop and placed in a cold stream of nitrogen (110 K). Low-temperature X-ray data were obtained on a Bruker APEXII CCD based diffractometer (Mo sealed X-ray tube, $K_\alpha$ = 0.71073 Å). All diffractometer manipulations, including data collection, integration and scaling were carried out using the Bruker APEXII software.[105] An absorption correction was applied using SADABS.[165] The space group was determined on the basis of systematic absences and intensity statistics and the structure was solved by direct methods and refined by full-matrix least squares on $F^2$. The structure was solved in the triclinic space group $P\bar{1}$ using XS[166](incorporated in SHELXTL). No missed symmetry was reported by the ADDSYM program within PLATON.[108] All non-hydrogen atoms were refined with anisotropic thermal parameters. Hydrogen atoms were located and fixed in idealized positions then refined using riding model. The structure was refined (weighted least squares refinement on $F^2$) to convergence. Three of the pyrrolyl groups were disordered and modeled accordingly.

**X-Ray data collection, solution, and refinement for 623.** A red crystal of suitable size and quality (0.14 x 0.09 x 0.05 mm) was selected from a representative sample of crystals of the same habit using an optical microscope, mounted onto a nylon loop and placed in a cold stream of nitrogen (110 K). Low-temperature X-ray data were obtained

on a Bruker APEXII CCD based diffractometer (Mo sealed X-ray tube, $K_\alpha$ = 0.71073 Å). All diffractometer manipulations, including data collection, integration and scaling were carried out using the Bruker APEXII software.[105] An absorption correction was applied using SADABS.[165] The space group was determined on the basis of systematic absences and intensity statistics and the structure was solved by direct methods and refined by full-matrix least squares on $F^2$. The structure was solved in the triclinic space group $P2_1/c$ using XS[166](incorporated in SHELXTL). No missed symmetry was reported by the ADDSYM program within PLATON.[108] All non-hydrogen atoms were refined with anisotropic thermal parameters. Hydrogen atoms were located and fixed in idealized positions then refined using riding model. The structure was refined (weighted least squares refinement on $F^2$) and the final least-squares refinement converged to $R_1$ = 0.0699 ($I > 2\sigma(I)$, 5164 data) and w$R_2$ = 0.1933 ($F^2$, 9277 data, 528 parameters).

# CHAPTER VII

# SUMMARY

In summary, this thesis presented the strong bond activation mediated by PNP pincer ligated group 9/10 transition metals (Pd, Rh, Ir).

In Chapter II, $[(PNP)Pd]^+$ fragment was found to be capable of net heterolytic cleavage of the B-H bond in catecholborane and the B-B bond in catecholdiboron. Cationic palladium hydrides and palladium boryl complexes were isolated and physically characterized. The activation of the B-H bond by $[(PNP)Pd]^+$ resulted in the formation of Pd-H and N-B bonds. The addition of a B-B bond across a Pd-N bond to form a palladium boryl complex is unique. It provides another route to palladium boryl complexes and to the cleavage of the B-B bond where oxidative addition of a B-B bond to the palladium center is difficult. Both the N-B and Pd-B bonds are subject to hydrolysis, forming the corresponding N-H and Pd-H bonds. Deprotonation of the partly hydrolyzed product **204-BAr$^{F}_{4}$** by $Et_3N$ gave the neutral palladium boryl complex (PNP)PdBCat.

Chapter III described the C-H activation at (PNP)Ir center. We have demonstrated that the thermodynamic preference for aryl or benzylic C-H oxidative addition may in certain cases depend on the coordination number of the metal center. A higher coordination number favors a less sterically demanding benzylic product instead of the preference for the mesityl isomer for the lower coordination number. We have also presented the C-H activation of cyclic ethers by (PNP)Ir and found that the results were

very substrate dependent. These findings highlight the challenge of catalytic functionalization of C-H bonds with ethers by using (PNP)Ir.

Chapter IV discussed the reaction of the (PNP)Rh fragment with Ph-$O_2$CR substrates with an eye towards Aryl-O bond activation  It appears that a bulky and/or more electron-donating R group helps block the undesirable $C_{acyl}$-O OA and channel the reaction towards $C_{aryl}$-O OA.  Our findings also highlight C-H OA as another potential side reaction and illustrate that pivalate and carbamate may be particularly suitable for pursuing $C_{aryl}$-O OA reactions regardless of the metal involved.

Chapter V presented the synthesis of a PNP pincer supported Rh(I) difluorocarbene complex (PNP)Rh(=$CF_2$) through the reaction of (PNP)Rh(TBE) with $Me_3SiCF_3$ in the presence of CsF.  Reaction of the rhodium difluorocarbene complex with the silylium resulted in a new compound, which we tentatively assigned as the cationic terminal fluorocarbyne species $[(PNP)Rh(\equiv CF)]^+(B(C_6F_5)_4)^-$.

A new π-accepting PNP ligand bearing pyrrolyl substituents was synthezied in Chapter VI.  Other PNP ligands with different substituents on the phosphorous atoms have also been synthesized by reacting $^{Me}PNP^{pryl}$ with organolithium reagents.  This study develops a completely new method to synthesize PNP ligands with different electronic and steric properties.  Several Rh(I) complexes with the $^{Me}PN(P)P^{pryl}$ ligand via N-P cleavage, direct transmetalation, or ligand substitution have been obtained.  Six-coordinate Rh(III) has been generated through oxidative addition of arylhalide to rhodium.  Fast C-C RE was observed in the new system.  However, attempts at the more challenging C-O RE were unsuccessful.

# REFERENCES

(1) (a) Choi, J.; MacArthur, A. H. R.; Brookhart, M.; Goldman, A. S. *Chem. Rev.* **2011**, *111*, 1761. (b) Fan, L.; Parkin, S.; Ozerov, O. V. *J. Am. Chem. Soc.* **2005**, *127*, 16772. (c) Ben-Ari, E.; Gandelman, M.; Rozenberg, H.; Shimon, L. J. W.; Milstein, D. *J. Am. Chem. Soc.* **2003**, *125*, 4714.

(2) (a) Gandelman, M.; Milstein, D. *Chem. Commun.* **2000**, 1603. (b) Ozerov, O. V.; Guo, C.; Papkov, V. A.; Foxman, B. M. *J. Am. Chem. Soc.* **2004**, *126*, 4792.

(3) (a) Choi, J.; Choliy, Y.; Zhang, X.; Emge, T. J.; Krogh-Jespersen, K.; Goldman, A. S. *J. Am. Chem. Soc.* **2009**, *131*, 15627. (b) van der Boom, M. E.; Liou, S. Y.; Ben-David, Y.; Shimon, L. J. W.; Milstein, D. *J. Am. Chem. Soc.* **1998**, *120*, 6531.

(4) (a) Morgan, E.; MacLean, D. F.; McDonald, R.; Turculet, L. *J. Am. Chem. Soc.* **2009**, *131*, 14234. (b) Zhao, J.; Goldman, A. S.; Hartwig, J. F. *Science* **2005**, *307*, 1080. (c) Kanzelberger, M.; Zhang, X.; Emge, T. J.; Goldman, A. S.; Zhao, J.; Incarvito, C.; Hartwig, J. F. *J. Am. Chem. Soc.* **2003**, *125*, 13644.

(5) (a) Tanaka, R.; Yamashita, M.; Nozaki, K. *J. Am. Chem. Soc.* **2009**, *131*, 14168. (b) Lee, D. W.; Jensen, C. M.; Morales-Morales, D. *Organometallics* **2003**, *22*, 4744.

(6) Young, K. J. H.; Oxgaard, J.; Ess, D. H.; Meier, S. K.; Stewart, T.; Goddard, W. A.; Periana, R. A. *Chem. Commun.* **2009**, 3270.

(7) Gnanaprakasam, B.; Ben-David, Y.; Milstein, D. *Adv. Synth. Catal.* **2010**, *352*, 3169.

(8) (a) Moulton, C. J.; Shaw, B. L. *J. Chem. Soc., Dalton Trans.* **1976**, 1020. (b) van Koten, G. *Pure Appl. Chem.* **1989**, *61*, 1681.

(9) Fryzuk, M. D.; MacNeil, P. A. *J. Am. Chem. Soc.* **1981**, *103*, 3592.

(10) Peters, J. C.; Harkins, S. B.; Brown, S. D.; Day, M. W. *Inorg. Chem.* **2001**, *40*, 5083.

(11) (a) Liang, L. C.; Lin, J. M.; Hung, C. H. *Organometallics* **2003**, *22*, 3007. (b) Fan, L.; Foxman, B. M.; Ozerov, O. V. *Organometallics* **2004**, *23*, 326.

(12) Segawa, Y.; Yamashita, M.; Nozaki, K. *J. Am. Chem. Soc.* **2009**, *131*, 9201.

(13) Mitton, S. J.; McDonald, R.; Turculet, L. *Organometallics* **2009**, *28*, 5122.

(14) Langer, R.; Leitus, G.; Ben-David, Y.; Milstein, D. *Angew. Chem. Int. Ed.* **2011**,

*50*, 2120.

(15) Weng, W.; Chen, C. H.; Foxman, B. M.; Ozerov, O. V. *Organometallics* **2007**, *26*, 3315.

(16) Weng, W.; Yang, L.; Foxman, B. M.; Ozerov, O. V. *Organometallics* **2004**, *23*, 4700.

(17) DeMott, J. C.; Basuli, F.; Kilgore, U. J.; Foxman, B. M.; Huffman, J. C.; Ozerov, O. V.; Mindiola, D. J. *Inorg. Chem.* **2007**, *46*, 6271.

(18) Pape, A.; Lutz, M.; Müller, G. *Angew. Chem. Int. Ed*. **1994**, *33*, 2281.

(19 (a) van der Boom, M. E.; Ben-David, Y.; Milstein, D. *Chem. Commun.* **1998**, 917. (b) van der Boom, M. E.; Liou, S. Y.; Ben-David, Y.; Gozin, M.; Milstein, D. *J. Am. Chem. Soc.* **1998**, *120*, 13415.

(20) Puri, M.; Gatard, S.; Smith, D. A.; Ozerov, O. V. *Organometallics* **2011**, *30*, 2472.

(21) van der Boom, M. E.; Ben-David, Y.; Milstein, D. *J. Am. Chem. Soc.* **1999**, *121*, 6652.

(22) Albrecht, M.; Dani, P.; Lutz, M.; Spek, A. L.; van Koten, G. *J. Am. Chem. Soc.* **2000**, *122*, 11822.

(23) This section is written by reference to Jean, Y. *Molecular Orbitals of Transition Metal Complexes*; Oxford University Press, 2005.

(24) Albano, V.; Bellon, P. L.; Scatturin, V. *Chem. Commun.* **1966**, 507.

(25) Hay-Motherwell, R.S.; Wilkinson, G.; Hussain-Bates, B.; Hursthouse, M. B. *J. Chem. Soc., Dalton Trans*. **1992**, 3477.

(26) Mindiola, D. J.; Hillhouse, G. L. *J. Am. Chem. Soc*. **2001**, *123*, 4623.

(27) Hedberg, L.; Iijima, T.; Hedberg, K. *J. Chem. Phys.* **1979**, *70*, 3224.

(28) Mutz, M.; Latscha, H. *Z. Naturforsch. B* **1998**, *53*, 694.

(29) (a) Grushin, V. V.; Alper, H. *Chem. Rev*. **1994**, *94*, 1047. (b) Gatard, S.; Çelenligil-Çetin, R.; Guo, C.; Foxman, B. M.; Ozerov, O. V. *J. Am. Chem. Soc.* **2006**, *128*, 2808.

(30) Liang, L. C.; Lin, J. M.; Lee, W. Y. *Chem. Commun.* **2005**, 2462.

(31) (a) Harkins, S. B.; Peters, J. C. *Organometallics* **2002**, *21*, 1753. (b) Harkins, S. B.; Peters, J. C. *Inorg. Chem.* **2006**, *45*, 4316.

(32) (a) van der Boom, M. E.; Kraatz, H. B.; Hassner, L.; Ben-David, Y.; Milstein, D. *Organometallics* **1999**, *18*, 3873. (b) van der Boom, M. E.; Liou, S. Y.; Shimon, L. J. W.; Ben-David, Y.; Milstein, D. *Organometallics* **1996**, *15*, 2562.

(33) Kanzelberger, M.; Singh, B.; Czerw, M.; Krogh-Jespersen, K.; Goldman, A. S. *J. Am. Chem. Soc.* **2000**, *122*, 11017.

(34) MacLean, D. F.; McDonald, R.; Ferguson, M. J.; Caddell, A. J.; Turculet, L. *Chem. Commun.* **2008**, 5146.

(35) (a) Barrios-Landeros, F.; Carrow, B. P.; Hartwig, J. F. *J. Am. Chem. Soc*. **2009**, *131*, 8141. (b) Senn, H. M.; Ziegler, T. *Organometallics* **2004**, *23*, 2980.

(36) Cariou, R.; Graham, T. W.; Dahcheh, F.; Stephan, D. W. *Dalton Trans.* **2011**, *40*, 5419.

(37) Wang, X.; Lane, B. S.; Sames, D. *J. Am. Chem. Soc.* **2005**, *127*, 4996.

(38) (a) van der Boom, M. E.; Liou, S. Y.; Shimon, L. J. W.; Ben-David, Y.; Milstein, D. *Inorg. Chim. Acta* **2004**, *357*, 4015. (b) van der Boom, M. E.; Liou, S. Y.; Shimon, L. J. W.; Ben-David, Y.; Vigalok, A.; Milstein, D. *Angew. Chem. Int. Ed*. **1997**, *36*, 625.

(39) Ittel, S. D.; Tolman, C. A.; English, A. D.; Jesson, J. P. *J. Am. Chem. Soc.* **1978**, *100*, 7577. (b) Tolman, C. A.; Ittel, S. D.; English, A. D.; Jesson, J. P. *J. Am. Chem. Soc.* **1979**, *101*, 1742.

(40) (a) Rosen, B. M.; Quasdorf, K. W.; Wilson, D. A.; Zhang, N.; Resmerita, A. M.; Garg, N. K.; Percec, V. *Chem. Rev.* **2011**, *111*, 1346. (b) Sergeev, A. G.; Hartwig, J. F. *Science* **2011**, *332*, 439. (c) Tobisu, M.; Yamakawa, K.; Shimasaki, T.; Chatani, N. *Chem. Commun*. **2011**, *47*, 2946. (d) Alvarez-Bercedo, P.; Martin, R. *J. Am. Chem. Soc*. **2010**, *132*, 17352. (e) Wenkert, E.; Michelotti, E. L.; Swindell, C. S.; Tingoli, M. *J. Org. Chem.* **1984**, *49*, 4894. (f) Wenkert, E.; Michelotti, E. L.; Swindell, C. S. *J. Am. Chem. Soc.* **1979**, *101*, 2246.

(41) (a) Takaya, J.; Kirai, N.; Iwasawa, N. *J. Am. Chem. Soc.* **2011**, *133*, 12980. (b) Caballero, A.; Sabo-Etienne, S. *Organometallics* **2007**, *26*, 1191. (c) Hartwig, J. F.; Cook, K. S.; Hapke, M.; Incarvito, C. D.; Fan, Y.; Webster, C. E.; Hall, M. B. *J. Am. Chem. Soc.* **2005**, *127*, 2538. (d) Hartwig, J. F. *Chem. Soc. Rev.* **2011**, *40*, 1992. (e) Sloan, M. E.; Clark, T. J.; Manners, I. *Inorg. Chem.* **2009**, *48*, 2429.

(42) Hartwig J. F. *Organotransition Metal Chemistry: From Bonding to Catalysis*;

University Science Books: Sausalito, CA, 2009, p. 188.

(43) Nguyen, P.; Lesley, G.; Taylor, N. J.; Marder, T. B.; Pickett, N. L.; Clegg, W.; Elsegood, M. R. J.; Norman, N. C. *Inorg. Chem.* **1994**, *33*, 4623.

(44) Ishiyama, T.; Matsuda, N.; Miyaura, N.; Suzuki, A. *J. Am. Chem. Soc.* **1993**, *115*, 11018.

(45) (a) Cui, Q.; Musaev, D. G.; Morokuma, K. *Organometallics* **1998**, *17*, 742. (b) Sakaki, S.; Kikuno, T. *Inorg. Chem.* **1997**, *36*, 226.

(46) (a) Onozawa, S.; Tanaka, M. *Organometallics* **2001**, *20*, 2956. (b) Onozawa, S.; Hatanaka, Y.; Sakakura, T.; Shimada, S.; Tanaka, M. *Organometallics* **1996**, *15*, 5450. (c) Braunschweig, H.; Gruss, K.; Radacki, K.; Uttinger, K. *Eur. J. Inorg. Chem.* **2008**, 1462.

(47) (a) Ahuja, R.; Punji, B.; Findlater, M.; Supplee, C.; Schinski, W.; Brookhart, M.; Goldman, A. S. *Nature Chem.* **2011**, *3*, 167. (b) Punji, B.; Emge, T. J.; Goldman, A. S. *Organometallics* **2010**, *29*, 2702. (c) Renkema, K. B.; Kissin, Y. V.; Goldman, A. S. *J. Am. Chem. Soc.* **2003**, *125*, 7770.

(48) Timpa, S. D.; Fafard, C. M.; Herbert, D. E.; Ozerov, O. V. *Dalton Trans.* **2011**, 5426.

(49) Selander, N.; Willy, B.; Szabó, K. *Angew. Chem. Int. Ed*. **2010**, *49*, 4051.

(50) Tanaka, R.; Yamashita, M.; Nozaki, K. *J. Am. Chem. Soc.* **2009**, *131*, 14168.

(51) Gupta, M.; Hagen, C.; Flesher, R. J.; Kaska, W. C.; Jensen, C. M. *Chem. Commun.* **1996**, 2083.

(52) (a) Göttker-Schnetmann, I.; White, P.; Brookhart, M. *J. Am. Chem. Soc*. **2004**, *126*, 1804. (b) Göttker-Schnetmann, I.; Brookhart, M. *J. Am. Chem. Soc*. **2004**, *126*, 9330.

(53) Morales-Morales, D.; Redon, R.; Yung, C.; Jensen, C. M. *Inorg. Chim. Acta* **2004**, *357*, 2953.

(54) Biswas, S.; Ahuja, R.; Ray, A.; Choliy, Y.; Krogh-Jespersen, K.; Brookhart, M.; Goldman, A. S. *Abstracts of Papers, 236th ACS National Meeting, Philadelphia, PA, Aug 17-21*, 2008; American Chemical Society: Washington, DC, 2008, INOR-125.

(55) (a) Rubina, M.; Gevorgyan, V. *J. Am. Chem. Soc*. **2001**, *123*, 11107. (b) Ogoshi, S.; Ueta .M; Oka. M.; Kurosawa, H. *Chem. Commun*. **2004**, 2732. (c) Chuluo, Y.; Nolan, S. P. *J. Org. Chem.* **2002**, *67*, 591. (d) Trost, B. M.; Sorum, M. T.; Chan, C.; Harms, A.

E.; Ruhter, G. *J. Am. Chem. Soc.* **1997**, *119*, 698.

(56) Weng, W.; Guo, C.; Celenligil-Cetin, R.; Foxman, B. M.; Ozerov, O. V. *Chem. Commun.* **2006**, 197.

(57) Nishiura, M.; Hou, Z.; Wakatsuki, Y.; Yamaki, T.; Miyamoto, T. *J. Am. Chem. Soc.* **2003**, *125*, 1184.

(58) Ghosh, R.; Zhang, X.; Achord, P.; Emge, T. J.; Krogh-Jespersen, K.; Goldman, A. S. *J. Am. Chem. Soc.* **2007**, *129*, 853.

(59) (a) Boebel, T. A.; Hartwig, J. F. *J. Am. Chem. Soc*. **2008**, *130*, 7534. (b) Shimada, S.; Batsanov, A. S.; Howard, J. A. K.; Marder, T. B. *Angew. Chem*. **2001**, *113*, 2226. (c) Chen, H. Y.; Schlecht, S.; Semple, T. C.; Hartwig, J. F. *Science* **2000**, *287*, 1995. (d) Ohmura, T.; Kijima, A.; Suginome, M. *J. Am. Chem. Soc*. **2009**, *131*, 6070.

(60) Boller, T. M.; Murphy, J. M.; Hapke, M.; Ishiyama, T.; Miyaura, N.; Hartwig, J. F. *J. Am. Chem. Soc*. **2005**, *127*, 14263.

(61) Suzuki, A. *Angew. Chem. Int. Ed*. **2011**, *50*, 2.

(62) (a) Driver, M. S.; Hartwig, J. F. *J. Am. Chem. Soc*. **1997**, *119*, 8232. (b) Pawlas, J.; Nakao, Y.; Kawatsura, M.; Hartwig, J. F. *J. Am. Chem. Soc*. **2002**, *124*, 3669. (c) Paul, F.; Patt, J.; Hartwig, J. F. *J. Am. Chem. Soc*. **1994**, *116*, 5969. (d) Guram, A. S.; Buchwald, S. L. *J. Am. Chem. Soc*. **1994**, *116*, 7901. (e) Yin, J.; Buchwald, S. L. *J. Am. Chem. Soc*. **2002**, *124*, 6043. (f) Guram, A. S.; Rennels, R. A.; Buchwald, S. L. *Angew. Chem. Int. Ed*. **1995**, *34*, 1348.

(63) (a) Kondo, T.; Misudo, T. *Chem. Rev.* **2000**, *100*, 3205. (b) Li, G. Y. *Angew. Chem. Int. Ed.* **2001**, *40*, 1513. (c) Schopfer, U.; Schlapbach, A. *Tetrahedron* **2001**, *57*, 3069. (d) Fernandez-Rodriguez, M. A.; Shen, Q.; Hartwig, J. F. *J. Am. Chem. Soc.* **2006**, *128*, 2180. (e) Torraca, K. E.; Huang, X.; Parrish, C. A.; Buchwald, S. L. *J. Am. Chem. Soc*. **2001**, *123*, 10770. (f) Vorogushin, A. V.; Huang, X.; Buchwald, S. L. *J. Am. Chem. Soc.* **2005**, *127*, 8146. (g) Gowrisankar, S.; Sergeev, A. G.; Anbarasan, P.; Spannenberg, A.; Neumann, H.; Beller, M. *J. Am. Chem. Soc*. **2010**, *132*, 11592. (h) Maimone, T. J.; Buchwald, S. L. *J. Am. Chem. Soc.* **2010**, *132*, 9990.

(64) Mkhalid, I. A. I.; Barnard, J. H.; Marder, T. B.; Murphy, J. M.; Hartwig, J. F. *Chem. Rev*. **2010**, *110*, 890.

(65) Burks, H. E.; Kliman, L. T.; Morken, J. P. *J. Am. Chem. Soc.* **2009**, *131*, 9134.

(66) Dang, L.; Lin, Z.; Marder, T. B. *Chem. Commun*. **2009**, 3987.

(67) Cipot, J.; Vogels, C. M.; McDonald, R.; Westcoot, S. A.; Stradiotto, M.

*Organometallics* **2006**, *25*, 5965.

(68) Kinder, R. E.; Widenhoefer, R. A. *Org. Lett*. **2006**, *8*, 1967.

(69) Braunschweig, H.; Kollann, C.; Rais, D. *Angew. Chem. Int. Ed.* **2006**, *45*, 5254.

(70) Cho, J. Y.; Tse, M. K.; Holmes, D.; Maleczka, R. E., Jr.; Smith, M. R., III. *Science* **2002**, *295*, 305.

(71) Ishiyama, T.; Takagi, J.; Ishida, K.; Miyaura, N.; Anastasi, N. R.; Hartwig, J. F. *J. Am. Chem. Soc.* **2002**, *124*, 390.

(72) Waltz, K. M.; Hartwig, J. F. *Science* **1997**, *277*, 211.

(73) Lantero, D. R.; Ward, D. L.; Smith, M. R., III. *J. Am. Chem. Soc.* **1997**, *119*, 9699.

(74) (a) Crabtree, R. H. *The Organometallic Chemistry of the Transition Metals*, 5th ed.; Wiley-Interscience: New York, 2009, pp 153-172. (b) Hartwig, J. F. *Organotransition Metal Chemistry: From Bonding to Catalysis*; University Science Books: Sausalito, CA, 2009, pp 261-320.

(75) (a) Lesley, G.; Nguyen, P.; Taylor, N. J.; Marder, T. B.; Scott, A. J.; Clegg W.; Norman, N. C. *Organometallics* **1996**, *15*, 5137. (b) Iverson, C. N.; Smith, M. R., III. *J. Am. Chem. Soc.* **1995**, *117*, 4403.

(76) (a) Chotona, G. A.; Rak, M. A.; Smith, M. R., III. *J. Am. Chem. Soc*. **2005**, *127*, 10539. (b) Irvine, G. J.; Lesley, M. J.; Marder, T. B.; Norman, N. C.; Rice, C. R.; Robins, E. G.; Roper, W. R.; Whittell, G. R.; Wright, L. *Chem. Rev.* **1998**, *98*, 2685.

(77) Gregor, L. C.; Chen, C. H.; Fafard, C. M.; Fan, L.; Guo, C.; Foxman, B. M.; Gusev, D. G.; Ozerov, O. V. *Dalton Trans.* **2010**, 3195.

(78) For an analogous net heterolytic addition of $H_2$ to $[(PNP^*)Ni]^+$, where PNP* = $(^tBu_2PCH_2SiMe_2)_2N$, see: He, T.; Tsvetkov, N. P.; Andino, J. G.; Gao, X. F.; Fullmer, B. C.; Caulton, K. G. *J. Am. Chem. Soc*. **2010**, *132*, 910.

(79) H-H addition to Noyori Ru amides: (a) Sandoval, C. A.; Ohkuma, T.; Muñiz, K.; Noyori, R. *J. Am. Chem. Soc.* **2003**, *125*, 13490. (b) Abdur-Rashid, K.; Clapham, S. E.; Hadzovic, A.; Harvey, J. N.; Lough, A. J.; Morris, R. H. *J. Am. Chem. Soc.* **2002**, *124*, 15104.

(80) (a) C-H addition across metal alkylidenes: Pamplin, C. B.; Legzdins, P. *Acc. Chem. Res.* **2003**, *36*, 223. (b) C-H addition across metal-imido: Slaughter, L. M.; Wolczanski, P. T.; Klinckman, T. R.; Cundari, T. R. *J. Am. Chem. Soc.* **2000**, *122*, 7953.

Bennett, J. L.; Wolczanski, P. T. *J. Am. Chem. Soc.* **1997**, *119*, 10696. Schaller, C. P.; Cummins, C. C.; Wolczanski, P. T. *J. Am. Chem. Soc.* **1996**, *118*, 591. (c) C-H addition across metal alkylidyne: Mindiola, D. J. *Acc. Chem. Res.* **2006**, *39*, 813.

(81) Stephan, D. W. *Dalton Trans.* **2009**, 3129.

(82) Fernandes, A. C.; Fernandes, J. A.; Paz, F. A.; Romão, C. C. *Dalton Trans.* **2008**, 6686.

(83) Salomon, M. A.; Braun, T.; Penner, A. *Angew. Chem. Int. Ed.* **2008**, *47*, 8867.

(84) (a) Ishiyama, T.; Murata, M.; Miyaura, N. *J. Org. Chem.* **1995**, *60*, 7508. (b) Takahashi, K.; Ishiyama, T.; Miyaura, N. *J. Organomet. Chem.* **2001**, *625*, 47. (c) Ishiyama, T.; Miyaura, N. *Pure Appl. Chem.* **2006**, *78*, 1369.

(85) Tran, B. L.; Adhikari, D.; Fan, H.; Pink, M.; Mindiola, D. J. *Dalton Trans.* **2010**, *39*, 358.

(86) Koren-Selfridge, L.; Query, I. P.; Hanson, J. A.; Isley, N. A.; Guzei, I. A.; Clark, T. B. *Organometallics* **2010**, *29*, 3896.

(87) (a) Shvo, Y.; Czarkie, D.; Rahamim, Y. *J. Am. Chem. Soc.* **1986**, *108*, 7400. (b) Karvembu, R.; Prabhakaran, R.; Natarajan, K. *Coord. Chem. Rev.* **2005**, *249*, 911. (c) Conley, B. L.; Pennington-Boggio, M. K.; Boz, E.; Williams, T. J. *Chem. Rev.* **2010**, *110*, 2294.

(88) (a) Brookhart, M.; Grant, B.; Volpe, A. F., Jr. *Organometallics* **1992**, *11*, 3920. (b) Bahr, S. R.; Boudjouk, P. *J. Org. Chem.* **1992**, *57*, 5545. (c) Kobayashi, H.; Sonoda, A.; Iwamoto, H.; Yoshimura, M. *Chem. Lett.* **1981**, *10*, 579.

(89) Yakelis, N. A.; Bergman, R. G. *Organometallics* **2005**, *24*, 3579.

(90) For a comprehensive review on carborane anions, see: Körbe, S.; Schreiber, P. J.; Michl, J. *Chem. Rev.* **2006**, *106*, 5208.

(91) For an example of hydrolysis of a metal-boryl bond to produce a metal hydride, see: Hartwig, J. F.; He, X. *Organometallics* **1996**, *15*, 5350.

(92) The NH resonances of compounds $[(PN(H)P)Ir(H)(SiR_3)][B(C_6F_5)_4]$ were found in the δ 7-8 ppm range in their $^1H$ NMR spectra in $C_6D_5Br$: Calimano, E.; Tilley, D. T. *Organometallics* **2010**, *29*, 1680.

(93) For an overview on the use of NMR spectroscopy in achieving sophisticated insight into interaction of ions in solution, see: Pregosin, P. S. *Pure Appl. Chem.* **2009**, *81*, 615.

(94) Burgess, K.; van der Donk, W. A.; Westcott, S. A.; Marder, T. B.; Baker, R. T.; Calabrese, C. J. *J. Am. Chem. Soc.* **1992**, *114*, 9350.

(95) (a) Kondoh, A.; Jamison, T. F. *Chem. Commun.* **2010**, 907. (b) Mkhalid, I. A.; Coapes, R. B.; Edes, S. N.; Coventry, D. N.; Souza, F. E. S.; Thomas, R. L.; Hall, J. J.; Bi, S. W.; Lin, Z.; Marder, T. B. *Dalton Trans*. **2008**, 1055. (c) Olsson, V. J.; Szabó, K. J. *Angew. Chem. Int. Ed.* **2007**, *46*, 6891.

(96) Adhikari, D.; Huffman, J. C.; Mindiola, D. J. *Chem. Commun.* **2007**, 4489.

(97) For selected references on σ-BH complexes, see: (a) Schlecht, S.; Hartwig, J. F. *J. Am. Chem. Soc.* **2000**, *122*, 9435. (b) Lachaize, S.; Essalah, K.; Montiel-Palma, V.; Vendier, L.; Chaudret, B.; Barthelat, J. C.; Sabo-Etienne, S. *Organometallics* **2005**, *24*, 2935. (c) Hebden, T. J.; Denney, M. C.; Pons, V.; Piccoli, P. M. B.; Koetzle, T. F.; Schultz, A. J.; Kaminsky, W.; Goldberg, K. I.; Heinekey, D. M. *J. Am. Chem. Soc.* **2008**, *130*, 10812.

(98) Lillo, V.; Mas-Marza, E.; Segarra, A. M.; Carbo, J. J.; Bo, C.; Peris, E.; Fernandez, E. *Chem. Commun.* **2007**, 3380.

(99) It is important to note that the splitting of CatB-H cannot be accomplished by proton migration, since it is the boryl that needs to be transferred to N of PNP.

(100) Crystal structures described in Chapter II were solved by Dr. Foxman's group at Brandeis University and these structures were published, see: Zhu, Y.; Chen, C. H.; Fafard, C. M.; Foxman, B.; Ozerov, O. V. *Inorg. Chem.* **2011**. *50*, 7980.

(101) Ozerov, O. V.; Guo, C.; Fan. L.; Foxman, B. M. *Organometallics* **2004**, *23*, 5573.

(102) Zhu, J.; Lin, Z.; Marder, T. B. *Inorg. Chem.* **2005**, *44*, 9384.

(103) Ortep drawing was prepared using *Persistence of Vision Ray Tracer (POV-Ray)*, available at http://www.povray.org/ and *Ortep-3 for Windows* (Farugia, L. *J. Appl. Crystallogr*. **1997**, *30*, 565).

(104) Fafard, C. M.; Ozerov, O. V. *Inorg. Chim. Acta* **2007**, *360*, 286.

(105) Apex2, Version 2 User Manual, M86-E01078, Bruker Analytical X-ray Systems, Madison, WI, June 2006.

(106) Altomare, A; Cascarano, G; Giacovazzo, G.; Guagliardi, A.; Burla, M. C.; Polidori, G.; Camalli, M. *J. Appl. Cryst*. **1994**, *27*, 435.

(107) Betteridge, P. W.; Carruthers, J. R.; Cooper, R. I.; Prout, K.; Watkin, D. J. *J.*

*Appl. Cryst.* **2003**, *36*, 1487.

(108) (a) van der Sluis, P.; Spek, A. *Acta Cryst.* **1990**, *A46*, 194. (b) Spek, A. L. *Acta Cryst*. **1990**, *A46*, C34. (c) PLATON, A Multipurpose Crystallographic Tool, Utrecht University, Utrecht, The Netherlands, Spek, A. L. 1998.

(109) (a) Shilov, A. E.; Shul'pin, G. B. *Chem. Re*v. **1997**, *97*, 2879. (b) Labinger, J. A.; Bercaw, J. E. *Nature* **2002**, *417*, 507. (c) Lersch, M.; Tilset, M. *Chem. Re*v. **2005**, *105*, 2471.

(110) (a) Campos, K. R. *Chem. Soc. Re*v. **2007**, *36*, 1069. (b) Kalyani, D.; Dick, A. R.; Anani, W. Q.; Sanford, M. S. *Tetrahedron* **2006**, *62*, 11483. (c) Daugulis, O.; Zaitsev, V. G.; Shabashov, D.; Pham, Q. N.; Lazareva, A. *Synlett.* **2006**, 3382. (d) Godula, K.; Sames, D. *Science* **2006**, *312*, 67. (e) Fiori, K. W.; Du Bois, J. *J. Am. Chem. Soc.* **2007**, *129*, 562. (f) Giri, R.; Maugel, N.; Li, J. J.; Wang, D. H.; Breazzano, S. P.; Saunders, L. B.; Yu, J. Q. *J. Am. Chem. Soc.* **2007**, *129*, 3510.

(111) Goldshleger, N. F.; Eskova, V. V.; Shilov, A. E.; Shteinman, A. A. *Zh. Fiz. Khim.* **1972**, *46*, 1353.

(112) (a) Janowicz, A. H.; Bergman, R. G. *J. Am. Chem. Soc.* **1982**, *104*, 352. (b) Hoyano, J. K.; Graham, W. A. G. *J. Am. Chem. Soc.* **1982**, *104*, 3723.

(113) (a) Jones, W. D. *Acc. Chem. Res.* **2003**, *36*, 140. (b) Jones, W. D.; Feher, F. J. *J. Am. Chem. Soc.* **1982**, *104*, 4240. (c) Jones, W. D.; Feher, F. J. *J. Am. Chem. Soc.* **1984**, *106*, 1650. (d) Jones, W. D.; Feher, F. J. *Acc. Chem. Res.* **1989**, *22*, 91. (e) Periana, R. A.; Bergman, R. G. *J. Am. Chem. Soc.* **1986**, *108*, 7332. (f) Wick, D. D.; Goldberg, K. I. *J. Am. Chem. Soc.* **1997**, *119*, 10235.

(114) Bergman, R. G. *Science* **1984**, *223*, 902.

(115) (a) Clot, E.; Megret, C.; Eisenstein, O.; Perutz, R. N. *J. Am. Chem. Soc.* **2006**, *128*, 8350. (b) Jones, W. D. *Inorg. Chem.* **2005**, *44*, 4475. (c) Wick, D. D.; Jones, W. D. *Organometallics* **1999**, *18*, 495. (d) Bennett, J. L.; Wolczanski, P. T. *J. Am. Chem. Soc.* **1997**, *119*, 10696.

(116) Adams, C. S.; Legzdins, P.; Tran, E. *Organometallics* **2002**, *21*, 1474.

(117) Nakamura et al. reported Ir-catalyzed benzylic C-C coupling of toluene with a bulky fullerene derivative; this selectivity may well be sterically enforced by the bulky substrate: Matsuo, Y.; Iwashita, A.; Nakamura, E. *Chem. Lett.* **2006**, *35*, 858.

(118) (a) Driver, T. G.; Day, M. W.; Labinger, J. A.; Bercaw, J. E. *Organometallics* **2005**, *24*, 3644. (b) Heyduk, A. F.; Driver, T. G.; Labinger, J. A.; Bercaw, J. E. *J. Am. Chem. Soc.* **2004**, *126*, 15034.

(119) (a) Lam, W. H.; Lam, K. C.; Lin, Z.; Shimada, S.; Perutz, R. N.; Marder, T. B. *Dalton Trans.* **2004**, 1556. (b) Shimada, S.; Batsanov, A. S.; Howard, J. A. K.; Marder, T. B. *Angew. Chem. Int. Ed.* **2001**, *40*, 2168.

(120) Collman, J. P.; Boulatov, R. *Inorg. Chem.* **2001**, *40*, 2461.

(121) (a) Cleary, B. P.; Eisenberg, R. *J. Am. Chem. Soc.* **1995**, *117*, 3510. (b) Cleary, B. P.; Eisenberg, R. *Organometallics* **1992**, *11*, 2335.

(122) (a) Gupta, M.; Hagen, C.; Kaska, W. C.; Cramer, R. E.; Jensen, C. M. *J. Am. Chem. Soc.* **1997**, *119*, 840. (b) Xu, W.; Rosini, G. P.; Gupta, M.; Jensen, C. M.; Kaska, W. C.; Krogh-Jespersen, K.; Goldman, A. S. *Chem. Commun.* **1997**, 2273.

(123) (a) Chen, H.; Schlecht, S.; Semple, T. C.; Hartwig, J. F. *Science* **2002**, *295*, 205. (b) Iverson, C. N.; Smith, M. R., III. *J. Am. Chem. Soc.* **1999**, *121*, 7696.

(124) (a) Ezbiansky, K.; Djurovich, P. I.; Laforest, M.; Sinning, D. J.; Zayes, R.; Berry, D. H. *Organometallics* **1998**, *17*, 1455. (b) Sadow, A. D.; Tilley, T. D. *J. Am. Chem. Soc.* **1997**, *127*, 643.

(125) (a) Wang, K.; Goldman, M. E.; Emge, T. J.; Goldman, A. S. *J. Organomet. Chem.* **1996**, *518*, 55. (b) Zhang, X. W.; Kanzelberger, M.; Emge, T. J.; Goldman, A. S. *J. Am. Chem. Soc.* **2004**, *126*, 13192.

(126) Crystal structure of **304c** was solved by Dr. Foxman's group at Brandeis University and was published, see Zhu, Y.; Lei, F.; Chen, C. H.; Finnell, S. R.; Foxman, B.; Ozerov, O. V. *Organometallics*, **2007**, *26*, 6066.

(127) Fryzuk observed benzylic C-H activation of toluene via ostensibly radical pathways (no reaction in the dark) by $[(Ph_2PCH_2SiMe_2)_2N]Rh(Me)(I)$ in the presence of MeI. In our case, the transformation of **301** to **304a** proceeds in the dark (see the Supporting Information); radical pathways are unlikely. See: Fryzuk, M. D.; MacNeil, P. A.; McManus, N. T. *Organometallics* **1987**, *6*, 882.

(128) (a) Goldman, A. S.; Roy, A. H.; Huang, Z.; Ahuja, R.; Schinski, W.; Brookhart, M. *Science* **2006**, *312*, 257. (b) Zhu, K.; Achord, P. D.; Zhang, X.; Krogh-Jespersen, K.; Goldman, A. S. *J. Am. Chem. Soc.* **2004**, *126*, 13044. (c) Krogh-Jespersen, K.; Czerw, M.; Summa, N.; Renkema, K. B.; Achord, P. D.; Goldman, A. S. *J. Am. Chem. Soc.* **2002**, *124*, 11404.

(129) Ben-Ari, E.; Cohen, R.; Gandelman, M.; Shimon, L. J. W.; Martin, J. M. L.; Milstein, D. *Organometallics* **2006**, *25*, 3190.

(130) Procelewska, J.; Zahl, A.; Liehr, G.; Van Eldik, R.; Smythe, N. A.; Williams, B. S.; Goldberg, K. I. *Inorg. Chem.* **2005**, *44*, 7732.

(131) Halpern, J.; Wong, C. S. *Chem. Commun.* **1973**, 629.

(132) (a) Whited, M. T.; Grubbs, R. H. *J. Am. Chem. Soc.* **2008**, *130*, 5874. (b) Romero, P. E.; Whited, M. T.; Grubbs, R. H. *Organometallics* **2008**, *27*, 3422. (c) Whited, M. T.; Grubbs, R. H. *Organometallics* **2008**, *27*, 5737. (d) Whited, M. T.; Grubbs, R. H. *J. Am. Chem. Soc.* **2008**, *130*, 16476. (e) Whited, M. T.; Grubbs, R. H. *Organometallics* **2009**, *28*, 161.

(133) Ziegler, T.; Versluis, L.; Tschinke, V. *J. Am. Chem. Soc.* **1986**, *108*, 612.

(134) Crystal of **312** was obtained by Sam Timpa and the structure was solved by Dr. Foxman's group at Brandeis Universiy. This structure was published, see: Whited, M. T.; Zhu, Y.; Timpa, S. D.; Chen, C. H.; Foxman, B. M.; Ozerov, O. V.; Grubbs, R. H. *Organometallics* **2009**,.*28*, 4560.

(135) Walker, J. F.; Chadwick, A. F. *Ind. Eng. Chem.* **1947**, *39*, 974.

(136) Luecke, H. F.; Arndtsen, B. A.; Burger, P.; Bergman, R. G. *J. Am. Chem. Soc*. **1996**, *118*, 2517.

(137) (a) Tsuji, J. *Palladium Reagents and Catalysts: New Perspectives for the 21st Century*, 2nd ed.; Wiley: New York, 2004. (b) de Meijere, A.; Diederich, F. *Metal Catalyzed Cross-Coupling Reactions*; Wiley-VCH: New York, 2004, Vols. 1 and 2. (c) Negishi, E. I., Ed. *Handbook of Organopalladium Chemistry for Organic Synthesis*; Wiley-Interscience: New York, 2002. (d) Hartwig, J. F. *Organotransition Metal Chemistry: From Bonding to Catalysis*; University Science Books: Sausalito, CA, 2009, Ch.7 and Ch. 19.

(138) (a) Negishi, E. *Bull. Chem. Soc. Jpn.* **2007**, *80*, 233. (b) Hassan, J.; Sevignon, M.; Gozzi, C.; Schulz, E.; Lemaire, M. *Chem. Rev.* **2002**, *102*, 1359.

(139) Anctil, J. G.; Snieckus, V. *J. Organomet. Chem.* **2002**, *653*, 150.

(140) Rosen, B. M.; Quasdorf, K. W.; Wilson, D. A.; Zhang, N.; Resmerita, A. M.; Garg, N. K.; Percec, V. *Chem. Rev.* **2011**, *111*, 1346.

(141) (a) Tobisu, M.; Yamakawa, K.; Shimasaki, T.; Chatani, N. *Chem. Commun*. **2011**, *47*, 2946. (b) Alvarez-Bercedo, P.; Martin, R. *J. Am. Chem. Soc*. **2010**, *132*, 17352.

(142) (a) Wenkert, E.; Michelotti, E. L.; Swindell, C. S.; Tingoli, M. *J. Org. Chem.* **1984**, *49*, 4894. (b) Wenkert, E.; Michelotti, E. L.; Swindell, C. S. *J. Am. Chem. Soc.* **1979**, *101*, 2246.

(143) (a) Quasdorf, K. W.; Antoft-Finch, A.; Liu, P.; Silberstein, A. L.; Komaromi,

A.; Blackburn, T.; Ramgren, S. D.; Houk, K. N.; Snieckus, V.; Garg, N. K. *J. Am. Chem. Soc.* **2011**, *133*, 6352. (b) Quasdorf, K. W.; Riener, M.; Petrova, K. V.; Garg, N. K. *J. Am. Chem. Soc.* **2009**, *131*, 17748. (c) Quasdorf, K. W.; Tian, X.; Garg, N. K. *J. Am. Chem. Soc.* **2008**, *130*, 14422.

(144) Yoshikai, N.; Matsuda, H.; Nakamura, E. *J. Am. Chem. Soc.* **2009**, *131*, 9590.

(145) (a) Huang, K.; Yu, D.; Zheng, S.; Wu, Z.; Shi. Z. J. *Chem. Eur. J.* **2011**, *17*, 786. (b) Yu, D.; Li, B.; Shi, Z. J. *Acc. Chem. Res.* **2010**, *43*, 1486. (c) Guan, B. T.; Wang,Y.; Li, B. J.; Yu, D. G.; Shi, Z. J. *J. Am. Chem. Soc.* **2008**, *130*, 14468.

(146) (a) Antoft-Finch, A.; Blackburn, T.; Snieckus, V. *J. Am. Chem. Soc.* **2009**, *131*, 17750. (b) Sengupta, S.; Leite, M.; Raslan, D. S.; Quesnelle, C.; Snieckus, V. *J. Org. Chem.* **1992**, *57*, 4066.

(147) Shimasaki, T.; Tobisu, M.; Chatani, N. *Angew. Chem. Int. Ed*. **2010**, *49*, 2929.

(148) Li, Z.; Zhang, S. L.; Fu, Y.; Guo, Q. X.; Liu, L. *J. Am. Chem. Soc.* **2009**, *131*, 8815.

(149) For an early example of Cacyl-O OA of aryl esters with Ni, see: Yamamoto,T.; Ishizu, J.; Kohara, T.; Komiya, S.; Yamamoto, A. *J. Am. Chem. Soc.* **1980**, *102*, 3758.

(150) Gatard, S.; Guo, C.; Foxman, B. M.; Ozerov, O. V. *Organometallics* **2007**, *26*, 6066.

(152) Verat, A. Y; Pink, M.; Fan, H.; Tomaszewski, J.; Caulton, K. G. *Organometallics* **2008**, 27, 166.

(152) For a discussion illuminating the thermodynamic, but not kinetic, directing role of the chelating group in C-H OA of arenes to (PCP)Ir, see ref. 125(b).

(153) Bentley, T. W.; Roberts, K. *J. Chem. Soc., Perkin Trans. II* **1989**, 1055.

(154) Panthi, B. D.; Gipson, S. L.; Franken, A. *Organometallics* **2010**, *29*, 5890.

(155) (a) Nagayama, K.; Shimizu, I.; Yamamoto, A. *Bull. Chem. Soc. Jpn.* **1999**, *72*, 799. (b) Nagayama, K.; Kawataka, F.; Sakamoto, M.; Shimizu, I.; Yamamoto, A. *Bull. Chem. Soc. Jpn*. **1999**, *72*, 573.

(156) (a) Cordaro, J. G.; Bergman, R. G. *J. Am. Chem. Soc*. **2004**, *126*, 16912. (b) Kakino, R.; Shimizu, I.; Yamamoto, A. *Bull. Chem. Soc. Jpn.* **2001**, *74*, 371. (c) Bennett, M. A.; Chee, H. K.; Robertson, G. B. *Inorg. Chem.* **1979**, *18*, 1061. (d) Blake, D. M.; Shields, S.; Wyman, L. *Inorg. Chem.* **1974**, *13*, 1595.

(157) Tentatively identified based on the following data: IR, $\nu_{CO}$ = 2062 cm-1; $^{19}$F

NMR: δ 3.5 ppm (apparent quartet, $J_{F\text{-}P} \approx J_{F\text{-}Rh} \approx 11$ Hz). These $^{19}F$ chemical shift and the coupling constants are similar to other known Rh-$CF_3$ complexes. See, for example, ref 155(a) and also: Bourgeois, C. J.; Garratt, S. A.; Hughes, R. P.; Larichev, R. B.; Smith, J. M.; Ward, A. J.; Willemsen, S.; Zhang, D.; DiPasquale, A. G.; Zakharov, L. N.; Rheingold, A. L. *Organometallics* **2006**, *25*, 3474.

(158) Brothers, P. J.; Roper, W. R. *Chem. Rev.* **1988**, *88*, 1293.

(159) We cannot rule out that some of the C-H to C-O OA rearrangement proceeds intramolecularly, without liberation of Ph-$O_2$CR.

(160) Hartwig, J. F. *Organotransition Metal Chemistry: From Bonding to Catalysis*; University Science Books: Sausalito, CA, 2009, pp 322-324.

(161) Single crystal of **407** was obtaind by Dr. Dan Smith and all the crystal structures described in Chapter IV were solved by Dr. Herbert. These structures are published, see: Zhu, Y.; Smith, D. A.; Herbert, D. E.; Gatard, S.; Ozerov, O. V. *Chem. Commun.* **2012**, 218.

(162) Drossman, H.; Johnson, H.; Mill, T. *Chemosphere* **1988**, *17*, 1509.

(163) Seganish, W. M.; Deshong, P. *J. Org. Chem.* **2004**, *69*, 6790.

(164) Niknam, K.; Saberi, D.; Molaee, H.; Zolfigol, M. *Can. J. Chem.* **2010**, *88*, 164.

(165) Sheldrick, G. M. *SADBS: Program for Absorption Correction for Data from Area Detector Frames*; University of Göttingen, 2008, version 2008/1.

(166) Sheldrick, G. M. *Acta Cryst*. **2008**, *A64*, 112.

(167) (a) Herrmann, W. A. *Angew. Chem. Int. Ed.* **2002**, *41*, 1291. (b) Arduengo, A. J. *Acc. Chem. Res.* **1999**, *32*, 913.

(168) (a) Reger, D. L.; Dukes, M. D. *J. Organomet. Chem.* **1978**, *153*, 67. (b) Crespi, A. M.; Shriver, D. F. *Organometallics* **1985**, *4*, 1830. (c) Koola, J. D.; Roddick, D. M. *Organometallics* **1991**, *10*, 591.

(169) (a) Brothers, P. J.; Burrell, A. K.; Clark, G. R.; Rickard, C. E. F.; Roper, W. R. *J. Organomet. Chem.* **1990**, *394*, 615. (b) Huang, D.; Koren, P. R.; Folting, K.; Davidson, E. R.; Caulton, K. G. *J. Am. Chem. Soc.* **2000**, *122*, 8916. (c) Campen, A. K.; Mahmoud, K. A.; Rest, A. J.; Willis, P. A. *J. Chem. Soc., Dalton Trans.* **1990**, 2817.

(170) Prakash, G. K. S.; Yudin, A. K. *Chem. Rev*. **1997**, *97*, 757.

(171) Trnka, T. M.; Day, M. W.; Grubbs, R. H. *Angew. Chem. Int. Ed*. **2001**, *40*, 3441.

(172) (a) Hughes, R. P.; Laritchev, R. B.; Yuan, J.; Golen, J. A.; Rucker, A. N.; Rheingold, A. L. *J. Am. Chem. Soc.* **2005**, *127*, 15020. (b) Huang, H.; Hughes, R. P.; Rheingold, A. L. *Dalton Trans.* **2011**, *40*, 47.

(173) Maggiarosa, N.; Tyrra, W.; Naumann, D.; Kirij, N. V.; Yagupolskii, Y. L. *Angew. Chem. Int. Ed.* **1999**, *38*, 2252.

(174) Tyrra, W.; Kremlev, M. M.; Naumann, D.; Scherer, H.; Schmidt, H.; Hoge, B.; Pantenburg, I.;Yagupolskii, Y. L. *Chem. Eur. J.* **2005**, *11*, 6514.

(175) The crystal structures of **501** and **502** were solved by Dr. Herbert and they have not been published yet.

(176) Goodman, J.; Grushin, V. V.; Larichev, R. B.; Macgregor, S. A.; Marshall, W. J.; Roe, D. C. *J. Am. Chem. Soc.* **2009**, *131*, 4236.

(177) (a) Browning, J.; Penford, B. R. *Chem. Commun.* **1973**, 198. (b) Evans, J. A.; Russell, D. R. *Chem. Commun.* **1971**, 197. (c) Guggenberger L. J.; Cramer, R. *J. Am. Chem. Soc.* **1972**, *94*, 3379.

(178) Karle, I. L.; Karle, J. *J. Chem. Phys.* **1950**, *18*, 963.

(179) Hitchcock, P. B.; McPartlin, M.; Mason, R. *Chem. Commun*. **1969**, 1367.

(180) Huang, H.; Hughes, R. P.; Landis, C. R.; Rheingold, A. L. *J. Am. Chem. Soc.* **2006**, *128*, 7454.

(181) (a) Douvris, C.; Ozerov, O. V. *Science* **2008**, *321*, 1188. (b) Douvris, C.; Nagaraja, C. M.; Chen, C. H.; Foxman, B. M.; Ozerov, O. V. *J. Am. Chem. Soc.* **2010**, *132*, 4946. (c) Scott, V. J.; Çelenligil-Çetin, R.; Ozerov, O. V. *J. Am. Chem. Soc*. **2005**, *127*, 2852.

(182) (a) Meier, G.; Braun, T. *Angew. Chem.* **2009**, *121*, 1575. (b) Zhang, Y.; Huynh, K.; Manners, I.; Reed, C. A. *Chem. Commun*. **2008**, 494. (c) Reed, C. A. *Acc. Chem. Res.* **2010**, *43*, 121.

(183) Example of halide abstraction using silylium cation: Egbert, J. D.; Bullock, R. M.; Heinekey, M. *Organometallics* **2007**, *26*, 2291.

(184) Lambert, J. B.; Zhang, S.; Ciro, S. M. *Organometallics* **1994**, *13*, 2430.

(185) (a) Tamao, K.; Sumitani, K.; Kumada, M. *J. Am. Chem. Soc.* **1972**, *94*, 4374. (b) Heck, R. F.; Nolley, J. P. *J. Am. Chem. Soc.* **1972**, *37*, 2320. (c) Miyaura, N.; Suzuki, A. *Chem. Rev.* **1995**, *95*, 2457. (d) Milstein, D.; Stille, J. K. *J. Am. Chem. Soc.* **1978**, *100*, 3636. (e) King, A. O.; Okukado, N.; Negishi, E. *Chem. Commun.* **1977**, 683. (f)

Sonogashira, K.; Tohda, Y.; Hagihara, N. *Tetrahedron Lett.* **1975**, *16*, 4467. (g) Trost, B. M.; Van Vranken, D. L. *Chem. Rev.* **1996**, *96,* 395. (h) Hartwig, J. F. *Acc. Chem. Res.* **2008**, *41*, 1534.

(186) Representive examples: (a) Bohm, V. P. W.; Weskamp, T.; Gstottmayr, C. W. K.; Herrmann, W. A. *Angew. Chem. Int. Ed.* **2000**, *39*, 1602. (b) Old, D. W.; Wolfe, J. P.; Buchwald, S. L. *J. Am. Chem. Soc.* **1998**, *120,* 9722. (c) Littke, A. F.; Fu, G. C. *Angew. Chem. Int. Ed.* **2002**, *41*, 4176. (d) Kawatsura, M.; Hartwig, J. F. *J. Am. Chem. Soc.* **1999**, *121*, 1473. (e) Baudoin, O. *Angew. Chem. Int. Ed.* **2007**, *46*, 1373.

(187) (a) Macgregor, S. A.; Roe, D. C.; Marshall, W. J.; Bloch, K. M.; Bakhmutov, V. I.; Grushin, V. V. *J. Am. Chem. Soc.* **2005**, *127*, 15304. (b) Douglas, T. M.; Chaplin, A. B.; Weller, A. S. *Organometallics* **2008**, *27*, 2918. (c) Chen, S.; Li, Y.; Zhao, J.; Li, X. *Inorg. Chem.* **2009**, *48*, 1198.

(188) Unpublished results by Sylvain Gatard.

(189) Moloy, K. G.; Petersen, J. L. *J. Am. Chem. Soc.* **1995**, *117,* 7696.

(190) Kossoy, E.; Iron, M. A.; Rybtchinski, B.; Ben-David, Y.; Shimon, L. J. W.; Konstantinovski, L.; Martin, J. M. L.; Milstein, D. *Chem. Eur. J.* **2005**, *11*, 2319.

(191) Kossoy, E.; Rybtchinski, B.; Ben-David, Y.; Shimon, L. J. W.; Leitus, G.; Milstein, D. *Organometalliscs* **2009**, *28*, 523.

(192) Welch, G. C.; Holtrichter-Roessmann, T.; Stephan, D. W. *Inorg. Chem.* **2008**, *47*, 1904.

(193) Yurkerwich, K.; Parkin, G. *Inorg. Chim. Acta* **2011**, *376*, 18.

(194) Fan, H.; Fullmer, B. C.; Pink, M.; Caulton, K. G. *Angew. Chem. Int. Ed.* **2008**, *47*, 9112.

(195) Bernskoetter, W. H.; Schauer, C. K.; Goldberg, K. I.; Brookhart, M. *Science*, **2009**, *326*, 553.

(196) Nifant'ev, E. A.; Grachev, M. K.; Burmistrov, S. Yu.; Bekker, A. R.; Vosyanina, L. K.; Antipin, M. Yu.; Struchkov, Yu. T. *Zh. Obshch. Khim.***1992**, *62*, 1461.

(197) The crystal structures described in Chapter VI were solved by Dr. Herbert and they have not been published yet.

(198) Forster, D. *Adv. Organomet. Chem.* **1979**, *17*, 255.

(199) Corey, J. Y. *Chem. Rev.* **2011**, *111*, 863.

(200) Taw, F. L.; Bergman, R. G.; Brookhart, M. *Organometallics* **2004**, *23*, 886.

(201) Hanson, S. K.; Heinekey, D. M.; Goldberg, K. I. *Organometallics* **2008**, *27*, 1454.

(202) (a) Racowski, J. M.; Dick, A. R.; Sanford, M. S. *J. Am. Chem. Soc*. **2009**, *131*, 10974. (b) Williams, B. S.; Goldberg, K. I. *J. Am. Chem. Soc*. **2001**, *123*, 2576. (c) Marquard, S. L.; Hartwig, J. F. *Angew. Chem. Int. Ed.* **2011**, *50*, 7119.

(203) (a) Burgos, C. H.; Barder, T. E.; Huang, X.; Buchwald, S. L. *Angew. Chem. Int. Ed.* **2006**, *45*, 4321. (b) Vorogushin, A. V.; Huang, X.; Buchwald, S. L. *J. Am. Chem. Soc.* **2005**, *127*, 8146. (c) Kataoka, N.; Shelby, Q.; Stambuli, J. P.; Hartwig, J. F. *J. Org. Chem.* **2002**, *67*, 5553. (d) Torraca, K. E.; Huang, X.; Parrish, C.; Buchwald, S. L. *J. Am. Chem. Soc*. **2001**, *123*, 10770. (e) Shelby, Q.; Kataoka, N.; Mann, G.; Hartwig, J. F. *J. Am. Chem. Soc*. **2000**, *122*, 10718. (f) Anderson, K. W.; Ikawa, T.; Tundel, R. E.; Buchwald, S. T. *J. Am. Chem. Soc*. **2006**, *128*, 10694.

(204) Andino, J. G.; Kilgore, U. J.; Pink, M.; Ozarowski, A.; Krzystek, J.; Telser, J.; Baik, M. H.; Mindiola, D. J. *Chem. Sci.* **2010**, *1*, 351.

(205) Giordano, G.; Crabtree, R. H. *Inorg. Synth*. **1979**, *19*, 218.

(206) Jackstell, R.; Klein, H.; Beller, M.; Wiese, K. D.; Rőttger, D. *Eur. J. Org. Chem.* **2001**, *20*, 3871.

# VITA


| | |
|---|---|
| Name: | Yanjun Zhu |
| Address: | Department of Chemistry<br>Texas A&M University<br>College Station, TX 77842-3012 |
| Email Address: | yjzhu0214@gmail.com |
| Education: | B.S., Chemistry, Soochow University, China, 2003<br>M.S., Chemistry, Brandeis University, Waltham, MA, 2009 |


Publications:


(1) Zhu, Y.; Smith, D; Herbert, D. E; Ozerov, O. V. *Chem. Commun.* **2012**, *48*, 218.

(2) Zhu, Y.; Chen, C. H.; Fafard, C. M.; Foxman, B. M.; Ozerov, O. V. *Inorg. Chem.* **2011**, *50*, 7980.

(3) Whited, M. T.; Zhu, Y.; Timpa, S. D.; Chen, C. H.; Foxman, B. M.; Ozerov, O. V. *Organometallics* **2009**, *28*, 4560.

(4) Zhu, Y.; Fan, L.; Chen, C.-H.; Finnell, S. R.; Foxman, B. M.; Ozerov, O. V. *Organometallics*, **2007**, *26*, 6701.